E-ISSN: 2148-6247

Turkish Journal of PHARMACEUTICAL SCIENCES

An Official Journal of the Turkish Pharmacists' Association, Academy of Pharmacy

Volume: 21 Issue: 3 June 2024

www.turkjps.org

PubMed Central PubMed Scopus TRDİZİN

galenos

Turkish Journal of
PHARMACEUTICAL SCIENCES

Turkish Journal of
PHARMACEUTICAL SCIENCES

Prof. Robert Rapoport, Ph.D.
ORCID: orcid.org/0000-0001-8554-1014
Cincinati University Faculty of Pharmacy, Department of Pharmacology and Cell Biophysics, Cincinati, USA
robertrapoport@gmail.com

Prof. Tayfun Uzbay, Ph.D.
ORCID: orcid.org/0000-0002-9784-5637
Üsküdar University Faculty of Medicine, Department of Medical Pharmacology, İstanbul, Türkiye
tayfun.uzbay@uskudar.edu.tr

Prof. Wolfgang Sadee, Ph.D.
ORCID: orcid.org/0000-0003-1894-6374
Ohio State University, Center for Pharmacogenomics, Ohio, USA
wolfgang.sadee@osumc.edu

Advisory Board

Turkish Journal of
PHARMACEUTICAL SCIENCES

Please refer to the journal's webpage (https://www.turkjps.org/) for "Editorial Policy" and "Instructions to Authors".

The editorial and publication process of the **Turkish Journal of Pharmaceutical Sciences** are shaped in accordance with the guidelines of ICMJE, WAME, CSE, COPE, EASE, and NISO. The Turkish Journal of Pharmaceutical Sciences is indexed in **PubMed, PubMed Central, Thomson Reuters / Emerging Sources Citation Index, Scopus, ULAKBİM, Türkiye Atıf Dizini, Embase, EBSCO Host, Türk Medline, Cabi, CNK**I.

The journal is published online.

Owner: Turkish Pharmacists' Association, Academy of Pharmacy

Responsible Manager: İlkay Erdoğan Orhan

galenos yayınevi

Publisher Contact
Address: Molla Gürani Mah. Kaçamak Sk. No: 21/1
34093 İstanbul, Türkiye
Phone: +90 (530) 177 30 97
E-mail: info@galenos.com.tr/yayin@galenos.com.tr
Web: www.galenos.com.tr | **Publisher Certificate Number:** 14521

Publication Date: July 2024
E-ISSN: 2148-6247
International scientific journal published bimonthly.

Turkish Journal of
PHARMACEUTICAL SCIENCES

CONTENTS

Original Articles

Turk J Pharm Sci 2024;21(3):167-173
DOI: 10.4274/tjps.galenos.2023.86727

ORIGINAL ARTICLE

Characterization of Equilibrative Nucleoside Transport of the Pancreatic Cancer Cell Line: Panc-1

Sıla APPAK BAŞKÖY[1,2*], Amardeep KHUNKHUNA[3], Bianca SCURIC[1], Zlatina NAYDENOVA[1], Imogen R. COE[1,2]

[1]Toronto Metropolitan University Faculty of Science, Department of Chemistry and Biology, Toronto, Ontario, Canada
[2]Institute for Biomedical Engineering, Science and Technology (iBEST), Toronto, Ontario, Canada
[3]University College London, Faculty of Pharmacy, London, United Kingdom

ABSTRACT

Objectives: Gemcitabine, a first-line chemotherapeutic nucleoside analog drug (NAD) for pancreatic cancer, faces limitations due to drug resistance. Characterizing pancreatic cancer cells' transport characteristics may help identify the mechanisms behind drug resistance, and develop more effective therapeutic strategies. Therefore, in this study, we aimed to determine the nucleoside transport properties of Panc-1 cells, one of the commonly used pancreatic adenocarcinoma cell lines.

Materials and Methods: To assess the presence of equilibrative nucleoside transporter-1 (ENT-1) in Panc-1 cells, we performed immunofluorescence staining, western blot analysis, and S-(4-nitrobenzyl)-6-thioinosine (NBTI) binding assays. We also conducted standard uptake assays to measure the sodium-independent uptake of [3H]-labeled chloroadenosine, hypoxanthine, and uridine. In addition, we determined the half-maximal inhibitory concentration (IC_{50}) of gemcitabine. Statistical analyses were performed using GraphPad Prism version 8.0 for Windows.

Results: The sodium-independent uptake of [3H]-labeled chloroadenosine, hypoxanthine, and uridine was measured using standard uptake assays, and the transport rates were determined as 111.1 ± 3.4 pmol/mg protein/10 s, 62.5 ± 4.8 pmol/mg protein/10 s, and 101.3 ± 2.5 pmol/mg protein/10 s, respectively. Furthermore, the presence of ENT-1 protein was confirmed using NBTI binding assays (B_{max} 1.52 ± 0.1 pmol/mg protein; equilibrium dissociation constant 0.42 ± 0.1 nM). Immunofluorescence assays and western blot analysis also revealed ENT-1 in Panc-1 cells. The determined IC_{50} of gemcitabine in Panc-1 cells was 2 μM, indicating moderate sensitivity.

Conclusion: These results suggest that Panc-1 is a suitable preclinical cellular model for studying NAD transport properties and potential therapies in pancreatic cancer and pharmaceutical research.

Keywords: Panc-1, ENT-1, gemcitabine, transport, pancreatic cancer

INTRODUCTION

Gemcitabine, a nucleoside analog drug (NAD) and deoxycytidine nucleoside analog is widely used as a chemotherapeutic agent for treating various solid tumors, particularly pancreatic cancer, where it serves as a first-line therapy.[1,2] Gemcitabine is metabolized to an active triphosphate derivative that inhibits ribonucleotide reductase, leading to the arrest of de novo DNA synthesis and induction of apoptosis.[2] Despite the initial sensitivity of pancreatic cancer cells to gemcitabine, most patients develop resistance within a few weeks of treatment initiation, resulting in poor survival rates.[3] Studies have shown that tumor cells deficient in nucleoside transporters are resistant to gemcitabine, highlighting the crucial role of these transport proteins in drug efficacy.[4] The levels of the predominant human nucleoside transporter, human equilibrative nucleoside transporter-1 (hENT-1), and the pyrimidine-preferring concentrative nucleoside transporter, human concentrative nucleoside transporter-1 (hCNT) have been found to correlate with gemcitabine sensitivity.[5,6] Therefore, understanding the role of nucleoside transporters in gemcitabine efficacy and developing novel approaches to enhance efficacy and overcome resistance are essential. Consequently, there is a need to better understand the role of nucleoside transporters in gemcitabine efficacy in pancreatic cells and to increase efficacy through the development of novel approaches that combine the established cytotoxicity of gemcitabine, considering the development

*Correspondence: sappakbaskoy@torontomu.ca, ORCID-ID: orcid.org/0000-0001-6105-1408
Received: 24.01.2023, Accepted: 20.06.2023

of chemoresistance. Several different pancreatic tumor cell lines are used in research, which exhibit varying sensitivity to gemcitabine, but only a few have well-characterized transporter profiles. Panc-1, a preclinical cellular model of pancreatic cancer, was cultured from a 56-year-old man with adenocarcinoma in the head of the pancreas that invaded the duodenal wall. Previous studies have reported a range of gemcitabine sensitivity (nM to mM) in Panc-1,[7,8] but the transport characteristics remain unknown. Therefore, our objective was to characterize nucleoside transport activity in Panc-1 and investigate the presence of hENT-1, which is both necessary and critical for gemcitabine efficacy.[4]

MATERIALS AND METHODS

Cell culture

Panc-1 cells American Type Culture Collection [(ATCC) + CRL-1469] were cultured in Dulbecco's Modified Eagle's Medium (Gibco™, Thermo Fisher Scientific, Milano, cat#LS11965092) supplemented with 10% (*v/v*) fetal calf serum (Gibco™, Thermo Fisher Scientific, Milano, cat#10437-036). The cells were maintained at 37 °C in a humidified incubator with 5% CO_2 and were subcultured at a 1:4 ratio using 0.025% Trypsin-EDTA solution (Thermo Fisher Scientific, cat#15090046). The authenticity of the Panc-1 cell line was confirmed by ATCC through RNA sequence analysis, which showed a 100% match to the original Panc-1 cell line.

Immunofluorescence microscopy

To determine the subcellular localization of hENT-1, immunofluorescence assays were conducted using Panc-1 cells. The cells were seeded in 6-well plates on round, 18-mm poly-D-lysine pre-coated German glass coverslips (Electron Microscopy Sciences, cat#72294-11) and grown in a humidified incubator at 37 °C with 5% CO_2 for 20-24 hours until they reached a minimum of 60% confluency. The cells were then washed twice with pre-warmed phenol-free HBSS++ (Hanks' balanced salt solution supplemented with calcium and magnesium, Thermo Fisher Scientific, cat#14025076) for 5 min, fixed for 15 min in 4% (*w/v*) paraformaldehyde in calcium and magnesium-free phosphate buffer saline (PBS), and rinsed. Following this, the cells were incubated with anti-hENT-1 antibody (Santa Cruz, cat#sc-377283-AF488) for 1 h at room temperature and then rinsed. Subsequently, the cells were incubated with wheatgerm Agglutinin 594 (WGA) at a concentration of 5.0 µg/mL and 4',6-diamidino-2-phenylindole for 5 min at 1:30.000 dilution. After rinsing, the cells were mounted in calcium- and magnesium-free PBS within a 35-mm Chamlide™ dish-type magnetic chamber (Quorum Technologies, cat#CM-B-30). Images were obtained using a Yokogawa X1 head with a Borealis Spinning Disk Microscope.

Total lysate and cytosolic protein extractions

To confirm the presence of hENT-1 within the membranes of Panc-1 cells, immunohistochemistry assays were performed. Panc-1 cells were seeded in 10-mm plates and grown in a humidified incubator at 37 °C with 5% CO_2 for 48 h. The cells were then washed twice with room temperature PBS. For total lysate collection, cells were harvested by scraping in NP-40 buffer (50 mM NaF, 1 mM Na2VO3) and protease inhibitor cocktail (Complete Mini, Roche, 11836153001), followed by membrane disruption by passing them through a 26-gauge needle attached to a 1 mL syringe three times within 5-min intervals on ice. The cell homogenate was fractionated by centrifugation at 8.000 gs for 5 min at 4 °C, and the supernatant containing the protein extract was collected and stored on ice. The protein concentration was quantified using the Bradford Protein Assay Kit (Bio-Rad, Hercules, CA, USA) according to the manufacturer's protocol. For the collection of cytosolic fractions, cells were harvested by scraping in PBS and collected using the Mem-PER Plus Membrane Protein Extraction Kit (ThermoFisher, cat#89842). Protein was collected following the manufacturer's protocol. Both cytosolic and membrane fractions were collected and stored on ice, and the protein concentration was quantified using the Bradford Protein Assay Kit (Bio-Rad, Hercules, CA, USA) according to the manufacturer's protocol.

Immunoblot analysis

All lysates were prepared in laemmli sample buffer [0.5 M Tris, pH 6.8, glycerol, 10% sodium dodecyl sulfate (SDS), 10% β-mercaptoethanol, and 5% bromophenol blue] and heated at 95 °C for 5 min. Proteins were resolved by glycine-Tris SDS-PAGE followed by transfer onto a nitrocellulose membrane (Bio-Rad). The membrane was then washed, blocked, and incubated overnight at 4 °C with a 1:1000 (*v/v*) dilution of anti-hENT-1 antibody (Santa Cruz, cat#sc-377283). After three washes, proteins were detected using a 1:2000 (*v/v*) dilution of goat anti-mouse (IgG) secondary antibody conjugated to horseradish peroxidase for 2 h at room temperature, followed by enhanced chemiluminescence (ECL) detection using the ECL Detection Kit (Bio-Rad, cat#1705061). Primary and secondary antibodies were removed using Restore™ PLUS Western Blot Stripping Buffer according to the manufacturer's protocol (Thermo Fisher Scientific, cat#46430). The blots were washed three times and probed to detect the loading control protein glyceraldehyde-3-phosphate dehydrogenase (GAPDH) using a 1:8000 (*v/v*) dilution of anti-GAPDH antibody [Santa Cruz, cat#(0411): sc-47724] for 2 h at room temperature. Proteins were detected using a 1:2000 (*v/v*) dilution of goat anti-mouse (IgG) secondary antibody conjugated to horseradish peroxidase for 1 h at room temperature, followed by ECL detection using the ECL Detection Kit (Bio-Rad, cat#1705061). Western blot assays were performed three times, and the data from each experiment were pooled. Signals corresponding to the intensity of the hENT-1 protein were obtained by analyzing the original files using ImageJ software to determine the area under the peak in the appropriate lane and band for each cell type. The area values collected for the replicate 3 samples were adjusted to show the corresponding value of expression in 10 µg of protein. The area values were normalized to the loading control (*e.g.*, GAPDH) signal obtained after replotting.

Transport assay

The transport characteristics of chloroadenosine (a purine analog), uridine (a pyrimidine analog), and hypoxanthine (a nucleobase) were determined using standard assays and [3H]-labeled substrates. Panc-1 cells were seeded into three 6-well plates at a density of approximately 300,000 cells per well and grown in a humidified incubator at 37 °C with 5% (*v/v*) CO_2 for 24-48 hours until they reached 80% confluency. Uptake was measured in sodium-free buffer (20 mM Tris-HCl, 3 mM K2HPO4, 1 mM MgCl2, 2 mM CaCl2.2H2O, 5 mM glucose, and 130 mM N-methyl-D-glucamine, pH 7.4) containing 10 µM cold substrate and 1 x 106 cpm/mL [3H]-labeled substrate. The cells were washed with sodium-free transport buffer and incubated for 10 s in 1.25 mL of permeant solution (sodium-free buffer containing either chloroadenosine, hypoxanthine, or uridine as the substrate). The uptake was stopped by rapid aspiration of the permeant solution and rapid washing of cells three times with sodium-free, ice-cold stop buffer [100 nM S-(4-nitrobenzyl)-6-thioinosine (NBTI) plus 30 µM dipyridamole]. Cells in each well were lysed in 1 mL of 2 M NaOH overnight at 4 °C. Aliquots were taken to measure the protein content using a modified Lowry protein assay (Bio-Rad), and the [3H]-labeled substrate uptake was measured by conducting standard liquid scintillation counting. Substrate uptake is expressed as picomoles per milligram of protein.

NBTI binding

To confirm the presence and correct orientation of the hENT-1 protein on the cell surface, NBTI binding was measured. NBTI is a high-affinity, non-transportable nucleoside analog that tightly binds to hENT-1 and inhibits ENT-1-mediated transport at nanomolar concentrations. Panc-1 cells were seeded in 10-cm plates and grown to 90-100% confluency. The cells were washed and collected by scraping, followed by resuspension in binding buffer (10 mM Tris-HCl, 100 mM KCl, 0.1 mM MgCl2, and 0.1 mM CaCl2, pH 7.4). NBTI binding experiments were performed by incubating the cells in the presence of increasing concentrations of [3H] NBTI (0.186-7.45 nM). Binding was calculated as the difference between binding in the absence (total binding) and presence (non-specific binding) of 10 µM unlabeled NBTI. The cells were incubated at room temperature with increasing concentrations of [3H] NBTI for 50 min to reach equilibrium, and the reaction was stopped by adding an ice-cold binding buffer. The samples were then subjected to scintillation counting to measure the accumulated radioactivity.

Determination of inhibitory concentration (IC_{50})

To determine the IC_{50} of gemcitabine in Panc-1 cells, the doubling time of Panc-1 was first established to be 40 h. The cells were then treated with a range of concentrations of gemcitabine (500 nM to 100 µM) for 48 hours, and 50% inhibition of cell growth was determined using a trypan exclusion viability assay measured with the Vi-CELL™ XR Cell Viability Analyzer (Beckman Coulter, USA).

Statistical analysis

Nucleoside and nucleobase uptake and NBTI binding assays were performed three times, and the data from each experiment were pooled. The data are expressed as means ± standard error of the mean. Uptake data were compared using One-Way analysis of variance with Tukey's multiple comparison test to determine statistical significance at $p < 0.05$. The [3H] NBTI binding constants, equilibrium dissociation constant (Kd) (binding affinity), and B_{max} (maximum specific binding) were obtained by non-linear regression analysis using GraphPad Software (PRISM version 8.0 for Windows).

All statistical analyses were performed using GraphPad Prism version 8.0 for Windows (GraphPad Software, San Diego, CA, 2018).

RESULTS

ENT-1 is a key transporter involved in the uptake of NAD drugs like gemcitabine.[9-11] In this study, we characterized the ENT-dependent uptake and presence of hENT-1 in Panc-1 cells. Colocalization analysis with the membrane marker WGA confirmed the presence of hENT-1 at the cellular membrane (Figure 1A), supporting previous findings.[12-14] We also observed the presence of hENT-1 intracellularly, consistent with previous reports of ENT-1 localization in internal structures such as membrane-bound vesicles, endosomes, and lysosomes in other cell lines.[15] To compare the levels of hENT-1 protein in Panc-1 cells with those in a well-established cell model, we examined HEK-293 cells (Figure 1B). Immunoblot analysis revealed that Panc-1 cells have approximately 13% higher levels of hENT-1 protein compared to HEK-293 cells (Figure 1C). However, the presence of the ENT-1 protein alone does not confirm its functional uptake. Therefore, we measured nucleoside and nucleobase uptake in the absence of sodium to exclude uptake via CNT. Our results showed that chloroadenosine, uridine, and hypoxanthine can all be transported into Panc-1 cells, at varying rates. Chloroadenosine and uridine exhibited higher uptake compared to hypoxanthine (Figure 2A), consistent with the preference of ENT-1 for nucleosides over nucleobases. The measurable uptake of hypoxanthine is likely attributable to ENT-2, which can transport both nucleosides and nucleobase.[16]

To confirm that ENT-1 is responsible for the majority of chloroadenosine and uridine transport, we performed inhibition assays using NBTI, a specific inhibitor of ENT-1 (Figure 2B). The effective inhibition of nucleoside uptake by NBTI further supported the involvement of ENT-1 in the transport process. NBTI binding assays were also performed to confirm the presence of hENT-1 on the cell surface membrane (Figure 2C). The binding capacity, represented by B_{max} (maximum binding capacity), of Panc-1 cells (B_{max}=1.52 pmol/mg protein, Kd=0.43 nM) suggested a higher number of hENT-1 proteins with high affinity compared with other cell lines, such as MCF-7 (B_{max}=1.01 pmol/mg protein), HL-1 (B_{max}=0.58 pmol/mg protein), and HEK293 (0.45 pmol/mg protein) cells.[17-19] The higher B_{max} in Panc-1 cells (111.18 ± 3.45 pmol/mg protein) correlated with significantly greater uptake of chloroadenosine compared with HEK293 cells (60 ± 2 pmol/mg protein).[20] The affinity (Kd) of NBTI binding in Panc-1 cells fell within the range of

published values for other cell lines, indicating similar binding site characteristics.[17,21,22]

Lastly, we determined the IC_{50} of gemcitabine in Panc-1 cells, which was found to be 2 μM (Figure 3). This value represents the concentration of gemcitabine required to inhibit 50% of cell growth after a 48-hour gemcitabine treatment.

DISCUSSION

Based on our findings, we can confirm the significant hENT-1-dependent uptake of gemcitabine in Panc-1 cells, which is consistent with hENT-1 playing a major role in determining the response to gemcitabine in patients with pancreatic cancer.[6,23] This reinforces the use of Panc-1 cells as a suitable model for studying the susceptibility of pancreatic tumors to gemcitabine treatment, either alone or in combination with other therapies.

It is worth noting that the IC_{50} level of gemcitabine in our study differed from previous reports, which have reported IC_{50} values ranging from nanomolar to millimolar levels.[7,8] The reasons for these discrepancies are not clear; however, they emphasize the importance of establishing the sensitivity of a cell line to a drug before using it for further research. The gemcitabine sensitivity of tumor cell lines can vary under different experimental conditions, including drug concentration, exposure time, and the assay used for evaluation (Table 1). The low-to-moderate sensitivity of Panc-1 cells to gemcitabine provides an opportunity to explore combination therapies, such as ultrasound and microbubbles, in conjunction with gemcitabine.[24,25] Studies have shown that this combination can enhance cytotoxicity in pancreatic cancer therapy compared with either treatment alone. In a study examining the cytotoxic effect of gemcitabine, various cell cultures were assessed by 3-(4,5-Dimethylthiazol-2-yl)-2,5-Diphenyltetrazolium Bromide cell viability assay. The cells included primary pancreatic tumor cells derived from ductal adenocarcinoma, pancreatic stellate cells, and established pancreatic ductal adenocarcinoma cell lines (BxPC-3, Mia PaCa-2, and Panc-1). Results indicated that gemcitabine exhibited a dose-dependent inhibition of cell viability in all primary tumor cell cultures and established cell lines. However, none of the pancreatic stellate cells displayed sensitivity to the cytotoxic effects of gemcitabine. At a specific concentration of gemcitabine (10 μM), the viability of primary cancer cells decreased by 58-70%, while the pancreatic ductal adenocarcinoma cell lines (BxPC-3, Mia PaCa-2, and Panc-1)

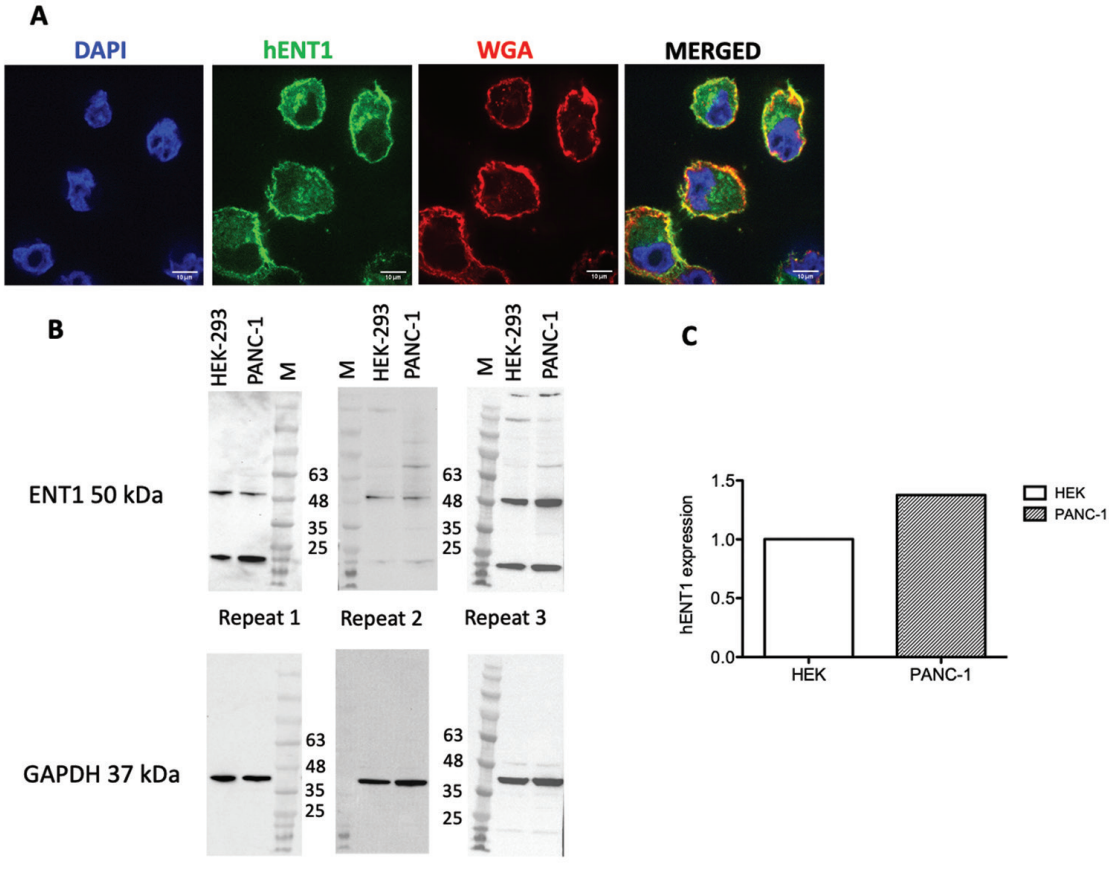

Figure 1. hENT-1 is present in the plasma membrane of Panc-1 cells. (A) Endogenous hENT-1 is found at the plasma membrane of Panc-1 cells based on co-localization with WGA, which localizes to the plasma membrane. Some hENT-1 was observed in intracellular structures distributed in a punctate pattern. (B) Three representative western blot analyses show the presence of hENT-1 at the predicted size of ~50 kDa in Panc-1 cells in comparison to HEK293 cells. Cytosolic fractions (repeat 1:10 ug) or whole-cell lysates (repeats 2-3:10 ug and 15 ug, respectively) were resolved by immunoblotting and probed with antibodies targeting hENT-1 (top) or loading control GAPDH (bottom). M represents the marker lane. (C) Quantification of western blots showing 13% higher expression of hENT-1 in Panc-1 cells compared with HEK-293 cells.

hENT-1: Human equilibrative nucleoside transporter-1, GAPDH: Glyceraldehyde 3-phosphate dehydrogenase, WGA: Wheat germ agglutinin

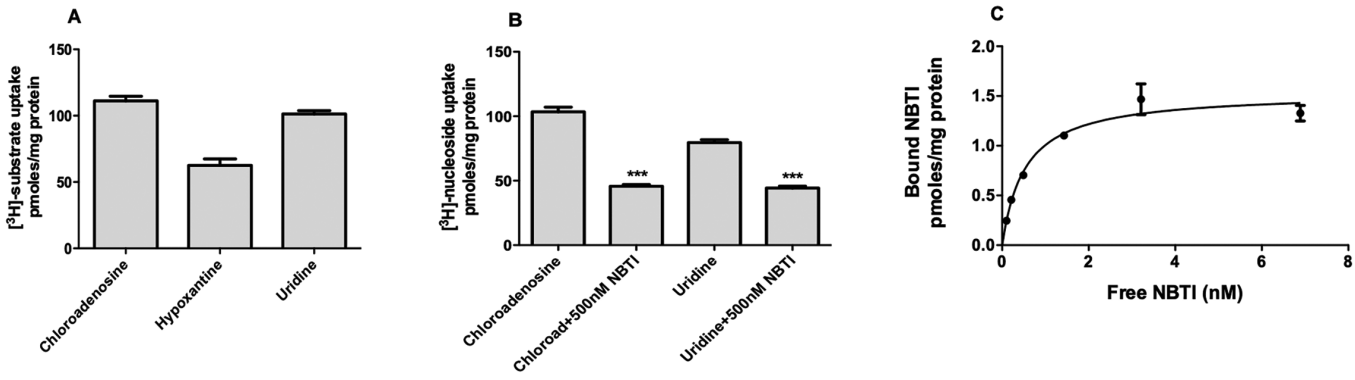

Figure 2. Panc-1 cells exhibit hENT-dependent nucleoside transport. (A) Panc-1 cells exhibit higher levels of uptake of the nucleosides chloroadenosine (1) and uridine (3) compared to the nucleobase hypoxanthine (2). Data are pooled from 3 independent experiments with 6 replicates for each substrate. Error bars represent mean ± SEM. (B) hENT-1 was confirmed to contribute to chloroadenosine (1) and uridine (3) uptake in Panc-1 cells because it was reduced in the presence of the hENT-1-specific inhibitor NBTI (500 nM), chloroadenosine + NBTI (2), and uridine + NBTI (4). Data are pooled from 3 independent experiments with 6 replicates for each substrate. Error bars represent mean ± SEM. ***$p < 0.001$ (C) presence of hENT-1 protein in Panc-1 cells was confirmed by NBTI binding. Representative experiment was repeated three times with similar results. Each point is the mean of two replicates ± SD.

hENT: Human equilibrative nucleoside transporter, SEM: Standard error of mean, NBTI: S-(4-nitrobenzyl)-6-thioinosine, SD: Standard deviation

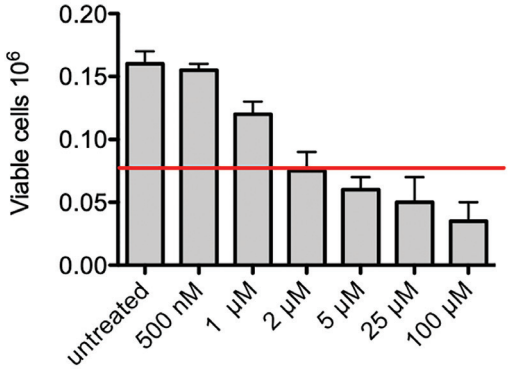

Figure 3. The IC_{50} of gemcitabine in Panc-1 cells.

IC_{50} of Panc-1 cells to gemcitabine was determined to be 2 µM by incubation in a range of concentrations of the drug (500 nM-100 µM) and measurement of viability after 48 hours. (0 = no treatment, 1 = 500 nM, 2 = 1 µM, 3 = 2 µM, 4 = 5 µM, 5 = 25 µM, 6 = 100 µM). Error bars represent mean ± SEM. $p < 0.005$. The experiment was repeated three times with similar results, and each treatment was performed in duplicate.

IC_{50}: Inhibitory concentration, SEM: Standard error of mean

exhibited a reduction in viability ranging from 40-56% (BxPC-3 the most and Panc-1 the least sensitive). Primary pancreatic cancer cells exhibited higher chemosensitivity than the pancreatic ductal adenocarcinoma cell lines. The resistance of satellite cells to gemcitabine has been attributed to the absence of membrane transporters.[26]

The development of novel approaches is crucial for pancreatic cancer treatment because the disease often presents at an advanced stage and tumor cells rapidly develop resistance.[27] Incubation of cells with NADs, such as gemcitabine, may lead to the downregulation of transporter expression and the selection of transporter-deficient cells, contributing to clinical resistance to gemcitabine chemotherapy.[10] These aspects of gemcitabine resistance can be investigated in Panc-1 cells because they reflect cellular behavior in response to drug treatment. For example, studies have demonstrated that gemcitabine resistance induced by the epithelial-to-mesenchymal transition in pancreatic cancer cells involves the functional loss of hENT-1.[14]

Tumors typically consist of heterogeneous populations of cells, each potentially having varying NT expression profiles.[28] High expression of ENT-1 in pancreatic cancer has been associated with increased patient survival in those receiving gemcitabine treatment, highlighting the significance of ENT-1 in therapeutic response.[6,23] Apart from ENT-1, hENT-2 was identified to transport gemcitabine into cells; however, it is not as effective as ENT-1 in drug uptake.[29] However, aberrant expression of hENT-2 is thought to contribute to gemcitabine resistance.[2] There has been an inverse proportion shown between hCNT3 amount and gemcitabine toxicity.[30] CNT-3 is considered a potential therapeutic target for addressing resistance to toxic nucleoside analog treatments. While much research has focused on hENT-1 as a target for overcoming gemcitabine resistance in pancreatic cancer patients, it was found that hCNT3-transfected cells with functional hENTs exhibited an 8-fold increase in gemcitabine uptake and cells without functional ENTs had much higher uptake, indicating that functional hENTs present in cells result in a decrease in gemcitabine uptake.[31] In another study, it was found that patients with high expression levels of ENT-1 had notably longer disease-free survival and overall survival than patients with low expression levels. High expression levels of hCNT3 were associated with longer overall survival but not with disease-free survival. However, pancreatic cancer patients who exhibited high expression levels of both hENT-1 and hCNT3 experienced a remarkable five-fold longer overall survival than other patients. This suggests that the combined presence of high expression levels of both hENT-1 and hCNT3 may lead to improved survival outcomes in pancreatic cancer patients.[32]

Table 1. Sensitivity of pancreatic adenocarcinoma cell lines to gemcitabine

Cell line	Sensitivity to gemcitabine
AsPc-1	Low to moderate[33,35]
BXPC-3	High to moderate[26,34]
Capan-1	High to moderate[35]
MiaPaca-2	High to moderate[26,35]
Panc-1	Low to moderate[8,26]

These findings suggest that the role of hCNT3 in gemcitabine treatment response and patient prognosis is complex. While increased hCNT3 expression may lead to decreased gemcitabine uptake, the presence of both high hENT-1 and hCNT3 expression levels appears to be associated with improved survival outcomes in patients with pancreatic cancer.

In summary, our data support the role of hENT-1-dependent uptake in Panc-1 cells, which has implications for gemcitabine response in pancreatic cancer patients. Panc-1 cells provide a valuable model for studying the efficacy of gemcitabine and for exploring combination therapies.

CONCLUSION

Our results demonstrate that Panc-1 cells exhibit high levels of hENT-1 protein expression and hENT-1-dependent uptake. Moreover, Panc-1 cells demonstrate moderate sensitivity to gemcitabine, with an IC_{50} of 2 μM, suggesting that this cell line is a suitable preclinical cellular model for studying both the transport properties and NAD therapies.The significant expression of hENT-1, the observed hENT-dependent uptake, and the sensitivity to gemcitabine in Panc-1 cells indicate that this cell line serves as a valuable model for investigating NAD therapies in combination with other strategies for pancreatic cancer treatment. Understanding the mechanisms of gemcitabine efficacy in Panc-1 cells can contribute to the development of improved treatment strategies for pancreatic cancer. Our findings contribute to the understanding of the molecular mechanisms underlying gemcitabine response and resistance in pancreatic cancer and pave the way for future studies aimed at improving therapeutic outcomes and exploring novel treatment approaches for this challenging disease.

Acknowledgments

This research was supported by the Natural Sciences and Engineering Research Council of Canada (#RGPIN 2017-05193).

Ethics

Ethics Committee Approval: No ethics approval as no animal or human work has been carried out for this manuscript.

Informed Consent: Not necessary.

Authorship Contributions

Concept: S.A.B., Z.N., I.R.C., Design: S.A.B., Z.N., I.R.C., Data Collection or Processing: S.A.B., A.K., B.S., Analysis or Interpretation: S.A.B., A.K., B.S., I.R.C., Literature Search: S.A.B., A.K., Writing: S.A.B., A.K.

Conflict of Interest: No conflict of interest was declared by the authors.

Financial Disclosure: The authors declared that this study received no financial support.

REFERENCES

1. Chand S, O'Hayer K, Blanco FF, Winter JM, Brody JR. The landscape of pancreatic cancer therapeutic resistance mechanisms. Int J Biol Sci. 2016;12:273-282.
2. Carter CJ, Mekkawy AH, Morris DL. Role of human nucleoside transporters in pancreatic cancer and chemoresistance. World J Gastroenterol. 2021;27:6844-6860.
3. Amrutkar M, Gladhaug IP. Pancreatic cancer chemoresistance to gemcitabine. Cancers (Basel). 2017;9:157.
4. Noble S, Goa KL. Gemcitabine. A review of its pharmacology and clinical potential in non-small cell lung cancer and pancreatic cancer. Drugs. 1997;54:447-472.
5. Mini E, Nobili S, Caciagli B, Landini I, Mazzei T. Cellular pharmacology of gemcitabine. Ann Oncol. 2006;17(Suppl 5):7-12.
6. Spratlin J, Sangha R, Glubrecht D, Dabbagh L, Young JD, Dumontet C, Cass C, Lai R, Mackey JR. The absence of human equilibrative nucleoside transporter 1 is associated with reduced survival in patients with gemcitabine-treated pancreas adenocarcinoma. Clin Cancer Res. 2004;10:6956-6961.
7. Quint K, Tonigold M, Di Fazio P, Montalbano R, Lingelbach S, Rückert F, Alinger B, Ocker M, Neureiter D. Pancreatic cancer cells surviving gemcitabine treatment express markers of stem cell differentiation and epithelial-mesenchymal transition. Int J Oncol. 2012;41:2093-2102.
8. Fryer RA, Barlett B, Galustian C, Dalgleish AG. Mechanisms underlying gemcitabine resistance in pancreatic cancer and sensitisation by the iMiD™ lenalidomide. Anticancer Res. 2011;31:3747-3756.
9. King AE, Ackley MA, Cass CE, Young JD, Baldwin SA. Nucleoside transporters: from scavengers to novel therapeutic targets. Trends Pharmacol Sci. 2006;27:416-425.
10. Young JD, Yao SY, Baldwin JM, Cass CE, Baldwin SA. The human concentrative and equilibrative nucleoside transporter families, SLC28 and SLC29. Mol Aspects Med. 2013;34:529-547.
11. Boswell-Casteel RC, Hays FA. Equilibrative nucleoside transporters-a review. Nucleosides Nucleotides Nucleic Acids. 2017;36:7-30.
12. Revalde JL, Li Y, Wijeratne TS, Bugde P, Hawkins BC, Rosengren RJ, Paxton JW. Curcumin and its cyclohexanone analogue inhibited human Equilibrative nucleoside transporter 1 (ENT1) in pancreatic cancer cells. Eur J Pharmacol. 2017;803:167-173.
13. Wang H, Word BR, Lyn-Cook BD. Enhanced efficacy of gemcitabine by indole-3-carbinol in pancreatic cell lines: the role of human equilibrative nucleoside transporter 1. Anticancer Res. 2011;31:3171-3180.
14. Weadick B, Nayak D, Persaud AK, Hung SW, Raj R, Campbell MJ, Chen W, Li J, Williams TM, Govindarajan R. EMT-induced gemcitabine resistance in pancreatic cancer involves the functional loss of equilibrative nucleoside transporter 1. Mol Cancer Ther. 2021;20:410-422.

15. Nivillac NM, Bacani J, Coe IR. The life cycle of human equilibrative nucleoside transporter 1: from ER export to degradation. Exp Cell Res. 2011;317:1567-1579.

16. Naes SM, Ab-Rahim S, Mazlan M, Abdul Rahman A. Equilibrative nucleoside transporter 2: properties and physiological roles. Biomed Res Int. 2020;2020:5197626.

17. Coe I, Zhang Y, McKenzie T, Naydenova Z. PKC regulation of the human equilibrative nucleoside transporter, hENT1. FEBS Lett. 2002;517:201-205.

18. Chaudary N, Shuralyova I, Liron T, Sweeney G, Coe IR. Transport characteristics of HL-1 cells: a new model for the study of adenosine physiology in cardiomyocytes. Biochem Cell Biol. 2002;80:655-665.

19. Zafar M, Naydenova Z, Coe IR. Extended exposure to substrate regulates the human equilibrative nucleoside transporter 1 (hENT1). Nucleosides Nucleotides Nucleic Acids. 2016;35:631-642.

20. Bicket A, Mehrabi P, Naydenova Z, Wong V, Donaldson L, Stagljar I, Coe IR. Novel regulation of equlibrative nucleoside transporter 1 (ENT1) by receptor-stimulated Ca^2 + -dependent calmodulin binding. Am J Physiol Cell Physiol. 2016;310:808-820.

21. Boumah CE, Hogue DL, Cass CE. Expression of high levels of nitrobenzylthioinosine-sensitive nucleoside transport in cultured human choriocarcinoma (BeWo) cells. Biochem J. 1992;288:987-996.

22. Boleti H, Coe IR, Baldwin SA, Young JD, Cass CE. Molecular identification of the equilibrative NBMPR-sensitive (es) nucleoside transporter and demonstration of an equilibrative NBMPR-insensitive (*ei*) transport activity in human erythroleukemia (K562) cells. Neuropharmacology. 1997;36:1167-1179.

23. Farrell JJ, Elsaleh H, Garcia M, Lai R, Ammar A, Regine WF, Abrams R, Benson AB, Macdonald J, Cass CE, Dicker AP, Mackey JR. Human equilibrative nucleoside transporter 1 levels predict response to gemcitabine in patients with pancreatic cancer. Gastroenterology. 2009;136:187-195.

24. Dimcevski G, Kotopoulis S, Bjånes T, Hoem D, Schjøtt J, Gjertsen BT, Biermann M, Molven A, Sorbye H, McCormack E, Postema M, Gilja OH. A human clinical trial using ultrasound and microbubbles to enhance gemcitabine treatment of inoperable pancreatic cancer. J Control Release. 2016;243:172-181.

25. Mariglia J, Momin S, Coe IR, Karshafian R. Analysis of the cytotoxic effects of combined ultrasound, microbubble and nucleoside analog combinations on pancreatic cells in vitro. Ultrasonics. 2018;89:110-117.

26. Amrutkar M, Vethe NT, Verbeke CS, Aasrum M, Finstadsveen AV, Sántha P, Gladhaug IP. Differential gemcitabine sensitivity in primary human pancreatic cancer cells and paired stellate cells is driven by heterogenous drug uptake and processing. Cancers (Basel). 2020;12:3628.

27. McGuigan A, Kelly P, Turkington RC, Jones C, Coleman HG, McCain RS. Pancreatic cancer: a review of clinical diagnosis, epidemiology, treatment and outcomes. World J Gastroenterol. 2018;24:4846-4861.

28. García-Manteiga J, Molina-Arcas M, Casado FJ, Mazo A, Pastor-Anglada M. Nucleoside transporter profiles in human pancreatic cancer cells: role of hCNT1 in 2',2'-difluorodeoxycytidine- induced cytotoxicity. Clin Cancer Res. 2003;9:5000-5008.

29. Pastor-Anglada M, Pérez-Torras S. Emerging roles of nucleoside transporters. Front Pharmacol. 2018;9:606.

30. Stecula A, Schlessinger A, Giacomini KM, Sali A. Human concentrative nucleoside transporter 3 (hCNT3, SLC28A3) forms a cyclic homotrimer. Biochemistry. 2017;56:3475-3483.

31. Paproski RJ, Yao SY, Favis N, Evans D, Young JD, Cass CE, Zemp RJ. Human concentrative nucleoside transporter 3 transfection with ultrasound and microbubbles in nucleoside transport deficient HEK293 cells greatly increases gemcitabine uptake. PLoS One. 2013;8:e56423.

32. Maréchal R, Mackey JR, Lai R, Demetter P, Peeters M, Polus M, Cass CE, Young J, Salmon I, Devière J, Van Laethem JL. Human equilibrative nucleoside transporter 1 and human concentrative nucleoside transporter 3 predict survival after adjuvant gemcitabine therapy in resected pancreatic adenocarcinoma. Clin Cancer Res. 2009;15:2913-2919.

33. Liu F, Gore AJ, Wilson JL, Korc M. DUSP1 is a novel target for enhancing pancreatic cancer cell sensitivity to gemcitabine. PLoS One. 2014;9:e84982.

34. Kong R, Qian X, Ying W. Pancreatic cancer cells spectral library by DIA-MS and the phenotype analysis of gemcitabine sensitivity. Sci Data. 2022;9:283.

35. Shi X, Liu S, Kleeff J, Friess H, Büchler MW. Acquired resistance of pancreatic cancer cells towards 5-Fluorouracil and gemcitabine is associated with altered expression of apoptosis-regulating genes. Oncology. 2002;62:354-362.

Turk J Pharm Sci 2024;21(3):174-183
DOI: 10.4274/tjps.galenos.2023.75668

ORIGINAL ARTICLE

Proteomic Analysis of HepG2 Cells Reveals FAT10 and BAG2 Signaling Pathways Affected by a Protease Inhibitor from *Tinospora cordifolia* (Willd.) Hook. f. and Thoms Stem. Extract Among the Different Plant and Microbial Samples Analyzed

Bramhi Suresh CHOUGULE, Kumar GAURAV, Mutthu KUMAR, Nayana MAHADEVAPRASAD, Nisarga Hosahalli KRISHNA, Sreya Lakshmi PONNADA, Somasekhara DERANGULA, Varalakshmi Kilingar NADUMANE*

Jain (Deemed-to-be-University), Department of Biotechnology, School of Sciences, Karnataka, India

ABSTRACT

Objectives: Dysregulation of proteolysis underlies diseases like cancer. Protease inhibitors (PIs) regulate many biological functions and hence have potential anticancer properties. With this background, the current study aimed to identify the PI from natural sources such as plants and microbes against trypsin (a protease), which was assayed against casein, using an ultraviolet spectrophotometer-based methodology.

Materials and Methods: PI extracted from a few plants and microbial samples were screened for their PI activity against trypsin. The PI from the most promising source in our study, Tinospora cordifolia (Willd.) Hook. f. and Thoms. stem, was partially purified using ammonium sulfate precipitation followed by dialysis. The PI activity of the partially purified inhibitor was analyzed against chymotrypsin and collagenase enzymes, and the cytotoxic effect of the PI was checked on HepG2 (liver carcinoma) cells by MTT- [3-(4, 5-dimethylthiazol-2-yl)-2, 5-diphenyltetrazolium bromide]- assay. Liquid Chromatograography Mass Spectrometry -based proteomic studies were performed on HepG2 cells to understand the signaling pathways affected by the PIs in the liver cancer cell line.

Results: Among the samples tested the PIs from *T. cordifolia* stem extract had the highest inhibitory activity (72.0%) against trypsin along with cytotoxicity to HepG2 cells. After partial purification by 80.0% ammonium sulfate precipitation, PI had increased inhibitory activity (83.0%) against trypsin and enhanced cytotoxicity (47.0%) to HepG2 cells. Proteomic analysis of the PI-treated HepG2 cells revealed that BAG2 and FAT10 signaling pathways were affected, which may have caused the inhibition of cancer cell proliferation.

Conclusion: PI from *T. cordifolia* stem has promising anticancer potential and hence can be used for further purification and characterization studies toward cancer drug development.

Keywords: *Tinospora cordifolia*, ammonium sulfate, trypsin, protease inhibitor, anticancer, BAG2 signaling

INTRODUCTION

Proteases are enzymes that play a very essential and basic role in many biological events, such as apoptosis, necrosis, angiogenesis, wound healing, transcription, translation, immune responses, differentiation, senescence, *etc.*, by a tightly regulated mechanism known as proteolysis. Dysregulation of the mechanism of proteolysis could lead to many underlying diseases such as cancer, cardiovascular disease, and neurological disorders. Regulation of proteolysis is therefore crucial for the regular developmental activities of an organism.[1,2]

*Correspondence: kn.varalakshmi@jainuniversity.ac.in, Phone: +918043430400, ORCID-ID: orcid.org/0000-0001-9979-5007
Received: 01.03.2023, Accepted: 20.06.2023

The functioning of proteases has been investigated for more than 3 decades for their potential role in cancer development. Protease inhibitors (PIs) inhibit specific classes of proteases by their ability to form a strong protease-PI complex, thereby maintaining the homeostatic balance necessary for preventing life-threatening diseases like cancer. With over 100 proteases already linked to various elements of tumor formation and its progression, there is a strong motive to use PIs in oncology.[3]

Surgery, chemotherapy, and radiotherapy are the three main cancer treatment techniques. Although these treatment modalities play an important role in controlling cancer to a certain extent, the associated adverse effects decrease the quality of life among patients.[4] As a result, scientists are attempting to identify alternative therapeutic strategies capable of suppressing cancer without causing additional morbidity.

The use of alternative cancer therapies from medicinal plants is gaining greater significance due to the existence of a variety of anti-tumor compounds in plants such as *Tinospora cordifolia* (Willd.) Hook. f. and Thoms.[5] *T. cordifolia*, belonging to the family Menispermaceae, can be found all over tropical regions like India and China, growing at altitudes up to 300 m. It is also referred to as guduchi or giloy and was called "amritha" or "heavenly elixir" in Hindu Vedic times. Guduchi is a veterinary folk medicine and Ayurvedic staple. Its stems and roots are anciently used as therapeutics due to their antispasmodic, general tonic, anti-arthritic, anti-diabetic, anti-inflammatory, anti-allergic, and anti-inflammatory properties.[6]

Not only plants but also some microorganisms have similar effects among natural resources. Recently, actinobacteria have also been identified as producers of enzyme inhibitors. A cysteine PI (2081) from *Streptomyces* sp. 2081 exhibited potent inhibition against papain and significant inhibition of tumor cell migration.[7] Thus, studies on the protease landscape associated with cancer have resulted in the emergence of better clinical technologies for diagnosis and therapy that use pathologic patterns of proteolytic activity.[8] Although much work has been conducted in the area of PIs for human immunodeficiency virus (HIV) and other viral diseases, their utility toward cancer therapy has not been extensively explored.[9] Hence, analyzing the ability of PIs for cancer treatment appears to be a very promising approach. The current study is aimed to isolate compounds from medicinal plants and screen them for their PI activity against trypsin and chymotrypsin, along with checking their cytotoxicity on the HepG2 (liver cancer) cell line.

MATERIALS AND METHODS

T. cordifolia cordifolia (Willd.) Hook. f. and Thoms. stem and leaves, *Cascabela thevetia* (L.) Lippold stem and leaves, and meth seeds (*Trigonella foenum-graecum* L.) were collected from Lalbagh in Bangalore in January 2022 and were identified (by Dr. Rama Rao, Research Officer, Central Council for Research in Ayurvedic Sciences, Bangalore, India). The herbarium specimens were kept at the herbarium of Jain University (with specimen numbers *T. cordifolia*-JUH96; *C. thevetia*- JUH97; *T. foenum-graecum* -JUH98). Pure cultures of microbes like *Acinetobacter vinetianus*, *Streptomyces* sp., maintained in our lab were used in the study. Chemicals included, trypsin EDTA, tris HCl, chymotrypsin, collagenase, phosphate buffer saline (PBS), casein, ammonium sulfate, trichloroacetic acid (TCA), sodium bicarbonate, ethylenediaminetetraacetic acid (EDTA) (1 mM), diphenyltetrazolium bromide and dimethyl sulfoxide. All analytical grade chemicals used in this study were procured from Himedia, India.

Extraction of the PI

All plant materials were separately dried at room temperature, and the stem, leaves and seeds were separately ground using a blender. Stem/leaf/seed powder (10 g) was mixed in 100 mL of PBS (0.1 M) having a pH of 7.2, and incubated at room temperature for 30 minutes. The mixture was then centrifuged to remove all the insoluble material at 6000 x g at 4 °C for 10 minutes. The clear supernatant was stored at 4 °C for further analysis. Microorganisms were cultured in nutrient broth for 48 hours, centrifuged at 6000 x g at 4 °C for 10 minutes. The clear supernatant was stored at 4 °C for further analysis. PI activity was determined for all these supernatants using trypsin and chymotrypsin as the proteases.

Assay of PI activity

As per the methodology given by Kunitz[10] with minor modifications, the PI activity against the proteases trypsin, chymotrypsin, and collagenase was assessed. Casein was used as the substrate, whose hydrolysis produces amino acids like tyrosine. The absorbance of the amino acids released was measured at 280 nm. The inhibitory activity was assessed as the residual proteolytic activity in the presence of the inhibitor and expressed as a percentage of the proteolytic activity of the uninhibited control.[11] One unit of enzyme activity is the amount of enzyme that releases 1 µmole/min/mL of tyrosine under the assay conditions. One unit of PI activity unit was defined as the quantity of inhibitor that reduced the absorbance (at 280 nm) by one unit of TCA-soluble casein hydrolysis product, due to the enzyme action per minute under the assay conditions. The PI activity was calculated and expressed as a percentage of the activity of uninhibited protease.[12]

Tyrosine standard

A standard graph of tyrosine was prepared at a final concentration of 200 µg/mL, which was used to quantify the amino acid liberated by the proteases.

Effects of pH, temperature, and metal ions on the PI activity of T. cordifolia

To analyze the effect of pH on the PI activity of the selected plant extract (*T. cordifolia* stem), the plant sample was extracted in buffers of various pH (pH 3, pH 5, pH 7, pH 9, and pH 11). All of these extracts were analyzed on trypsin for PI activity. The samples extracted with distilled water (DW) (TD) and PBS were diluted using DW and PBS, respectively (in the ratio 1:5 and 1:10). To check the effect of temperature, the extracts were incubated at different temperatures (25 °C, 50 °C, 75 °C, and 37 °C) for 30 minutes before performing the PI activity assay.

To check the effect of the metal ions on PI activity, 10 metal salts (barium chloride, manganous chloride, lead chloride, nickel chloride, mercuric sulfate, chromium chloride, cadmium chloride, cupric sulfate, and ferric chloride) were taken in 5 mM and 10 mM concentrations and added to 1 mL of *T. cordifolia* stem PBS extract (TP) and incubated at 37 °C for 30 minutes before performing the PI activity assay.

Purification of PI by ammonium sulfate precipitation

T. cordifolia was sourced from Lalbagh Botanical Garden Nursery. The stem was weighed and 80 g was ground with 400 mL of 0.1 M PBS at pH 7.2. The resulting mixture was filtered using a muslin cloth, and then the filtered sample was centrifuged at 10000 x g at 4 °C for 10 minutes to remove any insoluble plant material. The supernatant was collected and measured. The amount of extract was 380 mL, which was divided equally into two conical flasks. For 40.0% and 80.0% saturation, 46.67 g and 107.73 g of ammonium sulfate were added, respectively, at 4 °C and kept under constant stirring for approximately 12 hours. The solution was centrifuged at 6000 x g at 4 °C for 30 minutes to separate the precipitate and the supernatant. The precipitate was dissolved in 0.1 M PBS of 7.2 pH and further processed.

Dialysis

The PI precipitated by ammonium sulfate was dialyzed in PBS (0.01 M) with a pH of 7.2 to remove ammonium sulfate from it.[13] The dialysis membrane used was from HIMEDIA (LA 401-1 mt). The samples after dialysis were pipetted out and stored in vials at 4 °C for further analysis. The PI activity against trypsin was analyzed as mentioned earlier.

3-(4, 5-dimethylthiazol-2-yl)-2, 5-diphenyltetrazolium bromide (MTT)-assay

To assess the cytotoxicity of PI on MCF-7 and HepG2 cancer cell lines, MTT assay was performed according to the standard methodology.[14] The cancer cell lines (1 x 10^4 cells/mL) were seeded onto the wells of 96-well microtiter plates after trypsinization. The crude extract and ammonium sulfate precipitated (40% and 80%) PIs were added (10 µL) after 24 hours at varying concentrations (1:1, 1:10, 1:25 and 1:50 dilutions) for 24, 48, and 72 hours. After incubation, the MTT assay was performed, and the optical density was recorded at 540 nm. The viability percentage was calculated as follows:

$$\text{Percentage viability} = \frac{\text{OD of sample}_{(540)}}{\text{OD of control}_{(540)}} \times 100$$

where, OD represents the optical density of the sample and control at 540 nm

Assessment of cytotoxicity by lactate dehydrogenase (LDH) activity

The degree of toxicity of the PI in the treated cancer cells was analyzed by estimating LDH enzyme activity in the cytosol.[15] The increase in the LDH enzyme levels in the treated cells reflects the number of lysed cells. The assay was performed based on the instructions provided in the kit manual.

Relative protein quantification using electrospray Ionization-nano Liquid Chromatograography Mass Spectrometry (LC-MS/MS) (Proteomics)

Protein extraction

Confluent cancer cell lines (70%) were cultured in a serum-free medium for 12 hours and later lysed using 2% sodium dodecyl sulfate in 50 mM triethyl ammonium bicarbonate as the lysis buffer, followed by sonication. The concentration of protein in this sample was determined as per standard methods.

Trypsin digestion

The samples were reduced using 100 mM 1, 4-Dithiothreitol (Sigma Aldrich), alkylated using 200 mM iodoacetamide (Sigma Aldrich), and digested overnight with MS-grade trypsin (Sigma Aldrich) in a 1:25 ratio (1 µg of trypsin to 25 µg of protein). All the samples were injected in duplicate (2 injections per sample). The injection volume was 1.0 µL. The detailed in-solution protocol we employed is given in the web link.[16]

Liquid chromatography conditions

LC-MS/MS (Instrument): nanoACQUITY UPLC® chromatographic system (Waters, Manchester, UK) was used for proteomics study with MassLynx4.1 SCN781 software for acquisition, Trap column: Symmetry® 180 µm 20 mm C18 5 µm, water, Analytical column: 75 µm 200 mm HSS T3 C18 1.8 µm, (waters), Solvent flow rate: 300 nL/min, Column temperature being 35 °C, reverse phase chromatography mode: Autosampler temperature was 4 °C.

Mass spectrometry condition

MS runs were performed using ion mobility-enabled separation. MS system: Synapt G2 High Definition MS™ System (HDMS^E System) Waters, with Sodium iodide calibration.

Analysis of identified proteins by Bioinformatics

Making use of the STRING database (https://string-db.org), the differentially expressed proteins were subjected to network analysis. Ingenuity Pathway Analysis (IPA) (https:// ingenuity.com/products/ipa) was made use of for analysing molecular pathways and canonical pathways. The proteomics data were deposited at the ProteomeXchange Consortium.[17]

RESULTS

Residual protease activity and PI activity of selected plant and microbial extracts against trypsin

T. cordifolia leaves (Sample 1), *T. cordifolia* stem (Sample 2), *C. thevetia* leaves (Sample 3), *C. thevetia* stem (Sample 4), *A. vinetianus* (Sample 5), and *Streptomyces* sp. (Sample 6). The positive control was the uninhibited trypsin, *i.e.*, trypsin untreated with any plant extract. According to the results of this investigation, *T. cordifolia* stem extract at 1:5 dilution had the highest inhibition of trypsin activity (62.87%), followed by the same extract at a 1:10 dilution (Figure 1a). At any of the tested concentrations, the leaves of *T. cordifolia*, and the leaves and stem of *C. thevetia* did not exhibit any inhibitory effects on the protease enzyme trypsin, which resulted in enhanced enzyme activities (with negative values for protease inhibition

-44.0%, -52.0% and -106.0% respectively). In addition, at all the investigated concentrations, microbial isolates of *A. venetianus* and *Streptomyces* sp. did not show any inhibitory effects on trypsin with negative values, as shown in Figure 1a.

T. cordifolia stem buffer (PBS) extract was serially diluted before the protease inhibition assay was conducted (the OD was measured at 280 nm), and as per the formula, PI activity was calculated and presented graphically (Figure 1b). The *T. cordifolia* stem extract has good PI activity with 71.0% inhibition at 1:2 dilution (highest PI activity), followed by the 1:1 diluted sample with 60.0%.

Effect of temperature on the PI activity of T. cordifolia

Phosphate buffer (PBS) and DW (TD) extracts of the stem of *T. cordifolia* were checked at varying temperatures of 25 °C, 37 °C, 50 °C, and 75 °C for their effect on PI activity (Figure 1c). According to the findings, at 50 °C, the DW (TD) extract at a dilution of 1:10 showed the highest protease inhibition with 71.0%, followed by the PBS extract at 75 °C, at a dilution of 1:10 with 70.0% inhibition.

Effect of pH on PI activity of T. cordifolia stem extract

T. cordifolia stem buffer extract was analyzed for protease activity (trypsin) and PI activity in relation to pH. The stem of *T. cordifolia* was extracted in buffers of different pH. The pH 11 extract (1:10 dilution) exhibited the maximum protease inhibition with 67.0%, followed by pH 9 (1:10 dilution) with 63.0%, and again the pH 9 extract at 1:5 dilution with 53.0% (Figure 1d).

Metal ions effect on the PI activity of T. cordifolia

T. cordifolia stem extract was incubated with 10 different metal ions at 5- and 10-mM concentrations to analyze their effect on PI activity. As per the results, all metal ions significantly inhibited the PI activity of *T. cordifolia* stem extract (Figure 2a).

Partial purification of PI by salting out

For partial purification ammonium sulfate precipitation method was used. The *T. cordifolia* stem extract was added with ammonium sulfate to 40.0% and 80.0% saturation, and the precipitated inhibitor was used to perform the PI activity assay. Figure 2b displays the study findings, with the 80.0% sample at 1:30 dilution having the highest PI activity with 83.0% inhibition, followed by the 80.0% sample at 1:5 dilution with 79.0% inhibition. PI activity was maximum in the 80.0% ammonium sulfate precipitate and was also noticeable in the 40.0% precipitate.

PI's ability to inhibit Chymotrypsin and Collagenase enzymes

Because of the high PI activity of the partially purified inhibitor

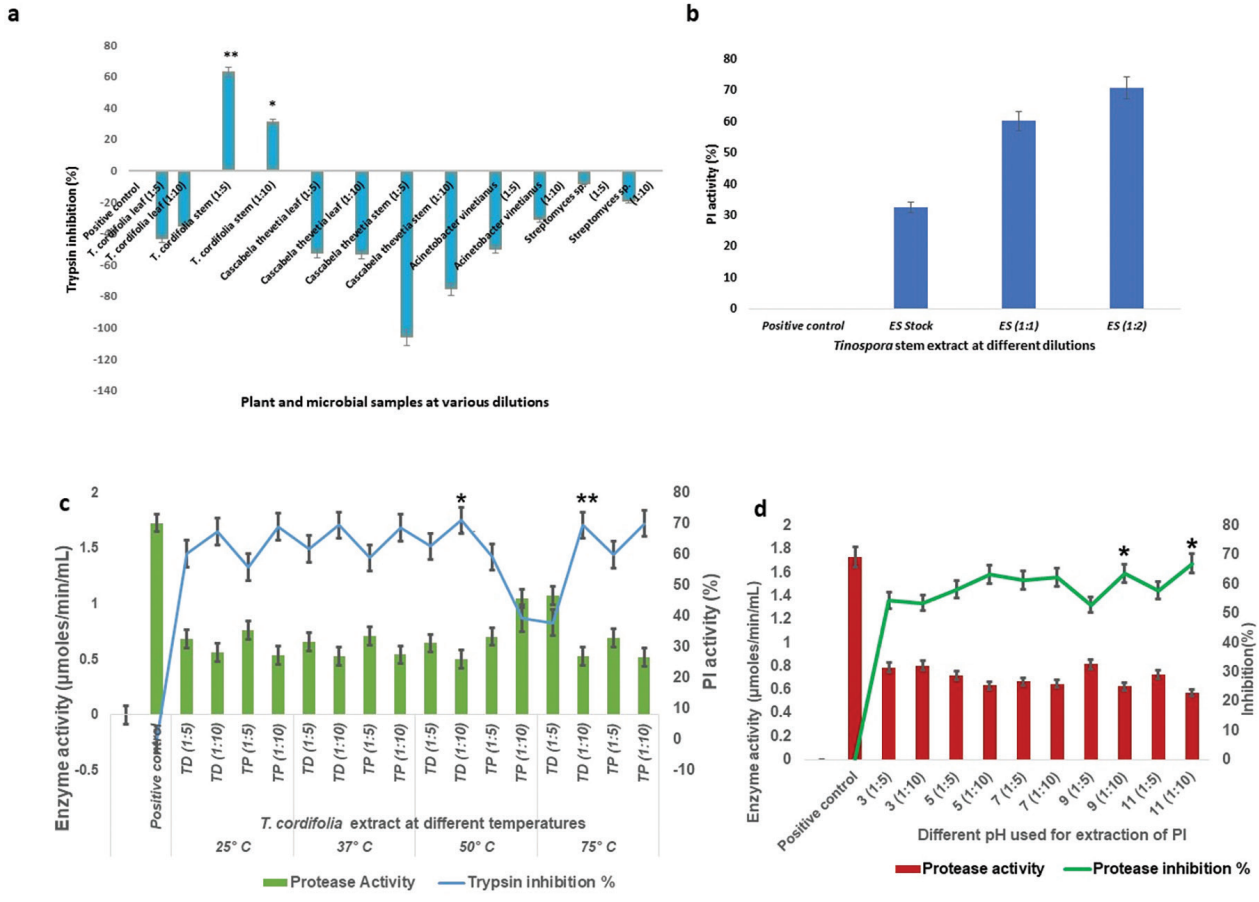

Figure 1. a) Screening the PI activity of plant and microbial samples, b) PI activity of *Tinospora cordifolia* stem extract, c) effect of temperature on PI activity of distilled water (TD) and Phosphate buffer extracts (TP) of *Tinospora cordifolia*, d) effect of pH on the PI of *T. cordifolia* stem extract

PI: Protease inhibitors

from *T. cordifolia* stem, it was tested on other proteases like chymotrypsin and collagenase. As per the results, chymotrypsin inhibitory activity was highest for the 40.0% ammonium sulfate precipitate of the PI with 96.0% inhibition, followed by the 80.0% sample with 78.0% inhibition, and slightly lower activity was observed with the crude PI with 45.0% inhibition (Figure 2c). The collagenase inhibitory potential was exhibited only by the 80.0% sample (53.0% inhibition), and both the crude extract and the 40.0% sample were not able to inhibit the activity of collagenase (Figure 2d).

Cytotoxicity studies on the HepG2 liver cancer cell line

As *T. cordifolia* stem extract and the ammonium sulfate precipitated samples showed good PI activity, these samples were treated with the liver cancer HepG2 cell line to assess their potential anticancer activity. According to the findings, after 48 hours of incubation, the ethanol extract exhibited 17.0% cytotoxicity, whereas the buffer extract displayed 13.0% cytotoxicity to HepG2 cells (Figure 3a).

Cytotoxicity of partially purified samples of PI from T. cordifolia stem extract

When the partially purified PI (40% and 80%) of *T. cordifolia* was analyzed for cytotoxicity to HepG2 (liver cancer) cells for varied lengths of time (24, 48, and 72 hours), the partially purified PI (40% sample) demonstrated considerable cytotoxicity at all the time periods with 81.0%, 80.0% and 65.0% viabilities respectively at 1:10 dilution. The maximum cytotoxicity was 35.0% (Figure 3b). The highest cytotoxicity was displayed by the PI (80.0% sample) at 72 hours of incubation and 1:20 dilution. The treated liver cancer cells had a viability of 53.0% with cytotoxicity of 47.0% (Figure 3c), and other dilutions also demonstrated considerable cytotoxicity after a 72-hours incubation period. The viability was 93.0% at 24 hours, 79.0% at 48 hours, and 69.0% at 72 hours of incubation with 1:5 diluted PI.

LDH activity assay

As per the LDH assay results, among the cancer cells treated with the PI (80.0% precipitate) from *T. cordifolia*, we observed 16.0% cytotoxicity on HepG2 cells and 13.0% cytotoxicity on MCF-7 (breast cancer) cells (Figure 3d).

Proteomic studies of HepG2 cells treated with PI from the T. cordifolia stem

When HepG2 cells treated with PI were subjected to LC-MS/MS-based proteomic analysis, the data showed altered expression of several proteins. Significant overexpression of 19 proteins, downregulation of 8 proteins, and the remaining unaltered proteins were observed (Figure 4a). These proteomics data were deposited to the ProteomeXchange Consortium with the dataset identifier PXD037511.[17] A fold change cutoff of 1.5-fold and $p < 0.05$ was considered to filter proteins for further analysis. As per the data, we found that proliferation-associated protein 2G4 (PA2G4) expression was 3.48-fold upregulated in treated HepG2 cells compared with

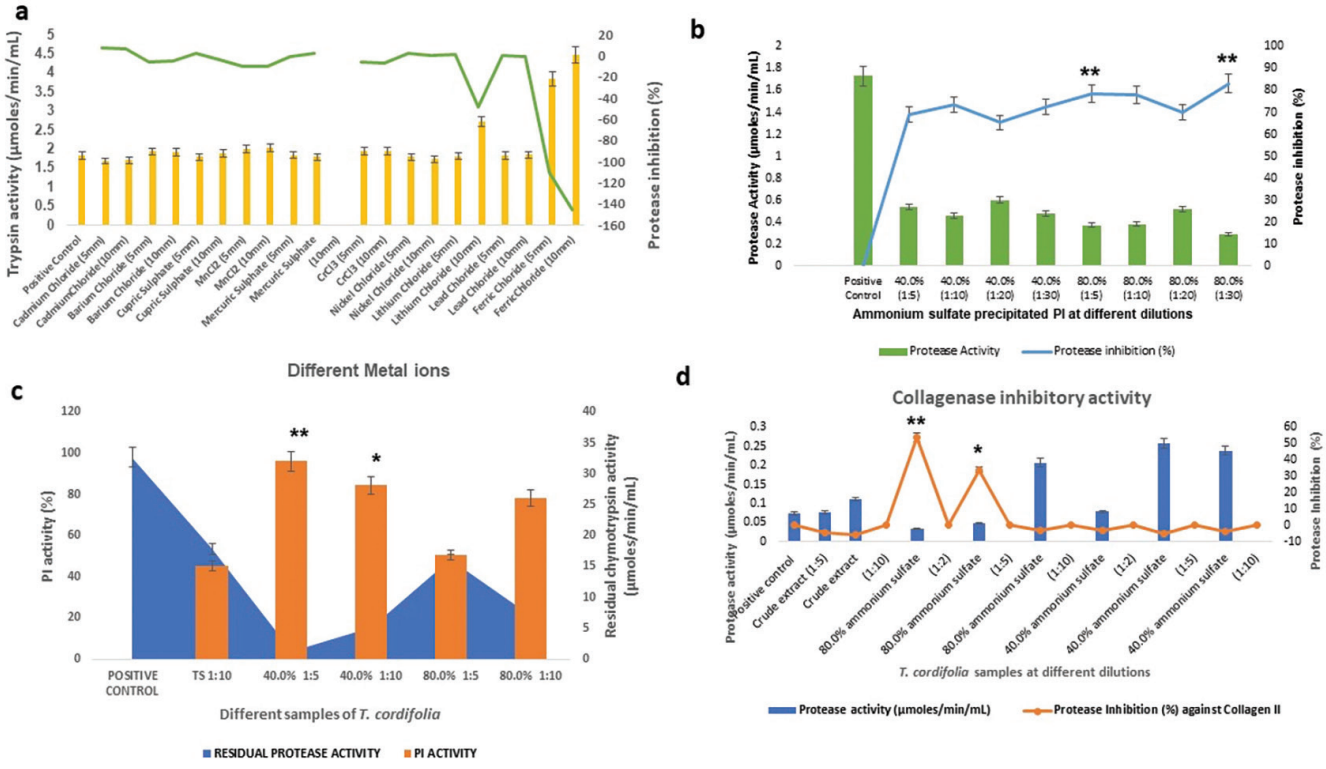

Figure 2. a) Effect of metal ions on PI activity of *Tinospora cordifolia,* b) PI activity of ammonium sulfate precipitate of *T. cordifolia* stem extract, c) chymotrypsin inhibitory activity of PI from *T. cordifolia*, and d) collagenase inhibitory activity of crude and partially purified PI from *T. cordifolia* stem

PI: Protease inhibitors

the controls. PA2G4 isoforms have opposing functions in cancer, which is well documented.[18] In our data, PEBP1 protein expression was 1.5-fold upregulated in treated HepG2 cells compared with the controls. EBP1 belongs to the PA2G4 family of DNA-binding proteins. The growth-inhibiting properties of EBP1 are multifaceted because it binds to RNA,[19] DNA[20] and proteins.[21] Overexpression of the ubiquitin-conjugating enzyme E2 L3 (UBE2L3) has been reported in non-small-cell lung cancer (NSCLC) tissues. A correlation was found between high expression of UBE2L3 and advanced tumor stage and negative outcomes, whereas UBE2L3 knockdown was reported to inhibit NSCLC cell growth.[22] In our current study results, UBE2L3 was downregulated 5.4-fold in treated HepG2 cells compared with control untreated cells. Mitogen-activated protein kinase kinase kinase 21 (MAP3K21) was observed to be 2.5-fold upregulated in treated HepG2 cells compared with controls, as per our result.

To understand the protein-protein interactions among the dysregulated proteins, a STRING database network analysis was performed.[23] As shown in the results of network analysis, mitochondrial and nuclear transport proteins, chaperon proteins, ribosomal proteins, proteasome proteins, translation initiation factors, spliceosomal proteins, glucose metabolism proteins, and mitochondrial inner membrane proteins were majorly affected by PI from *T. cordifolia* on HepG2 cells (Fig 4b).

T. cordifolia PI treatment affects BAG2 and FAT10 signaling pathways in HepG2

According to canonical pathway analysis, EIF2 signaling, BAG2 signaling, and FAT10 signaling pathways were found to be significantly altered in the PI-treated HepG2 cells (Figure 4c). Among these, we considered BAG2 and FAT10 signaling pathways because of the higher percentage of overlap (21.4 and 26.8% respectively) than EIF2 signaling, which has 17.2% overlap.

In our data, SQSTM1 and cathepsin B (CTSB) proteins were upregulated, and the upregulation of cathepsins increased the formation of autophagosomes.[24,25] Further in our Ingenuity Pathway analysis, 26s Proteasome proteins were found to be downregulated (Figure 5). In nuclei, the 26s proteasome complex increases the inhibition of ubiquitinated p53 protein. As per our results, the CTSB protein was upregulated (Figure 5).

Hsp70 is an important protein and has been studied for possible effects on energy metabolism. In our data, Hsp70 is downregulated, and downregulation of Hsp70 leads to

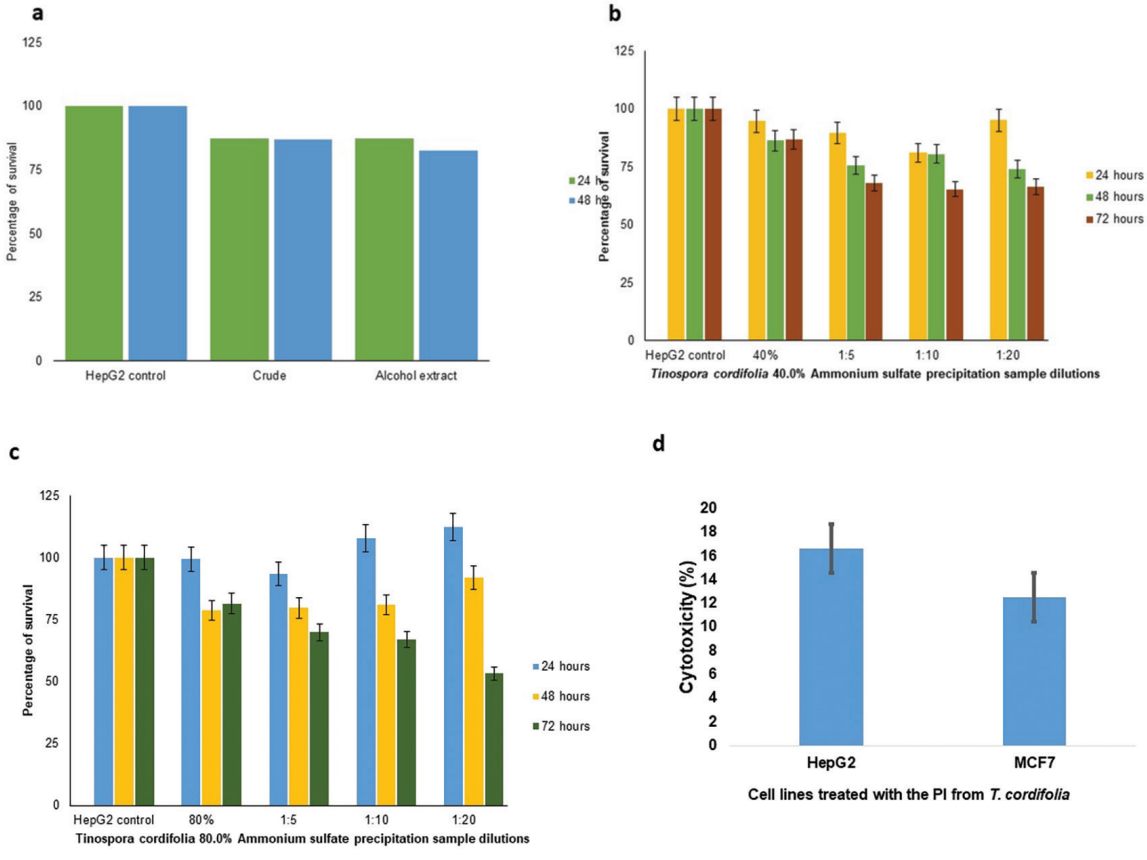

Figure 3. a) Effect of *Tinospora cordifolia* stem buffer extract and ethanol extract on HepG2 cells at 24 and 48 hours, b) effect of *T. cordifolia* 40.0% ammonium sulfate precipitated PI sample on Hep G2 cells, c) effect of *T. cordifolia* 80.0% ammonium sulfate precipitated PI sample on HepG2 cells, d) cytotoxicity of 80.0% ammonium sulfate precipitated PI of *T. cordifolia* by LDH assay

PI: Protease inhibitors, LDH: Lactate dehydrogenase

mitochondrial dysfunction. It can be inferred from our results that the downregulation of Hsp70, induced by PI in HepG2 cells, leads to mitochondrial dysfunction and cell death.

DISCUSSION

Proteolysis is considered the most important metabolic process involved in protein turnover and processing. Proteases are involved in the degradation of stored or unwanted proteins, which are essential for developmental processes such as differentiation and programmed cell death. Dysregulated proteolysis leads to many diseases, including cancer.[26] Hence, PIs have great therapeutic potential in controlling protease-mediated diseases. Plants and microbes are major sources of PIs. Therefore, in our current research, many plants, plant parts, and microbial isolates were screened for their PI activity. The plants *T. cordifolia* stem and leaves, *C. thevetia* stem and leaves, and meth (*T. foenum-graecum*) seeds (sprouted), along with the microbes *A. venetianus* and *Streptomyces* sp., were chosen for our PI activity study. All these samples were tested for PI activity. The *T. cordifolia* stem extract showed the highest PI activity against trypsin. As per our study results, *T. cordifolia* stem extract exhibited maximum inhibition of trypsin activity. *T. cordifolia* stem extract showed good PI activity, with the highest inhibition value observed being 71.0%, while the meth seed extract also had good inhibitory effects with the highest of 61.0% inhibition. To analyze the effects of physicochemical parameters on PI activity, buffers with different pH values, different temperatures, and different metal ions were considered. We found that a basic pH of 11 had positive effects on the PI activity of *T. cordifolia*, with 67.0% inhibition of trypsin activity. In comparison to this observation, it was reported that plant-based PIs have a broad pH range (from 2 to 10), with the highest activity at pH 7.5, and that the plant PIs are unstable at highly acidic pH.[26] For the PI from *T. cordifolia*, in temperature studies, we observed the highest percentage

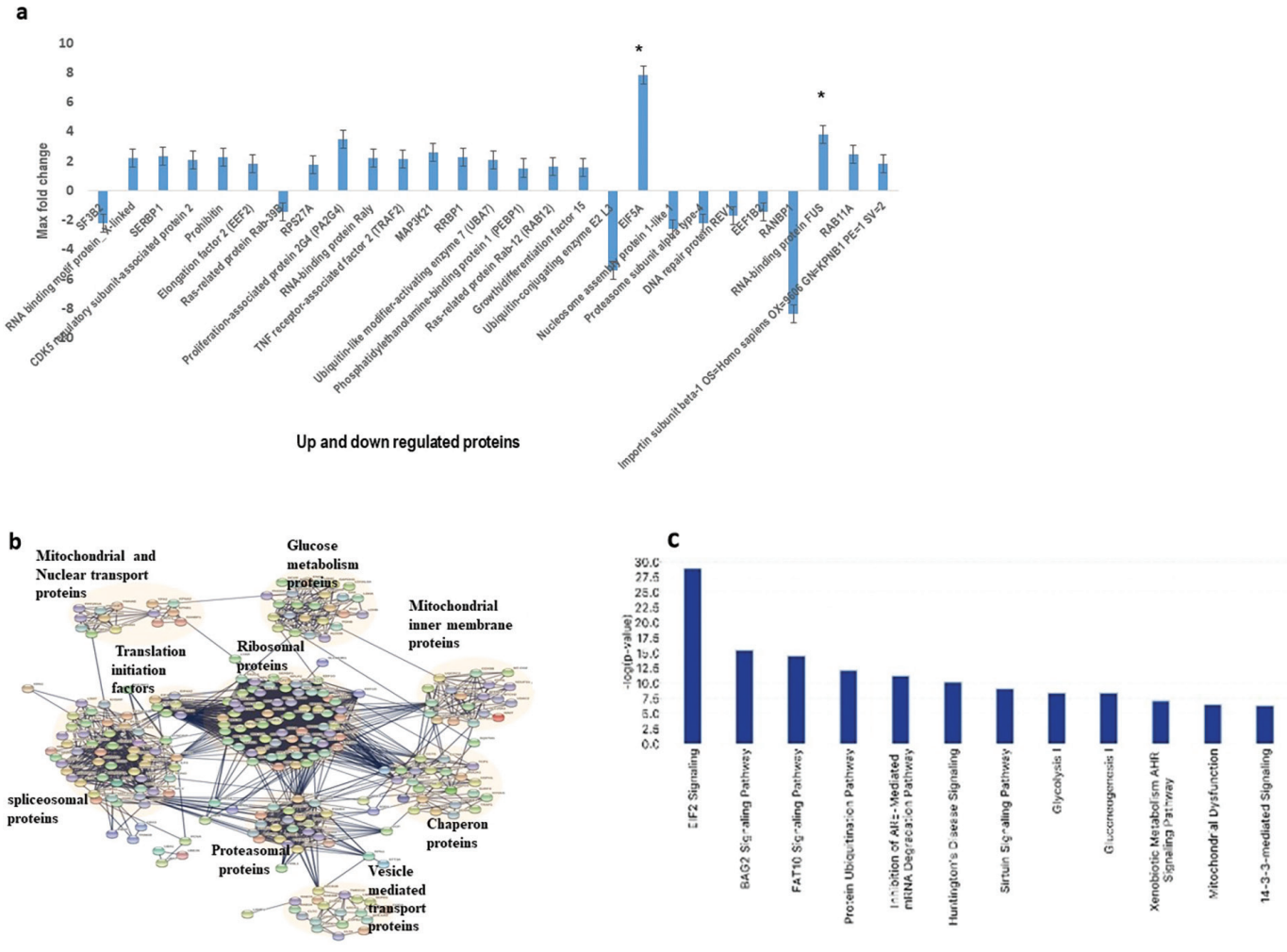

Figure 4. a) Protein expressions (having significance to cancer cell proliferation and survival) altered due to treatment with *T. cordifolia* PI sample in HepG2 cells, in comparison to the controls, b) Bioinformatic analysis of interaction of proteins using STRING database (https://string-db.org) in HepG2 cells treated with *Tinospora cordifolia* extract showing distinct molecular alterations, c) altered canonical pathways as per Ingenuity Pathway Analysis (https://ingen uity. com/ products/ipa) in *T. cordifolia* PI-treated HepG2 cells

PI: Protease inhibitors

of PI at 50 °C (71.0%), followed by 75 °C for the PBS extracted PI (70.0%). Most plant PIs are active at temperatures as high as 50 °C. As far as the metal ions are concerned, *T. cordifolia* PI was inhibited by all tested metals at 5- and 10-mM concentrations. In a previous study, it was reported that 1 mM Mg^{2+} addition increased the PI activity, whereas all other divalent metal ions decreased the activity.[26]

Because the PI from *T. cordifolia* had the highest activity, it was chosen for further purification studies by salting out using ammonium sulfate. Among the partially purified PI (by 40.0% and 80.0% ammonium sulfate precipitation), the highest protease inhibition was observed in the 80.0% precipitated sample. Even the 40.0% precipitated PI sample had considerable PI activity. Our results have shown that PI from *T. cordifolia* has potent cytotoxic and anticancer potential against the liver cancer (HepG2) cell line. In a previous study conducted on different cancer cell lines, it was reported that *T. cordifolia* showed 52-59% of protease inhibition.[27] Compared with this report, in our current study, the 40.0% ammonium sulfate precipitated PI from *T. cordifolia* exhibited highest trypsin inhibition (78.0%) with the best cytotoxic activity (35.0%), whereas the PI sample precipitated by 80.0% ammonium sulfate exhibited 83.0% trypsin inhibition along with the highest cytotoxic activity against HepG2 liver cancer cells (47.0%). In addition, 96.0% inhibition of chymotrypsin and 54.0% inhibition of collagenase was also demonstrated by the partially purified PI of *T. cordifolia* in our study, which substantiates its anticancer potential. As per previous reports, berberine, palmatine, tembetarine, and magnoflorine have been isolated from *T. cordifolia* stem.[4] Though anticancer properties of *T. cordifolia* were reported by earlier workers, PI activity and cytotoxicity of PI from *T. cordifolia* are being reported for the first time through the current study.[28-30]

When HepG2 cells treated with partially purified PI were subjected to proteomic studies, we found major signaling proteins involved in cancer to be dysregulated, such as EIF2 signaling, BAG2 signaling, and FAT10 signaling pathways. In our data, SQSTM1 and CTSB were upregulated, and an increase in these proteins enhances the formation of autophagosome. Autophagy has both roles as a tumor suppressor and a tumor growth promoter.[24,25] In tumor suppressor mechanisms, autophagy prevents the accumulation of damaged proteins and organelles, which can promote tumor survival.[31]

In the FAT10 signaling pathway, the inhibition of fat10ylated active SQSTM1 protein occurs due to the 26s proteasome in the cytoplasm, and in our data, 26s proteasome proteins are downregulated. In contrast, in the nuclei, the 26s proteasome complex increases the inhibition of ubiquitinated p53 protein.[32] In HepG2 cells treated with PI, we could predict that the p53 protein was upregulated due to the downregulation of the 26s

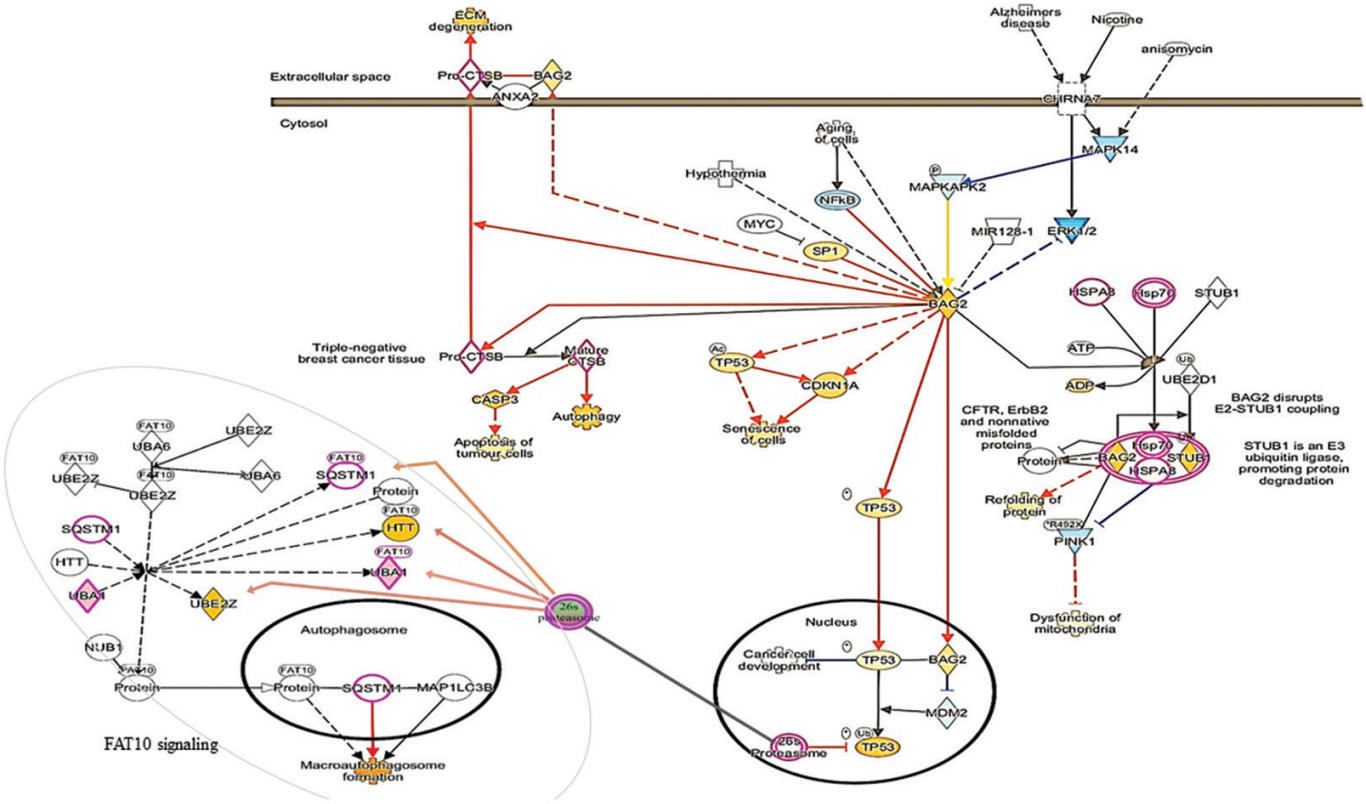

Figure 5. *Tinospora cordifolia* partially purified PI treatment on HepG2 cells affects BAG2 and FAT10 signaling pathways. Ingenuity Pathway analysis of proteins significantly dysregulated ($p \leq 0.05$) in treated HepG2/control HepG2 cells. The signaling network of BAG2, EIF2, FAT10 pathways based on differential expression of molecules in the HepG2 cells

proteasome.[33] This upregulation of p53 in the HepG2 cells might be a reason for the observed cytotoxicity due to the PI in the current study.

Caspases are enzymes primarily involved in mediating apoptosis, and caspase-3, the usually activated death protease, is needed for the specific breakdown of several cellular proteins. In our data, CTSB protein was found to be upregulated, and according to reports, mature CTSB protein increases activation of caspase 3 protein.[34]

Hsp70 is an important protein studied for its possible effects on energy metabolism. In our data, Hsp70 is downregulated, which leads to mitochondrial dysfunction through inhibition of oxidative phosphorylation and ROS generation.[35] Because mitochondria are primarily involved in cell apoptosis, we can assume that Hsp70-mediated mitochondrial dysfunction leads to the apoptosis of HepG2 cells treated with PI in our current study. There are studies and reports about the anti-HIV and anti-severe acute respiratory syndrome Coronavirus-19 (SARS-CoV-19) activity of the *T. cordifolia* PI.[9,36] However, the current study is the first report of anticancer activity of the PI from *T. cordifolia* to the best of our knowledge. It can be concluded from the outcomes of the proteomic studies, STRING analysis, Ingenuity pathway analysis, and canonical pathway analysis that the PI from *T. cordifolia* exerts its anticancer activity by majorly altering the signaling pathways of BAG2, EIF2, and FAT10 molecules.

CONCLUSION

It can be concluded that PI from *T. cordifolia* has potent PI and anticancer effects on the liver cancer cell line HepG2. *T. cordifolia* possesses several phytochemicals with significant anticarcinogenic activities, as per many earlier *in vivo* and *in vitro* studies. Although the PI activity of *T. cordifolia* was checked by earlier researchers on HIV and SARS-CoV proteases, the anticancer potential of this *T. cordifolia* PI is being analyzed and reported for the first time in the current study. The current study opens further scope for the complete characterization of this PI and the validation of its anticancer activity through *in vivo* and future clinical studies.

Ethics

Ethics Committee Approval: Not required.

Informed Consent: Not required.

Authorship Contributions

Concept: V.K.N., Design: V.K.N., B.S.C., K.G., M.K., N.M., N.H.K., S.L.P., Data Collection or Processing: B.S.C., K.G., M.K., N.M., N.H.K., S.L.P., S.D., Analysis or Interpretation: V.K.N., Literature Search: B.S.C., K.G., M.K., N.M., N.H.K., S.L.P., Writing: B.S.C., K.G., M.K., N.M., N.H.K., S.L.P.

Conflict of Interest: No conflict of interest was declared by the authors.

Financial Disclosure: The authors declared that this study received no financial support.

REFERENCES

1. López-Otín C, Bond JS. Proteases: multifunctional enzymes in life and disease. J Biol Chem. 2008;283:30433-30437.
2. López-Otín C, Hunter T. The regulatory crosstalk between kinases and proteases in cancer. Nat Rev Cancer. 2010;10:278-292.
3. Bond JS. Proteases: History, discovery, and roles in health and disease. J Biol Chem. 2019;294:1643-1651.
4. Tiwari P, Nayak PS, Prusty SK, Sahu PK. Phytochemistry and pharmacology of Tinospora cordifolia: a review. Syst Rev Pharm. 2018;9:70-78.
5. Gupta AK. Quality standards of Indian medicinal plants. (1st ed.). New Delhi; 2003:212-218.
6. Singh B, Sharma P, Kumar A, Chadha P, Kaur R, Kaur A. Antioxidant and *in vivo* genoprotective effects of phenolic compounds identified from an endophytic Cladosporium velox and their relationship with its host plant Tinospora cordifolia. J Ethnopharmacol. 2016;194:450-456.
7. Singh S, Srivastava R, Choudhary S. Antifungal and HPLC analysis of the crude extracts of Acorus calamus, Tinospora cordifolia and Celestrus paniculatus. J Agric Technol. 2010;6:149-158.
8. Vizovisek M, Ristanovic D, Menghini S, Christiansen MG, Schuerle S. The Tumor Proteolytic Landscape: A Challenging Frontier in Cancer Diagnosis and Therapy. Int J Mol Sci. 2021;22:2514.
9. Kalikar MV, Thawani VR, Varadpande UK, Sontakke SD, Singh RP, Khiyani RK. Immunomodulatory effect of *Tinospora cordifolia* extract in human immuno-deficiency virus positive patients. Indian J Pharmacol. 2008;40:107-110.
10. Kunitz M. Crystalline soybean trypsin inhibitor: II. General properties. J Gen Physiol 1947;30:291-310.
11. Venkatachalam P, Nadumane VK. Purification and characterization of a protease inhibitor with anticancer potential from *Bacillus endophyticus* JUPR15. Curr Cancer Ther Rev. 2019;15:74-82.
12. Nadig N, Dhanapala M, Venkatachalam P, Nadumane VK. Screening different plants and fungal isolates for protease inhibitory activity and evaluation of the cytotoxicity of the most promising sample. Adv Biores. 2021;12:237-247.
13. Thomas DH, Rob A, Rice DW. A novel dialysis procedure for the crystallization of proteins. Prot Eng Design Sel. 1989;2:489-491.
14. Mosmann T. Rapid colorimetric assay for cellular growth and survival: application to proliferation and cytotoxicity assays. J Immunol Methods. 1983;65:55-63.
15. Weyermann J, Lochmann D, Zimmer A. A practical note on the use of cytotoxicity assays. Int J Pharm. 2005;288:369-376.
16. In-solution sample digestion protocol. Available at https://www.rgcb.res.in/mass-protocolinsoldige.php (Accessed on 08 July 2022).
17. Monie TP, Perrin AJ, Birtley JR, Sweeney TR, Karakasiliotis I, Chaudhry Y, Roberts LO, Matthews S, Goodfellow IG, Curry S. Structural insights into the transcriptional and translational roles of Ebp1. EMBO J. 2007;26:3936-3944.
18. Stevenson BW, Gorman MA, Koach J, Cheung BB, Marshall GM, Parker MW, Holien JK. A structural view of PA2G4 isoforms with opposing functions in cancer. J Biol Chem. 2020;295:16100-16112.
19. Monie TP, Perrin AJ, Birtley JR, Sweeney TR, Karakasiliotis I, Chaudhry Y, Roberts LO, Matthews S, Goodfellow IG, Curry S. Structural insights into the transcriptional and translational roles of Ebp1. EMBO J. 2007;26:3936-3944.

20. Zhang Y, Hamburger AW. Heregulin regulates the ability of the ErbB3-binding protein Ebp1 to bind E2F promoter elements and repress E2F-mediated transcription. J Biol Chem. 2007;279:26126-26133.

21. Ahn JY, Liu X, Liu Z, Pereira L, Cheng D, Peng J, Wade PA, Hamburger AW, Ye K. Nuclear Akt associates with PKC-phosphorylated Ebp1, preventing DNA fragmentation by inhibition of caspase-activated DNase. EMBO J. 2006;25:2083-2095.

22. Ma X, Zhao J, Yang F, Liu H, Qi W. Ubiquitin conjugating enzyme E2 L3 promoted tumor growth of NSCLC through accelerating p27kip1 ubiquitination and degradation. Oncotarget. 2017;8:84193-84203.

23. STRING database available at https://string-db.org (Accessed on 08 July 2022).

24. Kageyama S, Gudmundsson SR, Sou YS, Ichimura Y, Tamura N, Kazuno S, Ueno T, Miura Y, Noshiro D, Abe M, Mizushima T, Miura N, Okuda S, Motohashi H, Lee JA, Sakimura K, Ohe T, Noda NN, Waguri S, Eskelinen EL, Komatsu M. p62/SQSTM1-droplet serves as a platform for autophagosome formation and anti-oxidative stress response. Nat Commun. 2021;12:16.

25. Bhoopathi P, Chetty C, Gujrati M, Dinh DH, Rao JS, Lakka S. Cathepsin B facilitates autophagy-mediated apoptosis in SPARC overexpressed primitive neuroectodermal tumor cells. Cell Death Differ. 2010;17:1529-1539.

26. Mohan M, Kozhithodi S, Nayarisseri A, Elyas KK. Screening, Purification and characterization of protease inhibitor from *Capsicum frutescens*. Bioinformation. 2018;14:285-293.

27. Mishra A, Kumar S, Pandey AK. Scientific validation of the medicinal efficacy of *Tinospora cordifolia*. ScientificWorldJournal. 2013;2013:292934.

28. Ahamad R, Shrivastava AN, Khan MA. Evaluation of *in vitro* anticancer activity of stem of *Tinospora cordiflia* against human breast cancer and Vero cell lines. J Med Plants Stud. 2015;3:33-37.

29. Maliyakkal N, Udupa N, Pai KSR, Rangarajan A. Cytotoxic and apoptotic activities of extracts of *Withania somnifera* and *Tinospora cordfolia* in human breast cancer cells. Int J Appl Res Nat Prod. 2013;6:1-10.

30. Priya MS, Venkateswaran KV, Vijayanand T. Determination of apoptosis by flow cytometric analysis inMCF-7 cells treated with *Tinospora cordifolia*. Ind Vet J. 2017;94:73-75.

31. Yang ZJ, Chee CE, Huang S, Sinicrope FA. The role of autophagy in cancer: therapeutic implications. Mol Cancer Ther. 2011;10:1533-1541.

32. Aichem A, Kalveram B, Spinnenhirn V, Kluge K, Catone N, Johansen T, Groettrup M. The proteomic analysis of endogenous FAT10 substrates identifies p62/SQSTM1 as a substrate of FAT10ylation. J Cell Sci. 2012;125:4576-4585.

33. do Patrocinio AB, Rodrigues V, Guidi Magalhães L. P53: Stability from the Ubiquitin-proteasome system and specific 26S proteasome inhibitors. ACS Omega. 2022;7:3836-3843.

34. Yang KM, Bae E, Ahn SG, Pang K, Park Y, Park J, Lee J, Ooshima A, Park B, Kim J, Jung Y, Takahashi S, Jeong J, Park SH, Kim SJ. Co-chaperone BAG2 determines the pro-oncogenic role of cathepsin B in triple-negative breast cancer cells. Cell Rep. 2017;21:2952-2964.

35. Wang L, Schumann U, Liu Y, Prokopchuk O, Steinacker JM. Heat shock protein 70 (Hsp70) inhibits oxidative phosphorylation and compensates ATP balance through enhanced glycolytic activity. J Appl Physiol (1985). 2012;113:1669-1676.

36. Sagar V, Kumar AHS. Efficacy of natural compounds from *Tinospora cordifolia* against SARS-CoV-2 protease, surface glycoprotein and RNA polymerase. BEMS Reports. 2020;6:6-8.

Turk J Pharm Sci 2024;21(3):184-191
DOI: 10.4274/tjps.galenos.2023.23855

ORIGINAL ARTICLE

Effect of Nutrition on Drug-Induced Liver Injury: Insights from a High-Fat Diet Mouse Model

Murali BADANTHADKA[1]*, Vinitha D'SOUZA[1], Meghashree SHETTY[1], Varsha AUGUSTIN[1], Madhura RATHNAKAR JALAJAKSHI[1], Mamatha BANGERA SHESHAPPA[2], Vijayanarayana KUNHİKATTA[3]

[1]Nittte (Deemed to be University), Nitte University Center for Science Education and Research (NUCSER), Paneer Campus, Deralakatte, Mangaluru, Karnataka State, India
[2]Nittte (Deemed to be University), Nitte University Center for Science Education and Research (NUCSER), Paneer Campus, Deralakatte, Mangaluru, Karnataka State, India
[3]Department of Pharmacy Practice, Manipal College of Pharmaceutical Sciences, Manipal Academy of Higher Education, Madhav Nagar, Manipal, Karnataka State, India

ABSTRACT

Objectives: Literature suggests that a high-fat diet (HFD) potentially increases the risk of chemical/drug-induced toxicity after an acute overdose. Drug/chemical-induced hepatotoxicity has been well studied, and the mechanism that regulates this toxicity has been extensively examined using different experimental animal models. Our study focuses on drug-induced hepatotoxicity in HFD-fed female Balb/C mice. This study addresses the effect of nutrition on the magnitude of acetaminophen (APAP)-induced hepatotoxicity at different time intervals.

Materials and Methods: Female Balb/C mice, after the weaning period separated into two different groups, normal diet (ND) and HFD receiving groups; after 15 weeks, they were dosed with a single dose (300 mg/kg *per os* (*p.o.*) of APAP. Blood samples were collected at different time intervals (0, 6 and 24 hours), and liver samples were collected at the end time point. Liver injury parameters [alanine aminotransferase (ALT) and aspartate aminotransferase (AST)], antioxidant assay (sodium dismutase, glutathione, and catalase), and histopathology study were conducted. Pharmacokinetic (PK) analysis was done using the RP-HPLC system and Phoenix WinNonlin 8.3 software.

Results: APAP-induced liver injury decreased AST and ALT in the HFD group compared with the ND group at 6 and 24 hours ($p < 0.01$ and $p < 0.001$), respectively. Antioxidant enzyme levels remained constant in the HFD group, whereas histopathology showed remarkable changes. The PK's of APAP in HFD indicate lower plasma concentrations of APAP ($p < 0.05$), with two-fold higher clearance and volume of distribution.

Conclusion: HFD significantly reduced susceptibility to APAP-mediated liver injury in Balb/C mice compared with ND mice. Our study mimics the clinical scenario where the same dose of the drug is prescribed to the normal and obese population. Our results suggest the potential need for dose titration to assess an individual's nutritional state in a clinical scenario.

Keywords: Acetaminophen, high-fat diet, liver injury, nutrition, pharmacokinetics, stage-II toxicity

INTRODUCTION

Nutrition plays an important role in drug kinetics and influences the efficacy or toxicity of a molecule.[1,2] Both fasting and malnutrition are risk factors for acetaminophen (APAP)-induced hepatotoxicity in healthy individuals.[3] In contrast, a high-fat diet (HFD) may increase the risk of chemical/drug-induced toxicity following an acute overdose. Short-term HFD causes changes in the liver and may alter the activity of hepatic drug-metabolizing enzymes. Such a change in enzyme expression or activity may increase APAP-induced hepatotoxicity.[4]

The liver plays a pivotal role in numerous processes such as food and drug biotransformation, protein synthesis, detoxification, and the generation of enzymes essential for digestion.[5] During these processes, both toxic chemicals and drug overdose may cause drug-induced liver injury (DILI), and hepatocytes become the primary target.[6] The classical hepatotoxic chemicals include alcohol, carbon tetrachloride, anticancer drugs, anti-inflammatory drugs, and analgesics.[7,8] During the process of DILI, hepatocytes play various roles in inflammatory and fibrotic processes.[8] The inflammatory response initiated by a

*Correspondence: murali@nitte.edu.in, Phone: +91 0824 2203991, ORCID-ID: orcid.org/0000-0002-4313-5111
Received: 26.05.2023, Accepted: 04.07.2023

damaged hepatocyte accelerates the injury process, leading to tissue damage. Early toxic injury (toxicity) also depends upon innate immune activation, and APAP-induced hepatotoxicity is one of the best examples of this type of injury.[9]

APAP is also referred to as paracetamol and is used over the counter as an efficient pain reliever. Although APAP is typically considered a safe medicine, an overdose can cause immediate liver damage or failure.[10] Depending on the body mechanism, the maximum advised dose might cause mild or moderate hepatotoxicity, resembling non-alcoholic fatty liver disorders (NAFLD), even in a healthy individual.[10,11] At therapeutic doses, 90% of APAP is metabolized without toxicity through glucuronidation and sulfation and is eliminated through the kidney. The remaining 10%, however, is metabolized in phase I, where CYP2E1 and CYP450 enzymes convert small amounts of APAP into toxic N-acetyl-p-benzoquinone imine (NAPQI), which disrupts the immune system and causes oxidative stress, lipid peroxidation, and eventually liver injury.[8,12]

Both the risk and severity of APAP-induced hepatotoxicity are increased by other factors such as alcohol, fasting, undernutrition, and diet.[4] Diet is the most significant environmental factor linked to the prevalence of drug or chemical toxicity.[13,14] Current lifestyle modifications have encouraged a large increase in the use of high-energy diets such as HFD.[14] HFD's have substantially higher fat than what is typically consumed. HFD increases the risk of developing numerous metabolic and cardiovascular complications and drug-mediated toxicity.[14] Recently, studies combining APAP and HFD have been conducted clinically but require more in-depth mechanistic research queries using experimental animals.[4,15,16] HFD increases the expression of CYP 2E1 in C57BL/C mice, explaining APAP-mediated NAFLD susceptibility.[17] Most overweight and obese individuals suffer from fatty liver disease; however, symptom-free fatty liver patients may unknowingly take a higher dose of APAP. Recent research suggests that oxidative stress is critical for the onset of NAFLD, causing energy depletion, liver cell destruction, and accumulation of fatty acids in hepatocytes. Oxidative stress is also a major factor in the etiology of APAP-induced toxicity.[18]

The present study is a time-course experiment demonstrating the role of nutrition (HFD and 18% protein diet) on a single dose of APAP-mediated liver injury. Furthermore, biomarkers of liver injury and histopathology data were correlated with the pharmacokinetic (PK) profile of APAP.

MATERIALS AND METHODS

Chemicals

APAP from Ce-Chem Pharmaceuticals Pvt. Ltd. 4th phase, #336, 9th Cross Rd, Ganapathy Nagar, Phase 3, Peenya, Bengaluru, Karnataka 560 058, India. Methanol was obtained from HIMEDIA (cat#AS061), ethyl acetate was acquired from RANKEM (cat#LTR/RANK30200), and alanine aminotransferase (ALT) and aspartate aminotransferase (AST) kits were obtained from Aspen Laboratories Pvt. Ltd.

Animal study

Female 3-week-old Balb/C mice (n= 24) were housed at NUCARE, NGSM Institute of Pharmaceutical Sciences, Paneer campus, Mangalore, Karnataka, India. Animals (n= 6) were provided free access to food and water under controlled temperature (22 °C) and humidity (50%) with a 12:12, light: dark cycle. Mice were randomly assigned into two groups (n= 6 each). 1) Normal diet group (ND, 18% protein) fed with ND and 2) high-fat diet group (HFD) fed with HFD. Dietary compositions of HFD[19] are listed in Table 1. After 15 weeks, mice were treated with a single dose of APAP-300 mg/kg; *per os* (*p.o.*). Blood samples were collected at different time intervals

Table 1. Dietary compositions of ND and HFD

Serial number	Ingredients (ND, 18% protein)	%	Serial number	Ingredients (HFD)	%
1	Wheat flour	56.2	1	Milk casein	24.50
2	DCP (rock base)	1.8	2	Egg white	5.00
3	Calcite powder	1.0	3	L-cystine	0.43
4	LAF mix	1.0	4	Powdered beef tallow	15.88
5	Linseed	5.0	5	Safflower oil (high oleic acid)	20.00
6	Maize gluten	5.0	6	Crystalline cellulose	5.50
7	Roasted gram flour	25.0	7	Maltodextrin	8.25
8	Skimmed milk powder	5.0	8	Lactose	6.93
			9	Sucrose	6.75
			10	AIN93 vitamin mix	1.40
			1	AIN93G mineral mix	5.00
			12	Choline bitartrate	0.36
			13	Tertiary butylhydroquinone	0.00

ND: Normal diet, HFD: High-fat diet, DCP: Dicalcium phosphate

(0, 6 and 24 hours) using isoflurane anesthesia through the retro-orbital sinus. The choice of time points mentioned (0, 6, and 24 hours) for blood collection after APAP administration is a common approach in PK and pharmacodynamic studies. These time points allow for capturing the immediate (0 hour), short-term (6 hours), and long-term (24 hours) effects of the drug. Collecting blood samples at 24 hours allows researchers to assess liver function markers and investigate delayed toxic effects, if any.[20] After the 24th hour of collection of blood samples, the animals were euthanized and dissected, and liver samples were removed. Part of the fresh liver sample was stored at -20 ˚C, and the other part of the tissue sample was stored in 10% formalin for histopathology studies. Separate sets of animals (n= 6) were taken for PK study and blood samples were collected at 0, 0.5, 1.0, 2.0, and 4.0 hours time intervals after APAP treatment.

Ethical clearance

All animal experiments were performed according to institutional guidelines for the care and use of laboratory animals as approved by the IAEC, under the committe for control and supervision of experiments on animals (CCSEA). In accordance with the Institutional Animal Ethics Committee of NGSM Institute of Pharmaceutical Science (approval number: NGSMIPS/IAEC/DEC-2020/2021, date: 29.11.2020).

Measurement of AST and ALT

Blood samples were collected at 0, 6 and 24 hours after a single dose of APAP 300 mg/kg *p.o.*, serum separated and stored at -20 ˚C until further analysis. Serum AST and ALT were measured using commercially available kits (Aspen Laboratories Pvt. Ltd.) as per the manual instruction by semi-auto analyzer model: Star 21+ from a rapid diagnostic group of companies.

Measurement of hepatic antioxidant enzymes [sodium dismutase (SOD), glutathione (GSH) and catalase]

Fresh liver samples were used to prepare 5% tissue homogenate using 0.25 M phosphate buffer, centrifuged at 10000 rpm for 20 minutes, and the supernatant separated. Antioxidant assays, catalase,[21] SOD[22] and GSH[23,24] were measured as per the respective protocol using an ultraviolet (UV) spectroquant prove 600 analyzer from Merck.

Histopathological examination of liver tissue

Liver tissue samples stored in 10% formalin were used to make paraffin-embedded sections. The sections were used to prepare slides, stained using hematoxylin and eosin (H&E) dyes, and observed under various magnifications.

PK study

This study was conducted to examine the role of nutrition in the absorption, distribution, metabolism and elimination (ADME) profile of APAP in mice. After weaning, female Balb/C mice were separated into two groups receiving ND and HFD. After 15 weeks, both groups were treated with APAP (300 mg/kg *p.o.*) and blood samples (100 µL) were drawn from the retro orbital sinus under the influence of isoflurane anesthesia at 0, 0.5, 1.0, 2.0 and 4.0 hour time intervals (from a separate set of animals), centrifuged (3000 rpm for 10 min) and stored at -20 ˚C until analysis. The liquid-liquid extraction method was used to extract APAP from plasma. Briefly, to a 50 µL plasma sample, 1.5 mL ethyl acetate was added, vortexed for 5 min and centrifuged at 3000 rpm for 5 min, supernatant separated and vacuum dried. To the dried residue, 200 µL of mobile phase was added and vortexed. 10 µL of aliquot was injected into the HPLC system.

PK sample analysis

Sample analysis was performed using a Waters RP-HPLC system (Model-1525 separation module and model 2998, photodiode array detector) and a C18 column (Waters SPHERISORB 5 m, ODS 1, 4.6*150 mm) as described in the literature.[2,25] A60:40 *v/v* methanol: water solution was used as the mobile phase (filtered through a 0.45 m nylon syringe membrane filter). The injection volume was 10 µL, and the effluent was monitored with a UV detector at a flow rate of 1 mL/min at 254 nm.

PK parameter calculation

We employed Phenix WinNonlin 8.3 software to conduct a non-compartment analysis to analyze the time profiles of plasma concentrations versus time data obtained from each mouse. Maximum plasma concentrations (C_{max}) and time to reach maximum plasma concentrations (t_{max}) were calculated directly from individual plasma concentration-time curves. The areas under the plasma concentrations area under the curve $(AUC)_{0-4}$, $AUC_{0-\infty}$were estimated. Drug elimination half-life ($t_{1/2}$), obvious total body clearance or oral clearance CL/F, and volume of distribution V_Z/F were calculated and interpreted.

Statistical analysis

Data are presented as mean ± SEM. Graph pad prism 8.0.1 software was used to analyze the statistical difference between groups using the Student's t-test. Also, One-Way analysis of variance with Newman-Keuls post hoc test. The level of statistical significance was considered at $p < 0.05$.

RESULTS

Biochemical analysis data

Both ND and HFD groups had similar levels of ALT at 0 hour, suggesting no nutritional role at 0 hour time point. The challenge with a single dose of APAP (300 mg/kg; *p.o.*) increased ALT level by 6th hour in both ND and HFD ($p < 0.05$ and $p < 0.01$, respectively) as compared to 0 hour time point. Surprisingly, injury was further increased in the ND group ($p < 0.001$). In contrast, injury was regressed ($p < 0.001$) in the HFD group at 24th hour compared to ND group (Figure 1A). AST estimation (Figure 1B) follows a similar trend and strengthens the ALT data.

Antioxidant assay

SOD, catalase, and GSH in fresh liver samples were estimated at the end of the study. HFD decreased antioxidant enzyme levels of SOD, catalase, and GSH (Figure 2). APAP challenge significantly ($p < 0.01$) decreased antioxidant levels in the ND group, but not in the HFD group.

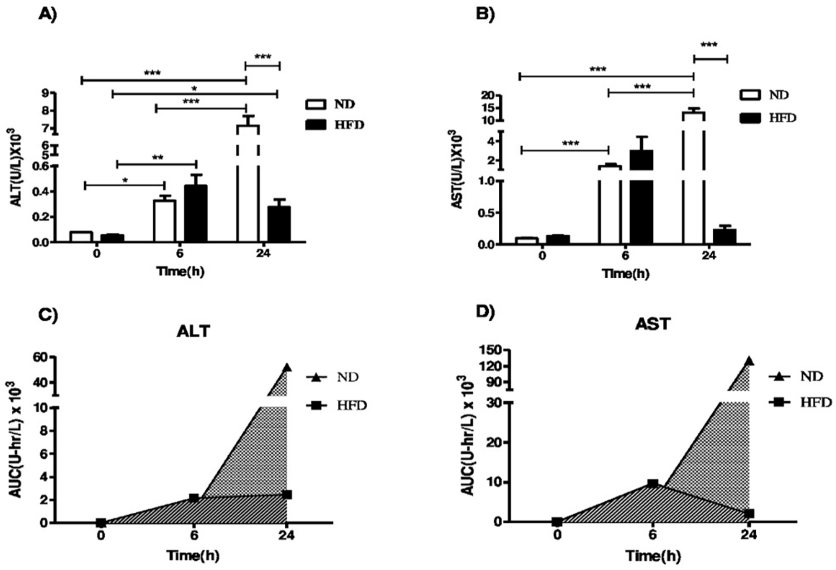

Figure 1. Serum ALT, AST levels in APAP-treated mice. (A) ALT, (B) AST levels, C) and D) AUC graphs of ALT and AST of APAP (300 mg/kg *p.o.*) treated mice at various time points. ND and HFD. ND mice received ND and HFD mice received HFD. Data are presented as mean ± SEM, n= 6. Statistical analysis was performed by t-test analysis, *$p < 0.05$, **$p < 0.01$, ***$p < 0.001$

ALT: Alanine aminotransferase, AST: Aspartate aminotransferase, APAP: Acetaminophen, AUC: Area under the curve, ND: Normal diet, HFD: High-fat diet, SEM: Standard error of the mean

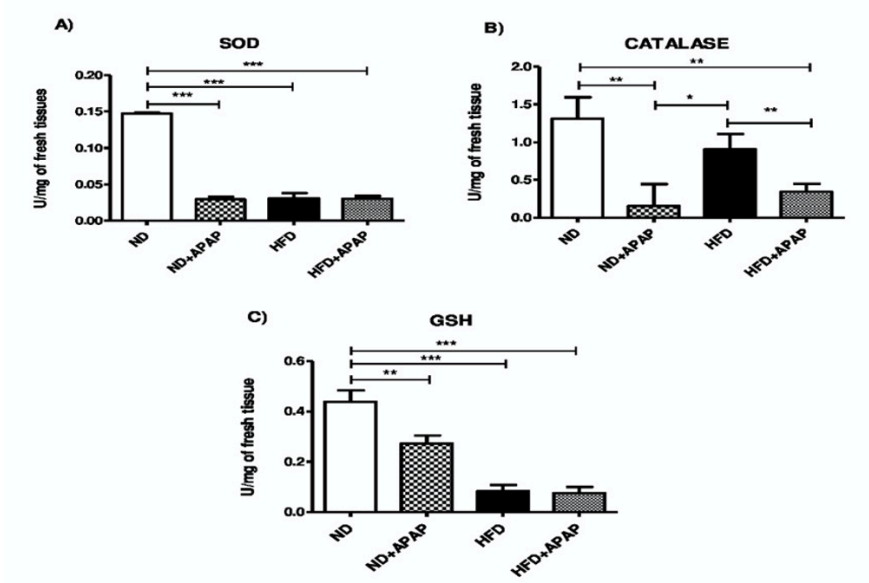

Figure 2. Effect of HFD on cellular antioxidants (A) SOD, (B) catalase, (C) GSH in the liver. ND and HFD of control and 24-hour time point after APAP 300 mg/kg *p.o.* treatment. ND mice received ND and HFD mice received HFD. ND + APAP, ND receiving group treated with APAP (300 mg/kg *p.o.*) and HFD + APAP, HFD group treated with APAP (300 mg/kg *p.o.*). Data are presented as mean ± SEM, n= 6. Statistical analysis was performed using One-Way ANOVA with Newman-Keuls post hoc test. Statistical significance is considered *$p < 0.05$, **$p < 0.01$, ***$p < 0.001$

SOD: Sodium dismutase, GSH: Glutathione, ND: Normal diet, HFD: High-fat diet, APAP: Acetaminophen, SEM: Standard error of the mean, ANOVA: Analysis of variance

Histopathological examination of liver tissue

H&E staining of HFD liver tissue showed obvious fat accumulation in the form of droplets, a characteristic feature of HFD-consuming mice.[26] Livers of ND animals showed minimal or no changes (Figure 3A), whereas those from animals fed with HFD showed severe fatty infiltration in the liver (Figure 3C, 3D). APAP administration caused extensive centrilobular injury with apoptotic cells in the livers of the ND group (Figure 3B). On the other hand, there were few inflammatory cells in the centrilobular regions of the liver from APAP-treated animals fed HFD. However, fat accumulation remained similar to that in the HFD-fed group (Figure 3C-F), confirming less liver injury in the HFD group.

PK's study

PK results were obtained from ND and HFD animals for 300 mg/kg APAP. PK study was designed to investigate the ADME profile of APAP in plasma samples from mice given ND and HFD. On the 15th week of the study, all of the mice (ND and HFD) were given single-dose APAP (300 mg/kg, *p.o.*). The average APAP retention time was 3,407 min. Peak area and APAP retention duration in ND and HFD were 3,409 and 3,409 min, respectively. HFD- receiving mice had lower plasma concentrations (37,141± 22.98, $p < 0.05$) than ND (74.38 ± 18.63). In contrast, APAP clearance and volume of distribution were two-fold higher in HFD-treated mice. As a result, the systemic exposure parameters (C_{max} and AUC) in HFD groups are lower than in ND groups (Table 2). Plasma concentrations of APAP in HFD and ND are in a ratio of 1:2.

DISCUSSION

Dietary protein and fat influence drug metabolism, altering drug toxicity and therapeutic response.[27] Clinical research examines the effects of diets, malnutrition, diet restriction, and high-fat on the PK of drugs.[3,28] Evaluating drug toxicity and PK in the clinical setting is difficult because of high cost, time, volunteer unavailability, *etc*. This study aimed to analyze the effect of HFD on APAP-mediated toxicity and PK profile in a mouse model.

APAP is chiefly metabolized by the liver, where 90% is renally eliminated after sulfide or glucuronide conjugation. The remaining 10% is metabolized *via* CYP2E1, generating the toxic metabolite NAPQI.[4] At therapeutic doses, APAP generates NAPQI in quantities that conjugate with cellular GSH without producing toxicity on hepatocytes. However, toxic doses of APAP deplete cellular GSH, and NAPQI covalently binds with the sulfhydryl group of many proteins to form APAP protein adducts in hepatocytes, leading to mitochondrial dysfunction and necrosis.[29-31] As expected, a single dose of APAP (300 mg/kg, *p.o.*) caused liver injury as reflected by elevated liver injury biomarkers (ALT and AST) in the ND and HFD groups, confirming hepatotoxicity as early as 6 hours after APAP challenge. This increase in ALT and AST is comparable in both the ND and HFD groups, suggesting similar bioactivation-mediated liver injury (stage I toxicity).[32-34] Extensive liver injury in the ND group (reflected by high AST and ALT at 24 hours) confirms greater susceptibility to APAP toxicity (stage-II toxicity). In sharp contrast, liver injury regressed in HFD-receiving animals, underlining the toxicodynamics (progression V regression of injury) of dietary fat. The HFD group probably encounters stage-II toxicity much before the 24th hour time point. Nevertheless, early publications have documented that liver progression of injury continues even after 24 hours and peaks at 36-48 hours after toxin challenge.[35] The difference in the timing of maximal injury depends on the nature of the molecule and its dose.[36] In the present study, HFD-receiving mice experienced regression of liver injury by 24 hours itself; thereby suggesting that recovery will be complete by 48 hours. Differences in liver injury between ND and HFD are reflected in the graphs showing AUC for AST and ALT (Figure 1C, 1D). However, we could not collect blood samples after the 24 hour time point. Liver histopathology provides additional evidence supporting the difference in injury (Figure 3, 4).

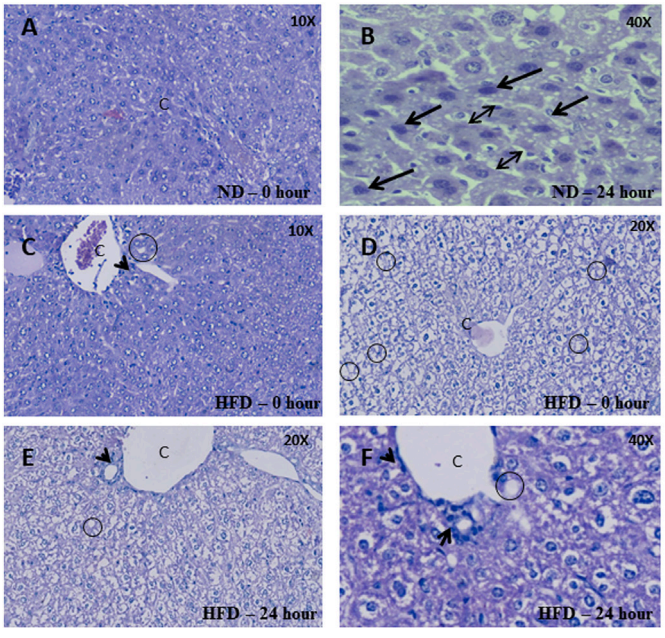

Figure 3. Liver histology of mice (A) control ND group 10. (B) 40X ND + APAP treated group, at 24 hours (C) 10 and (D) 20X HFD control group, (E) 20 and (F) 40X HFD + APAP. ND and HFD n= 6, of control and 24-hour time point after APAP 300 mg/kg *p.o.* treatment in Balb/C mice representative gures were stained with H&E. Arrows indicate apoptotic cells, arrowheads indicate inammatory cell clusters, circles indicate small fat droplets and double-headed arrows indicate sinusoids in hepatocytes

ND: Normal diet, HFD:High-fat diet, APAP: Acetaminophen, H&E: Hematoxylin and eosin

Different animal models have been used to study the impact of NAFLD on APAP toxicity. Many conflicting reports imply that HFD either increases or decreases hepatotoxicity.[2,18,37] Clinical research appears to discount the impact of HFD on APAP toxicity[4,15] which correlates with the current study's assertion that HFD suffers little or no toxicity compared with ND. There are conflicting reports in which some models reflected greater injury in the HFD group at 300 mg/kg doses of APAP, and others showed similar or lower toxicity. Multiple reports suggest a decrease in CYP2E1 enzyme activity in the HFD group.[37] The difference between previous reports and the present study could be due to differences in animal species, dose of APAP, route of administration, time points of blood sampling, *etc*. Recently, Achterbergh et al.[3] reported that short-term fasting increases APAP toxicity. However, healthy subjects did not experience APAP toxicity after an HFD, demonstrating the importance of diet in APAP-induced toxicity.

We evaluated the PK difference in APAP between the ND and HFD groups to examine the role of blood levels of APAP in liver injury. The initial absorption of APAP is more rapid in the ND group than in the HFD group. Likewise, ND had greater C_{max} and AUC than HFD. Furthermore, APAP was eliminated faster in the HFD group, explaining the lower plasma concentration

(Table 2). Similar liver injury in the ND and HFD groups at 6 hours (Figure 1) was possible because CYP2E1 enzyme levels were similar in both groups, generating similar bioactivation-mediated liver injury.

Study limitations

Further research is needed to understand the molecular mechanisms underlying the protective effects of a high-fat diet against APAP-induced liver injury, and caution should be exercised when applying these findings to obese patients without human studies.

CONCLUSION

The present study has demonstrated that HFD protects mice from APAP-mediated liver injury. Additionally, the ADME profile is considerably different in the HFD group than in the ND group. The reason for lower stage II injury in the HFD group needs further investigation. Our findings indicate that obese patients may respond differently to APAP efficacy or toxicity because of altered drug kinetics. Therefore, such victims may be treated differently from normal ones. A detailed mechanistic study is essential at the molecular level to understand the effects of nutritional status on stage-II toxicity. The outcomes of such a study will help in decision-making while treating APAP overdose victims.

Table 2. Plasma PK parameters of APAP (300 mg/kg, *p.o.*) in ND and HFD receiving Balb/C mice (n= 6)

Serial number	Parametersa	Unit	ND	HFD
1	C_{max}	µg/mL	74.38 ± 18.63	37.141 ± 22.99*
2	AUC_{0-4}	h* µg/mL	77.37 ± 17.26	37.558 ± 28.89*
3	$AUC_{0-\infty}$	h* µg/mL	79.41 ± 16.71	39.328 ± 28.52*
4	t_{max}	H	0.58 ± 0.20	0.500 ± 0.00
5	$t_{1/2}$	H	0.65 ± 0.18	0.737 ± 0.69
6	CL/F	mL/h	111.90 ± 25.58	238.788 ± 142.83
7	V_z/F	L	102.25 ± 23.30	295.662 ± 178.76

[a]Parameters values are expressed as mean ± SEM, * $p < 0.05$, when compared with the ND group, C_{max}: Maximum plasma concentration, AUC_{0-4}: Area under the drug concentration-time curve from time zero to the time of the last measurable concentration, $AUC_{0-\infty}$: Area under the drug concentration-time curve from time zero to infinity, t_{max}: Times to achieve maximum plasma concentrations, $t_{1/2}$: Elimination half-life period of the drug, CL/F: Apparent total body clearance or oral clearance, V_z/F: Volume of distribution, PK: Pharmacokinetics, APAP: Acetaminophen, ND: Normal diet, HFD: High-fat diet, AUC: Area under the curve, SEM: Standard error of the mean

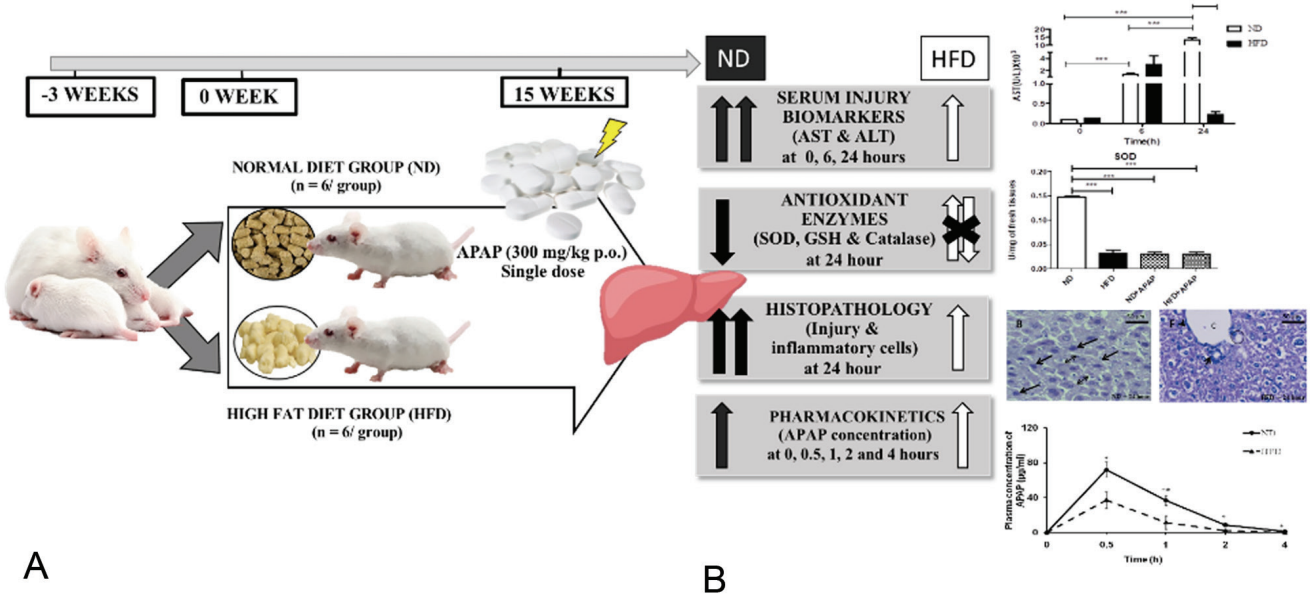

Figure 4. Graphical abstract representing animal experimental methodology. Female Balb/C mice after the weaning period were separated (0 week of the study period) into two different groups: A) ND and B) HFD receiving groups. After 15 weeks, they were administered a single dose (300 mg/kg *p.o.*) of APAP. Blood samples were collected at different time intervals (0, 6, and 24 hours), and liver samples were collected at the end time point. Liver injury parameters (ALT and AST), SOD assay (catalase and GSH), and histopathology study were conducted. Aseparate set of animals (n= 6, each group) was used for PK analysis

ND: Normal diet, HFD: High-fat diet, APAP: Acetaminophen, ALT: Alanine aminotransferase, AST: Aspartate aminotransferase, SOD: Sodium dismutase, PK: Pharmacokinetics

Acknowledgments

The research work was supported by internal funding to the NUCARE department from Nitte (Deemed to be University). Mazhuvancherry Kesavan Unnikrishnan MD, Professor, Pharmacy Practice, NGSMIPS for corrections and proofreading.

Ethics

Ethics Committee Approval: All animal experiments were performed according to institutional guidelines for the care and use of laboratory animals as approved by the IAEC. In accordance with the Institutional Animal Ethics Committee of NGSM Institute of Pharmaceutical Science (approval number: NGSMIPS/IAEC/DEC-2020/2021, date: 29.11.2020).

Informed Consent: Not necessary.

Authorship Contributions

Concept: M.B., Design: M.B., V.D'S., M.S., Data Collection or Processing: V.D'S., M.S., Analysis or Interpretation: M.B.S., V.K., V.D'S., Literature Search: V.D'S., Writing: M.B., V.D'S., V.A., M.R.J.

Conflict of Interest: No conflict of interest was declared by the authors.

Financial Disclosure: This work was supported by Nitte (Deemed to be University) [Grant: N/RG/NUFR2/NGSMIPS/2021/5].

REFERENCES

1. Mehendale HM. Tissue repair: an important determinant of final outcome of toxicant-induced injury. Toxicol Pathol. 2005;33:41-51.
2. Souza VD, Shetty M, Badanthadka M, Mamatha BS, Vijayanarayana K. The effect of nutritional status on the pharmacokinetic profile of acetaminophen. Toxicol Appl Pharmacol. 2022;438:115888.
3. Achterbergh R, Lammers LA, Kuijsten L, Klümpen HJ, Mathôt RAA, Romijn JA. Effects of nutritional status on acetaminophen measurement and exposure. Clin Toxicol (Phila). 2019;57:42-49.
4. Achterbergh R, Lammers LA, Klümpen HJ, Mathôt RAA, Romijn JA. Short-term high-fat diet alters acetaminophen metabolism in healthy individuals. Ther Drug Monit. 2022;44:797-804.
5. Ozougwu JC. Physiology of the liver. Int J Res Pharm Biosci. 2017;4:13-24.
6. Zillen D, Movig KLL, Kant G, Masselink JB, Mian P. Impact of malnourishment on the pharmacokinetics of acetaminophen and susceptibility to acetaminophen hepatotoxicity. Clin Case Rep. 2021;9:e04611.
7. Ramadori G, Moriconi F, Malik I, Dudas J. Physiology and pathophysiology of liver inflammation, damage and repair. J Physiol Pharmacol. 2008;59(Suppl 1):107-117.
8. Edwards L, Wanless IR. Mechanisms of liver involvement in systemic disease. Best Pract Res Clin Gastroenterol. 2013;27:471-483.
9. Imaeda AB, Watanabe A, Sohail MA, Mahmood S, Mohamadnejad M, Sutterwala FS, Flavell RA, Mehal WZ. Acetaminophen-induced hepatotoxicity in mice is dependent on Tlr9 and the Nalp3 inflammasome. J Clin Invest. 2009;119:305-314.
10. Salaj R, Stofilová J, Soltesová A, Hertelyová Z, Hijová E, Bertková I, Strojný L, Kružliak P, Bomba A. The effects of two Lactobacillus plantarum strains on rat lipid metabolism receiving a high fat diet. Sci World J. 2013;2013:135142.
11. Sasidharan SR, Joseph JA, Anandakumar S, Venkatesan V, Ariyattu Madhavan CN, Agarwal A. An experimental approach for selecting appropriate rodent diets for research studies on metabolic disorders. Biomed Res Int. 2013;2013:752870.
12. Li H, Xi Y, Xin X, Tian H, Hu Y. Salidroside improves high-fat diet-induced non-alcoholic steatohepatitis by regulating the gut microbiota-bile acid-farnesoid X receptor axis. Biomed Pharmacother. 2020;124:109915.
13. Hariri N, Thibault L. High-fat diet-induced obesity in animal models. Nutr Res Rev. 2010;23:270-299.
14. Santos Lacerda DS, Garbin de Almeida M, Teixeira C, De Jesus A, Da Silva Pereira Júnior É, Martins Bock P, Pegas Henriques JA, Gomez R, Dani C, Funchal C. Biochemical and physiological parameters in rats fed with high-fat diet: the protective effect of chronic treatment with purple grape juice (bordo variety). Beverages. 2018;4:100.
15. Michaut A, Moreau C, Robin MA, Fromenty B. Acetaminophen-induced liver injury in obesity and nonalcoholic fatty liver disease. Liver Int. 2014;34:171-179.
16. Speakman JR. Use of high-fat diets to study rodent obesity as a model of human obesity. Int J Obes (Lond). 2019;43:1491-1492.
17. Wang P, Shao X, Bao Y, Zhu J, Chen L, Zhang L, Ma X, Zhong XB. Impact of obese levels on the hepatic expression of nuclear receptors and drug-metabolizing enzymes in adult and offspring mice. Acta Pharm Sin B. 2020;10:171-185.
18. Wang J, Jiang W, Xin J, Xue W, Shi C, Wen J, Huang Y, Hu C. Caveolin-1 alleviates acetaminophen-induced fat accumulation in non-alcoholic fatty liver disease by enhancing hepatic antioxidant ability *via* activating AMPK Pathway. Front Pharmacol. 2021;12:717276.
19. Ganz M, Csak T, Szabo G. High fat diet feeding results in gender specific steatohepatitis and inflammasome activation. World J Gastroenterol. 2014;20:8525-8534.
20. Gao Y, Cao Z, Yang X, Abdelmegeed MA, Sun J, Chen S, Beger RD, Davis K, Salminen WF, Song BJ, Mendrick DL, Yu LR. Proteomic analysis of acetaminophen-induced hepatotoxicity and identification of heme oxygenase 1 as a potential plasma biomarker of liver injury. Proteomics Clin Appl. 2017;11:10.
21. Aebi H. Catalase. In: Bergmeyer HU, ed. Methods of Enzymatic Analysis. Academic Press; 1974:673-684.
22. Kakkar P, Das B, Viswanathan PN. A modified spectrophotometric assay of superoxide dismutase. Indian J Biochem Biophys. 1984;21:130-132.
23. Ellman GL. A colorimetric method for determining low concentrations of mercaptans. Arch Biochem Biophys. 1958;74:443-450.
24. Eyer P, Podhradský D. Evaluation of the micromethod for determination of glutathione using enzymatic cycling and Ellman's reagent. Anal Biochem. 1986;153:57-66.
25. Pingili RB, Pawar AK, Challa SR. Systemic exposure of Paracetamol (acetaminophen) was enhanced by quercetin and chrysin co-administration in Wistar rats and *in vitro* model: risk of liver toxicity. Drug Dev Ind Pharm. 2015;41:1793-1800.
26. Küçükkurt I, Ince S, Keleş H, Akkol EK, Avci G, Yeşilada E, Bacak E. Beneficial effects of Aesculus hippocastanum L. seed extract on the body's own antioxidant defense system on subacute administration. J Ethnopharmacol. 2010;129:18-22.
27. Niederberger E, Parnham MJ. The Impact of Diet and Exercise on Drug Responses. Int J Mol Sci. 2021;22:7692.

28. Wang C, Allegaert K, Tibboel D, Danhof M, van der Marel CD, Mathot RA, Knibbe CA. Population pharmacokinetics of paracetamol across the human age-range from (pre)term neonates, infants, children to adults. J Clin Pharmacol. 2014;54:619-629.

29. Qiu Y, Benet LZ, Burlingame AL. Identification of the hepatic protein targets of reactive metabolites of acetaminophen *in vivo* in mice using two-dimensional gel electrophoresis and mass spectrometry. J Biol Chem. 1998;273:17940-17953.

30. Jaeschke H, McGill MR, Ramachandran A. Oxidant stress, mitochondria, and cell death mechanisms in drug-induced liver injury: lessons learned from acetaminophen hepatotoxicity. Drug Metab Rev. 2012;44:88-106.

31. Ni HM, McGill MR, Chao X, Du K, Williams JA, Xie Y, Jaeschke H, Ding WX. Removal of acetaminophen protein adducts by autophagy protects against acetaminophen-induced liver injury in mice. J Hepatol. 2016;65:354-362.

32. Mehendale HM. Role of hepatocellular regeneration and hepatolobular healing in the final outcome of liver injury. A two-stage model of toxicity. Biochem Pharmacol. 1991;42:1155-1162.

33. Murali B, Korrapati MC, Warbritton A, Latendresse JR, Mehendale HM. Tolerance of aged Fischer 344 rats against chlordecone-amplified carbon tetrachloride toxicity. Mech Ageing Dev. 2004;125:421-435.

34. Bhushan B, Apte U. Liver Regeneration after Acetaminophen Hepatotoxicity: Mechanisms and Therapeutic Opportunities. Am J Pathol. 2019;189:719-729.

35. Yoon E, Babar A, Choudhary M, Kutner M, Pyrsopoulos N. Acetaminophen-Induced Hepatotoxicity: a Comprehensive Update. J Clin Transl Hepatol. 2016;4:131-142.

36. McGill MR, Williams CD, Xie Y, Ramachandran A, Jaeschke H. Acetaminophen-induced liver injury in rats and mice: comparison of protein adducts, mitochondrial dysfunction, and oxidative stress in the mechanism of toxicity. Toxicol Appl Pharmacol. 2012;264:387-394.

37. Piccinin E, Ducheix S, Peres C, Arconzo M, Vegliante MC, Ferretta A, Bellafante E, Villani G, Moschetta A. PGC-1β induces susceptibility to acetaminophen-driven acute liver failure. Sci Rep. 2019;9:16821.

Turk J Pharm Sci 2024;21(3):192-198
DOI: 10.4274/tjps.galenos.2023.83451

ORIGINAL ARTICLE

Optimization of Enterocin Production from Probiotic *Enterococcus faecium* Using Taguchi Experimental Design

Dina MAANY[1], Amr EL-WASEIF[2]*, Eslam Abd EL-WAHED[2]

[1]National Research Centre, Pharmaceutical and Drug Industries Research Institute, Department of Chemistry of Natural and Microbial Products, Giza, Egypt
[2]Al-Azhar University Faculty of Science, Department of Botany and Microbiology, Cairo, Egypt

ABSTRACT

Objectives: Enterocin is a significant broad-spectrum peptide antibiotic produced by *Enterococcus faecium (E. faecium)*. Enterocin production by *E. faecium* was investigated using the Taguchi experimental design. The Taguchi models were used to save the time and effort required for optimizing the different conditions affecting its production. They were applied to optimize the conditions for enterocin production using the least number of experiments and the least number of required materials.

Materials and Methods: Seven factors i.e., pH, temperature, time of incubation, aeration rate, inoculum size, carbohydrate concentration, and bile salt concentrations, each at three levels were selected and an orthogonal array layout of $L27^3$ was performed.

Results: The experimental results indicated that the best incubation conditions were; 48 hours incubation on a nutrient medium at pH 6.5, temperature at 25 °C, aeration rate at 0 round per minute, inoculum size 20 mL, and bile salt concentration. It was 5%, and the carbon concentration was 2.0%. All these factors combined led to the best enterocin production by *E. faecium*.

Conclusion: This optimization of enterocin production by the Taguchi experimental models emphasized some important results regarding the interaction of the different driving factors leading to the best enterocin production in one experiment.

Keywords: *Enterococcus faecium*, enterocin, optimization, Taguchi design, antibacterial activity

INTRODUCTION

Probiotics are the microflora living in the human intestinal tract. These bacteria are capable of producing peptides called bacteriocins, which have antimicrobial properties. *Enterococcus faecium (E. faecium)* is among these enterocin-producing bacteria.[1]

Enterocins can be used for pathogen control purposes in laboratory experiments, clinical trials, and in the food industry. Enterocins are extracellular products mainly produced by enterococci such as; *E. faecium*, *Enterococcus faecalis*, and *Toxoplasma gondii*. Bacteriocins produced by *Enterococcus* include bacteriocin 35, enterocins A, B, L50A/B, and P, which belong to class II bacteriocins.[2]

Enterocin A of *E. faecium* is a stable peptide that can be potentially used for the treatment of pathogens and cancer. It is a cyclic peptide with an isoelectric point of approximately 10.[3]

Enterocin works as an antimicrobial agent for Gram-positive as well as Gram-negative bacteria, whereas most of the recorded literature states that lactic acid bacteria-derived bacteriocins have an antimicrobial effect only on Gram-positive bacteria.[4]

It has been scientifically reported that enterocins have an antibacterial effect against several types of bacteria such as *Listeria monocytogenes* and *Staphylococcus aureus*.[5] *Enterococci* carry resistance genes in their genetic profile, and bacteriocin a is heat stable, so they can be used as antibacterial agents against foodborne pathogenic microorganisms. Safe bacteria with the same properties can be used to inhibit foodborne pathogens.[6]

The results of any scientific experiment depend on several chemical and physical factors. To obtain the best results from any experiment, those factors have to be optimized in reference

*Correspondence: amrelwaseif@azhar.edu.eg, Phone: +20 1006543350, ORCID-ID: orcid.org/0000-0002-8605-9067
Received: 25.04.2023, Accepted: 11.07.2023

to each other, and it is much more efficient and time-saving when this aim is achieved with fewer experiments, saving time, effort, and expenses.[7,8]

The Taguchi design has been successfully used to optimize the parameters involved in several experiments.[9] The design was used to adjust the interaction of several variables and their interaction in any given experiment in one process instead of requiring a more significant number of experiments that are often costly and time-consuming. The Taguchi design allows us to obtain the information needed from any experiment by optimizing the variables involved in this experiment and allowing more facility for the best outcome of the system performance, using a smaller number of experiments.[10]

The research explored the power of Taguchi experimental design to optimize and validate the factors affecting enterocin production from the probiotic *E. faecium*.

MATERIALS AND METHODS

Enterocin biosynthesis from E. faecium

E. faecium was isolated and identified in a previous study.[11] It was propagated as 10 mL of *E. faecium* liquid culture was inoculated into 1 L of MRS broth medium. The turbidity of bacterial growth was calibrated using 0.5 McFarland standard where a hundred microliter (1 x 10^7 cells/mL) of bacterial growth culture was used as the standard inoculum and incubated for 48 hours at 30 ˚C under static conditions.

Antibacterial assay

The antibacterial activity was assayed using the agar well diffusion method as follows: 40.0 mL of nutrient agar medium incubated at 55-60 ˚C was inoculated with 200.0 µL of the pathogenic bacteria cell suspensions under test separately and poured into 150.0 mm diameter Petri dishes, mixed well, and allowed to solidify. After solidification, holes of 5.0 mm in diameter were made in the agar plate with the aid of a sterile cork borer. For each sample, duplicate wells were made and then 100.0 µL of the culture filtrate was poured into the prepared holes using an automatic micropipette. The Petri dishes were kept in a refrigerator for 1 hour to permit homogeneous diffusion of the antimicrobial agent before the growth of *S. aureus* American Type Culture Collection (ATCC) 6538 and *Escherichia coli* ATCC 8739, and then the plates were incubated at 37 ˚C for 24 hours for Gram-positive and Gram-negative bacteria. Antimicrobial activities were determined by measuring the diameter of the inhibition zone.[12]

Optimization of enterocin production

Several experiments were carried out to investigate the production rate and the antibacterial activity.

In this experiment, an L-27 standard orthogonal array (OA) was generated for the examination of seven factors, *i.e.*, pH, temperature, incubation time (hour), inoculum size (mL), aeration [round per minute (RPM)] (-1; static, 0; 50 RPM, 100; 100 RPM), carbohydrate concentration (glucose g/L), and bile salt concentration $X10^{-1}$, which were selected on the basis of the results of biosynthesis. The L-27 symbolic array of the experimental matrix represents the number of runs (*i.e.*, 27 experimental trials). The three levels of the seven factors were coded as levels 1, 2, and 3 (Table 1), and the layout of L27 Taguchi's OA is shown in Table 2. The total degrees of freedom (DF) for the OA L-27 set was 26 (number of runs minus one). Runs involved a particular combination of levels to which the factors were set, and the diversity of factors was studied by crossing the factors. Experiments were conducted in duplicate, and factors were studied at three levels.

Statistical analysis

Statistical analysis and graph plotting were conducted using Design-Expert software. Analysis of variance (ANOVA) was used to evaluate the effect of each independent variable on the response, and $p < 0.05$ was considered significant. The multiple correlation coefficient (R^2) and adjusted R^2 were used to evaluate the fitness of the equation. Three-dimensional surface plots were employed to demonstrate the relationships and interactions between the variables and response.

RESULTS

Optimization of enterocin production

This optimization process using Taguchi models enables us to determine the ideal factors in the experimental area. Using Minitab in the experiment provided us with the experimental data for enterocin production and incorporated the quadratic polynomial prototype with ideal parameters.

The maximum enterocin production was achieved at pH= 6.5, temperature= 25 ˚C, incubation time= 48 hours, inoculum size= 20 mL, aeration= 1, carbohydrate concentration= 20, bile salt concentration 5. The variables tested were pH (A), temperature (B), incubation time (C), inoculum size (D), aeration (E), carbohydrate concentration (F), and bile salt concentration (G). The Pareto chart revealed that pH was the best factor that had an effect on enterocin production and carbohydrate concentration but did not show any effect on enterocin production.

A plot of the expected normal values of residuals versus residuals (Figures 1 and 2) showed that data were very close to the straight line and situated on both sides. Where values below the straight line were insignificant and those above

Table 1. Factors and levels selected for experimental use

Factors	Level 1	Level 2	Level 3
pH	5	6.5	8
Temperature	25	35	40
Incubation time (hour)	24	48	72
Inoculum size (mL)	5	10	20
Aeration (RPM)	-1	0	100
Carbohydrate concentration	10	20	30
Bile salt concentration $X10^{-1}$	1	3	5

RPM: Revolutions per minute

the straight line were significant. Where values below the line are insignificant and those above the line are significant. Residuals represent the difference between true and predicted values using our final logistic regression models, whereas the histogram of frequency versus residual had a dumbbell shape. It could be seen that residuals were most concentrated around 5 and had a right skewed distribution.

The main effects for the means of various parameters

Each medium component was tested for enterocin production and was investigated using Taguchi models.

The provided data revealed that the level of enterocin production increases as pH level, aeration, and bile salt concentration decrease. On the other hand, enterocin production increased as the temperature, incubation time, and inoculum size increased, whereas the level of bacteriocin was constant at any carbohydrate concentration.

Statistical analysis

The provided data were used for ANOVA. The different values (*p* value, *f* value, coeffcient of variation, and determination coeffcient) obtained from ANOVA confirmed the significance of the selected model. If the *p* value is less than 0.5, the variables were statistically significant.

ANOVA was used to determine the model's significance. Various values (*p* value, *f* value, coefficient of variation

Table 2. Taguchi experimental layout

Row	pH	Temperature	Incubation time (hour)	Inoculum size (mL)	Aeration (RPM)	Carbohydrate concentration	Bile salt concentration 10X
1	5.0	25	24	5	-1	10	1
2	5.0	25	24	5	0	20	3
3	5.0	25	24	5	100	30	5
4	5.0	35	48	10	-1	10	1
5	5.0	35	48	10	0	20	3
6	5.0	35	48	10	100	30	5
7	5.0	40	72	20	-1	10	1
8	5.0	40	72	20	0	20	3
9	5.0	40	72	20	100	30	5
10	6.5	25	48	20	-1	20	5
11	6.5	25	48	20	0	30	1
12	6.5	25	48	20	100	10	3
13	6.5	35	72	5	-1	20	5
14	6.5	35	72	5	0	30	1
15	6.5	35	72	5	100	10	3
16	6.5	40	24	10	-1	20	5
17	6.5	40	24	10	0	30	1
18	6.5	40	24	10	100	10	3
19	8.0	25	72	10	-1	30	3
20	8.0	25	72	10	0	10	5
21	8.0	25	72	10	100	20	1
22	8.0	35	24	20	-1	30	3
23	8.0	35	24	20	0	10	5
24	8.0	35	24	20	100	20	1
25	8.0	40	48	5	-1	30	3
26	8.0	40	48	5	0	10	5
27	8.0	40	48	5	100	20	1

RPM: Revolutions per minute

and determination coefficient) obtained from ANOVA demonstrate that the selected model was significant at $p < 0.5$, the analysis of variance for means ratio with the DF. From Table 3, we found that pH, incubation time, inoculum size, and aeration had significant effects on response due to ($p < 0.5$). The adjacent sum of squares, adjacent mean square, and probability (P) are shown in Table 4. The point at which the effect estimates were statistically significant was $p= 0.5$.

These results emphasize the impact of each parameter on metabolite synthesis depending on the other factors involved in the fermentation process. The percentage of involvement of each factor is shown in the ANOVA Table 4. The last column of the ANOVA shows how much each factor was involved in the optimization process. The ANOVA results of all studies showed that all factors were effective for the response variables.

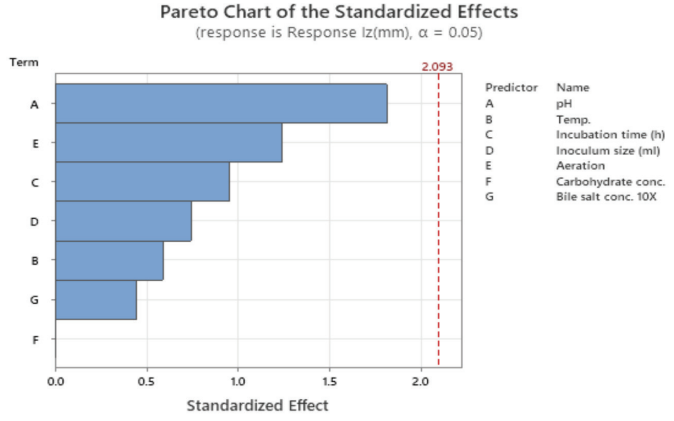

Figure 1. Pareto graph showing the different factors tested and their standardized estimates for enterocin production

DISCUSSION

The optimized parameters in this experiment were: pH, temperature, incubation time, inoculum size, aeration, carbohydrate concentration, and bile salt concentration, all of which have a great effect on enterocin production.[13]

During the optimization process of the antibacterial products of *E. faecium*, we considered both physical and chemical factors. The physical factors were pH, temperature, time of incubation, aeration rate, and inoculum size, and chemical factors included carbohydrate concentration and bile salt concentrations. These factors had a major effect on the growth and enterocin biosynthesis by *E. faecium*.[14] Optimization and enhancement of the efficiency of presently available drugs require novel research approaches to accelerate the speed of antimicrobial drug development.[15] Both the type of microbial strain and their growth conditions affect the antibiotic biosynthesis of bacteria quantitatively and qualitatively.[16] In this study, the production was optimized under different conditions using the Taguchi method, which gives us the best results for optimizing the different factors interacting to produce the maximum amount of enterocin in the fermentation process.[17]

The Taguchi design includes an analysis of results leading to a response model that clearly demonstrates the relationship of each variable toward the response, as well as the interactions between factors. In regression with a single variable, the coefficient shows how much the variable is expected to increase or decrease (if the coefficient is

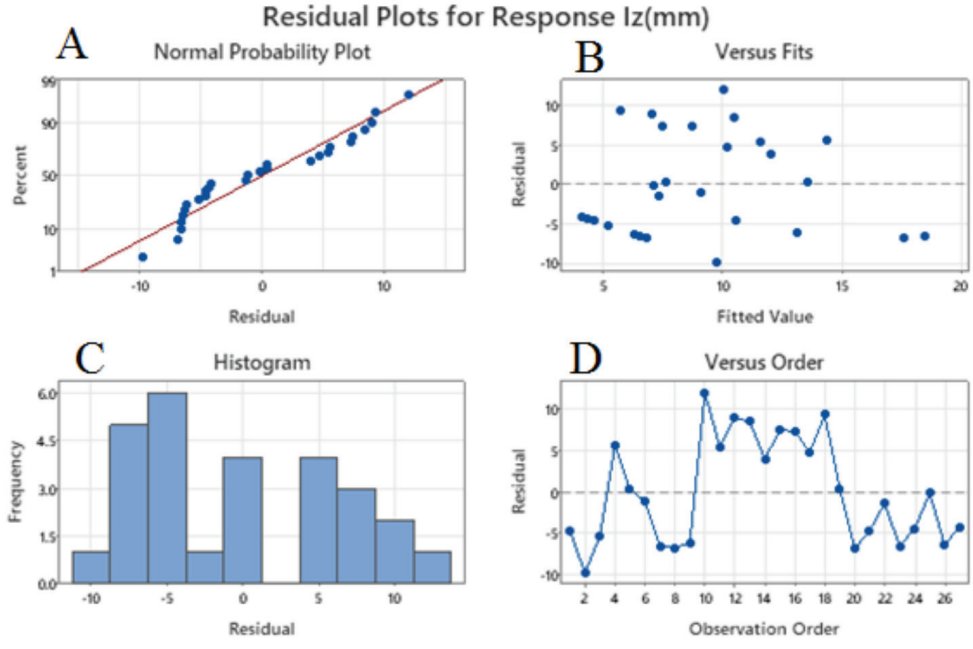

Figure 2. A) Normal probability plot of standardized residuals for bacteriocin production, the probability showed linearity. (B) Residual versus fitted samples were randomly scattered. (C) Frequency of each value interval versus residual values. (D) Residual versus observation order had an asymmetrical pattern

Table 3. Design of the experiment and results of the response

Run	pH	Temperature	Incubation time (hour)	Inoculum size (mL)	Aeration	Carbohydrate concentration	Bile salt concentration 10X	Response Iz (mm)
1	5.0	25	24	5	-1	10	1	6
2	5.0	25	24	5	0	20	3	0
3	5.0	25	24	5	100	30	5	0
4	5.0	35	48	10	-1	10	1	20
5	5.0	35	48	10	0	20	3	14
6	5.0	35	48	10	100	30	5	8
7	5.0	40	72	20	-1	10	1	12
8	5.0	40	72	20	0	20	3	11
9	5.0	40	72	20	100	30	5	7
10	6.5	25	48	20	-1	20	5	22
11	6.5	25	48	20	0	30	1	17
12	6.5	25	48	20	100	10	3	16
13	6.5	35	72	5	-1	20	5	19
14	6.5	35	72	5	0	30	1	16
15	6.5	35	72	5	100	10	3	15
16	6.5	40	24	10	-1	20	5	16
17	6.5	40	24	10	0	30	1	15
18	6.5	40	24	10	100	10	3	15
19	8.0	25	72	10	-1	30	3	8
20	8.0	25	72	10	0	10	5	0
21	8.0	25	72	10	100	20	1	0
22	8.0	35	24	20	-1	30	3	6
23	8.0	35	24	20	0	10	5	0
24	8.0	35	24	20	100	20	1	0
25	8.0	40	48	5	-1	30	3	7
26	8.0	40	48	5	0	10	5	0
27	8.0	40	48	5	100	20	1	0

Table 4. Analysis of the variance for means

Source	DF	Adj SS	Adj MS	*f* value	*p* value
Regression	7	375.51	53.645	0.97	0.477
pH	1	180.50	180.500	3.28	0.086
Temperature	1	19.11	19.114	0.35	0.563
Incubation time (hour)	1	50.00	50.000	0.91	0.352
Inoculum size (mL)	1	30.29	30.288	0.55	0.467
Aeration	1	84.72	84.724	1.54	0.230
Carbohydrate concentration	1	0.00	0.000	0.00	1.000
Bile salt concentration 10X	1	10.89	10.889	0.20	0.661
Error	19	1045.67	55.035		
Total	26	1421.19			

DF: Degrees of freedom, Adj SS: Adjacent sum of squares, Adj MS: Adjacent mean square

positive or negative, respectively) when that independent variable increases by one, and the *p* value with confidence correlates with both variables.

Orthodox optimization techniques proceeded by varying a single factor at one time while other factors remained constant, which enabled us to measure the influence of those factors on antimicrobial agent activity. The limitations of this process, such as time loss, burdensomeness, and the need more experimental research to provide a better conclusion about the interactions of these factors.[18] The Taguchi design has been used for the improvement of several factors named "orthogonal arrays" (OA) to decrease experimental errors and to increase the desired product in this experiment.[19]

The Taguchi models have been useful for improving bioreactors on an industrial scale for a better yield of antimicrobial metabolites. On the other hand, Taguchi enables researchers to investigate several factors and provides a lot of data in a limited number of experiments.[17,20] In our research, the best optimized conditions included an incubation time of 48 hours, pH of 6.5, temperature of 25 ˚C, aeration rate of 0 RPM, inoculum size of 20 mL, bile salt concentration of 5% and carbon concentration of 2.0%.

The Taguchi technique was used by Venil and Lakshmanaperumalsamy to determine the importance of nutritional media components. This was achieved by optimizing the amount of chemical components and physical factors affecting the protease enzyme produced by *Bacillus subtilis* strain HB04.[20]

CONCLUSION

The Taguchi experiment was used to optimize the production of enterocin by *E. faecium* to obtain the advantage of a lower number, shorter time of experiments, and fewer experimental errors. A standard variance procedure was then used to determine the statistically important factors. Because there were three levels for each factor (7), the L-27 OA was selected for the experimental design. The test outcomes were best under the following conditions: incubation for 48 hours, pH of the medium at 6.5, temperature at 25 ˚C, aeration rate at 0 RPM, inoculum size of 20 mL, bile salt concentration of 5%, and carbon concentration of 2.0%. Average effects of the affecting parameters and their relevant interactions at the given levels on enterocin synthesis.

Ethics

Ethics Committee Approval: This study does not require any ethical permission.

Informed Consent: Not ablicable an in vitro study.

Authorship Contributions

Concept: A.E-W., Design: D.N., A.E-W., E.A.E.-W., Data Collection or Processing: D.N., A.E-W., E.A.E.-W., Analysis or Interpretation: D.N., A.E-W., E.A.E.-W., Literature Search: D.N., A.E-W., E.A.E.-W., Writing: D.N., A.E-W., E.A.E.-W.

Conflict of Interest: Authors declare that there is no conflict of interests.

Financial Disclosure: The authors declared that this study received no financial support.

REFERENCES

1. Konings WN, Kok J, Kuipers OP, Poolman B. Lactic acid bacteria: the bugs of the new millennium. Curr Opin Microbiol. 2000;3:276-282.
2. Satish Kumar R, Kanmani P, Yuvaraj N, Paari KA, Pattukumar V, Arul V. Purification and characterization of enterocin MC13 produced by a potential aquaculture probiont *Enterococcus faecium* MC13 isolated from the gut of Mugil cephalus. Can J Microbiol. 2011;57:993-1001.
3. Franz CM, Stiles ME, Schleifer KH, Holzapfel WH. Enterococci in foods-a conundrum for food safety. Int J Food Microbiol. 2003;88:105-122.
4. Line JE, Svetoch EA, Eruslanov BV, Perelygin VV, Mitsevich EV, Mitsevich IP, Levchuk VP, Svetoch OE, Seal BS, Siragusa GR, Stern NJ. Isolation and purification of enterocin E-760 with broad antimicrobial activity against gram-positive and gram-negative bacteria. Antimicrob Agents Chemother. 2008;52:1094-1100.
5. Martín M, Gutiérrez J, Criado R, Herranz C, Cintas LM, Hernández PE. Cloning, production and expression of the bacteriocin enterocin a produced by *Enterococcus faecium* PLBC21 in *Lactococcus lactis*. Appl Microbiol Biotechnol. 2007;76:667-675.
6. Gutiérrez J, Larsen R, Cintas LM, Kok J, Hernández PE. High-level heterologous production and functional expression of the sec-dependent enterocin P from *Enterococcus faecium* P13 in *Lactococcus lactis*. Appl Microbiol Biotechnol. 2006;72:41-51.
7. Bezerra MA, Santelli RE, Oliveira EP, Villar LS, Escaleira LA. Response surface methodology (RSM) as a tool for optimization in analytical chemistry. Talanta. 2008;76:965-977.
8. Teofilo RF, Ferreira MMC. Quimiometria Ii: planilhas eletrônicas para cálculos de planejamentos experımentais, um tutorial. Quim Nova 2006;29:338-350.
9. Zhang J, Fan Y, Smith E. Experimental design for the optimization of lipid nanoparticles. J Pharm Sci. 2009;98:1813-1819.
10. Qadah AM, El-Waseif AA., Yehia H. Novel use of probiotic as acetylcholine esterase inhibitor and a new strategy for activity optimization as a biotherapeutic agent. Journal of Applied Biology and Biotechnology. 2023;11: 202-215.
11. Abd-Elwahed ES, El-Waseif AA, Maany DA. Biosynthesis and FPLC purification of antibacterial peptide from the biotherapeutic agent *Enterococcus faecium*. Egypt Pharm J. 2023;22:202-208.
12. Elghwas DE, El-Waseif AA. The synthesis of silver nanoparticals from *Streptomyces* sp. with antimicrobial activity. Int J Pharm Tech Res. 2016;9:179-186.
13. Webster JM, Chen CG, Hu K, Jianxiong L. Bacterial metabolites. In Entomopathogenic Nematology ed. Gaugler R, ed. Wallingford: CAB International; 2002:99-114.
14. Falagas ME, Kopterides P. Old antibiotics for infections in critically ill patients. Curr Opin Crit Care. 2007;13:592-597.
15. Chen G, Maxwell P, Dunphy GB, Webster JM. Culture conditions for Xenorhabdus and Photorhabdus symbionts of entomopathogenic nematodes. Nematologica. 1996;42:124-127.

16. Houng JY, Liao JH, Wu JY, Shen SC, Hsu HF. Enhancement of asymmetric bioreduction of ethyl 4- chloro acetoacetate by the design of composition of culture medium and reaction conditions. Process Biochem. 2006;42:1-7.

17. Beg QK, Sahai V, Gupta R. Statistical media optimization and alkaline protease production from *Bacillus mojavensis* in a bioreactor. Process Biochem. 2003;39:203-209.

18. Parasad KK, Mohan SV, Rao RS, Pati BR, Sarma PN. Laccase production by Pleurotus ostreatus 1804: Optimization of submerged culture conditions by Taguchi DOE methodology. Biochem Eng J. 2005;24:17-26.

19. Stone RA, Veevers A. The Taguchi influence on designed experiments. J Chemom. 1994;8:103-110.

20. Venil CK, Lakshmanaperumalsamy P. Taguchi experimental design for medium optimization for enhanced protease production by *Bacillus subtilis* HB04. Journal of Science and Technology. 2009;4:1-10.

Turk J Pharm Sci 2024;21(3):199-210
DOI: 10.4274/tjps.galenos.2023.93765

ORIGINAL ARTICLE

Olmesartan Medoxomil-Loaded Niosomal Gel for Buccal Delivery: Formulation, Optimization, and *Ex Vivo* Studies

Narahari Narayan PALEI[1]*, Bibhash Chandra MOHANTA[2], Jayaraman RAJANGAM[3], Prathap Madeswara GUPTHA[4]

[1]Amity Institute of Pharmacy, Amity University, Lucknow, Uttar Pradesh, India
[2]Department of Pharmacy, Faculty of Health Science, Central University of South Bihar, Gaya, India
[3]Shri Venkateshwara College of Pharmacy, Ariyur, Puducherry, India
[4]Amity Institute of Pharmacy, Amity University, Gwalior, Madhya Pradesh, India

ABSTRACT

Objectives: Olmesartan medoxomil (OLM) is a low bioavailability antihypertensive drug. This study aimed to prepare and optimize an OLM niosomal gel and investigate drug permeation *via* a chicken buccal pouch.

Materials and Methods: OLM-loaded niosome were prepared using a film hydration technique. The vesicle size, zeta potential, entrapment efficiency, and percentage cumulative drug release of niosome were evaluated. The niosomes were incorporated into a Carbopol 974P (1.5% *w/v*) gel, and the drug permeability of the niosomal gel was evaluated. The formulations of the niosomal gel were optimized using the Box-Behnken design. The optimized formulation was further characterized by transmission electron microscopy (TEM) and Fourier transform infrared radiation analysis.

Results: The particle size and zeta potential of the optimized niosomal formulations were 296.4 nm and -38.4 mV, respectively. Based on TEM analysis, the niosomes were found to be spherical in shape. The permeability, flux, and permeability coefficient of the optimized niosomal gel were 0.507 mg/cm^2, 0.083 mg/cm^2 × hour, and 041 cm/hour, respectively. Histopathological evaluation revealed that the niosomal gel had better permeability than the OLM gel.

Conclusion: Based on the results of the OLM niosomal gel, it can be concluded that the formulation can be beneficial in increasing bioavailability, resulting in better therapeutic efficacy.

Keywords: Box-Behnken design, buccal delivery, histopathology, niosomal gel, olmesartan medoxomil, permeability

INTRODUCTION

The buccal route of drug administration is an alternative to the oral route, particularly for gastro irritants and drugs with low bioavailability. The high vascularization of the buccal mucosa allows for direct blood flow to the systemic circulation *via* the jugular vein, avoiding drug metabolism through the gastrointestinal and liver routes.[1] Niosomes are novel drug delivery systems in which the drug is encapsulated in a bilayer of non-ionic surface active agents consisting of a vesicle. They can accommodate both hydrophobic and hydrophilic drugs and act as reservoirs for sustained drug release. Niosomes also help increase targeted drug delivery and oral bioavailability of poorly bioavailable drugs, therapeutic efficacy, and minimizing drug toxicity. Niosome can resolve some drawbacks associated with liposomes, *i.e.*, leakage, aggregation, and stability, even though they are structurally similar. Mucoadhesive films containing niosome can improve drug permeation, reduce skin irritation, and prevent the first-pass effect. Profound penetration of nanovesicles into the buccal mucosa can be achieved because of the small size of the particles and surface properties. Due to the small size of the noisome and its lipid nature, drug permeation in the buccal mucosa can be improved compared with that

*Correspondence: narahari.palei@gmail.com, Phone: +8374557445, ORCID-ID: orcid.org/0000-0002-2041-1849
Received: 17.04.2023, Accepted: 14.07.2023

of the plain drug. Buccal delivery of niosomal formulations has been reported by various researchers to improve the bioavailability as well as local action of a drug like metoprolol, benzocaine, and lornoxicam.[2-4] Various formulations such as self-micro emulsifying drug delivery system, nanocapsules, nanostructured lipid carriers, nanosuspension, nanocrystals, and liquisolid compacts of olmesartan medoxomil (OLM) improved oral bioavailability.[5-10] OLM belongs to the class of drugs known as angiotensin II receptor antagonists. It inhibits the action of certain natural substances that stiffen blood vessels, enabling better blood flow and heart pumping. OLM is a poorly bioavailable drug (28%) through the oral route.[11] Owing to its low aqueous solubility (8 µg/mL) and high lipophilicity (log P 4.31), OLM is classified as a BCS class II drug.[12] The absorption potential of the buccal mucosa is influenced by the lipid solubility and molecular weight of the drug. The molecular weight of OLM is 558.5 g/mol, and its proper elimination half-life ($t_{1/2}$ = 13 h) makes it a suitable candidate for administration by the buccal route. During gastrointestinal absorption, OLM is converted to olmesartan by ester hydrolysis.[13] Thus, the buccal mucosa has been explored as a potential location for the delivery of drugs because of its excellent accessibility, low enzymatic activity, and avoidance of first-pass hepatic metabolism.[14] Although works have been done to improve the bioavailability of OLM by administering oral route, OLM loaded niosomal buccal gel has not been performed so far. Therefore, an attempt was made to develop an OLM-loaded niosomal gel as a carrier for buccal delivery, which can improve drug permeation and reduce the pre-systemic metabolism of the drug. This study aimed to prepare and optimize niosomal gel for buccal delivery of OLM and evaluate drug permeation through chicken mucosa.

MATERIALS AND METHODS

Materials

OLM was obtained from a gift sample from Glenmark Pharmaceuticals, Mumbai. Sorbitan monostearate (Span 60), dialysis bag, were purchased from Hi Media, Mumbai. *Aloe vera* oil (AO) and Carbopol 974P were procured from Yarrow chem, India. Cholesterol was purchased from SD Fine Chemicals, Mumbai. The chemicals used in the study were all of analytical grade.

Preparation of the OLM calibration curve

Stock solution of olmesartan for ultraviolet (UV) determination was prepared at a concentration of 50 µg/mL in 10% (*v/v*) methanol in phosphate buffer (pH 6.8). The working standard solutions were prepared by diluting the stock solution in the concentration range from 2.5 to 25 µg/mL. The solutions were scanned in a UV-visible spectrophotometer (Shimadzu UV-1800). The samples were analyzed for their respective absorbance at a λ_{max} of 257 nm. The experiment was performed three times for each sample. The limit of detection (LOD) and limit of quantification (LOQ) for OLM using the proposed method were determined using calibration standards. LOD and LOQ were calculated as 3.3 σ/S and 10 σ/S, respectively, where S is the slope of the calibration curve and σ is the standard deviation of the y-intercept of the regression equation.[15]

Preparation and optimization of OLM-loaded niosome

Niosome were prepared using the lipid film hydration method with slight modification.[16] Span 60, cholesterol, and AO were dissolved in 10 mL of chloroform and methanol (2:1 *v/v* ratio) in a round bottom flask (Tables 1, 2). To the above mixture, 40 mg of OLM was added and mixed properly. The solvent was evaporated from the round bottom flask using a rotary flash evaporator (R-3 Rotavapour, Buchi) under a vacuum of 10 bar at a temperature of 50 °C at 80 rpm until a smooth, dry lipid film was obtained. The dried film was then hydrated with 10 mL of 7.4 phosphate buffer saline and sonicated for 1 min at 50% and 40 pulses using an ultrasonicator (Model 300 V/T ultrasonic homogenizer, Biologics) to obtain niosomal dispersion. The niosomal dispersion was kept at 2-8 °C overnight. The niosomal formulations were optimized using a Box-Behnken design (Design Expert version 10; Stat-Ease Inc.). Independent variables such as Span 60, cholesterol, and AO were used at low, medium, and high levels for preparing 17 formulation sand are depicted in Tables 1 and 2. Vesicle size (Y1), cumulative drug release (CDR) (Y2), and permeability (Y3) were chosen as dependent variables. In addition, response surface 3D graphs were plotted to show the effects of the predetermined variables on the measured responses.

Characterization of the niosomes

Particle size and zeta potential

The mean vesicle size and zeta potential were measured using dynamic light scattering techniques (Horiba SZ 100, Japan). The measurement was performed at an angle of 90° in 10mm diameter cells at a temperature of 25 °C. The measurements of vesicle size and zeta potential were performed three times.

Entrapment efficiency

The ultracentrifugation method was used to assess the entrapment efficiency of the niosomal formulations. Niosomal suspension (10 mL) was poured into a centrifuge tube and centrifuged at a speed of 25000 relative centrifugal force (RCF) using a cooling centrifuge for 90 min at 4 °C and then filtered to obtain a clear fraction using Whatman filter paper. The free drug was analyzed using a UV-visible spectrophotometer (Shimadzu UV-1800) at 257 nm on the clear fraction, and the entrapment efficiency was estimated using the formula.

$$\text{Entrapment efficiency (\%)} = \frac{Wt\text{-}wf}{Wt\text{-}wf} \times 100$$

Where, Wt= total amount of drug and Wf= amount of free drug

CDR studies

The dialysis bag was washed with distilled water. The niosomal dispersion (5 mL) was transferred into a dialysis bag, and both ends were sealed. The dialysis bag was placed in a beaker containing 100 mL phosphate buffer (pH 6.8). The beaker was then positioned above the magnetic stirrer. Three milliliter samples were taken out and substituted with fresh medium at different time intervals up to 24 h. Samples were diluted properly and the drug was quantified using a UV-

visible spectrophotometer (Shimadzu UV-1800) at 257 nm. The percentage CDR from different formulations was calculated. The CDR (%) of each formulation was calculated three times.

Formulation of the niosomal gel

The known volume of the niosomal formulation was centrifuged for 90 min at 4 °C and 25000 RCF in a cooling centrifuge. The highly viscous portion of the niosomes was collected by decanting the supernatant and added to the 1.5% Carbopol 974P gel base. The gel containing OLM niosome was mixed properly using a mortar and pestle. Afterward, glycerin (1% *w/w*) and sucrose (quantum satis) were added to the gel, while it was continuously triturated. Triethanolamine was used to adjust the pH to buccal pH.

Table 1. Process variables in Box-Behnken design for niosomal formulations

Independent variable	Low (-1)	Medium (0)	High (+1)
Span 60 (mmol)	0.25	0.375	0.5
Cholesterol (mmol)	0.125	0.187	0.25
Aloe vera oil (mL)	0.25	0.375	0.5

Evaluation of the niosomal gel

The calibration of the pH meter was performed before measuring the pH of the gel, and measurements were obtained by immersing the glass electrode in the gel formulations. The spreadability of gel formulations was determined by placing 1 g of gel on the lower slide and positioning the upper slide on the top of the gel. The weight (500 g) was placed on the upper slide, and the diameter of the spread gel was measured in cm.[17] The content uniformity of the gel was determined by taking the gel from three parts of the beaker. The gel (1 g) was added to methanol and sonicated for 15 min. The filtrate was collected after filtration of the mixture using Whatman filter paper, and the OLM concentration was analyzed using a UV-visible spectrophotometer at 257 nm after proper dilution with methanol.

Ex vivo permeation study of the niosomal gel

Permeation studies on chicken buccal mucosa were conducted using a Franz diffusion cell with an effective diffusion area of 3.14 cm^2 and a receiver compartment capacity of 60 mL. The mucosa was tied to the donor compartment and phosphate buffer (pH 6.8) was placed in the receiver compartment. The Franz diffusion cell was positioned on a magnetic stirrer

Table 2. Formulation and characterization of niosomal formulations. Data presented as mean ± SD (n= 3)

FC	Independent variable			Gelling agent	Response niosomal suspension		Response niosomal gel
	Factor 1 (X1)	Factor 2 (X2)	Factor 3 (X3)		Response 1 (Y1)	Response 2 (Y2)	Response 3 (Y3)
	A: Span 60	B: Cholestrol	C: AO	Carbopol 974P	Vesicle size	CDR	Permeability
	mmol	mmol	mL	%	nm	%	mg/cm^2
NF1	0.375	0.1875	0.375	1.5	270.4 ± 3.2	73.54 ±2.6	0.385 ± 0.015
NF2	0.375	0.1875	0.375	1.5	274.5 ± 4.1	72.21 ±3.1	0.372 ± 0.023
NF3	0.25	0.25	0.375	1.5	298.3 ± 3.6	85.13 ±2.9	0.411 ± 0.013
NF4	0.5	0.1875	0.25	1.5	331.6 ± 2.9	73.1 ± 3.1	0.366 ± 0.019
NF5	0.375	0.25	0.25	1.5	265.3 ± 5.3	72.13 ± 2.6	0.362 ± 0.026
NF6	0.25	0.1875	0.25	1.5	325.7 ± 3.7	65.13 ± 3.2	0.321 ± 0.025
NF7	0.5	0.1875	0.5	1.5	329.1 ± 4.1	77.34 ± 3.1	0.392 ± 0.023
NF8	0.375	0.25	0.5	1.5	296.4 ± 3.9	96.22 ± 2.9	0.507 ± 0.017
NF9	0.375	0.1875	0.375	1.5	269.6 ± 3.1	74.14 ± 2.3	0.38 ± 0.021
NF10	0.375	0.125	0.5	1.5	282.5 ± 3.5	93.12 ± 2.3	0.434 ± 0.019
NF11	0.25	0.125	0.375	1.5	282.8 ± 4.3	85.11 ± 3.2	0.394 ± 0.026
NF12	0.375	0.1875	0.375	1.5	271.6 ± 3.9	73.54 ± 2.9	0.385 ± 0.022
NF13	0.5	0.125	0.375	1.5	310.6 ± 3.6	86.22 ± 3.2	0.39 ± 0.018
NF14	0.5	0.25	0.375	1.5	276.1 ± 4.1	76.11 ± 2.3	0.384 ± 0.026
NF15	0.375	0.125	0.25	1.5	304.3 ± 3.2	84.23 ± 3.1	0.4 ± 0.021
NF16	0.25	0.1875	0.5	1.5	344.6 ± 4.2	94.22 ± 1.9	0.474 ± 0.018
NF17	0.375	0.1875	0.375	1.5	276.7 ± 4.1	71.35 ± 2.9	0.376 ± 0.025

SD: Standard deviation, AO: Aloe vera oil, CDR: Cumulative drug release, FC: Formulation code

that rotated at 50 rpm while maintaining a temperature of 37 ± 0.5 °C. The niosomal gel (1 g) was transferred to the donor compartment and covered with aluminum foil. Two milliliters of samples were taken out at specific intervals up to 6 h and the drug content was quantified by UV-visible spectrophotometer. The drug permeability (mg/cm^2) versus time graph was plotted and compared with the OLM gel. The flux (J), permeability coefficient (P), at 6 h, and enhancement ratio (ER) were estimated using the following equations:

$$\text{Flux (J)} = \left(\frac{\text{Amount of drug permeated}}{\text{Surface area of buccal mucosa}}\right) \times \frac{1}{\text{Time}}$$

$$\text{Permeability coefficient (P)} = \frac{\text{Flux}}{\text{Concentration}}$$

$$\text{ER} = \frac{\text{Flux of niosomal gel formulation}}{\text{Flux of gel formulation}}$$

Fourier transform infrared radiation (FTIR) study

FTIR (Bruker, Alpha-E, Germany) was used to analyze OLM, Span 60, cholesterol, and niosome ranging from 4000 to 600 cm^{-1} at room temperature.

Transmission electron microscopy (TEM)

Niosomal formulations were stained with 1% phosphotungstic acid and the shape of niosomes was monitored using a transmission electron microscope (JEM 2100, Jeol, Japan).

Histopathology

After the application of gel, the cross-sectioned chicken mucosa was stained with hematoxylin and eosin to observe the histological alterations. The results were compared with control chicken mucosa.[7]

Statistical analysis

The results are expressed as mean ± SD (n= 3). The group means were compared using Student's t-test. A value of $p < 0.05$ was used to denote statistical significance.

RESULTS

Calibration curve of the OLM

The calibration curve of OLM was plotted using drug concentration on the X-axis and absorbance on the Y-axis. The calibration curve of the OLM is depicted in Figure 1. The calibration plot of OLM showed a good linear relationship with the standard regression equation, y= 0.037x-0.003 in 10% (*v/v*) methanol in phosphate buffer (pH 6.8) medium over the concentration range studied. The correlation coefficient (R^2= 0.9997) indicated high significance. The linear regression data for the calibration plot are indicative of a good linear. The LOD for OLM was found to be 0.46 µg/mL, whereas the value of LOQ was found to be 1.39 µg/mL. The LOD and LOQ were found to be at the microgram level, indicating the sensitivity of the method.

Characterization of the niosomes

The size of the niosome vesicles ranged from 265.3 ± 5.3 nm to 344.6 ± 4.2 nm. The Polydispersity index (PDI) of niosome ranged from 0.21 ± 0.06 to 0.33 ± 0.09. The zeta potential was found in the range between -32.6 ± 1.8 and -38.4 ± 2.3 mV. The entrapment efficiency was found range between 69.34 ± 1.9% and 86.23 ± 2.7%.

Analysis of the design

Three levels, *i.e.* high, middle, and low, were used for investigating each independent factor in the Box-Behnken design. In this study, the manufacturing process of niosomal formulations was optimized by considering three independent variables at three levels (Table 2), as well as their binary interactions and polynomial outcomes. The three independent variables were optimized in 17 formulations with five replicates of the center point. Based on the above evaluation studies, vesicle size, CDR (%), and permeability were chosen as responses for optimizing niosomal formulation.

Vesicle size

The effects of A, B, and C represent the average result of changing one variable at a time from its low level to its high level. From the above formula, it is stated that the high concentration of Span 60 (A; $p < 0.6789$ and f value 0.1865) showed a more prominent effect on vesicle size than cholesterol concentration (B; $p < 0.0021$ and f value 22.66) and AO (C; $p < 0.0275$ and f value 7.70). The p value (< 0.0001) indicated that cholesterol (B), AO (C), and their combination, respectively, have synergistic and antagonistic effects on vesicle size as a response variable. The combination of AB (Span 60 and cholesterol) and AC (Span 60 and AO) had a greater negative effect on vesicle size, whereas BC (cholesterol and AO) had a positive effect. It is asserted by the respective p value and coded equation. In addition, the coded factor claims that a synergistic effect was observed in binate amounts of constrained independent variables such as A and C. The analysis of variance (ANOVA) table of vesicle size, CDR (%), and permeability of the niosomal formulations is depicted in Table 3. The interaction between Span 60 and AO had a significant negative effect on vesicle size. The interaction between Span 60 and cholesterol had a significant negative effect on vesicle size. The vesicle size ranged from 265.3 nm to 344.6 nm.

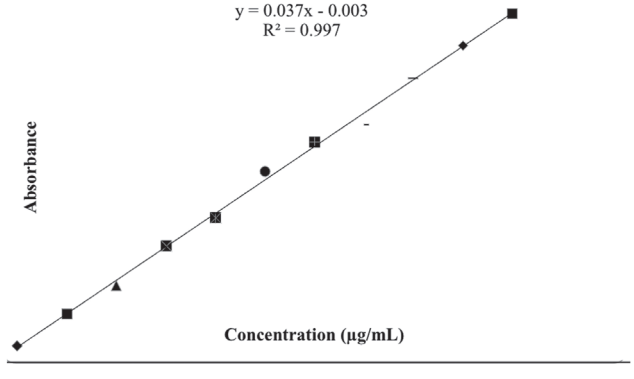

Figure 1. Calibration curve of OLM in 10% (v/v) methanol in phosphate buffer (pH 6.8)

OLM: Olmesartan medoxomil

Table 3. ANOVA table of vesicle size, CDR, and permeability

Parameters	Source	Sum of squares	DF	Mean square	*f* value	*p* value	
Vesicle size (nm)	Model	10268.63	9	1140.96	106.37	< 0.0001	Significant
	A-Span 60	2.00	1	2.00	0.1865	0.6789	
	B-cholestrol	243.10	1	243.10	22.66	0.0021	
	C-AO	82.56	1	82.56	7.70	0.0275	
	AB	625.00	1	625.00	58.27	0.0001	
	AC	114.49	1	114.49	10.67	0.0137	
	BC	699.60	1	699.60	65.22	< 0.0001	
	A^2	4449.42	1	4449.42	414.81	< 0.0001	
	B^2	724.50	1	724.50	67.54	< 0.0001	
	C^2	3226.61	1	3226.61	300.81	< 0.0001	
	Residual	75.08	7	10.73			
	Lack of fit	39.83	3	13.28	1.51	0.3415	Not significant
	Pure error	35.25	4	8.81			
	Cor total	10343.72	16				
CDR (%)	Model	0.0292	9	0.0032	110.56	< 0.0001	Significant
	A-Span 60	0.0006	1	0.0006	19.67	0.0030	
	B-cholestrol	0.0003	1	0.0003	9.00	0.0199	
	C-AO	0.0160	1	0.0160	545.18	< 0.0001	
	AB	0.0001	1	0.0001	4.50	0.0716	
	AC	0.0040	1	0.0040	137.22	< 0.0001	
	BC	0.0031	1	0.0031	104.82	0.0001	
	A^2	0.0005	1	0.0005	17.89	0.0039	
	B^2	0.0029	1	0.0029	99.30	< 0.0001	
	C^2	0.0017	1	0.0017	56.32	0.0001	
	Residual	0.0002	7	0.0000			
	Lack of fit	0.0001	3	0.0000	0.7895	0.5595	Not significant
	Pure error	0.0001	4	0.0000			
	Cor total	0.0294	16				
Permeability	Model	1344.10	9	149.34	189.78	< 0.0001	Significant
	A-Span 60	35.36	1	35.36	44.94	0.0003	
	B-cholestrol	45.55	1	45.55	57.89	0.0001	
	C-AO	549.63	1	549.63	698.44	< 0.0001	
	AB	25.65	1	25.65	32.60	0.0007	
	AC	154.38	1	154.38	196.18	< 0.0001	
	BC	57.76	1	57.76	73.40	< 0.0001	
	A^2	1.54	1	1.54	1.96	0.2047	
	B^2	386.59	1	386.59	491.26	< 0.0001	
	C^2	63.62	1	63.62	80.84	< 0.0001	
	Residual	5.51	7	0.7869			
	Lack of fit	0.2888	3	0.0963	0.0738	0.9709	Not significant
	Pure error	5.22	4	1.30			
	Cor total	1349.61	16				

ANOVA: Analysis of variance, CDR: Cumulative drug release, DF: Degrees of freedom, AO: Aloe vera oil

Graph claims that term BC (cholesterol and AO) is associated with positive effects on vesicle size under constrained conditions of increasing cholesterol from low concentration (0.125 mmol) to high concentration (0.25 mmol) and AO at moderate level (0.375 mL) with constant level of Span 60 (0.25 mmol) shown antagonistic effect of response factor. It is possible that at greater levels of cholesterol, it can directly cause vesicle fusion and reduce the vesicle size from 301 to 259 nm, as shown in the graph. On the other hand, in the case of high AO concentration under constrained conditions, the cholesterol concentration increased and vesicle size increased. Based on the analysis of the three (AB, AC, BC) second-order interactions, BC showed a greater influence on the response factor (vesicle size).

At low levels of AO and increasing cholesterol concentration, it was found that the vesicle size decreased, but at a high level of AO and increasing cholesterol concentration, it was found that the vesicle size increased (Figure 2). The response surface plot revealed that the independent variables Span 60, cholesterol, and AO significantly influenced vesicle size (Figure 3). The quadratic equation for vesicle size was generated as follows:

Vesicle size = + 272.56 - 0.51A - 5.51B + 3.21C - 12.50AB - 5.35AC + 13.22BC + 32.51A^2 -13.12B^2 + 27.68C^2

CDR (%)

It was stated that AO (C; $p < 0.0001$ and f value 545.18) showed a prominent effect on CDR compared to the non-ionic surfactant (A; $p < 0.003$ and f value 19.67) and cholesterol (B; $p < 0.019$ and f value 9.0). AB, AC, and BC terms were tested for their effects on CDR (%) using the factor tool. The results of the study claim that AC does not obey additive fashion. Instead, AC (Span 60 and AO) showed a negative effect on decreasing percentage CDR with constrained conditions AO at low level to high level (0.25 mL to 0.5 mL). The percentage CDR was found to be between 65.13% and 96.22%. At a higher level of AO (C) term and low level of Span 60 (A) term, showed CDR (%) as 94.22%. On further increment of Span 60 (A), the graph witnessed a decline of CDR (%) as 77.34%. A high concentration of cholesterol significantly influenced the CDR (%) and had a negative effect on CDR. The interaction between non-ionic surfactant and cholesterol had a negative effect on CDR (%). The interaction between non-ionic surfactant and AO had a negative effect on CDR (%). The CDR (%) of the optimized niosomal formulation is depicted in Figure 4. The quadratic equation of CDR (%) was generated as follows:

CDR (%)= + 72.96 - 2.10A - 2.39B + 8.29C - 2.53AB - 6.21AC + 3.80BC + 9.58B^2 + 3.89C^2

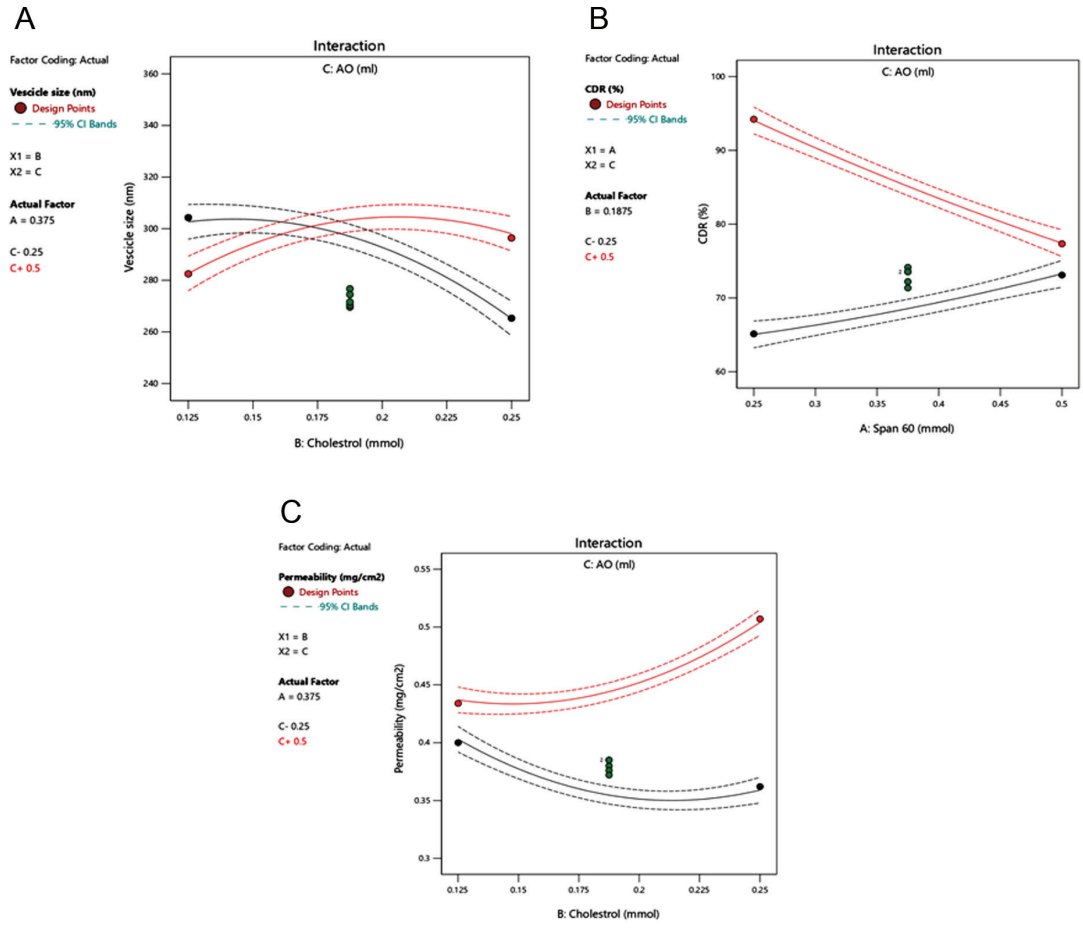

Figure 2. Interaction of (A) vesicle size (nm), (B) CDR (%), and (C) permeability (mg/cm^2)

CDR: Cumulative drug release

Permeability

It was stated that AO (C; $p < 0.0001$, f value 698.44) had an eminent effect compared with surfactant concentration (A; $p < 0.0003$, f value 44.94) and cholesterol concentration (B; $p < 0.0001$, f value 9.00). The cholesterol and AO concentrations (C; $p < 0.0001$, f value 698.44) showed a positive effect on permeability as a result the permeation increases from 0.421 mg/cm^2 to 0.507 mg/cm^2 at the constrained condition as AO (C) at high level (0.5 mL) and temperature at room condition. High permeability of the drug obtained with high concentrations of cholesterol and AO. High concentrations of non-ionic surfactant had a negative effect on permeability. The interaction between the non-ionic surfactant and AO showed a negative effect on permeability. The drug permeation was found to range from 0.321 mg/cm^2 to 0.507 mg/cm^2. The permeability study of the formulations is depicted in Table 4 and Figure 5. The presence of AO and increased drug permeation could be attributed to the disruption of the structural arrangement of the lipid sequences in the mucosa, which promotes lipid fluidity. At a high AO concentration, the permeability of the drug was increased by increasing the cholesterol concentration. The quadratic equation of permeability was generated as follows:

Permeability= + 0.3796 - 0.0085A + 0.0058B + 0.0448C - 0.0318AC + 0.0278BC - 0.0112A^2 + 0.0263B^2 + 0.0198C^2

The effect of any two variables on the response parameter was used to generate the response surface plot of vesicle size, CDR (%), and permeability which is depicted in Figure 3.

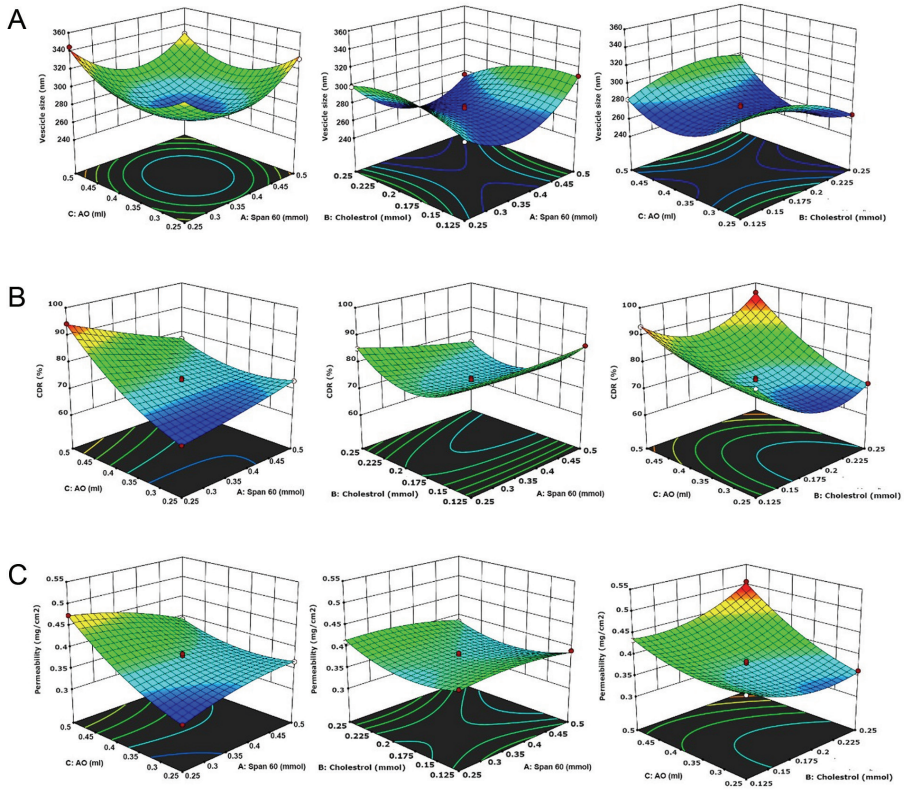

Figure 3. Response surface plot of (A) vesicle size (nm), (B) CDR (%), and (C) permeability (mg/cm^2)
CDR: Cumulative drug release

Table 4. Data generated from Box-Behnken design analysis of niosomal formulations and predicted and observed values of the optimized formulation (NF8)

Responses	Vesicle size (nm)	CDR (%)	Permeability (mg/cm^2)
R^2	0.9927	0.9959	0.9930
Adjusted R^2	0.9834	0.9907	0.9840
Predicted R^2	0.9331	0.9905	0.9516
Adeq precision	30.5098	45.6792	44.1961
Predicted value of the optimized formulation (NF8)	291.56	97.11	0.498
Observed value of the optimized formulation (NF8)	296.4	96.22	0.507

CDR: Cumulative drug release

Formulation optimization

In all responses, the predicted R^2 values were found to be in good agreement with the adjusted R^2. It was preferable to have a signal-to-noise ratio greater than 4 (Table 4). The trial runs were fitted in the design of the experiment software and analyzed by ANOVA. The niosomal gel formulation was optimized on the basis of particle size, CDR, and permeability studies. Based on the desirability value obtained by the software, the closest value to 1 was chosen as the optimized formulation. Based on the analysis, NF8, where Span 60 (0.375 mmol), cholesterol (0.25 mmol), and AO (0.5 mL) (desirability= 0.89) were considered the optimized formulation.

TEM

It was revealed that the niosome had a spherical shape and uniform size, which was confirmed by the TEM study (Figure 5). The vesicle size of niosome found in the TEM study showed good agreement with the dynamic light scattering method.

FT-IR

The FTIR spectra of the OLM, Span 60, cholesterol, AO, and niosomal formulations are depicted in Figure 6. The FTIR spectra of OLM showed peaks at 2995.37 cm^{-1}, 2923.16 cm^{-1} due to C-H stretching, 1708.12 cm^{-1}, 1831.99 cm^{-1} due to C-O stretching and 3299.12 cm^{-1} due to N-H stretching. The same peaks were found in the niosomal formulation, and there were no significant changes in the wavenumber in the formulations. Thus, it can be confirmed that the drug was entrapped in the formulations.

Evaluation of niosomal gel

The drug content of OLM niosomal gel and OLM gel was found to be 97.9 ± 3.5% and 98.60 ± 3.2% respectively. The pH of the OLM niosomal gel and OLM gel was found to be 6.5 and 6.7, respectively, which could be within tolerable limits. Spreadability is responsible for supplying the right dose to the intended place and adding it to the substrate rapidly. In the results of spreadability studies, OLM niosomal gel was found to be 5.6 ± 0.3 cm and revealed significantly higher ($p < 0.05$) than the OLM gel (4.3 ± 0.5 cm).

Ex vivo permeation studies

Chicken pouch mucosa is believed to be a suitable model for *ex vivo* permeation studies because it is widely available and offers an alternative to the keratinized mucosa of rats and partially keratinized rabbit mucosa.[27] Because of the non-keratinized nature of chicken mucosa, *ex vivo* investigations could alter it to mimic human mucosa.

The *ex vivo* buccal permeation of the OLM niosomal gel and OLM gel is shown in Table 5 and Figure 7. After 6 h, the results showed that *ex vivo* mucosal permeation was greater in the case of OLM niosomal gel than in the case of OLM gel loaded with an equivalent amount of drug. It was probably the presence of the surfactant and AO in the niosomal gel. The smaller size range of the niosomes also accounted for this penetration enhancement. The results showed that the drug permeation characteristics of the optimized niosomal gel (0.507 mg/cm^2)

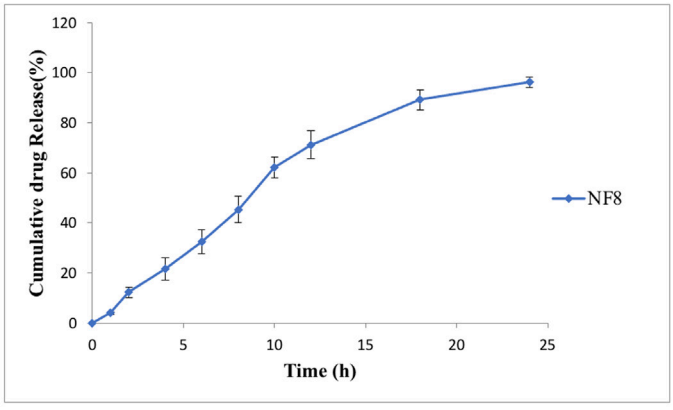

Figure 4. Cumulative drug release (%) of optimized niosomal formulation (NF8). Data are presented as mean ± SD (n= 3)

SD: Standard deviation

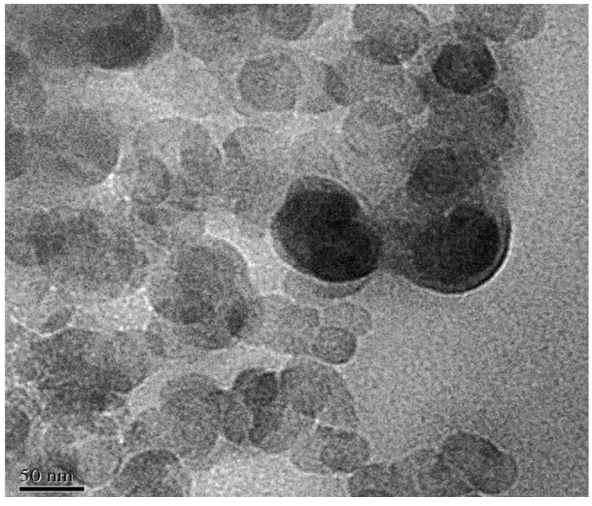

Figure 5. TEM study of optimized niosomal formulation (NF8)

TEM: Transmission electron microscopy

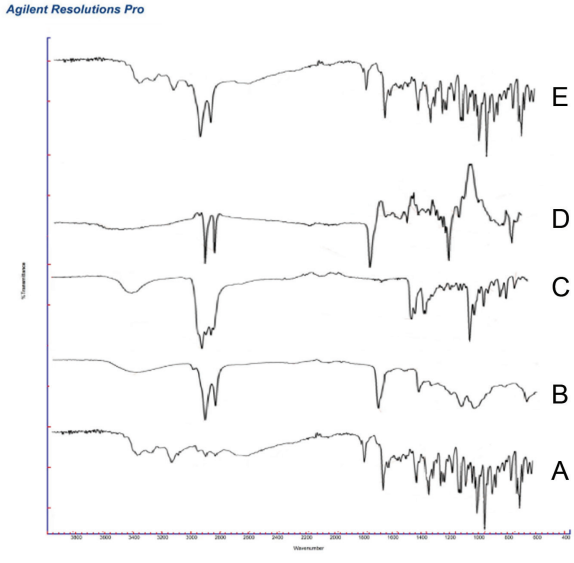

Figure 6. FT-IR analysis of (A) OLM, (B) Span 60, (C) cholesterol, (D) AO, and (E) niosomes (NF8)

FT-IR: Fourier transform infrared spectroscopy, OLM: Olmesartan medoxomil, AO: Aloe vera oil

Table 5. *Ex vivo* permeation studies of niosomal gel formulations (data presented as mean ± SD (n= 3)

FC	Permeability (mg/cm²)	Flux (J) (mg/cm² h)	Permeability coefficient (P) (cm/h)
NF1	0.385 ± 0.015	0.057 ± 0.003	0.028 ± 0.002
NF2	0.372 ± 0.023	0.051 ± 0.006	0.025 ± 0.003
NF3	0.411 ± 0.013	0.063 ± 0.004	0.032 ± 0.002
NF4	0.366 ± 0.019	0.057 ± 0.005	0.028 ± 0.002
NF5	0.362 ± 0.026	0.054 ± 0.007	0.027 ± 0.004
NF6	0.321 ± 0.025	0.048 ± 0.006	0.024 ± 0.003
NF7	0.392 ± 0.023	0.060 ± 0.006	0.030 ± 0.003
NF8	0.507 ± 0.017	0.083 ± 0.005	0.041 ± 0.003
NF9	0.38 ± 0.021	0.057 ± 0.006	0.028 ± 0.003
NF10	0.434 ± 0.019	0.067 ± 0.005	0.033 ± 0.002
NF11	0.394 ± 0.026	0.062 ± 0.007	0.031 ± 0.004
NF12	0.385 ± 0.022	0.058 ± 0.005	0.029 ± 0.002
NF13	0.39 ± 0.018	0.062 ± 0.004	0.031 ± 0.002
NF14	0.384 ± 0.026	0.062 ± 0.006	0.031 ± 0.003
NF15	0.4 ± 0.021	0.055 ± 0.005	0.027 ± 0.002
NF16	0.474 ± 0.018	0.076 ± 0.004	0.038 ± 0.002
NF17	0.376 ± 0.025	0.057 ± 0.007	0.028 ± 0.004

SD: Standard deviation, FC: Formulation code

were significantly (p <0.05) better than those of the plain gel (0.261 mg/cm²). Based on the ER results, it was found that OLM from the niosomal buccal gel permeates significantly (p < 0.05) faster (approximately more than 2 times) compared to the OLM suspension (Table 6).

Histopathology

Chicken buccal mucosa without gel, OLM gel, and niosomal gel application are shown in Figure 8. Histological observation revealed that control of the buccal mucosa was lined by stratified squamous epithelium with ducts in the submucosa. A layer of smooth muscles was noticed below the submucosa. OLM gel treated buccal showed no severe damage to the buccal mucosa integrity compared with the untreated control. A slight thinning of the epithelium, fewer ducts in the smooth mucosa, and a thin layer of smooth muscle were noticed in the buccal mucosa treated with OLM gel.

DISCUSSION

PDI shows homogeneity of vesicle size. The lower value of PDI shows that formulation is more homogeneous in nature.[18] Based on the zeta potential results, the OLM niosomes showed sufficient dispersion stability. Stable formulations have a zeta potential between +30 mV and -30 mV.[19] Higher concentrations of Span 60 may increase the possibility of vesicle aggregation, which frequently lowers the possibility of forming a stable film surface. As a result, there is drug leakage, which lowers the drug entrapment efficacy. It was found that raising the cholesterol level improved the effectiveness of drug entrapment.[17] Based on these results, cholesterol played a

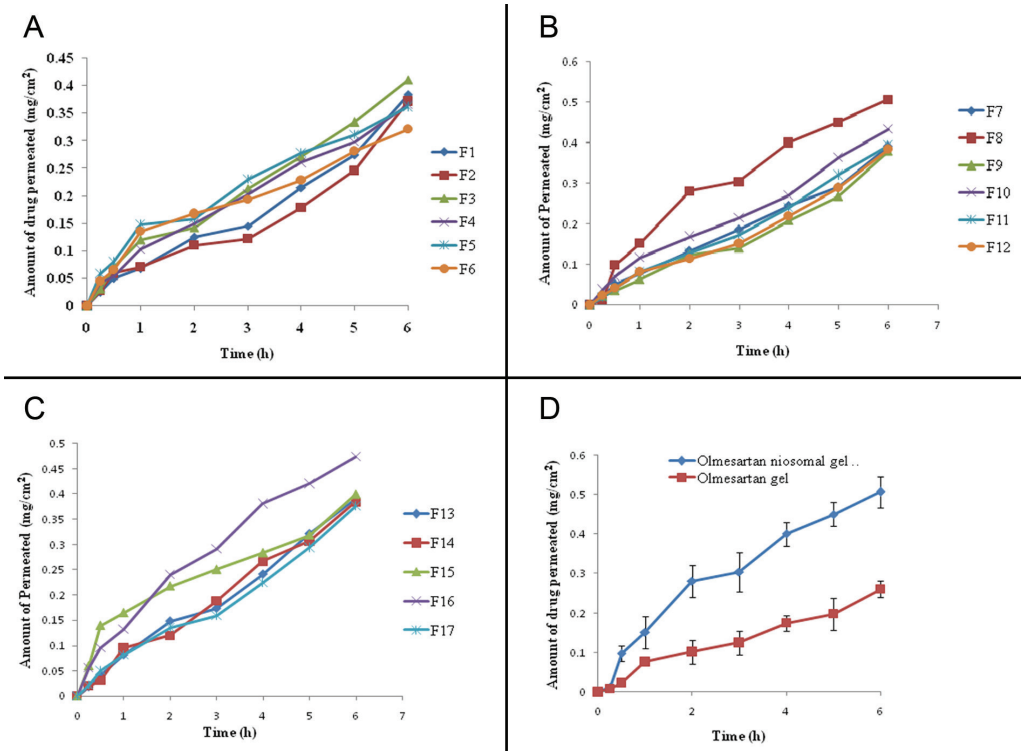

Figure 7. *Ex vivo* permeation studies of (A) NF1-NF6, (B) NF7-NF12, (C) NF13-NF17, and (D) OLM gels. Data are presented as mean ± SD (n= 3)
OLM: Olmesartan medoxomil, SD: Standard deviation

significant role in particle size. It was predicted that at low cholesterol levels, non-ionic surfactant and cholesterol would pack tightly together, increasing curvature and shrinking in size.[20] As the AO concentration increases, the high surfactant charge increases vesicle aggregation and cohesive force by reducing the interfacial tension between phases.[21] When the concentration of cholesterol increases, the hydrophobicity of the bilayer membrane increases, resulting in an increase in the vesicle size to achieve a more thermodynamically stable shape.[22,23] This mechanism influences the increase in vesicle size. This may be due to AO occupying the space of the surfactant molecule influencing the increase in vesicle size. It was determined that the vesicle size increased as the Span 60 concentration increased, possibly because stronger contraction caused vesicle aggregation. By increasing the level of surfactant, the formulation becomes more consistent and the diffusional path length of the vesicles increases.[24] In addition, the surfactant concentration acts as a depot, reducing drug leakage from niosomal to dissolution media. Drug release from niosomal vesicles was reduced as the concentration of Span 60 increased. This may be because an improvement in the surfactant concentration acts as a depot, reducing drug leakage from niosome to dissolution media.[25] Drug release was decreased by increasing the cholesterol concentration. This may be due to the rigidization of vesicles, resulting in the minimization of drug transport from the vesicles to the dissolution medium. Cholesterol influences the fluidity of the membrane; at low temperatures, it increases fluidity. In addition, AO at a high level enhances permeability by facilitated permeation, *i.e.* transient reduction in barrier resistance of stratum corneum (SC). The composition of chicken buccal mucosa and AO also alters lipid bilayer fluidity. The observations show that there is a possibility of high drug permeation by AO, as evidenced by the keratinization of coenocytes in the chicken buccal mucosa (SC).[26] Non-ionic surfactant concentration showed a promising effect on permeability.The addition of surfactant, which helps to solubilize lipids in the mucosa and allows for high vesicle penetration, may result in higher drug permeability.[17] The lower permeation of OLM from the suspension than from the niosomal formulation may be due to the higher log *p* value of OLM.[28] Niosome can alter drug transport through the mucosa because of adsorption on the surfaceof the mucosa, which results in a high thermodynamic activity gradient of the drug at the interface, which helps act as a driving force for permeating the lipophilic drug. The ability of vesicles to enhance penetration is related to a decrease in the barrier properties of the mucosa by niosome. This may be explained by the superiority of niosomal carriers, which have high permeation in mucosal layers due to carrier portion integration with mucosal lipids. Surfactants in vesicular form reduce the crystallinity of the skin's intracellular lipid bilayer, improving drug permeation.[29] Reduced layers of epithelium, no ducts in the submucosa, a thin layer of the submucosa, and smooth muscles were noticed in the buccal mucosa treated with OLM niosomal gel, which could be additional evidence of enhanced drug permeability.

CONCLUSION

The Box-Behnken design was used to optimize the OLM niosomal gel formulations. Noisome formulation (NF8) was chosen as an optimized formulation of the niosomal gel because of its small vesicle size (296.4 ± 3.9 nm, PDI= 0.21

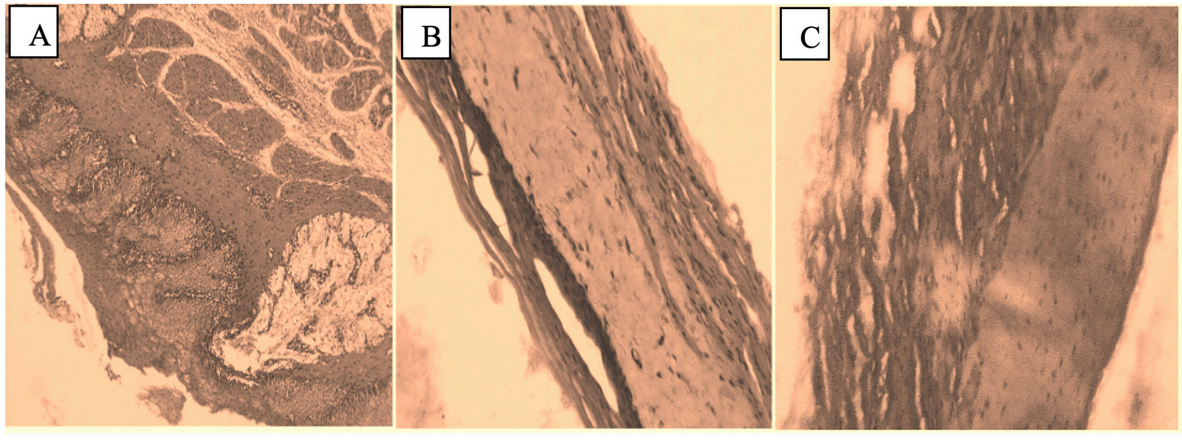

Figure 8. Histopathology of chicken buccal mucosa after 6 hours of permeation study (A) control, (B) OLM gel, and (C) OLM niosomal gel
OLM: Olmesartan medoxomil

Table 6. *Ex vivo* permeation study of the OLM gel and OLM niosomal gel (NF8). Data presented as mean ± SD (n= 3)

FC	Permeability (mg/cm^2)	Flux (J) (mg/cm^2 h)	Permeability coefficient (J/C) (cm/h)	ER
OLM gel	0.261 ± 0.013	0.040 ± 0.002	0.020 ± 0.001	-
OLM niosomal gel (NF8)	0.507 ± 0.017	0.083 ± 0.005	0.041 ± 0.003	2.05 ± 0.18

OLM: Olmesartan medoxomil, ER: Enhancement ratio, FC: Formulation code

± 0.06) and high CDR (96.22 ± 2.9%). Permeability studies of niosomal gel formulations were performed using chicken buccal pouches. The optimized niosomal formulations showed higher permeation rates (0.507 ± 0.017 mg/cm^2) than plain OLM gel (0.261 ± 0.013), which may be useful in increasing the systemic presence of OLM in the body. The niosomal gel exhibited significant permeation with an almost 2.05-fold increase in flux compared with the OLM gel. Thus, the buccal administration of niosomal gel could help improve OLM bioavailability.

Ethics

Ethics Committee Approval: The *ex vivo* permeation studies were conducted using chicken buccal mucosa. The buccal mucosa was procured from local slughter house. So this study does not require animal ethics approval.

Informed Consent: Not required.

Authorship Contributions

Concept: N.N.P, Design: N.N.P, B.C.M., Data Collection or Processing: N.N.P, J.R., Analysis or Interpretation: N.N.P, P.M.G., Literature Search: N.N.P, B.C.M., Writing: N.N.P, B.C.M.

Conflict of Interest: Authors declared no conflicts of interest.

Financial Disclosure: This research did not receive any specific grant from funding agencies in the public, commercial, or not-for-profit sectors.

REFERENCES

1. Madhav NV, Shakya AK, Shakya P, Singh K. Orotransmucosal drug delivery systems: a review. J Control Release. 2009;140:2-11.
2. Abdelbary GA, Aburahma MH. Oro-dental mucoadhesive proniosomal gel formulation loaded with lornoxicam for management of dental pain. J Liposome Res. 2015;25:107-121.
3. Allam A, Fetih G. Sublingual fast dissolving niosomal films for enhanced bioavailability and prolonged effect of metoprolol tartrate. Drug Des Devel Ther. 2016;10:2421-2433.
4. El-Alim SA, Kassem A, Basha M. Proniosomes as a novel drug carrier system for buccal delivery of benzocaine. J Drug Deliv Sci Technol. 2014;24:452-458.
5. Kaithwas V, Dora CP, Kushwah V, Jain S. Nanostructured lipid carriers of olmesartan medoxomil with enhanced oral bioavailability. Colloids Surf B Biointerfaces. 2017;154:10-20.
6. Khattab WM, Zein El-Dein EE, El-Gizawy SA. Formulation of lyophilized oily-core poly-ε-caprolactone nanocapsules to improve oral bioavailability of Olmesartan Medoxomil. Drug Dev Ind Pharm. 2020;46:795-805.
7. Alsofany JM, Hamza MY, Abdelbary AA. Fabrication of nanosuspension directly loaded fast-dissolving films for enhanced oral bioavailability of olmesartan medoxomil: *in vitro* characterization and pharmacokinetic evaluation in healthy human volunteers. AAPS PharmSciTech. 2018;19:2118-2132.
8. Komesli Y, Burak Ozkaya A, Ugur Ergur B, Kirilmaz L, Karasulu E. Design and development of a self-microemulsifying drug delivery system of olmesartan medoxomil for enhanced bioavailability. Drug Dev Ind Pharm. 2019;45:1292-1305.
9. Jain S, Patel K, Arora S, Reddy VA, Dora CP. Formulation, optimization, and in vitro-*in vivo* evaluation of olmesartan medoxomil nanocrystals. Drug Deliv Transl Res. 2017;7:292-303.
10. Prajapati ST, Bulchandani HH, Patel DM, Dumaniya SK, Patel CN. Formulation and evaluation of liquisolid compacts for olmesartan medoxomil. J Drug Deliv. 2013;2013:870579.
11. Nooli M, Chella N, Kulhari H, Shastri NR, Sistla R. Solid lipid nanoparticles as vesicles for oral delivery of olmesartan medoxomil: formulation, optimization and in vivo evaluation. Drug Dev Ind Pharm. 2017;43:611-617.
12. Singh S, Pathak K, Bali V. Product development studies on surface-adsorbed nanoemulsion of olmesartan medoxomil as a capsular dosage form. AAPS PharmSciTech. 2012;13:1212-1221.
13. Thakkar HP, Patel BV, Thakkar SP. Development and characterization of nanosuspensions of olmesartan medoxomil for bioavailability enhancement. J Pharm Bioallied Sci. 2011;3:426-434.
14. Fantini A, Giulio L, Delledonne A, Pescina S, Sissa C, Nicoli S, Santi P, Padula C. Buccal permeation of polysaccharide high molecular weight compounds: effect of chemical permeation enhancers. Pharmaceutics. 2023;15:129.
15. Nobilis M, Kopecký J, Kvetina J, Chládek J, Svoboda Z, Vorísek V, Perlík F, Pour M, Kunes J. High-performance liquid chromatographic determination of tramadol and its O-desmethylated metabolite in blood plasma. Application to a bioequivalence study in humans. J Chromatogr A. 2002;949:11-22.
16. Das MK, Palei NN. Sorbitan ester niosomes for topical delivery of rofecoxib. Indin J Exp Biol. 2011;49:438-445.
17. Shilakari Asthana G, Asthana A, Singh D, Sharma PK. Etodolac containing topical niosomal gel: formulation development and evaluation. J Drug Deliv. 2016;2016:9324567.
18. Hegdekar NY, Priya S, Shetty SS, Jyothi D. Formulation and evaluation of niosomal gel loaded with asparagus racemosus extract for anti-inflammatory activity. Ind J Pharm Edu Res. 2023;57:63-74.
19. Nagaich U, Gulati N. Nanostructured lipid carriers (NLC) based controlled release topical gel of clobetasol propionate: design and in vivo characterization. Drug Deliv Transl Res. 2016;6:289-298.
20. Rahman SA, Abdelmalak NS, Badawi A, Elbayoumy T, Sabry N, El Ramly A. Formulation of tretinoin-loaded topical proniosomes for treatment of acne: *in-vitro* characterization, skin irritation test and comparative clinical study. Drug Deliv. 2015;22:731-739.
21. Ng N, Rogers MA. Surfactants. In: Melton L, Shahidi F, Varelis P, (eds). Encyclopedia of Food Chemistry. Oxford: Academic Press; 2019:276-282.
22. Essa E. Effect of formulation and processing variables on the particle size of sorbitan monopalmitate niosomes. Asian J Pharm. 2010;4:227-233.
23. Patel KK, Kumar P, Thakkar HP. Formulation of niosomal gel for enhanced transdermal lopinavir delivery and its comparative evaluation with ethosomal gel. AAPS PharmSciTech. 2012;13:1502-1510.
24. Elmotasem H, Awad GEA. A stepwise optimization strategy to formulate *in situ* gelling formulations comprising fluconazole-hydroxypropyl-beta-cyclodextrin complex loaded niosomal vesicles and Eudragit nanoparticles for enhanced antifungal activity and prolonged ocular delivery. Asian J Pharm Sci. 2020;15:617-636.
25. Line JE, Svetoch EA, Eruslanov BV, Perelygin VV, Mitsevich EV, Mitsevich IP, Levchuk VP, Svetoch OE, Seal BS, Siragusa GR, Stern NJ.

Isolation and purification of enterocin E-760 with broad antimicrobial activity against gram-positive and gram-negative bacteria. Antimicrob Agents Chemother. 2013;5:525-535.

26. Vashisth I, Ahad A, Aqil M, Agarwal SP. Investigating the potential of essential oils as penetration enhancer for transdermal losartan delivery: Effectiveness and mechanism of action. Asian J Pharm Sci. 2014;9:260-267.
27. El-Nahas AE, Allam AN, El-Kamel AH. Mucoadhesive buccal tablets containing silymarin Eudragit-loaded nanoparticles: formulation, characterisation and ex vivo permeation. J Microencapsul. 2017;34:463-474.
28. Butreddy A, Dudhipala N, Veerabrahma K. Development of olmesartan medoxomil lipid-based nanoparticles and nanosuspension: preparation, characterization and comparative pharmacokinetic evaluation. Artif Cells Nanomed Biotechnol. 2018;46:126-137.
29. Kumbhar D, Wavikar P, Vavia P. Niosomal gel of lornoxicam for topical delivery: *in vitro* assessment and pharmacodynamic activity. AAPS PharmSciTech. 2013;14:1072-1082.

Turk J Pharm Sci 2024;21(3):211-218
DOI: 10.4274/tjps.galenos.2023.91267

ORIGINAL ARTICLE

The Effect of Sucrose and Yeast Extract on Total Phenolic, Flavonoid, and Anthocyanin of Lactic-Acid-Fermented Mangosteen Fruit Peel (*Garcinia mangostana* L.)

Komang Dian Aditya PUTRA, G. A. Desya PRADNYASWARI, Putu Sanna YUSTIANTARA, I Made Agus Gelgel WIRASUTA, Eka Indra SETYAWAN*

Udayana University Faculty of Mathematics and Natural Sciences, Department of Pharmacy, Bali, Indonesia

ABSTRACT

Objectives: This study aimed to determine the most suitable concentration of sucrose and yeast extract (SYE) and its impact on the levels of total phenol, flavonoid, and anthocyanin (TPFA) for lactic acid fermentation in mangosteen fruit peel.

Materials and Methods: In this study, the primary components were mangosteen fruit peel, SYE, and lactic acid bacteria starter. The experimental design was conducted using the Factorial Design method. The colorimetric method was used to determine the total phenol (Folin-Ciocalteu reagent) and total flavonoid ($AlCl_3$ reagent). In addition, the differential pH method was used to determine the total anthocyanins using KCl and the CH_3COONa reagent.

Results: The addition of SYE during the fermentation of mangosteen fruit peel significantly increased the concentrations of TPFA compared with the control (*p* value of 0.0001). The high sucrose concentration and low yeast extract produced the highest TPFA levels in mangosteen rind fermentation.

Conclusion: The use of SYE affects the levels of TPFA in lactic acid-fermented mangosteen fruit peel, with the most suitable concentrations obtained using sucrose (45 g/L) and yeast extract (2.5 g/L).

Keywords: Fermentation, *Garcinia mangostana* fruit peel, sucrose, yeasts

INTRODUCTION

Herbal products are parts of plants intended for health use according to their properties and can be developed into medicinal products, food supplements, and cosmetics.[1-3] One of the plants that can be developed into herbal products is the mangosteen fruit (*Garcinia mangostana* L.). It has health benefits for the body and is dubbed the Queen of Fruits.[4] The amount of waste generated by the mangosteen processing industry is considerable, as approximately 60% of the mangosteen fruit is made up of inedible fruit peel.[5] Mangosteen fruit peel extract has been reported to contain many phenolic compounds that can help overcome health issues such as cancers, tumors, diabetes, hypertension, inflammation, and skin aging.[6-8]

The extraction process is one of the important steps that need to be determined by a researcher to obtain the desired bioactive compounds.[9,10] Fermentation is one of the natural extraction processes involving microorganisms and enzymatic processes that result in the degradation of plant cell walls

*Correspondence: indrasetyawan@ymail.com, Phone: +6281364892853, ORCID-ID: orcid.org/0000-0003-3236-5904
Received: 17.05.2023, Accepted: 19.07.2023

so that phytochemical components can be released from the matrix.[11] Lactic acid fermentation has been shown in previous studies to significantly enhance the nutrient and phytochemical profile of the substrate.[12-14] A different research also suggested that lactic acid fermentation on mulberry fruit substrate significantly influences the levels of total phenol, flavonoid, and anthocyanin (TPFA) compounds.[15,16] In addition, lactic acid fermentation also causes the fermentation environment to become acidic, which correlates with the release of bioactive compounds and by-products of fermentation.[17,18] Several factors that influence the fermentation of lactic acid are the source of carbon and nitrogen, in particular their type and concentration. The carbon source used in this research is sucrose, and the nitrogen source is yeast extract.[19,20] In another study, a sucrose concentration of 15-45 g/L was used as a carbon source, and yeast extract of 2.5-7.5 g/L was used as a nitrogen source during fermentation.[19] However, the fermentation of mangosteen peel has not been widely studied as an advanced processing step to increase phytochemical components; therefore, further studies are necessary. This study aimed to determine the most suitable concentration of sucrose and yeast extract (SYE) and its impact on the levels of TPFA for lactic acid fermentation in mangosteen fruit peel.

MATERIALS AND METHODS

Mangosteen fruit peel dry simplicia (*G. mangostana* L.) was purchased from the Center for Post-Harvest Processing of Medicinal Plants (Bali, Indonesia). Other materials provided at the Unud Forensic and Criminology Laboratory included SYE, lactic acid bacteria starter, potassium chloride, sodium acetate trihydrate, hydrochloric acid, aluminum chloride, ethanol, quercetin standard, gallic acid standard, Folin-Ciocalteu, and distilled water. All materials used were of analytical grade.

Mangosteen fruit peel fermentation

The concentrations of SYE used varied; sucrose with a concentration range of 15-45 g/L and yeast extract with a concentration range of 2.5-7.5 g/L were designed with Design Expert Software using the Regular Two-Level 2^2 Factorial Design method. The design of the experiment is listed in Table 1.

Fermentation was performed on 100 g of dried simplicia of mangosteen fruit peel, SYE lactic acid bacteria starter, and water in an Erlenmeyer flask. The fermentation runs on a shaker at 100 rpm at room temperature for 4 days, equipped with an airlock. Sampling for analysis was performed at 96 hours of fermentation. The sample was centrifuged for 20 minutes at 5 C˚ and 6000 rpm. In preparation for further analysis, the samples were collected and stored at a low temperature.

Total phenolic content (TPC) determination

TPC was determined using the Folin-Ciocalteu reagent and NaOH in a colorimetric method. The sample was placed into a vial, and 10% *v/v* Folin-Ciocalteu solution was added and allowed to stand for 8 minute. 1% *v/v* NaOH solution was added and incubated for 1 hour. A blank solution was prepared in the same manner without the addition of the test solution. A ultraviolet (UV)-vis spectrophotometer was used to determine the absorbance of each solution at a wavelength of 730 nm. TPC was calculated using the linear regression equation and expressed in mg gallic acid equivalents per liter (mg GAE/L).

Total flavonoid content (TFC) determination

TFC was determined using a colorimetric technique with $AlCl_3$ and CH_3COONa reagents. The sample was put into a vial, and ethanol, $AlCl_3$ 10%, CH_3COONa 1M CH3COONa, and water. Shaken and incubated at room temperature for 30 minutes. Similarly, a blank solution was prepared without using the test solution. A UV-vis spectrophotometer was used to determine the absorbance at a wavelength of 425 nm. TFC was calculated using the linear regression equation and expressed in mg QE/L.

Total anthocyanin content (TAC) determination

The sample was initially dissolved in KCl buffer at pH 1, which was used to establish the proper dilution factor for the sample. The sample was placed into several different vials. While the remaining vials received a pH 4.5 buffer solution (0.4 M CH_3COONa), the other vials received a pH one buffer solution (0.025 M KCl). After incubation for 15 minutes, the absorbance of all test solutions was measured at 520 and 700 nm. The quantity of all anthocyanins was calculated using the following calculation:

$$TAC = [(A_{520}-A_{700})_{pH1.0}-(A_{520}-A_{700})_{pH4.5}]/(\varepsilon \times l) \times \text{molecular weight (MW)} \times \text{dilution factor (DF)} \times 1000$$

where TAC stands for TAC (mg Cyanidin-3-glucoside/L), A stands for absorbance of each wavelength at a different pH, stands for molar absorptivity coefficient (26.900 L/mol.cm), MW stands for molecular weight (449.2 g/mol), DF stands for dilution factor, l stands for path length in cm (1 cm), and 1000 stands for the factor of conversion from g to mg.

Table 1. Mangosteen peel fermentation run using the factorial design method: regular two level 2^2

Run	Level		Concentration	
	A: Sucrose	B: Yeast extract	Sucrose (g/L)	Yeast extract (g/L)
1	-1	-1	15	2.5
2	-1	+1	15	7.5
3	+1	-1	45	2.5
4	+1	+1	45	7.5

Statistical analysis

In this study, experimental design was used using the Regular Two Factorial Design 2^2 method. Determination of the optimum conditions based on the highest response of TPC, TFC, and TAC levels during 96 hours of fermentation. The effect of SYE and their optimum levels to be used in mangosteen rind fermentation were analyzed using analysis of variance (ANOVA) integrated in the design expert software with several parameters, such as *f* value, *p value*, R squared, Predicted R squared and Adeq Precision. In addition, the influential factors in fermentation can be described in a linear equation.[21]

RESULTS

TPC determination

The link between the standard concentration of gallic acid and its absorbance was calculated in this study and the equation y= 0.0094 x 0.1317 was obtained, as shown in Figure 1. The results of the TPC determination are shown in Table 2.

TFC determination

The link between the standard concentration of quercetin and its absorbance was calculated in this study, and the equation y= 0.0077 x 0.4372 was obtained, as shown in Figure 2. The results of the TFC determination are shown in Table 3.

TAC determination

The results of the TAC determination are shown in Table 4.

Analysis

All data inputted and analyzed using ANOVA can be seen in Table 5.

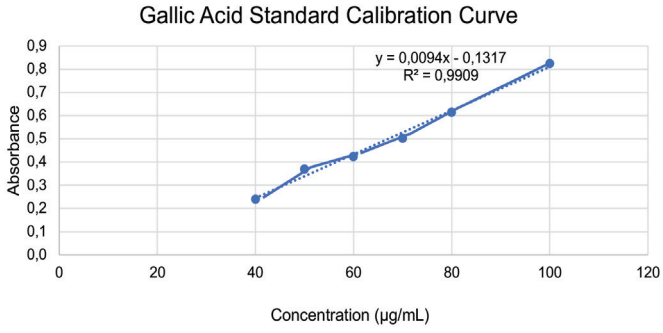

Figure 1. Gallic acid standard calibration curve

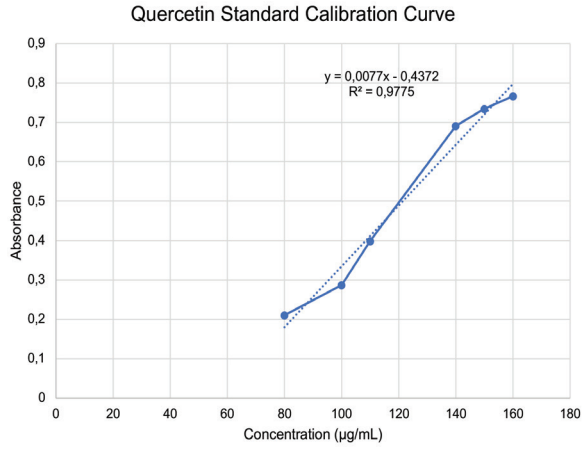

Figure 2. Quercetin standard calibration curve

Table 2. Results of the TPC determination of lactic acid-fermented mangosteen fruit peel

Sample	Replication	TPC (mg GAE/L)	Average value of the TPC (mg GAE/L) ± SD
Non-fermented mangosteen fruit peel (control)	1	592.65	593.62 ± 0.84
	2	593.93	
	3	594.25	
Run 1	1	665.96	666.10 ± 0.16
	2	666.10	
	3	666.28	
Run 2	1	684.47	684.47 ± 0.21
	2	684.26	
	3	684.68	
Run 3	1	791.91	792.20 ± 0.33
	2	792.13	
	3	792.55	
Run 4	1	681.06	681.17 ± 0.18
	2	681.06	
	3	681.38	

TPC: Total phenolic content, GAE: Gallic acid equivalents, SD: Standard deviation

DISCUSSION

Mangosteen fruit peel fermentation

Fermentation of mangosteen fruit peel was carried out using four Erlenmeyer, each filled with 100 g of mangosteen fruit peel dry simplicia, sucrose at a concentration between 15 and 45 g/L, yeast extract at a concentration between 2.5 and 7.5 g/L, and lactic acid bacteria starter at a concentration as high as 10 mL. The elements needed by lactic acid bacteria for growth and reproduction are carbon and nitrogen sources, which can be obtained through SYE.[19] Fermentation runs at room temperature, which is around 30 C˚ with constant stirring, where temperatures between 30 and 40 C˚ are ideal for promoting the development of lactic acid bacteria.[22] Constant stirring during fermentation was also performed on a shaker at

Table 3. Results of TFC determination of lactic acid-fermented mangosteen fruit peel

Sample	Replication	TFC (mg QE/L)	Average value of the TFC (mg QE/L) ± SD
Non-fermented mangosteen fruit peel (control)	1	200.13	200.03 ± 0.10
	2	200.05	
	3	199.92	
Run 1	1	239.17	239.37 ± 0.19
	2	239.43	
	3	239.53	
Run 2	1	252.94	253.01 ± 0.33
	2	252.73	
	3	253.38	
Run 3	1	311.48	311.28 ± 0.19
	2	311.27	
	3	311.09	
Run 4	1	301.77	301.94 ± 0.96
	2	301.09	
	3	302.98	

TFC: Total flavonoid content, QE: Quercetin equivalent, SD: Standard deviation

Table 4. Results of TAC determination of lactic acid-fermented mangosteen fruit peel

Sample	Replication	TAC (mg C3GE/L)	Average value of the TAC (mg C3GE/L) ± SD
Non-fermented mangosteen fruit peel (control)	1	3.45	3.49 ± 0.03
	2	3.51	
	3	3.52	
Run 1	1	4.67	4.67 ± 0.04
	2	4.64	
	3	4.71	
Run 2	1	3.53	3.58 ± 0.05
	2	3.58	
	3	3.62	
Run 3	1	6.60	6.64 ± 0.21
	2	6.45	
	3	6.88	
Run 4	1	2.08	2.14 ± 0.05
	2	2.19	
	3	2.15	

TAC: Total anthocyanin content, SD: Standard deviation

100 rpm. Constant stirring at 100 rpm will improve lactic acid bacteria's rate of growth during fermentation.[23]

With microbes, the process of fermentation helps break down organic macromolecules into simpler ones.[9] The purpose of fermentation on mangosteen peel is to increase the phytochemical components contained in it, namely phenol group compounds, flavonoids, and anthocyanins, which produce fermentation by-products in the form of lactic acid, which has many benefits. The production of organic acids that make the environment acidic will increase the solubility of phenolic compounds in water. The optimal pH in the extraction process of phenol compounds is in acidic conditions in the 3.0-5.3 pH range. The degradation of phenolic compounds is directly related to the pH level.[24]

In lactic acid fermentation, sucrose first undergoes hydrolysis to become the simplest sugar, namely glucose. Hexokinase, phosphogluconolactonase, and epimerase enzymes were produced by lactic acid bacteria and play a role in converting glucose through a series of chemical modifications. It also enters the phosphoketolase pathway and undergoes new chemical modifications to produce pyruvate, which can then be converted to lactic acid by the enzyme lactate dehydrogenase. The nitrogen source used in fermentation, namely yeast extract, also contains many nutrients in the form of vitamins, amino acids, and pyruvate so this will also affect the proliferation of lactic acid bacteria.[25]

The fermented mangosteen fruit peel samples were then subjected to phase separation using a centrifuge at 6000 rpm for 20 minutes. Centrifugation is performed to separate yeast extract, lactic acid bacteria, and powdered simplicia so that the fermentation process can be stopped. Sample centrifugation has a working principle, namely the application of centrifugal force and sedimentation to separate particles based on their specific gravity or density. The centrifugation results will separate two phases, namely, the supernatant and pellet. The supernatant is the result of centrifugation with a lower specific gravity than the pellets, whereas the pellets are the result of centrifugation with a higher specific gravity than the supernatant. The pellet is at the bottom of the centrifugation tube.[26] Water has a density of 0.99 g/mL, sucrose has a density of 1.6 g/mL, and yeast extract has a density of 1.4 g/mL. This shows that compared with water, SYE have a larger density. The components of sucrose, yeast extract, and simplicia will be at the bottom of the tube.

Table 5. Data analysis

Source	*f* value	*p* value	
Determination of the TPC			
Model	218642.77	< 0.0001	Significant
A-Sucrose	244356.76	< 0.0001	
B-Yeast extract	139042.57	< 0.0001	
AB	272698.57	< 0.0001	
Determination of the TPC			
Model	22933.01	< 0.0001	Significant
A-Sucrose	66446.12	< 0.0001	
B-Yeast extract	109.11	< 0.0001	
AB	2243.79	< 0.0001	
Determination of TAC			
Model	826.88	< 0.0001	Significant
A-Sucrose	16.24	0.0038	
B-Yeast extract	1796.47	< 0.0001	
AB	667.93	< 0.0001	

TPC: Total phenolic content, TFC: Total flavonoid content, TAC: Total anthocyanin content

TPC determination

The Folin-Ciocalteu and NaOH reagents were used in the spectrophotometric method to measure TPC levels. The basic principle of this method is the oxidation of phenolic-hydroxyl groups. Folin-Ciocalteu reagent will oxidize phenol and reduce heteropoly acids into a molybdenum-tungsten (Mo-W) complex. When the sample is treated with the Folin-Ciocalteu reagent, a greenish-yellow hue is produced, which indicates a phenolic compound. The amount of phenolic compounds present correlates exactly with the amount of blue color produced by this reaction.[27-29] TPC is expressed in mg GAE/L.

Compared with the control group in this study, the TPC of the lactic acid-fermented mangosteen fruit peel was significantly higher. Lactic acid bacteria produce several enzymes like β-glycosidase that play a role in β-glycoside hydrolysis, as well as the production of decarboxylase, esterase, hydrolase, and reductase, which have a significant influence on increasing the phenolic levels in mangosteen fruit peel fermentation.[30-32] In addition, it is also influenced by the constant stirring carried out during fermentation. According to previous research, constant stirring during fermentation causes hydrolysis of the glycoside bond but does not degrade the phenolic aglycone.[33] The increase in phenolic components is also caused by an

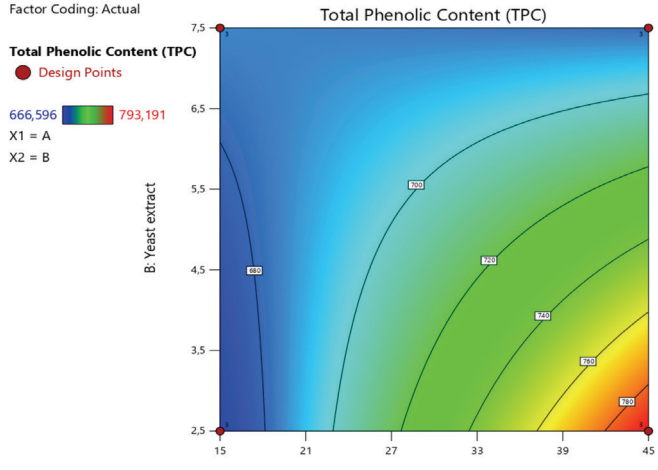

Figure 3. Contour plot of the relationship between SYE concentration in mangosteen fruit peel fermentation to its TPC

TPC: Total phenolic content, SYE: Sucrose and yeast extract

increase in extraction ability and the release of phenolic compounds from bound forms to free forms.[34] The contour plot of the relationship between SYE concentration in mangosteen fruit peel fermentation and its TPC is shown in Figure 3.

Based on the *p* value of 0.0001, the contour plot of the TPC test results of mangosteen (*G. mangostana* L.) fruit peel fermentation with different amounts of SYE showed significant results. This value indicates that the mathematical model used to calculate the TPC of the fermentation products can accurately capture the real conditions. The following linear equation represents the total phenol test results from the factorial design calculation.

y= 6.36 (A) +16.66 (B) -0.83 (A*B)

Where y= TPC; A= sucrose; B= yeast extract; and A*B= interaction between SYE. Based on the equation obtained, it can be interpreted that an increase in the SYE components can increase the total phenol content during fermentation. However, the interaction between the two can reduce the total phenol content. The resulting *R squared* value is 1.000, and the resulting pred *R squared* value is 1.000. This indicates that the predicted value is the same as the *R* value generated in actual experiments. The resulting Adeq Precision value is 1016.4183. Adeq Precision is required to measure the noise level of an experiment, and this value is expected to be more than 4.

TFC determination

The UV-vis Spectrophotometric technique with an $AlCl_3$ and CH_3NOONa reagent was used in this study to determine the TFC. The basic principle behind the use of this method is the high affinity to bind $AlCl_3$ metal ions to form Al (III)-flavonoid chelates. The addition of $AlCl_3$ will cause the OH group on C3 and C5 to form a stable complex, causing the solution to turn yellow. Furthermore, the addition of CH3NOONa is known to create an acidic atmosphere that will form a complex compound so that the solution turns pink, where the absorbance will be measured.[35] TFC was measured at a wavelength of 425 nm using quercetin standards and $AlCl_3$ and CH_3NOONa reagents. TFC is expressed as the amount of quercetin in milligrams per liter of sample (mg QE/L) or mg quercetin.

A significant difference was found between the TFC of the lactic acid-fermented mangosteen fruit peel and the control group. The increase in flavonoid compounds is caused by changes in the environment, which becomes more acidic because of organic acid synthesis by lactic acid bacteria, which triggers the release of bound flavonoid components and increases their availability in water in their free form.[36] Figure 4 shows the contour plot showing the relationship between the concentration of SYE in mangosteen fruit peel fermentation and the total amount of flavonoids present.

Based on the p value of 0.0001, the contour plot of the TFC test results of mangosteen (*G. mangostana* L.) fruit peel fermentation with different amounts of SYE showed significant results. This value indicates that the mathematical model used to calculate the TFC of the fermentation results can accurately capture the real conditions. The following linear equation shows the results of the factorial design calculation for the total flavonoid assay.

y= 2.768 (A) +4.957 (B) -0.148 (A*B)

Where Y is the TFC; A is sucrose; B is yeast extract; and A*B is the interaction between SYE. According to the equation, an increase in the SYE components can increase the TFC during fermentation. However, the interaction between the two can decrease the TFC. The resulting R squared value is 0.999, as is the resulting pred R squared value. This means that the predicted value is the same as the R value obtained from the experiments. The resulting Adeq Precision value is 434.3983. Adeq Precision is required to measure the noise level of an experiment, and this number is predicted to be greater than 4.

TAC determination

The difference in absorbance caused by the change in anthocyanin structure due to pH changes drives the differential pH technique used to measure the TAC. Anthocyanins in strongly acidic conditions at pH 1 have a colored flavellum cation (oxonium) form, whereas those in weak acidic conditions at pH 4.5 have a pseudo base carbinol (hemiketal) form that does not produce color.[37,38] At pH 4.5, most anthocyanin monomers are in the hemiketal state; however, polymerized anthocyanins and non-enzymatic browning pigments are not reversible to pH changes and must be omitted from absorbance calculation.[37,39] As a result, the difference in absorbance values between pH 1 and 4.5 at the maximum wavelength of the anthocyanins is directly proportional to the anthocyanin content.[37]

In comparison with the control group, the mangosteen fruit peel's TAC was considerably greater. The use of sugar and yeast extract during fermentation contributes to the increase in TAC. Pyruvate from the fermentation process and yeast extract is converted to acetaldehyde during sucrose glycolysis, which acts as a terminal electron acceptor in the production of ethanol. Pyruvate and acetaldehyde are produced in the cytoplasm of yeast extracts and metabolized simultaneously,

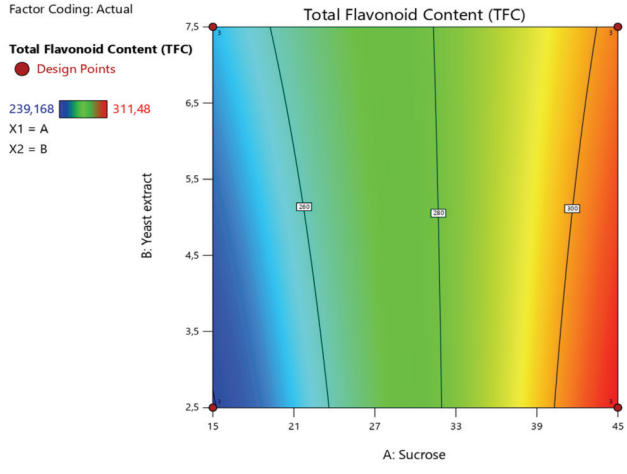

Figure 4. Contour plot of the relationship between SYE concentrations in mangosteen fruit peel fermentation to its TFC

TFC: Total flavonoid content, SYE: Sucrose and yeast extract

with pyruvate being decarboxylated to acetaldehyde or used to produce acetyl CoA. However, some of them will diffuse out of the cell and become reactive, allowing them to attack other molecules and facilitate the transition of anthocyanins into various derivative compounds such as proanthocyanins. The most important anthocyanin derivatives in the fermentation products are proanthocyanidin. Pyruvate and anthocyanins react to form proanthocyanidin carboxy compounds (visitin type A), whereas acetaldehyde and anthocyanins react to form anthocyanin 3-O-glycoside-4-vinyl (visitin type B).[40] However, compared with the control group, run 4 had lower numbers of total anthocyanins. This is due to the degradation of anthocyanin compounds through hydrolysis by glucosidase and polyphenol oxidase enzymes, which break the glycoside bond between the aglycone and glycine groups. The hydrolysis process converts anthocyanin molecules to the chalcone form and ultimately to aldehydes and phenolic acids. As a result, the component identified as cyanidin-3-glucoside on the spectrophotometer was lower in the test group than in the control group. Figure 5 shows a contour plot of the relationship between sugar and yeast extract concentrations in mangosteen fruit peel fermentation and TAC.

The contour plot of the TAC test results of mangosteen (*G. mangostana* L.) peel fermentation with varying amounts of SYE indicates significant results based on a p value of 0.0001. This figure shows how the equation model used can describe the actual conditions for calculating the TAC of the fermentation results. The results of the factorial design calculation for the total anthocyanin assay are shown in the linear equation below.

$$Y = 0.12\,(A) + 0.12\,(B) - 0.02\,(A*B)$$

Where Y is the TAC, A is sucrose, B is yeast extract, and A*B is the reaction between the two. Based on the equation found, it can be deduced that during fermentation, an increase in the components of yeast extract and sucrose can lead to an increase in the total amount of anthocyanins. However, the combined anthocyanin content may decrease because of their interaction. The *R squared* value obtained is 0.9968, whereas the pred *R squared* value obtained is 0.9928. This shows that the *R* value obtained from the actual experiments and the predicted value is identical. 68.2291 is the derived Adeq Precision value. To quantify the noise level of an experiment, Adeq Precision is required, and this value is expected to be greater than 4.

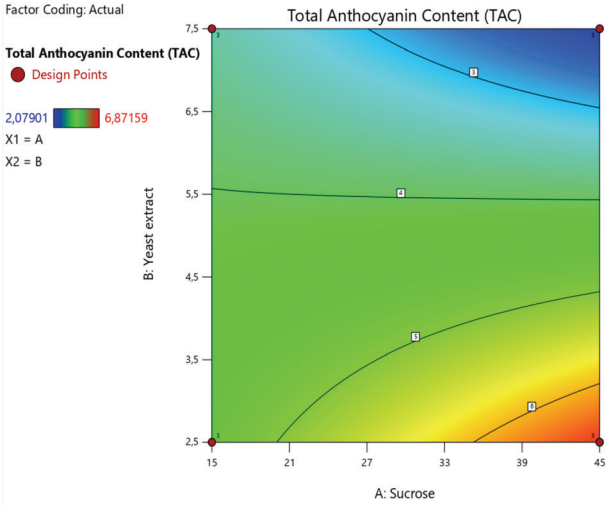

Figure 5. Contour plot of the relationship between SYE concentration in mangosteen fruit peel fermentation to its TAC

TAC: Total anthocyanin content

CONCLUSION

The use of sucrose as a carbon source at a high concentration (45 g/L) and yeast extract as a nitrogen source at a low concentration (2.5 g/L) resulted in a significant increase in total phenol, flavonoid, and anthocyanin levels compared with the control group. An increase in the components of yeast extract and sucrose can increase the concentrations of total phenol, flavonoids, and anthocyanin. However, their interaction may decrease its concentration.

Acknowledgments

The author would like to thank the Pharmacy Study Program, Faculty of Mathematics and Natural Science, Bali, Indonesia, which has facilitated this research.

Ethics

Ethics Committee Approval: Not required.

Informed Consent: Not required.

Authorship Contributions

Concept: I.M.A.G.W., E.I.S., Design: P.S.Y., I.M.A.G.W., Data Collection or Processing: K.D.A.P., G.A.D.P., Analysis or Interpretation: K.D.A.P., E.I.S., P.S.Y., Literature Search: K.D.A.P., Writing: K.D.A.P., G.A.D.P.

Conflict of Interest: No conflict of interest was declared by the authors.

Financial Disclosure: The authors declared that this study received no financial support.

REFERENCES

1. Başaran N, Paslı D, Başaran AA. Unpredictable adverse effects of herbal products. Food Chem Toxicol. 2022;159:112762.
2. Tegtmeier M, Knierim L, Schmidt A, Strube J. Green manufacturing for herbal remedies with advanced pharmaceutical technology. Pharmaceutics. 2023;15:188.
3. Sharma RR, Deep A, Abdullah ST. Herbal products as skincare therapeutic agents against ultraviolet radiation-induced skin disorders. J Ayurveda Integr Med. 2022;13:100500.
4. Karim N, Tangpong J. Biological properties in relation to health promotion effects of *Garcinia mangostana* (queen of fruit): A short report. J Heal Res. 2018;5:364-370.
5. Albuquerque BR, Dias MI, Pinela J, Calhelha RC, Pires TCSP, Alves MJ, Corrêa RCG, Ferreira ICFR, Oliveira MBPP, Barros L. Insights into the chemical composition and *in vitro* bioactive properties of mangosteen (*Garcinia mangostana* L.) pericarp. Foods. 2023;12:994.
6. Tousian Shandiz H, Razavi BM, Hosseinzadeh H. Review of *Garcinia mangostana* and its xanthones in metabolic syndrome and related complications. Phytother Res. 2017;31:1173-1182.

7. Aizat WM, Jamil IN, Ahmad-Hashim FH, Noor NM. Recent updates on metabolite composition and medicinal benefits of mangosteen plant. PeerJ. 2019;7:6324.
8. Kalick LS, Khan HA, Maung E, Baez Y, Atkinson AN, Wallace CE, Day F, Delgadillo BE, Mondal A, Watanapokasin R, Barbalho SM, Bishayee A. Mangosteen for malignancy prevention and intervention: Current evidence, molecular mechanisms, and future perspectives. Pharmacol Res. 2023;188:106630.
9. Sharma K, Mahato N, Cho MH, Lee YR. Converting citrus wastes into value-added products: Economic and environmently friendly approaches. Nutrition. 2017;34:29-46.
10. Jha Kumar A, Sit N. Extraction of bioactive compounds from plant materials using combination of various novel methods: A review. Trends Food Sci Technol. 2022; 119:579-591.
11. Prerna, Vidhu A. Fermentation: A green herbal extraction process for polyphenols. Biomed J Sci & Tech Res. 2020;31:24391-24392.
12. Trigueros L, Wojdyło A, Sendra E. Antioxidant activity and protein-polyphenol interactions in a pomegranate (*Punica granatum* L.) yogurt. J Agric Food Chem. 2014;62:6417-6425.
13. Gumienna M, Szwengiel A, Górna B. Bioactive components of pomegranate fruit and their transformation by fermentation processes. Eur Food Res Technol. 2016;242:631-640.
14. Cano-Lamadrid M, Trigueros L, Wojdyło A, Carbonell-Barrachina AA, Sendra E. Anthocyanins decay in pomegranate enriched fermented milks as a function of bacterial strain and processing conditions. LWT. 2017;80:193-199.
15. Kwaw E, Ma Y, Tchabo W, Apaliya MT, Wu M, Sackey AS, Xiao L, Tahir HE. Effect of *Lactobacillus* strains on phenolic profile, color attributes and antioxidant activities of lactic-acid-fermented mulberry juice. Food Chem. 2018;250:148-154.
16. Wang L, Zhang H, Lei H. Phenolics profile, antioxidant activity and flavor volatiles of pear juice: influence of lactic acid fermentation using three *Lactobacillus* strains in monoculture and binary mixture. Foods. 2022;11:11.
17. Bangar SP, Suri S, Trif M, Ozogul F. Organic acids production from lactic acid bacteria: A preservation approach. Food Biosci. 2022;46:101615.
18. Ji G, Liu G, Li B, Tan H, Zheng R, Sun X, He F. Influence on the aroma substances and functional ingredients of apple juice by lactic acid bacteria fermentation. Food Biosci. 2023;51:102337.
19. Lunelli BH, Andrade RR, Atala DI, Wolf Maciel MR, Maugeri Filho F, Maciel Filho R. Production of lactic acid from sucrose: strain selection, fermentation, and kinetic modeling. Appl Biochem Biotechnol. 2010;161:227-237.
20. Abbasiliasi S, Tan JS, Tengku Ibrahim TA, Bashokouh F, Ramakrishnan NR, Mustafa S, Ariff AB. Fermentation factors influencing the production of bacteriocins by lactic acid bacteria: A review. RSC Adv. 2017;7:29395-29429.
21. Setyawan EI, Rohman A, Setyowati EP, Nugroho AK. The combination of simplex lattice design and chemometrics in the formulation of green tea leaves as transdermal matrix patch. Pharmacia. 2021;68:275-282.
22. Taale E, Savadogo A, Zongo C, Ilboudo AJ, Traore AS. Bioactive molecules from bacteria strains: case of bacteriocins producing bacteria isolated from foods. Curr Res Microbiol Biotechnol. 2013;1:80-88.
23. Ibrahim SB, Rahman NAA, Mohamad R, Rahim RA. Effects of agitation speed, temperature, carbon and nitrogen sources on the growth of recombinant Lactococcus lactis NZ9000 carrying domain 1 of Aerolysin gene. African J Biotechnol. 2010;9:5392-5398.
24. Vuong QV, Golding JB, Stathopoulos CE, Roach PD. Effects of aqueous brewing solution pH on the extraction of the major green tea constituents. Food Res Int. 2013;53:713-719.
25. Abdel-Rahman MA, Tashiro Y, Sonomoto K. Recent advances in lactic acid production by microbial fermentation processes. Biotechnol Adv. 2013;31:877-902.
26. Naufal A, Kusdiyantini E, Raharjo B. Identifikasi jenis pigmen dan uji potensi antioksidan ekstrak pigmen bakteri serratia marcescens hasil isolasi dari sedimen sumber air panas gedong songo. Bioma. 2018;19:95.
27. Ariyanthini KS, Angelina E, Parta Wiratama IPRK, Naripradnya PS, Dewantara Putra IGAN, Setyawan EI. Implementation of principal component analysis-cluster analysis on the extraction of green tea leaf (*Camellia sinensis* (L.) Kuntze). Biointerface Res Appl Chem. 2023;13:1-14.
28. Blainski A, Lopes GC, DeMello JCP. Application and analysis of the folin ciocalteu method for the determination of the total phenolic content from *Limonium brasiliense* L. Molecules. 2013;18:6852-6865.
29. Behrad Z, Sefidkon F, Ghasemzadeh H, Rezadoost H, Balandari A. Determination of phenolic compounds and antioxidant activities of 55 Iranian berberis genotypes. J Med Plants By-Prod. 2023;2:181-188.
30. Mousavi ZE, Mousavi SM, Razavi SH, Hadinejad M, Emam-Djomeh Z, Mirzapour M. Effect of fermentation of pomegranate juice by *Lactobacillus plantarum* and *Lactobacillus acidophilus* on the antioxidant activity and metabolism of sugars, organic acids and phenolic compounds. Food Biotechnol. 2013;27:1-13.
31. Ávila M, Hidalgo M, Sánchez-Moreno C, Pelaez C, Requena T, de Pascual-Teresa S. Bioconversion of anthocyanin glycosides by *Bifidobacteria* and *Lactobacillus*. Food Res Int. 2009;42:1453-1461.
32. Gulsunoglu-Konuskan Z, Kilic-Akyilmaz M. Microbial bioconversion of phenolic compounds in agro-industrial wastes: a review of mechanisms and effective factors. J Agric Food Chem. 2022;70:6901-6910.
33. Mustafa SM, Chua LS, El-Enshasy HA. Effects of agitation speed and kinetic studies on probiotication of pomegranate juice with *Lactobacillus* casei. Molecules. 2019;24:2357.
34. Adebo OA, Gabriela Medina-Meza I. Impact of Fermentation on the Phenolic Compounds and Antioxidant Activity of Whole Cereal Grains: A Mini Review. Molecules. 2020;25:927.
35. Shraim AM, Ahmed TA, Rahman MM, Hijji YM. Determination of total flavonoid content by aluminum chloride assay: A critical evaluation. LWT. 2021;150:11932.
36. Adetuyi FO, Ibrahim TA. Effect of Fermentation Time on the Phenolic, Flavonoid and Vitamin C Contents and Antioxidant Activities of Okra (Abelmoschus esculentus) Seeds. Niger Food J. 2014;32:128-137.
37. Lee J, Durst RW, Wrolstad RE. Determination of total monomeric anthocyanin pigment content of fruit juices, beverages, natural colorants, and wines by the pH differential method: collaborative study. J AOAC Int. 2005;88:1269-1278.
38. Abedi-Firoozjah R, Yousefi S, Heydari M, Seyedfatehi F, Jafarzadeh S, Mohammadi R, Rouhi M, Garavand F. Application of Red Cabbage Anthocyanins as pH-Sensitive Pigments in Smart Food Packaging and Sensors. Polymers (Basel). 2022;14:1629.
39. Wrolstad RE, Durst RW, Lee J. Tracking color and pigment changes in anthocyanin products. Trends Food Sci Technol. 2005;16:423-428.
40. Ruta LL, Farcasanu IC. Anthocyanins and Anthocyanin-Derived Products in Yeast-Fermented Beverages. Antioxidants (Basel). 2019;8:182.

Turk J Pharm Sci 2024;21(3):219-223
DOI: 10.4274/tjps.galenos.2023.96020

ORIGINAL ARTICLE

Efficacy of ABCA1 Transporter Proteins in Patients with Endometrial Cancer: an *In Vitro* Study

Şerife Efsun ANTMEN[1,*], Cem YALAZA[2], Necmiye CANACANKATAN[1], Hakan AYTAN[3], Ferah TUNCEL[4], Sema ERDEN ERTÜRK[5]

[1]Mersin University Faculty of Pharmacy, Department of Biochemistry, Mersin, Türkiye
[2]Toros University, Vocational School of Health Services, Mersin, Türkiye
[3]Mersin University Faculty of Medicine, Department of Obstetrics and Gynecology, Mersin, Türkiye
[4]Mersin University Faculty of Medicine, Department of Pathology, Mersin, Türkiye
[5]Mersin University, Vocational School of Health Services, Mersin, Türkiye

ABSTRACT

Objectives: Endometrial carcinoma (EC) is a typical gynecological malignant tumor that occurs more frequently every year. Obesity is a significant contributor to the development of EC and its prognosis. Lipid metabolism and malignant tumors have a long history of association. Elevated cholesterol levels are made possible by adenosine triphosphate-binding cassette protein A1 (ABCA1) deficiency, which eventually promotes cancer cell survival. The aim of this study was to examine at the ABCA1 gene expression levels in EC patients. The relationship between ABCA1 and the occurrence, progression, and prognosis of EC is discussed in this article as a potential mechanism.

Materials and Methods: The samples of 45 endometrial adenocarcinoma patients were retrospectively included in this study and they were further divided into Grade 1 (15), Grade 2 (15), Grade 3 (15) tumors, control group. Twenty-nine endometrial tissues without a confirmed diagnosis of endometrial cancer made up the control group. ABCA1 gene expression was examined using real-time polymerase chain reaction.

Results: According to the results, the gene expressions of the patient group were higher than the control group When each Grade was compared with the control group, statistically significant results were obtained. After analyzing the data, it was found that the patient group was generally higher than the control group ($p < 0.05$) and there were differences in the grades of the patient group ($p < 0.05$). When the ABCA1 expressions of the grade groups and control groups were compared separately, a difference was found between Grade 1, Grade 2 and Grade 3 and the control group ($p= 0.0001$).

Conclusion: According to the findings of our study, a key component in the growth of EC tumors is the increase in cholesterol production caused by a reduction in ABCA1.

Keywords: ABCA1, endometrial cancer, cholesterol, ATP binding cassette protein, gene expression

INTRODUCTION

The most frequent gynecological tumor in developed nations is endometrial cancer (EC), a tumor that develops in the endometrium, and its frequency is rising.[1]

The main risk factor is having access to estrogens, both endogenous and exogenous, which are connected to conditions such as diabetes, obesity, early menarche age, nulliparity, late-onset menopause, and older age (55 years).[2,3] EC has been largely divided into two categories over the past 30 years on the basis of histological features, hormone receptor expression, and grade.[4] The most typical subtype of EC has a fair prognosis and is low-grade, endometrioid, diploid, and hormone receptor-positive, referred to as type I. Non-endometrioid, high-grade, aneuploid, TP53-mutated, and hormone receptor-negative tumors with a poor prognosis and a higher likelihood of metastasis are referred to as type II endometrial malignancies.[4]

According to certain studies, alterations in cancer cell metabolism, particularly aberrant cholesterol metabolism, play a significant role in their increased ability to proliferate and invade.[5]

*Correspondence: eantmen@mersin.edu.tr, Phone: +90 533 690 22 83, ORCID-ID: orcid.org/0000-0003-1270-2408
Received: 28.03.2023, Accepted: 19.07.2023

Adenosine triphosphate (ATP)-binding cassette (ABC) transporters are a family of lipid transporters that are confined to the plasma membrane.[6] ABC transporter A1 (ABCA1) is the first ABC protein to be discovered.[7] The liver, gut, brain, and macrophages all exhibit significant levels of the transmembrane protein ABCA1. Its main job is to facilitate the transfer of unbound phospholipids and free cholesterol from cells to apolipoprotein I to produce nascent high-density lipoprotein (nHDL) particles.[8] When ATP is hydrolyzed for energy, free cholesterol and intracellular phospholipids are ejected from cells and joined with non- or low-fat apo A-I to produce HDL, which subsequently kickstarts the process of reverse cholesterol transport.[6]

ABCA1 and Apo A1 interact through the Janus kinase/signal transducer activator of the transcription 3 signaling pathway. Tyrosine kinase/transcription factor 3 has anti-inflammatory effects and reduces chronic inflammation; both can be activated. This decreases the generation of pro-inflammatory cytokines, which cause increased cholesterol production from cells and inhibits ABCA1 degradation to prevent macrophage activation.[9] Dysregulation of cholesterol homeostasis, or decreased lipid export and increased cholesterol production in cancer cells, is a significant contributor to tumor formation.[10]

In this study, it was aimed to examine ABCA1 gene expression levels in patients with EC.

MATERIALS AND METHODS

Four groups of endometrial tissues were used in the study: patient groups, Group 1 including patients with EC Grade 1 (n= 15), Group 2 including patients with EC Grade 2 (n= 15), Group 3 including patients with EC Grade 3 (n= 15), and control group including patients with endometrial tissues without EC diagnosis (n= 29). The control group was classified into two: Control 1, which included 14 proliferative samples, and Control 2, which included 15 secretory phase healthy samples. During this study, formali-fixed paraffin embedded (FFPE) tissue samples retrospectively analyzed which were stored in Mersin University Faculty of Medicine, Department of Obstetrics and Gynecology and Pathology Department between 2010-2020. The Mersin University Ethics Committee accepted this study as a component of the "The Role of De Novo Lipogenesis and Cholesterol Synthesis Enzymes in Endometrial Cancer Development" project (2020/418, date: 10.06.2020).

The samples to be included in the study were graded as Grade 1, 2, and 3 according to their differentiation, belonging to patients diagnosed with endometrioid adenocarcinoma, which is the most common type of EC, without any prognostic factor. The International Federation of Gynecology and Obstetrics grading system for carcinomas of the uterine corpus is exclusively designated for endometrioid carcinomas and is based on architectural features as follows.[11]

Grade 1, 5% or less non-squamous solid growth pattern, Grade 2, 6-50% non-squamous solid growth pattern, Grade 3, > 50% non-squamous solid growth pattern.

Samples were taken from healthy individuals who were not diagnosed with EC. Control group samples were collected and stored in the same way as the patient group samples. The proper locations on the preparations were indicated after samples with little to no necrosis and no detection-tracking artifact were evaluated under a microscope (Figure 1). The right regions were then extracted from microtome sections of FFPE tissue blocks using the marked regions as a guide. From the paraffin block, 4-mm diameter by 10 µm thick microtome sections were removed and placed on clean slides. After that, 8-10 pieces of leaf tissue were removed from the slides.

All primers are composed of TaqMan Gene Expression Assays (ABI/Thermo, ThermoFisher Scientific).

Sample separation from the paraffin block was performed according to the protocol of the innu PREP FFPE Total RNA Kit from Analytikjena (PN: 845-KS-2050050/Jena-Germany). After the necessary procedures were done, total RNA was filtered into the tube for cDNA extraction. High-capacity cDNA Reverse Transcription Kits from Appliedbiosystems (PN: 4375222 Carlsbad, CA, USA) were used to convert the RNAs obtained into complementary DNA. TaqMan Gene Expression Master Mix from Appliedbiosystems (PN: 4371135/Carlsbad, CA, USA) was used for the gene expression method. The Uracil-DNA glycosylase enzyme is activated by maintaining the mixture at 50 C° for 2 minutes throughout the initial stage of the real-time PCR (RT-PCR) procedure. For 10 minutes, AmpliTaq Gold was maintained at 95 C° to stimulate the ultra pure enzyme.

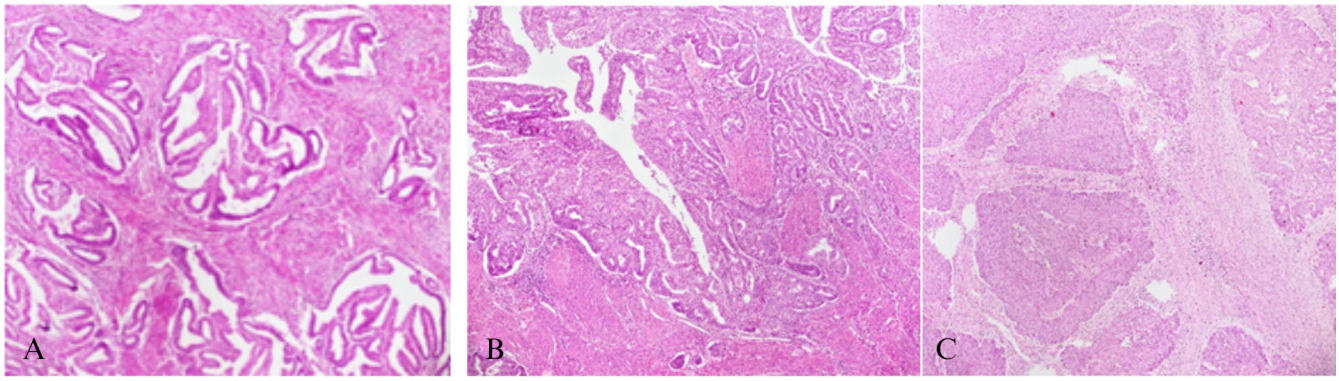

Figure 1. Determination of target tissues by marking in archive tissue preparations. A) Grade 1 (H&E X 100), B) Figo Grade 2 (H&E X 40), C) Figo Grade 3 (H&E X 40)

Amplification was carried out in 2 stages; Step 1) The transition of DNA from double-stranded to single-stranded structure (denaturation) for 15 seconds at 95 C°, Step 2) Beta-actin was used as an endogenous control in the quantitative analysis of RT-PCR to normalize the distinguishing expression of tissues. Calculated values of Delta Ct ($^{\Delta Ct}$) and $2^{-\Delta\Delta Ct}$ were employed in the statistical analysis.[12]

Statistical analysis

The IBM SPSS 22.0 Statistics program was used for statistical analysis. The Shapiro-Wilk test was used for the normality test. Because the variables did not show normal distribution in the comparisons between the groups, the Mann-Whitney U test was used for the comparisons of two groups, and the Kruskal-Wallis H test was used for the comparisons of more than two groups. When a difference was found as a result of Kruskal-Wallis H test, Conover's Post Hoc Test was used. Significant *p* values were defined as those 0.05.

RESULTS

This study involved 29 healthy participants and 45 patients with EC. All samples were used anonymously. It was revealed that there was a statistically significant difference between the means of ABCA1 gene expression in the patient and control groups when the means of the two groups were compared (p= 0.001) (Figure 2).

There was a significant difference in terms of ABCA1 gene expressions between the groups determined according to the stages of the patients ($p < 0.05$) (Figure 3).

Post Hoc test results showed a difference between the control and Grade 1 (p= 0.0001), Grade 2 (p= 0.0001) and Grade 3 (p= 0.0001), respectively. There was no difference between grades ($p > 0.05$). Although there was no statistically significant difference between the grades, when we compared the mean values, ABCA1 gene expression showed the highest increase in Grade 1. There was a slight decrease in Grade 3 and a serious decrease in expression in Grade 2 (Table 1).

No statistically significant difference was determined when the expressions in the secretory and proliferative phase samples were compared among themselves in the control group ($p > 0.05$).

DISCUSSION

The absence of a progesterone antagonistic effect with extended estrogen activity is linked to the pathophysiology of EC, which leads to sustained endometrial growth, atypical hyperplasia, and ultimately carcinogenesis. Obesity, which is among the factors that cause an increase in endogenous estrogen, constitutes 26-47% of all cases, and the risk of EC is 2-10%. Lipid metabolism in patients is directly related to tumor cell proliferation. Therefore, it is important to examine lipid metabolism in patients with EC for whom obesity is an important risk factor.[13]

All vertebrates require cholesterol, which is obtained from cells through de novo synthesis and uptake of lipoproteins from the blood using lipoprotein receptors. But more is not always better.[14] Although every cell in the body is capable of producing cholesterol, the majority of them do not have effective metabolic pathways and must instead expel the

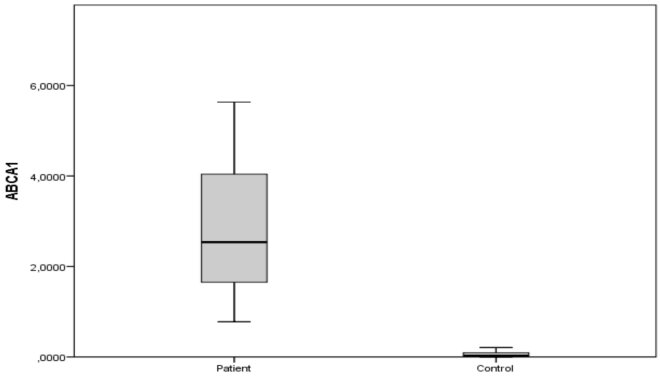

Figure 2. Comparison of *ABCA1* gene expression
ABCA1: ABC transporter A1

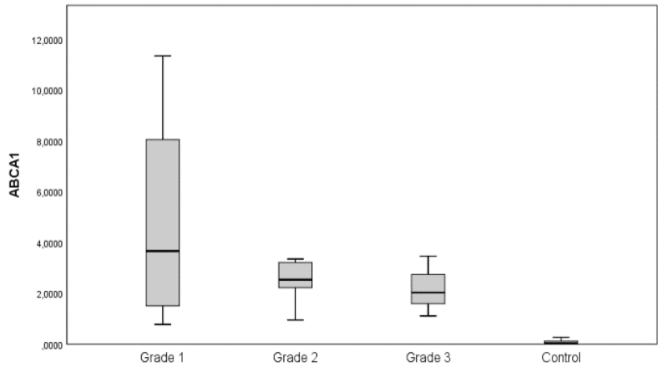

Figure 3. Comparison of ABCA1 gene expression in groups
ABCA1: ABC transporter A1

Table 1. Comparison of patient, baseline characteristics of case Grade1, Grade2, Grade3, and the controls

Gene	Controls (n= 29) mean ± SD	Patients (n= 45) mean ± SD			*p* value
		3.797 ± 3.710			0.0001*
		Grade 1 (n= 15) mean ± SD	Grade 2 (n= 15) mean ± SD	Grade 3 (n= 15) mean ± SD	
ABCA1	0.113 ± 0.207	4.699 ± 3.522	4.262 ± 5.111	2.432 ± 1.275	0.0001*

Mean, * shows a statistically significant difference between Grade 1, Grade 2, and Grade 3 and the control group (p= 0.0001), SD: Standard deviation

substance from cells through a variety of transporters. The ability of one of them, ABCA1, to join with apo A-I on the cell surface to create new HDL and use ATP energy to encourage the outflow of free cholesterol and phospholipids from cells is one of its key functions. This in turn starts the process of reverse cholesterol transport, which transports cholesterol from peripheral tissues back to the liver.[15,16] The ability of cells to move has been shown to be influenced by the cholesterol regulation in the plasma membrane.[17] Furthermore, it has been proposed that the adherence and migrating of cancer cells are significantly influenced by lipid rafts rich in cholesterol.[18,19] The expression of ABCA1 surface protein can be controlled by the activity of phosphoinositide 3 kinase (PI3K), which dramatically raises the risk of cancer cells migrating into the bloodstream and forming metastases.[20] According to our study results, ABCA1 expression was increased in the patient group compared with that in the control group ($p < 0.05$). In our team's previous study, PI3K increased in the patient group compared with the control group.[21]

According to previous studies, cancer-specific ABCA1 methylation and protein expression loss directly caused higher intracellular cholesterol levels in cancer cells, creating a microenvironment conducive to the spread of the disease.[22]

When the patient grade groups were compared with the control group, an increase was observed in each group compared with the control group ($p= 0.001$). When the grades were compared with each other, there was no statistically significant difference; however, when the mean values were examined, an increase was observed in Grade 1 and Grade 2 groups and a significant decrease in Grade 3. This shows that disease progression is inversely related to ABCA1 expression. The decrease in ABCA1 expression in Grade 3 differentiation of the disease indicates that cell proliferation may be increased and expression may be correlated with disease progression. In addition, our previous study showed that in accordance with the working mechanism of PI3K and ABCA1, PI3K, like ABCA1, increases as expected in the early stages of cancer and decreases as the tumor progresses.[21]

According to a study on mitochondrial ABCA1, ABCA1 can keep cells functioning normally by keeping their cholesterol levels low, and it also has some inhibitory effects on the growth of cancer cells.[23]

According to a study, it is easier for tumors to progress when ABCA1 expression is downregulated. High amounts of Apo A1 can decrease EC formation, and HDL and Apo A1 both have the capacity to remove cholesterol from cells, which reduces lipid metabolism.[24]

Apo A1 levels should be used as a tumor marker for the early detection of EC because elevated levels can halt the progression of EC. High amounts of Apo A1 might slow down lipid metabolism, and HDL and Apo A1 may remove cholesterol from cells, lowering lipid metabolism.[13]

In another study, it was stated that ABCA1 deficiency provides high mitochondrial cholesterol and ultimately promotes cancer cell survival. Theoretically, this entails an increase in the retention of chemicals that encourage cell death in the mitochondria, perhaps as a result of a decrease in membrane fluidity and blockage of the mitochondrial permeability transition.[25,26] According to a different study that came to the opposite conclusion as this one, ABCA1 anti-tumor activity is dependent on efflux function and is mediated by lower mitochondrial cholesterol with a higher likelihood of the release of molecules that promote cell death, like cytochrome C, from mitochondria.[22]

Normal breast epithelium exhibits strong ABCA1 expression, and breast cancer exhibits lower ABCA1 expression, which appears to be related to a bad prognosis.[27] In particular, a study on breast cancer found that elevating protein expression of ABCA1 can maintain the body's cholesterol balance and inhibit the development of cancer cells by inhibiting the proliferative effects of high cholesterol levels on breast cancer cells in a mouse transgenic model.[28]

In addition, it was revealed that cholesterol efflux plays a significant part in the management of lung cancer. According to a study using microRNA 200b-3p, ABCA1 overexpression dramatically reduces lung cancer cell proliferation, migration, and penetrating lung adenocarcinoma samples, human cell lines A549 and H1299, by functioning as an oncogene.[29] In all prostate tumors, ABCA1 was downregulated, which was noticeable. There have been reports that cells with prostate cancer metastasis have elevated cholesterol levels.[5]

When our study and all these results are evaluated, it can be revealed that ABCA1 may play an important role in the development of EC.

CONCLUSION

Given the possibility of pharmacological regulation using new or existing drugs, future research should focus on understanding the effect of ABCA family transporter activity on the tumor microenvironment and EC cells. The potential of ABCA1, one of the major intracellular cholesterol efflux transporters, to transport cholesterol has enormous potential for use in treating cancer. According to our results, it was determined that it may be possible to develop new therapeutic approaches for the prevention and treatment of cancer by modifying ABCA1 gene expression.

Cancer cells have adapted to employ cholesterol efflux links to promote malignancy, whereas healthy cells reduce the possibility of cell harm from excess cholesterol. The results of our study support this finding, and it has been associated with decreased ABCA1 expression and poor prognosis in the later stages of the disease. Based on this result, we can say that cancer cell growth mechanisms can be interfered with by modifying the ABCA1 gene.

Ethics

Ethics Committee Approval: This research was approved by Mersin University Clinical Research Ethics Committee (approval number: 2020/418, date: 10.06.2020).

Informed Consent: Created anonymously.

Authorship Contributions

Surgical and Medical Practices: H.A., F.T., Concept: Ş.E.A., C.Y., N.C., Design: Ş.E.A., C.Y., N.C., H.A., F.T., S.E.E., Data Collection or Processing: Ş.E.A., F.T., Analysis or Interpretation: Ş.E.A., C.Y., S.E.E., Literature Search: Ş.E.A., Writing: Ş.E.A.

Conflict of Interest: No conflict of interest was declared by the authors.

Financial Disclosure: This study was carried out within the scope of the project The Role of De Novo Lipogenesis and Cholesterol Synthesis Enzymes in the Development of Endometrial Cancer and was supported by Mersin University Scientific Research Projects Unit (Grant No: 2021-1-AP1-4139).

REFERENCES

1. Ferlay J, Soerjomataram I, Dikshit R, Eser S, Mathers C, Rebelo M, Parkin DM, Forman D, Bray F. Cancer incidence and mortality worldwide: sources, methods and major patterns in GLOBOCAN 2012. Int J Cancer. 2015;136:359-386.
2. Key TJ, Pike MC. The dose-effect relationship between 'unopposed' oestrogens and endometrial mitotic rate: its central role in explaining and predicting endometrial cancer risk. Br J Cancer. 1988;57:205-212.
3. Purdie DM, Green AC. Epidemiology of endometrial cancer. Best Pract Res Clin Obstet Gynaecol. 2001;15:341-354.
4. Bokhman JV. Two pathogenetic types of endometrial carcinoma. Gynecol Oncol. 1983;15:10-17.
5. Wu K, Zou L, Lei X, Yang X. Roles of ABCA1 in cancer. Oncol Lett. 2022;24:349.
6. van Meer G, Halter D, Sprong H, Somerharju P, Egmond MR. ABC lipid transporters: extruders, flippases, or flopless activators? FEBS Lett. 2006;580:1171-1177.
7. Kara ZP, Öztürk N, Öztürk D, Okyar A. ABC transporters: circadian rhythms and sex related differences. Müsbed. 2013;3:1-13.
8. Li G, Gu HM, Zhang DW. ATP-binding cassette transporters and cholesterol translocation. IUBMB Life. 2013.
9. Cochran BJ, Ong KL, Manandhar B, Rye KA. APOA1: a Protein with Multiple Therapeutic Functions. Curr Atheroscler Rep. 2021;23:11.
10. Ding X, Zhang W, Li S, Yang H. The role of cholesterol metabolism in cancer. Am J Cancer Res. 2019;9:219-227.
11. Lou L, Zhu H. Progress in the Study of the Correlation between Apolipoproteins and Endometrial Cancer. J Biosci. 2022;10:110-121.
12. Ogura M. HDL, cholesterol efflux, and ABCA1: Free from good and evil dualism. J Pharmacol Sci. 2022;150:81-89.
13. Wang N, Silver DL, Thiele C, Tall AR. ATP-binding cassette transporter A1 (ABCA1) functions as a cholesterol efflux regulatory protein. J Biol Chem. 2001;276:23742-23747.
14. Wu K, Zou L, Lei X, Yang X. Roles of ABCA1 in cancer. Oncol Lett. 2022;24:349.
15. Thysell E, Surowiec I, Hörnberg E, Crnalic S, Widmark A, Johansson AI, Stattin P, Bergh A, Moritz T, Antti H, Wikström P. Metabolomic characterization of human prostate cancer bone metastases reveals increased levels of cholesterol. PLoS One. 2010;5:e14175.
16. Murai T, Maruyama Y, Mio K, Nishiyama H, Suga M, Sato C. Low cholesterol triggers membrane microdomain-dependent CD44 shedding and suppresses tumor cell migration. J Biol Chem. 2011;286:1999-2007.
17. Ramprasad OG, Srinivas G, Rao KS, Joshi P, Thiery JP, Dufour S, Pande G. Changes in cholesterol levels in the plasma membrane modulate cell signaling and regulate cell adhesion and migration on fibronectin. Cell Motil Cytoskeleton. 2007;64:199-216.
18. Plösch T, Gellhaus A, van Straten EM, Wolf N, Huijkman NC, Schmidt M, Dunk CE, Kuipers F, Winterhager E. The liver X receptor (LXR) and its target gene ABCA1 are regulated upon low oxygen in human trophoblast cells: a reason for alterations in preeclampsia? Placenta. 2010;31:910-918.
19. Efsun Antmen S, Canacankatan N, Gürses İ, Aytan H, Erden Ertürk S. Relevance of lipogenesis and AMPK/Akt/mTOR signaling pathway in endometrial cancer. Eur Rev Med Pharmacol Sci. 2021;25:687-695.
20. Smith B, Land H. Anticancer activity of the cholesterol exporter ABCA1 gene. Cell Rep. 2012;2:580-590.
21. Huang CX, Zhang YL, Wang JF, Jiang JY, Bao JL. MCP-1 impacts RCT by repressing ABCA1, ABCG1, and SR-BI through PI3K/Akt posttranslational regulation in HepG2 cells. J Lipid Res. 2013;54:1231-1240.
22. Lee BH, Taylor MG, Robinet P, Smith JD, Schweitzer J, Sehayek E, Falzarano SM, Magi-Galluzzi C, Klein EA, Ting AH. Dysregulation of cholesterol homeostasis in human prostate cancer through loss of ABCA1. Cancer Res. 2013;73:1211-1218.
23. Colell A, García-Ruiz C, Lluis JM, Coll O, Mari M, Fernández-Checa JC. Cholesterol impairs the adenine nucleotide translocator-mediated mitochondrial permeability transition through altered membrane fluidity. J Biol Chem. 2003;278:33928-33935.
24. Montero J, Morales A, Llacuna L, Lluis JM, Terrones O, Basañez G, Antonsson B, Prieto J, García-Ruiz C, Colell A, Fernández-Checa JC. Mitochondrial cholesterol contributes to chemotherapy resistance in hepatocellular carcinoma. Cancer Res. 2008;68:5246-5256.
25. Schimanski S, Wild PJ, Treeck O, Horn F, Sigruener A, Rudolph C, Blaszyk H, Klinkhammer-Schalke M, Ortmann O, Hartmann A, Schmitz G. Expression of the lipid transporters ABCA3 and ABCA1 is diminished in human breast cancer tissue. Horm Metab Res. 2010;42:102-109.
26. Maslyanko M, Harris RD, Mu D. Connecting Cholesterol Efflux Factors to Lung Cancer Biology and Therapeutics. Int J Mol Sci. 2021;22:7209.
27. Liu K, Zhang W, Tan J, Ma J, Zhao J. MiR-200b-3p Functions as an Oncogene by Targeting ABCA1 in Lung Adenocarcinoma. Technol Cancer Res Treat. 2019;18:1533033819892590.
28. Jacobo-Albavera L, Domínguez-Pérez M, Medina-Leyte D.J, González-Garrido A, Villarreal-Molina T. The role of the ATP-binding cassette A1 (ABCA1) in human disease. Int J Mol Sci. 2021;22:1593.
29. Min HY, Lee HY. Mechanisms of resistance to chemotherapy in non-small cell lung cancer. Arch Pharm Res. 2021;44:146-164.

Turk J Pharm Sci 2024;21(3):224-233
DOI: 10.4274/tjps.galenos.2023.99148

ORIGINAL ARTICLE

Characterization of Forced Degradation Products of Netarsudil: Optimization and Validation of a Stability-Indicating RP-HPLC Method for Simultaneous Quantification of Process-Related Impurities

Venkateswara Rao ANNA[1]*, Bodasingi Sai KUMAR[1], Jammu HARISH[1], Bhagya Kumar TATAVARTI[2], Tamma ESWARLAL[3]

[1]Koneru Lakshmaiah Education Foundation, Department of Engineering, Chemistry College of Engineering, Andhra Pradesh, India
[2]Kakaraparti Bhavanarayana College (Autonomous), Department of Chemistry, Andhra Pradesh, India
[3]Koneru Lakshmaiah Education Foundation, Department of Engineering Mathematics, College of Engineering, Andhra Pradesh, India

ABSTRACT

Objectives: The aim of this study is to examine resolution, identification, and characterization of forced degradation products of netarsudil by liquid chromatography-tandem mass spectrometry by validating a simple and sensitive high-performance liquid chromatography method for the resolution, identification, and quantification of two process-related impurities in netarsudil.

Materials and Methods: Chromatographic separation was accomplished on a ZORBAX Eclipse XDB C18 (250 x 4.6 mm; 5 µ id) column at room temperature as the stationary phase and 257 nm as the detector wavelength with the mobile phase consisting of acetonitrile, methanol, and pH 4.6 phosphate buffer in 45:35:20 (*v/v*) at 1.0 mL/min flow rate in isocratic elution.

Results: The method reported very sensitive detection limits of 0.008 µg/mL for impurity 1 and 0.003 µg/mL for impurity 1. The method produces a calibration curve linear in the concentration level of 25-200 for netarsudil and 0.025-0.2 µg/mL for impurities. The proposed method gives acceptable results for other validation parameters such as accuracy, precision, ruggedness, and robustness. The drug was subjected to various stress conditions such as acid, base, peroxide, and thermal and ultraviolet light to investigate the stability-indicating ability of the method. Considerable degradation was observed in stress studies, and the degradation products were well resolved from process-related impurities. The characterization of degradation products was performed on the basis of collision-induced dissociation mass spectral data, and the possible structures of the six degradation compounds of netarsudil were proposed.

Conclusion: The outcomes of other validation studies were likewise satisfactory and proven adequate for the regular analysis of netarsudil and its process-related impurities in bulk drug and pharmaceutical dosage forms and can also be applied for the evaluation of the stress degradation mechanism of netarsudil.

Keywords: Netarsudil, process related impurities, HPLC analysis, forced degradation studies, characterization of degradation compounds

INTRODUCTION

The pharmaceutical industry is rising day by day with the aim of investigating novel drugs that are isolated from natural products or synthesized chemically. The main challenge that always remains is that the compound should be pure, and purity was treated as a significant factor for ensuring drug quality.[1] In the process of synthesis of a pure drug, there is a possibility of some unwanted compounds remaining in the pure drug, and these unwanted compounds are considered as impurities. The presence of these impurities even in very low quantities may influence the quality, efficacy, and safety of the drug

*Correspondence: avrchemistry@gmail.com, Phone: +91 9705678270, ORCID-ID: orcid.org/0000-0002-1705-2822
Received: 20.06.2023, Accepted: 23.07.2023

product. Hence, identification and quantification of impurities are considered essential for producing safe drugs, and high-performance liquid chromatography (HPLC) is considered a simple and convenient procedure for identifying and quantifying impurities from any source.[2]

Netarsudil is a Rho kinase inhibitor and norepinephrine transporter inhibitor drug approved for decreasing elevated intraocular pressure in patients with open-angle glaucoma or ocular hypertension.[3] The key difference between netarsudil and other Rho kinase inhibitors is that it not only minimizes intraocular pressure by reducing outflow resistance but also minimizes aqueous humor production and episcleral venous pressure.[4] The side effects possible during the usage of netarsudil include eye pain upon instillation, eye or eyelid redness changes in vision, discoloration of the eye, and teary eyes.[5] Its molecular structure is shown in Figure 1 with the International Union of Pure and Applied Chemistry name of *[4-[(2S)-3-Amino-1-(isoquinolin-6-ylamino)-1-oxopropan-2-yl] phenyl]methyl 2,4-dimethylbenzoate* with a molecular formula of $C_{28}H_{27}N_3O_3$ and a mass of 453.542 g/mol.

A literature survey was conducted to determine the available analytical method for quantification of netarsudil using various analytical techniques. In the literature, it was observed that few analytical methods have been reported for the quantification of netarsudil along with latanoprost using HPLC[6-10] and Ultra Performance Liquid Chromatography.[11] One Ultra Performance Liquid Chromatography/Mass Spectrometry method has been reported for the quantification of netarsudil along with timolol and latanoprost.[12] One Liquid Chromatography-Quadrupole Time-of-Flight Mass Spectrometry/Tandem Mass Spectrometry method has been reported for the identification and characterization of netarsudil and its hydrolytic degradation products.[13] The literature review suggests that no method is available for the resolution, identification, and quantification of process-related impurities of netarsudil. Hence, this study intended to fill the gaps identified in the literature. Process-related impurities 1 and 2 were available for the study and hence were selected. The molecular structure of netarsudil and its process related impurities is presented in Figure 1.

Netarsudil

The origin of process-related impurities in the netarsudil synthetic drug was evaluated by observing the synthesis route of netarsudil[14] and is presented in Figure 2. In the process of synthesis of netarsudil, the starting product of the reaction, *i.e.*, (4-[(2,4-dimethylbenzoyl)oxy]methylphenyl)acetic acid (4), and the intermediate product (6) remain in the final product, and these compounds are designated as impurities 1 and 2, respectively.

MATERIALS AND METHODS

Chemicals and reagents

The analytical standard compound netarsudil with purity of 98.17% and impurities 1 and 2 were procured from Ajanta Pharma Limited, Hyderabad, Salangana. The eye drop formulation containing 0.02% *w/v* netarsudil was obtained from a local pharmacy. HPLC grade methanol, acetonitrile, and Milli-Q® water were obtained from Merck Chemicals, Mumbai. Reagent grade chemicals such as acetic acid, sodium acetate, hydrochloric acid (HCl), sodium hydroxide (NaOH), and hydrogen peroxide were purchased from Fisher Scientific, Mumbai.

Instrumentation

HPLC analysis was performed on an Agilent 1100 (USA) instrument coupled with a quaternary pump (G1311 A) for solvent delivery. The analytes were injected through a temperature-adjustable autosampler (G1329A) with an injection capacity of 0.1-1500 µL. The column eluents were detected using a programable ultraviolet (UV) detector (G1314A), and the chromatographic integration was performed using Agilent chem-station software. Liquid Chromatography-Mass Spectrometry (LCMS) analysis was performed on a Waters LCMS (Japan) equipped with a triple quadruple mass detector. During the mass spectral analysis, a splitter was placed between the column and detector to allow 40% of the chromatographic eluents to be entered into the electrospray Ionization (ESI) source. The mass detector was operated in positive ESI mode with suitable fragmentor voltage (70 V), capillary voltage (3200-3600 V), and skimmer voltage (60 V). Nebulization (40

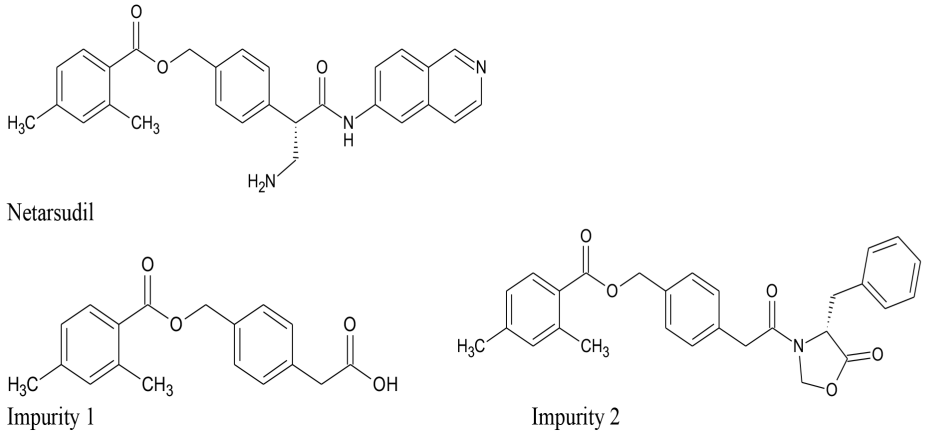

Figure 1. Molecular structure of netarsudil and its impurities in the study

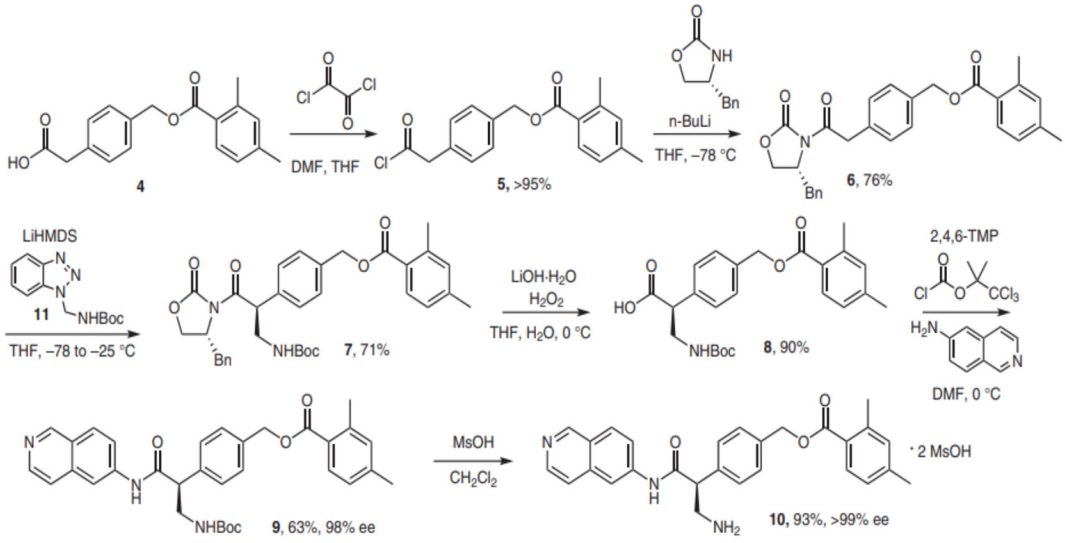

Figure 2. Netarsudil synthesis route

Psi) and drying (300 °C, 9 L/h) were performed using nitrogen gas. The spectra throughout the analysis were recorded under similar experimental conditions and 20-30 average scans were conducted.

Preparation of solutions

Netarsudil and impurity solutions

The standard netarsudil and its impurities at 1 mg/mL (1000 µg/mL) were prepared separately by accurately weighing 25 mg of analyte in 25 mL of volumetric flask containing 15 mL of methanol. The analytes were dissolved in a solvent using an ultrasonic bath sonicator. Then, the analytes were filtered through a 0.2 µ membrane filter, and the final volume was made up to the mark using the same solvent to obtain a 1000 µg/mL concentration of netarsudil and its impurities separately. During the analysis, the selected volume of the required concentration of individual analytes was mixed separately.

Formulation solution

The eye drop formulation containing 0.02% *w/v* of netarsudil was used for preparing the formulation solution. An accurately measured netarsudil solution (25 mL) was taken in a 50 mL calibrated flask containing 10 mL methanol. The flask was sonicated to dissolve the formulation completely in the solvent and then the volume was made up to mark with the same solvent. The solution was filtered through a 0.2 µ membrane filter to obtain the formulation solution at a concentration of 100 µg/mL, and the same solution was used for formulation analysis.

Method development

The method development was initiated by identifying a suitable wavelength for the detection of netarsudil and its impurities using a UV detector. The UV-visible spectrophotometer was used for the identification of suitable wavelength for the detection of netarsudil and its impurities. The standard solution at 10 µg/mL concentration of netarsudil and its impurities was scanned individually at a scan range of 400-200 nm. The overlay UV absorption spectra of netarsudil and its impurities confirm that the isoabsorption wavelength is suitable for detecting netarsudil and its impurities.

The suitable stationary phase for the separation of netarsudil and its impurities in the study was selected based on the resolution and chromatographic responses of the analytes in each column studied. Various C18 columns such as zodiac, zorbax XDB, phenomenex luna, and prontoSIL ODS columns with 250- and 100-mm column lengths were studied. The solvents like methanol and acetonitrile were selected as organic modifiers, and various strengths of acetate and phosphate buffer were selected as pH modifiers. Various compositions of these solvents were pumped at a flow range of 0.5 to 1.5 mL/min was studied for the best resolution of netarsudil and its impurities. In the method development conditions performed, the 100% standard solution containing 0.01% of impurities 1 and 2 was analyzed. The condition that gives the best resolution of netarsudil and its impurities with acceptable system suitability was considered suitable for the study.

Method validation

The method optimized for the evaluation of netarsudil and its impurities was validated as per methodology reported in literature[15-18] as well as International Conference on Harmonization (ICH) guidelines.[19]

System suitability

The 100% concentration level solution was analyzed six times in the proposed method to establish the system suitability of the developed method. The chromatographic response of the resultant chromatograms in each study was summarized to evaluate the system suitability of the developed method. Chromatographic parameters such as retention time (RT), asymmetric factor (tail factor), plate count (number of theoretical plates), and resolution factor were used to evaluate method system suitability.

Sensitivity

The method sensitivity of the proposed method for the detection of impurities was evaluated by assessing the detection limit (LOD) and quantification limit (LOQ). The signal (s) to noise (n) ratio method was adopted for evaluating the sensitivity levels of impurities in the developed method. The minimal concentration of netarsudil impurities was analyzed using the developed method, and the chromatographic response (signal) along with the baseline (noise) response was summarized. The signal-to-noise ratio of 3 and 10 was considered as LOD and LOQ, respectively.

Linearity and range

The calibration concentrations were prepared such that the netarsudil solution contained 0.1% impurity. Various levels of netarsudil standard solution spiked with 0.1% of the studied impurities were analyzed in the developed method. The chromatographic response of each analyte was tabulated, and the calibration curve was plotted individually by considering the obtained peak area response on the y-axis and its prepared concentration on the x-axis. The best-fit calibration range for each analyte was considered to be a suitable range of analysis in the developed method.

Precision

The 100% concentration level in the linearity level spiked with 0.1% of each impurity was used to evaluate the repeatability and reproducibility of the developed method. The solution was prepared and injected six times in one day (intraday), three days (interday), and by different analysts on the same day (ruggedness). The peak area response of each analyte in each study was tabulated, and the percentage relative standard deviation (RSD) was calculated for each analyte in each study. A RSD% of less than 2 was acceptable in each study as per the guidelines.

Robustness

The influence of minor variations in the developed method conditions for the separation and quantification of netarsudil and its impurities was evaluated in robustness. The ± 5 mL variation in the composition of the mobile phase, ± 5 nm variation in the wavelength of the detector and ± 0.1 factor variation in the mobile phase pH were intentionally made, and a 100% concentration of netarsudil containing 0.1% of each impurity was injected in each changed method condition. The chromatographic response and system suitability of the obtained chromatograms under each condition are summarized. The percentage change in the peak area response of each analyte was calculated by comparing it with the corresponding regression equation, and a percentage change of less than 2 was treated as acceptable.

Recovery

The 50, 100 and 150% levels to a known concentration (100%) in the linearity range were used for evaluating the method's accuracy. The percentage recovery in each analysis was calculated by correlating the recovery results with the calibration results. The percentage RSD in every studied spiked level was calculated for netarsudil and its impurities. The percentage recovery in the range of 98-102 and percentage RSD of < 2 in each level was considered acceptable.

Force degradation studies

The applicability of this method for the separation and analysis of stress degradation compounds generated during the stress exposure of netarsudil was confirmed by performing forced degradation studies. The standard netarsudil at a quantity of 50 mg was separately mixed with 50 mL of 0.1 N HCl, 0.1 N NaOH, and 3% peroxide solution for acid, base, and peroxide degradation studies, respectively. The stressed samples were incubated for 24 hours to induce degradation of the netarsudil drug. Then, the solution was neutralized, diluted to a 100% concentration level, and analyzed. The standard netarsudil was taken in a Petri dish and exposed to 60 °C for 24 hours in an air oven for thermal degradation and exposed to UV light at 254 nm for 24 hours for photolytic degradation study. The stressed sample was then diluted to a 100% concentration level, and the dilute solution was analyzed using the developed method. The chromatograms observed for each stress sample analysis were used to evaluate the efficiency of the method for the separation and analysis of stress degradation compounds. The percentage degradation of netarsudil was calculated by comparing the peak area response of the stressed sample with that of the un-stressed sample of the same concentration level. The peaks corresponding to degradation products were characterized using mass spectral analysis.

Sample analysis

The netarsudil solution was analyzed using the developed method. The formulation solution spiked with known and concentration of the impurities was also analysed. Based on results noticed during formulation analysis, the % assay of netarsudil and its impurities was calculated using its corresponding calibration equation.

RESULTS

The literature survey for the available analytical methods proved that there is no method reported for the resolution and quantification of process-related impurities of netarsudil in synthetic drugs or pharmaceutical formulations. In view of the above, this study was intended to develop a simple and sensitive HPLC method for quantification of two process-related impurities, namely impurities 1 and 2, along with netarsudil in formulations.

In the process of method development, various method conditions were optimized by comparing the results attained in each studied condition. The method optimization was concluded by achieving the best resolution of analytes with acceptable system suitability. The mobile phase composition of acetonitrile, methanol and pH 4.6 phosphate buffer in 45:35:20 (*v/v*) as mobile phase at 1.0 mL/min flow rate, ZORBAX Eclipse XDB C18 (250 x 4.6 mm; 5 µ id) column at room temperature as stationary phase and 257 nm as detector wavelength. Under the proposed method conditions, the chromatogram of the blank (Figure 3A) did not show any chromatographic detection

throughout the run time, whereas 100% solution of netarsudil spiked with 0.1% impurities was noticed to be well resolved and retained peaks corresponded to analytes in the study (Figure 3B). This result proved that the method was specific for detecting netarsudil and its impurities.

A) Chromatogram obtained for bank analysis in the developed method; B) standard chromatogram observed for analysing netarsudil standard solution at 100 µg/mL concentration spiked with 0.1% impurities

A tail factor of less than 1.5, plate count of more than 2500, and resolution of more than 2 were noticed for netarsudil, and its impurities suggest that the method passes system suitability and has good selectivity. The s/n method was used for evaluating method sensitivity, and the results were expressed in terms of LOD and LOQ. The LOD was observed to be 0.008 µg/mL and 0.003 µg/mL, whereas the LOQ was identified as 0.025 µg/mL and 0.010 µg/mL for impurities 1 and 2, respectively. The results obtained for both I impurities indicate the higher sensitivity of the method.

The higher LOQ concentration of impurities, *i.e.* 0.025 µg/mL) was taken as the initial concentration for constructing the calibration curve for both impurities. The netarsudil standard solution was prepared such that the solution contained 0.1% of each impurity, and an accurate fit calibration curve was obtained in the concentration level of 25-200 for netarsudil and 0.025-0.2 µg/mL for impurities.

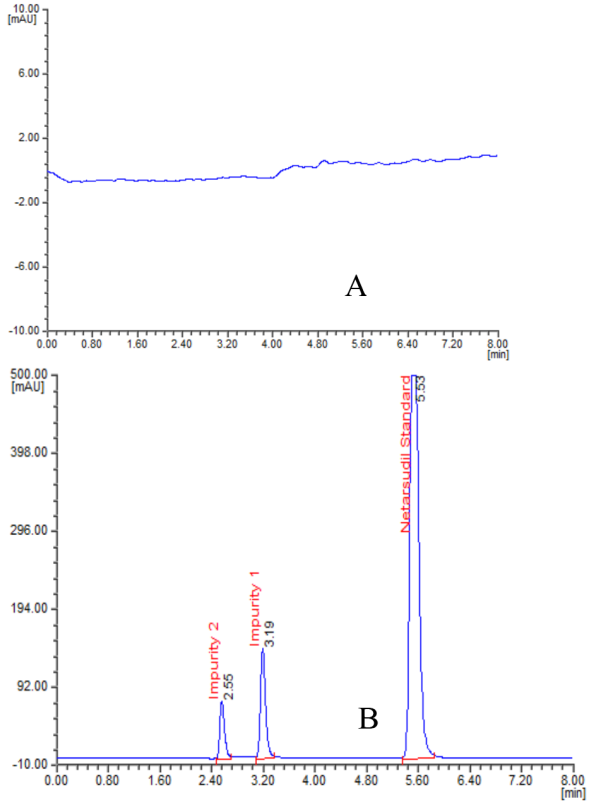

Figure 3. Specificity chromatograms observed in the proposed method, A) chromatogram obtained for bank analysis in the developed method; B) standard chromatogram observed for analysing netarsudil standard solution at 100 µg/mL concentration spiked with 0.1% impurities

The RSD% values of peak areas obtained were below 2 for impurities and netarsudil in intraday, interday precision, precision at the LOQ level, and ruggedness study, indicating good precision of the method. The summary results observed in the system suitability, linearity, precision, accuracy, and sensitivity study in the proposed method are presented in Table 1.

Spiked recovery at three spiked levels was performed to evaluate the accuracy of the proposed method for evaluating netarsudil and its impurities. The percentage recovery in each analysis as well as the percentage RSD in each studied level was noticed to be within the acceptable level for netarsudil and its impurities studied. The acceptable percent recovery and percentage RSD were observed, suggesting that the method was accurate. Results in the recovery study are presented in Table 2.

In all deliberately altered chromatographic conditions, such as mobile phase composition, pH, and detector wavelength, all analytes were resolved and the order of elution was unchanged. A very nominal percentage variation of less than 1 was noticed

Table 1. Summary results of method validation study

Parameter	Drugs		
	Netarsudil	Impurity 1	Impurity 2
System suitability[$]			
t_R (minute)	5.53	3.19	2.55
RRT	-	0.58	0.46
RRF	-	0.088	0.067
R_S	9.14	3.97	-
K^I	1.81	0.62	0.29
A_S	0.98	1.04	1.07
N	6525	7908	12410
Linearity			
Range in µg/mL	25-200	0.025-0.2	0.025-0.2
Slope	7108.2	627533	479773
Intercept	19692	-809.74	-258.73
r^2	0.9995	0.9992	0.9994
Precision[$$]			
Intraday	0.22	0.23	0.85
Interday (day 1)	1.31	0.89	1.30
Interday (day 2)	0.94	0.72	0.34
LOQ level	-	0.83	1.02
Sensitivity			
LOD (µg/mL)	-	0.008	0.003
LOQ (µg/mL)	-	0.025	0.010

[$]Average of three determinations, [$$]average of six determinations, t_R (minute): Retention time, RRT: Relative retention time, RRF: Relative response factor, R_S: Resolution, K^I: Retention factor, A_S: Tail factor, N: No of theoretical plates, r^2: Slope

for netarsudil and its studied impurities. The variability in the estimation of netarsudil and impurities was within the acceptable level of 2, indicating the robustness of the method. Table 3 presents the robustness study results obtained using the developed method.

No considerable degradation of netarsudil was observed under thermolytic stress conditions. Significant degradation of the netarsudil drug substance was observed in other degradation conditions studied. The assay of netarsudil for three determinations in acid degradation was calculated to be 91.09%, whereas, in the presence of impurities and degradation products, it was 99.73%. The chromatogram clearly resolves three degrdation products (DPs) identified at RTs of 0.89, 1.65, and 7.28 minutes, and these impurities are marked as DP 1, DP 2, and DP 6, respectively. Three degradation products were identified in the base degradation study with a percentage degradation of 6.32%. The percentage degradation of 4.01 and 9.85 was noticed in the peroxide and UV light degradation studies. Based on the t_R of the degradation products identified, it was confirmed that 6 DPs were observed in the stress degradation study of netarsudil.

Table 2. Recovery results in the study

Accuracy level	Drugs		
	Netarsudil	Impurity 1	Impurity 2
50%[$]			
Amount added (µg/mL)	50	0.05	0.05
Amount recovered (µg/mL)	49.478	0.04939	0.04940
Recovery %	98.96	98.78	98.7900
RSD %	0.79	0.90	0.76
100%[$]			
Amount added (µg/mL)	100	0.10	0.10
Amount recovered (µg/mL)	99.05	0.09879	0.09891
Recovery %	99.05	98.79	98.91
RSD %	0.49	0.99	0.78
150%[$]			
Amount added (µg/mL)	150	0.15	0.15
Amount recovered (µg/mL)	147.86	0.15086	0.15081
Recovery %	98.57	100.57	100.54
RSD %	0.47	0.37	0.60

[$]Average of three determinations, RSD: Relative standard deviation

The purity of netarsudil in each stress study was evaluated using a photodiode array detector, and the results proved that the peak was homogeneous and pure. A very high mass balance in the level of 99.02-99.84% was noticed in the stress study, and the results suggest that the method was specific and stable. Table 4 presents the results and Figure 4 shows the representative chromatograms observed in the forced degradation study.

A) Acid degradation chromatogram of netarsudil showing DP 1, 2, and 6; B) base degradation chromatogram of netarsudil showing DP 2, 4, and 5; C) peroxide degradation chromatogram of netarsudil showing DP 4 and 6; D) UV light degradation chromatogram of netarsudil showing DP 2 and 3.

Characterization of DPs by LC-MS/MS

Netarsudil and its DPs (DP 1 to DP 6) were well resolved by LC and identified at the specified RT. All DPs, along with standard netarsudil, exhibited abundant protonated molecular ions ($[M+H]^+$) in the positive ionization mode. Structural confirmation of DPs was performed using collision-induced dissociation (CID) spectra of the molecular ions of netarsudil. The ESI MS spectrum of DP 1 identified at t_R of 0.8 min showed abundant parent ions at an m/z of 298 (m+1), which might be due to *4-(2-amino-2-oxoethyl)benzyl 2,4-dimethylbenzoate* (loss of $C_{10}H_8N_2$ from $C_{28}H_{27}N_3O_3$ of netarsudil). In addition, the spectrum also showed a low abundance of product ions at m/z of 122 (m+1), which corresponds to benzoate ions with the molecular formula of $C_7H_6O_2$ by losing $C_{11}H_{14}NO$. The fragmentation spectra are shown in Figure 5A.

Table 3. Results observed in robustness study

Chromatographic conditions	t_R			Number of theorietical plates			Change in peak area %		
	NTD	Impurity 1	Impurity 2	NTD	Impurity 1	Impurity 2	NTD	Impurity 1	Impurity 2
Mobile phase composition (*v/v* of acetonitrile, methanol and buffer)[$]									
40:40:20	5.51	3.19	2.57	6904	8015	12328	0.42	0.47	0.76
50:30:20	5.53	3.20	2.54	6858	8146	12507	0.26	0.99	0.98
Detector wavelength[$]									
252 nm	5.53	3.08	2.55	6562	7858	12269	0.51	0.88	0.57
262 nm	5.50	3.10	2.53	6749	7940	12351	0.96	0.74	0.13
Mobile phase pH[$]									
4.5	5.55	3.11	2.54	6631	8414	12499	0.28	0.52	0.61
4.7	5.52	3.10	2.56	6503	8329	12407	0.69	0.95	0.31

[$]Average of three determinations (n= 3), NTD: Netarsudil

The mass fragmentation spectra of DP 2 (Figure 5B) show an abundant parent ion at an m/z of 314 (m+1) under the negative ionization mode. The spectrum also shows fragment ions at m/z of product ions at m/z of 122 (m+1), which corresponds to benzoate ions with a molecular formula of $C_7H_6O_2$. Based on the achieved date, DP 2 was confirmed to be *4-(1-amino-3-hydroxypropan-2-yl)benzyl 2,4-dimethylbenzoate* with a molecular formula of $C_{19}H_{23}NO_3$.

The ESI-MS spectrum identified at a RT of 2.0 min shows a parent ion at m/z= 152 corresponding to the $[M+H]^+$ of DP 3 formed under acidic stress (Figure 5C). The spectrum showed abundant product ions at m/z 78, and the production fragments correlated well with the fragmentation pattern of benzene. The purity test and CID studies of DP 3 suggest that it is one of the degradation products of DP-2 observed in the study. All these product ions and patent ions confirm DP 3 as *(2,4-dimethylphenyl)(hydroxy)methanolate* with the molecular formula $C_9H_{11}O_2$.

The ESI-MS spectrum of DP 4 (Figure 5D) identified at a RT of 4.1 min shows a parent ion at m/z= 322 (m+1) with a parent ion at m/z= 123 (m+1). The parent ion shows a molecular formula of $C_{19}H_{19}N_3O_2$ and a fragment ion with a molecular formula of $C_7H_{10}N_2$ by losing $C_{12}H_9NO_2$. DP 4 was identified as *3-amino-2-[4-(hydroxymethyl)phenyl]-N-(isoquinolin-6-yl)propanamide* with a molecular mass of 322 (m+1), DP 5 (Figure 5E) observed at an RT of 4.5 min was identified as *isoquinolin-6-amine* with

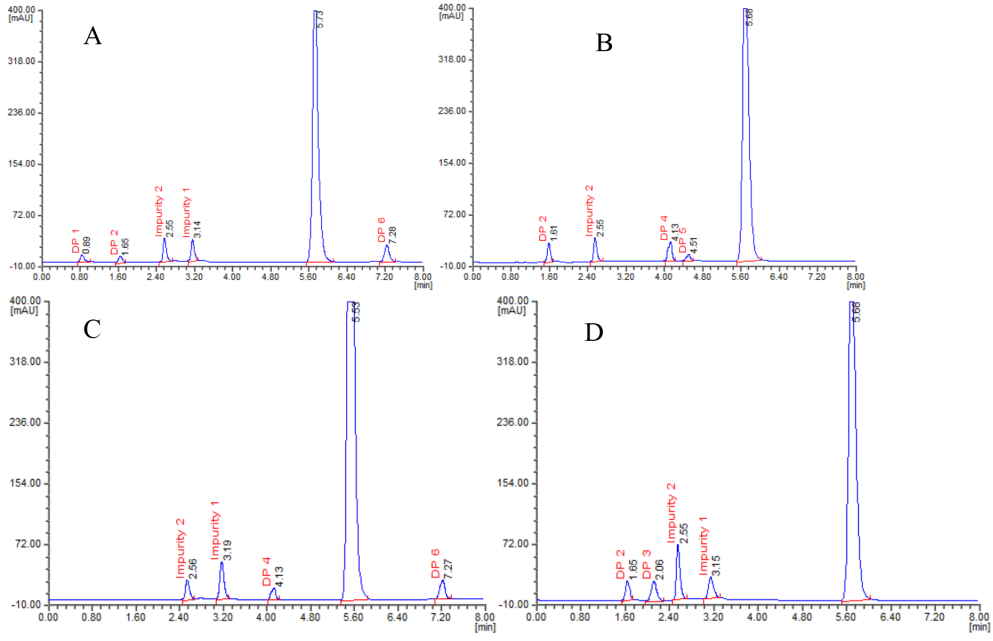

Figure 4. Chromatogram observed in forced degradation study of netarsudil in the proposed method, A) acid degradation chromatogram of netarsudil showing DP 1, 2 and 6; B) base degradation chromatogram of netarsudil showing DP 2, 4 and 5; C) peroxide degradation chromatogram of netarsudil showing DP 1, 4 and 6; D) UV light degradation chromatogram of netarsudil showing DP 2 and 3

UV: Ultraviolet, DP: Degrdation product

Table 4. Summary of netarsudil forced degradation results in the proposed method

Stress condition	% Degradation[$] of netarsudil	% Assay[$] of netarsudil	% Mass balance[$] (assay + total impurities)	Remark
Acid	8.91	91.09	99.47	DP 1 (0.89 minute), 2 (1.65 minute) and 6 (7.28 minute) were identified
Base	6.32	93.68	99.78	DP 2 (1.61 minute), 4 (4.13 minute) and 5 (4.51 minute) were identified
Peroxide	4.01	95.99	99.63	DP 4 (4.13 minute) and 6 (7.27 minute) were identified
Thermal	3.28	96.72	99.95	No degradation was identified
UV light	9.85	90.15	99.58	DP 2 (6.15 minute) and 3 (2.06 minute) were identified

[$]Average of three replicate experiments, UV: Ultraviolet, DP: Degrdation product

a molecular formula of $C_9H_8N_2$ and a molecular mass of 145 (m+1).

The characterization of DP 6 (Figure 5F) was carried out based on its ESI MS spectrum $[M+H]^+$ that showed abundant product ions at m/z 304 (m+1). The production at m/z 105 may be formed by the loss of $C_{11}H_9NO_3$ from m/z 304, resulting in a p-xylylene ion. The peak purity CID studies of DP 6 confirm that it is one of the degradation products of DP 4 observed in the study. Based on these studies, DP 6 was identified as *3-amino-N-(isoquinolin-6-yl)-2-(4-methylidenecyclohexa-2,5-dien-1-ylidene)propanamide* with a molecular mass of 303 g/mol and formula of $C_{19}H_{17}N_3O$. The DP 1 to 6 generated during the stress study of netarsudil was presented in Figure 6.

The developed HPLC method was applied to quantify process-related impurities of netarsudil in pharmaceutical formulations. The formulation sample was directly analyzed for the evaluation of impurities present in it, and the formulation sample spiked with impurities was analyzed to evaluate the effectiveness of the method for the resolution and quantification of impurities in the formulation. The chromatogram obtained for the impurity spiked formulation solution (Figure 7A) shows a clear identification of peaks corresponding to the impurities in the study. The chromatogram observed for the unspiked formulation solution (Figure 7B) shows peaks corresponding to impurity 1 only. Impurity 2 was not identified in the chromatogram, proving that the quantity of impurity in the sample was less than the LOD of impurity B. The peak area response of impurity 1 was substituted in its corresponding regression equation, and the percentage assay was calculated. The percentage assay of impurity 1 was estimated to be 0.02%. This confirms that the quantity of impurity in the sample was noticed to be under the permissible level, and the proposed method can be successfully applied for the quantification of process-related impurities in netarsudil.

DISCUSSION

The study addresses a critical gap in existing literature by developing a novel HPLC method for the precise quantification of process-related impurities (impurities 1 and 2) along with netarsudil in pharmaceutical formulations. Through syntematic method optimization including the optimization of mobile phase composition, column selection, and detector wavelength, optimal conditions were established to ensure effective resolution

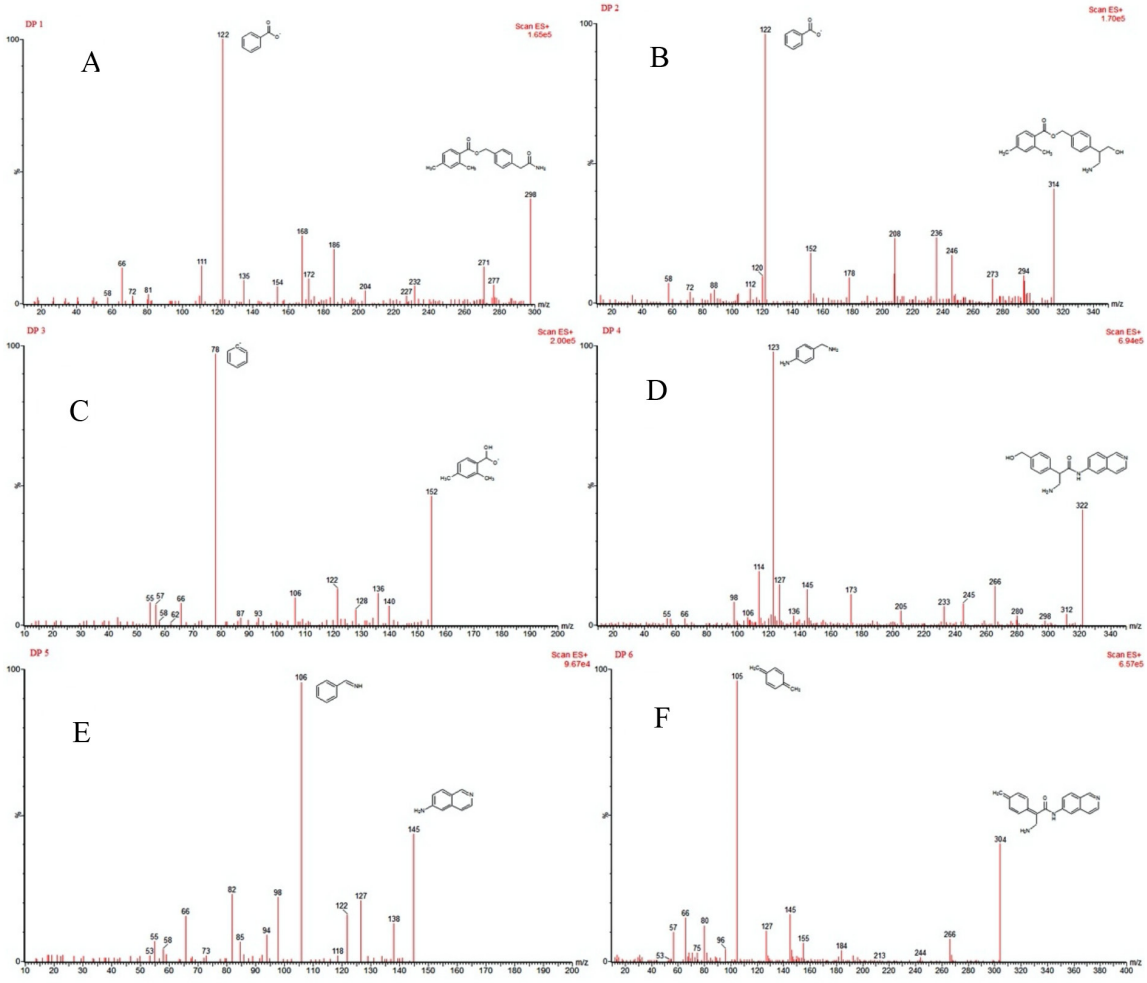

Figure 5. Mass spectra of DPs observed in forced degradation study, mass spectra identified at tR of 0.8 min for DP 1 (A), 1.6 min for DP 2 (B), 2.0 min for DP 3 (C), 4.1 min for DP 4 (D), 4.5 min for DP 5 (E) and 7.2 min for DP 6 (F)

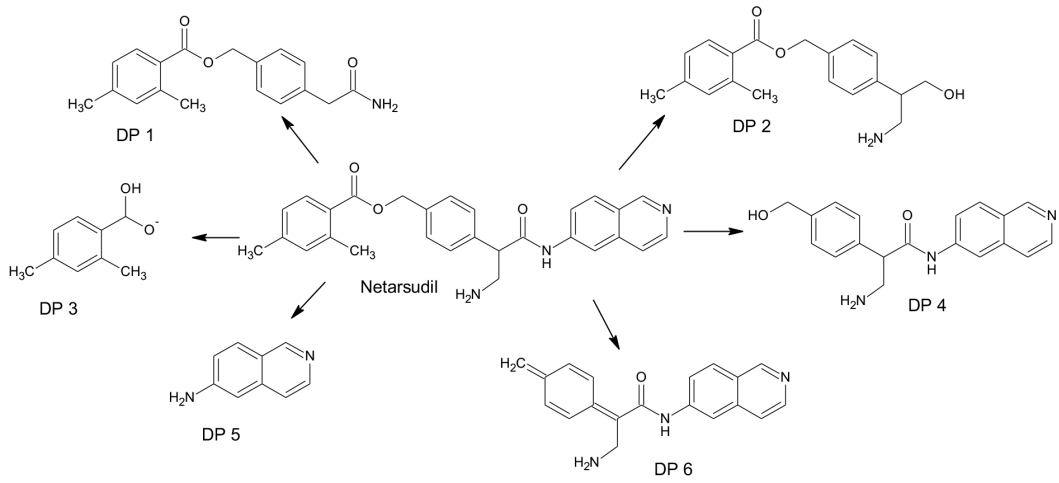

Figure 6. Degradation products formed during the forced degradation study of netarsudil

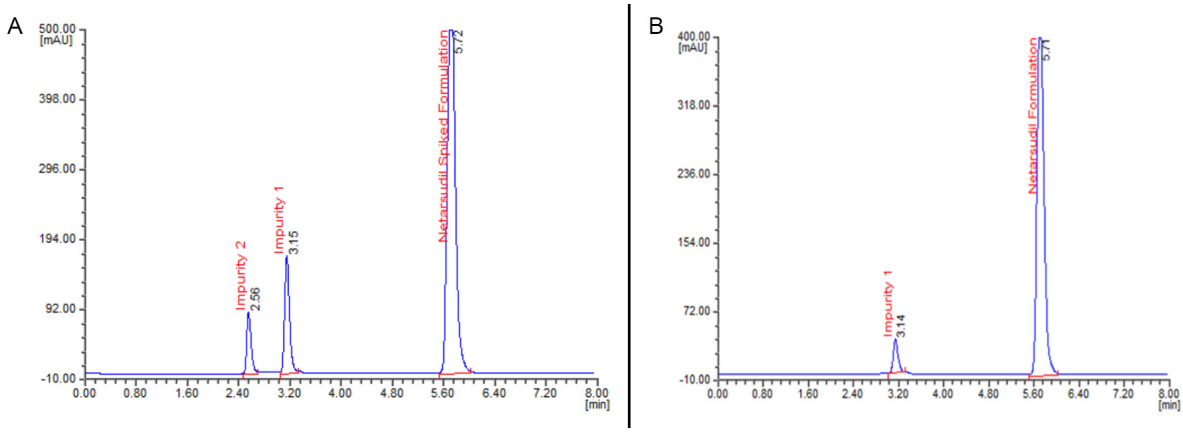

Figure 7. Formulation chromatogram of netarsudil in the developed method, A) chromatogram observed for analysing netarsudil solution spiked with 0.1% impurities; B) chromatogram observed for analysing netarsudil formulation solution spiked with no impurities

and system suitability. The finalized method exhibited robust chromatographic parameters, including tailing factors below 1.5, plate counts exceeding 2500, and resolution values greater than 2, confirming its specificity and reliability. Sensitivity assessments revealed low limits of detection (LOD) at 0.008 µg/mL and 0.003 µg/mL for impurities 1 and 2, respectively, underscoring the method's ability to detect trace impurities. Calibration curves constructed across a broad concentration range (25-200 µg/mL for netarsudil and 0.025-0.2 µg/mL for impurities) demonstrated excellent linearity, essential for accurate quantification. Precision studies demonstrated consistent results with RSD% values below 2, both within-day and between-day, reinforcing the method's reliability. Furthermore, robustness testing under varied chromatographic conditions showed minimal impact on quantification, affirming the method's stability and reproducibility. Application of the method to pharmaceutical formulations effectively identified and quantified impurities, with analysis of spiked and unspiked samples confirming its suitability for routine quality control. The study's comprehensive approach, including forced degradation studies and characterization of degradation products through LC-MS/MS, provided valuable insights into netarsudil's stability under stress conditions, enhancing its applicability in pharmaceutical analysis and ensuring compliance with regulatory standards.

CONCLUSION

A simple, sensitive isocratic reversed-phase HPLC method has been optimized and subsequently used for the evaluation of a stability-indicating assay of netarsudil and its two process-related impurities in bulk drugs and its dosage forms. The developed method was validated to be selective, sensitive, linear, accurate, precise, and sensitive and is applicable for evaluating process-related impurities and degradation products at trace levels in bulk drugs and formulations. The degradation behavior of netarsudil was assessed under different stress conditions as per the ICH prescribed guidelines. In total, six degradation products were formed and characterized by LCMS. The DPs were characterized as *4-(2-amino-2-oxoethyl)benzyl 2,4-dimethylbenzoate* (DP 1), *4-(1-amino-3-hydroxypropan-2-yl)benzyl 2,4-dimethylbenzoate* (DP 2), *(2,4-dimethylphenyl)(hydroxy)methanolate* (DP 3), *3-amino-2-[4-(hydroxymethyl)phenyl]-N-(isoquinolin-6-yl)propanamide* (DP 4), *isoquinolin-6-amine* (DP 5), and *3-amino-N-(isoquinolin-6-yl)-2-(4-*

methylidenecyclohexa-2,5-dien-1-ylidene) propanamide (DP 6). Thus, this method can be used for process development and quality assurance of netarsudil in bulk drugs.

Ethics

Ethics Committee Approval: This study does not involve the use of animals, and therefore ethical approval is not required to complete my research study.

Informed Consent: In this study, a no-consent model was employed to complete this research work.

Authorship Contributions

Concept: V.R.A., B.S.K., J.H., Design: V.R.A., B.K.T., T.E., Data Collection or Processing: V.R.A., B.S.K., J.H., Analysis or Interpretation: V.R.A., B.S.K., J.H., Literature Search: V.R.A., B.K.T., T.E., Writing: V.R.A., B.S.K., J.H.

Conflict of Interest: No conflict of interest was declared by the authors.

Financial Disclosure: The authors declared that this study received no financial support.

REFERENCES

1. Rahman N, Azmi SNH, Fen Wu H. The importance of impurity analysis in pharmaceutical products: an integrated approach. Accred Qual Assur. 2006;11:69-74.
2. Görög S. The importance and the challenges of impurity profiling in modern pharmaceutical analysis. TrAC Trends in Analytical Chemistry. 2006;25:755-757.
3. Dasso L, Al-Khaled T, Sonty S, Aref AA. Profile of netarsudil ophthalmic solution and its potential in the treatment of open-angle glaucoma: evidence to date. Clin Ophthalmol. 2018;12:1939-1944.
4. Li G, Mukherjee D, Navarro I, Ashpole NE, Sherwood JM, Chang J, Overby DR, Yuan F, Gonzalez P, Kopczynski CC, Farsiu S, Stamer WD. Visualization of conventional outflow tissue responses to netarsudil in living mouse eyes. Eur J Pharmacol. 2016;787:20-31.
5. Kahook MY, Serle JB, Mah FS, Kim T, Raizman MB, Heah T, Ramirez-Davis N, Kopczynski CC, Usner DW, Novack GD; ROCKET-2 Study Group. Long-term safety and ocular hypotensive efficacy evaluation of netarsudil ophthalmic solution: rho kinase elevated IOP treatment trial (ROCKET-2). Am J Ophthalmol. 2019;200:130-137.
6. Manoranjani M. Stability indicating assay method development and validation of netarsudil and latanoprost by RP-HPLC and its degradation. JETIR. 2019;6:825-832.
7. Padmalatha K, Vijaya Durga D, Jagadeeswari N. A novel study on Rp-Hplc method development and validation for estimation of netarsudil and latanoprost in api and pharmaceutical dosage form. World J Pharm Res. 2021;10:1624-1633.
8. Kunala A, Gummadi S. Simultaneous estimation of netarsudil and latanoprost by stability indicating RP-HPLC-PDA in pure binary blend and their ophthalmic solution. Int J Pharm Qual Assur. 2022;13:308-314.
9. Ramana LV, Narendra D, Lakshmi G. Method development and validation for simultaneous estimation of netarsudil & latanoprost by RP-HPLC method. Eur J Pharm Med Res. 2020;7:888-894.
10. Sai Sharanya P, Shoba Rani S. Development and Validation of stability indicating analytical method for the simultaneous estimation of netarsudil and latanoprost by RP-HPLC. World J Pharm Sci. 2022;10:104-112.
11. Dharmamoorthy G, Nataraj KS, Manjari Pawar AK. Development and validation of a stabilityindicating reverse-phase ultra-performance liquid chromatography method for the simultaneous determination of netarsudil and latanoprost in bulk and pharmaceutical formulation. Int J Green Pharm. 2020;14:179-185.
12. Wang T, Zhang Y, Chi M, Zhao C, Cao L, Tian C, Kamei K, Zheng Y, Jiang Q. A novel fixed-combination timolol-netarsudil-latanoprost ophthalmic solution for the treatment of glaucoma and ocular hypertension. Asian J Pharm Sci. 2022;17:938-948.
13. Kumar Raju SP, Reddy JR. Identification and characterization of novel hydrolytic degradation products of netarsudil by LC-Q-TOF-MS/MS: In silico toxicity prediction. J Liq Chromatogr Relat Technol. 2022:45:1-9.
14. deLong MA, Sturdivant JM. Asymmetric Synthesis of Netarsudil: a new therapeutic for open-angle glaucoma. Synthesis. 2019;51:953-959.
15. Kasimala BB, Mallu UR, Anna VR, Reddy LM. Intended high-performance liquid chromatography procedure for the quantification of norfloxacin and its potential impurities in active pharmaceutical ingredient and tablet dosage forms. Thai J Pharm Sci. 2018;42:27-36.
16. Mallu UR, Anna VR, Kasimala BB. Rapid stability indicating HPLC method for the analysis of leflunomide and its related impurities in bulk drug and formulations. Turk J Pharm Sci. 2019;16:457-465.
17. Kasimala BB, Anna VR, Reddy Mallu U. Stability-indicating reversed-phase HPLC method for the separation and estimation of related impurities of cilnidipine in pharmaceutical formulations. Indian Drugs. 2018;55:41-49.
18. Sri Girija K, Kasimala BB, Anna VR. A new high-performance liquid chromatography method for the separation and simultaneous quantification of eptifibatide and its impurities in pharmaceutical injection formulation. Int J App Pharm. 2021;13;165-172.
19. ICH validation of analytical procedures: text and methodology Q2(R1). Access Date: 27.10.1994.

Turk J Pharm Sci 2024;21(3):234-242
DOI: 10.4274/tjps.galenos.2023.08504

ORIGINAL ARTICLE

Evaluation of Herbal Products and Dietary Supplements Use in Patients with Respiratory Diseases Applied to Tertiary Health Institution

Tuğba SUBAŞ[1]*, Ufuk ÖZGEN[1], Yılmaz BÜLBÜL[2], Tevfik ÖZLÜ[2], Gülin RENDA[1], Abdul Kadir ALBAYRAKTAR[3]

[1]Karadeniz Technical University Faculty of Pharmacy, Department of Pharmacognosy, Trabzon, Türkiye
[2]Karadeniz Technical University Faculty of Medicine, Department of Chest Diseases, Trabzon, Türkiye
[3]Karadeniz Technical University Faculty of Medicine, Department of Public Health, Trabzon, Türkiye

ABSTRACT

Objectives: In recent years, especially with the Coronavirus Disease of 2019 (COVID-19) pandemic, the use of herbal products for various health problems has been increasing worldwide. This study aimed to determine the frequency of herbal product/dietary supplement use, the most used products, and the factors affecting the use of these products in patients who applied to the Chest Diseases Clinic.

Materials and Methods: This descriptive survey study was conducted at Chest Diseases Clinic using a face-to-face interview technique. Adult individuals with subacute respiratory complaints for > 3 weeks or a diagnosis of chronic chest disease were included in the study. The questionnaire form included questions about personal characteristics, data related to disease and treatment, use of herbal products/dietary supplements, and attitudes toward these products. A total of 444 participants with all the data included in the study. Descriptive statistics, chi-square, and binary logistic regression tests were used.

Results: It was determined that 49.3% of the participants used herbal products/dietary supplements, and the most frequently used products were honey, linden, ginger, lemon, and carob. According to the results of the binary logistic regression test, it was determined that patients over 60 years old [odds ratio (OR)= 2.0, 95% confidence interval (CI): 1.1-3.8, p= 0.042], those with a high education level (OR= 2.0, 95% CI: 1.1-3.6, p= 0.018), those who live in urban (OR= 1.8, 95% CI: 1.1-3.0, p= 0.018), and those with a diagnosis of post-COVID syndrome (OR= 2.7, 95%, CI: 1.3-5.5, p= 0.007) are more likely to use these products. It was determined that 57.9% of the participants used these products to relieve the symptoms of the disease.

Conclusion: Considering the high probability of using these products in patients with respiratory tract disease, it is essential for public health that health professionals question the use of these products and provide counseling on this issue.

Keywords: Medicinal herb, dietary supplements, respiratory diseases, herb-drug interactions, pharmacist

INTRODUCTION

Respiratory diseases, particularly asthma, chronic obstructive pulmonary disease (COPD), and lung cancer, affect many people around the world. According to World Health Organization data, COPD, lower respiratory tract infections, and lung cancer were determined as three of the ten diseases that caused the most deaths in 2019.[1] "Coronavirus Disease of 2019" (COVID-19), which has emerged recently and caused a pandemic, significantly affects the respiratory system. Post-COVID syndrome is a condition in which there are new, recurrent, or ongoing symptoms and clinical findings after an acute infection with COVID-19. COVID-19 and post-COVID syndrome have increased morbidity and mortality rates.[2]

With important developments in treating respiratory diseases in recent years, these diseases are controlled, and morbidity rates are decreasing.[3] However, there is a tendency for different searches in patients due to the increase in the incidence of diseases, the inability to fully recover with known treatment

*Correspondence: tugbasubas08@gmail.com, Phone: +90 539 200 90 87, ORCID-ID: orcid.org/0000-0002-0956-6567
Received: 25.03.2023, Accepted: 26.07.2023

methods, drug side effects, dissatisfaction with treatment and health services, and fear and anxiety caused by the COVID-19 pandemic experienced in recent years.[4,5] In this context, traditional and complementary treatment methods such as medicinal plants, acupuncture, homeopathy, hypnotherapy, aromatherapy, breathing, and relaxation techniques are used for respiratory system disorders.[6,7] Plants have been used for centuries for purposes such as controlling, treating, and preventing diseases.[8] In Türkiye, herbal products are available in the form of finished products as traditional herbal medicinal products and herbal medicines approved by the Ministry of Health, and dietary supplements approved by the Ministry of Agriculture and Forestry, apart from forms such as raw drugs and teas.[9]

There are studies evaluating the use of herbal products/dietary supplements in people with respiratory disorders.[10-13] The use of herbal products was found to be 61.8% in a study conducted in participants with respiratory tract diseases in Germany.[8] In another study conducted with 274 students in Saudi Arabia, it was determined that 62.7% of the participants used herbal products for the prevention of respiratory tract infections and 48.5% of them occasionally used herbal products when they had an illness related to respiratory tract infections.[5] In studies conducted in Türkiye, the frequency of use of herbal products and supplements in patients with various respiratory diseases (asthma, COPD, pharyngitis, cough, flu-cold, rhinitis, tonsillitis, and respiratory tract infections) varies between 64.5% and 90.8%.[13,14]

While there were studies investigating the use of herbal products in patients with asthma, COPD, allergic rhinitis, and lung cancer, no study was found in patients with pulmonary embolism, interstitial lung diseases, respiratory symptoms, and post-COVID syndrome. This study aimed to determine the frequency of herbal products/dietary supplement use, the most used products, the factors affecting the use of these products, and the attitudes of patients toward these products in patients who applied to the Chest Diseases Clinic.

MATERIALS AND METHODS

Study design and sample size

This descriptive study was conducted at Chest Diseases Clinic between 15.11.2021 and 01.05.2022. Adult individuals (≥ 18 years of age) with subacute respiratory complaints for more than 3 weeks or a diagnosis of chronic chest disease who agreed to participate in this study were included in the study. The questionnaire form was administered to the participants using the face-to-face questionnaire technique. Participants were informed about the content and purpose of the study, and their consent was obtained. The interview with each patient lasted approximately 15 minutes.

Questionnaire form

The questionnaire form was created by examining the literature and consists of four parts: personal characteristics, disease and treatment characteristics, use of herbal products/dietary supplements, and attitudes toward herbal products/dietary supplements.

Personal characteristics included age, gender, education level, place of residence, having a job, self-reported general health status, and body mass index (BMI) (kg/m^2). BMI was calculated by dividing weight (kg) by the square of height (m). In the next section, chest-related diseases/symptoms, the duration of diagnosis (week, month, year), the medicines used, whether there is a problem with the treatment, and self-reported satisfaction with the treatment were evaluated. Diseases/symptoms were evaluated in four categories: post-COVID syndrome, respiratory airway and allergic diseases (asthma, COPD, bronchiectasis and allergic rhinitis), respiratory symptoms (cough, dyspnea, and chest pain), and other diseases group (pulmonary embolism, interstitial lung diseases, lung cancer, and structural disorders in the lung). The Global Initiative for Asthma symptom control assessment algorithm-scale was used to determine the level of symptom control in asthma patients.[15] According to the results of the pulmonary function test in diseases involving the airways, when the forced expiratory volume 1 second (FEV1)/forced vital capacity (FVC) ratio is below 80%, it is classified as an obstructive disease, and when the ratio is normal and the FVC is below 80%, it is classified as a restrictive disease.[16]

In the section on herbal products/dietary supplements use, there are questions such as the use of herbal products/dietary supplements, the products used, how these products are used, the reason for use, sources of information about these products, place of supply, side effects, and whether the information about the use was given to the doctor. All plant-derived products, such as raw drugs, teas, herbal medicinal products, dietary supplements, and herbal preparations were evaluated. The contents of the preparations containing herbal products/dietary supplements were investigated and the mixtures were evaluated separately. In the determination of the products used, the statements of the participants were taken as the basis, and no species identification was made. In the last section, there are six questions that evaluate the opinions of all patients toward herbal products/dietary supplements. Before the data were collected, a pre-test was conducted with 20 participants. The questionnaire was finalized according to the feedback.

Ethics committee approval of the study was received from the Karadeniz Technical University Faculty of Medicine, Scientific Research Ethics Committee (date: 24.11.2021, number: 24237859-856, protocol number: 2021/329).

Statistical analysis

The IBM SPSS 23.0 (SPSS Inc., Chicago, IL, USA) statistical package program was used for data analysis. Descriptive statistics were presented as number (n), percent (%), mean, standard deviation (SD), minimum (min.), and maximum (max.) values. The chi-square test was used to compare categorical variables.

Multivariate analyses of the factors affecting the use of herbal products were performed using the logistic regression test. The model was created using the enter method. The independent variables included in the model were age, gender,

education level, place of residence, working a job, general health status, BMI, diagnosis/symptoms that are the reason for application, duration of diagnosis/symptoms, and regular use of medicines. Results are presented with odds ratio (OR) and 95% confidence interval (CI) values. Hosmer-Lemeshow test results and Nagelkerke R^2 values were calculated. The statistical significance level was set as $p < 0.05$.

RESULTS

The mean age of the participants was 50.7 ± 17.6 years (min.= 18, max.= 90). 324 (73.0%) of the participants were women. The personal characteristics of the participants and their use of herbal products/dietary supplements according to these characteristics are presented in Table 1. It was determined that 219 (49.3%) participants used herbal products/dietary supplements. The most used products were honey (n= 126, 57.5%), linden (n= 74, 33.8%), ginger (n= 60, 27.4%), lemon (n= 53, 24.2%), and carob (n= 24, 10.9%). These products were used in different ways: directly, as an infusion/decoction, alone, or in combination with other herbs, mostly internally. For example, honey was consumed directly or mixed with different herbs such as ginger or turmeric, linden as a decoction, lemon directly as an infusion or added to tea, and carob as molasses. Herbal products and dietary supplements used by the participants are presented in Table 2.

Gender, general health status, and BMI were not associated with herbal product use. Seventy-one (55.0%) patients between the ages of 18 and 40, 73 (42.0%) patients between the ages of 41 and 60, and 75 (53.2%) patients over the age of 60 were using herbal products/dietary supplements (p= 0.043). Urban residence (p= 0.003), high school and above education status (p= 0.004), and having a job (p= 0.039) were associated with a higher frequency of herbal products/dietary supplements use (Table 1).

Of the participants, 160 (36.0%) presented with respiratory airway diseases and allergic diseases (22.5% asthma, 4.7% COPD, 1.8% bronchiectasis, 7.0% allergic rhinitis), 124 (27.9%) with respiratory symptoms (14.2% cough, 8.3% dyspnea, 5.4% chest pain), 78 (17.6%) with ongoing complaints after COVID, and 82 (18.5%) with other diseases (5.9% interstitial lung diseases, 4.7% lung cancer, 4.5% pulmonary embolism, 4.5% structural disorders in the lung). The mean duration of individuals' diagnoses/symptoms was 3.68 ± 5.85 years. There was no significant association between the use of herbal products/dietary supplements and the duration of the disease/symptoms (p= 0.788), medicine use (p= 0.290), regular use of medicines (p= 0.056), treatment satisfaction (p= 0.942), treatment problems (p= 0.492), and FEV1/FVC ratio (p= 1.000). Forty-nine (62.8%) people with post-COVID syndrome, 77 (48.1%) people with respiratory airway diseases and allergic diseases, 62 (50.0%) people with respiratory symptoms, and 31 (37.8%) people with other diseases were using herbal products/dietary supplements (p= 0.017). It was determined that these products were used more in asthma patients than in well-controlled patients with inadequate and uncontrolled symptoms (p= 0.034). The characteristics of the participants regarding the disease/symptom and treatment and the use of herbal products/dietary supplements according to these characteristics are shown in Table 3.

According to multivariate analysis, the use of herbal products/dietary supplements was not associated with gender, job status, general health status, BMI, duration of diagnosis/symptoms, and regular use of medicines. Herbal products/dietary supplements use was higher in patients who were older than 60 years (OR= 2.0; 95% CI: 1.1-3.8, p= 0.042), had high school or higher education (OR= 2.0; 95% CI: 1.1-3.6, p= 0.018), and urban resident (OR= 1.8; 95% CI: 1.1-3.0, p= 0.018). Participants with post-COVID syndrome were more likely to use these products than those with other diseases (OR= 2.7; 95% CI: 1.3-5.5, p= 0.007). The results of the logistic

Table 1. Use of herbal products/dietary supplements and personal characteristics (n= 444)

	Total	User	Non-user	*p* value
	n (%)*	n (%)**	n (%)**	
Herbal products and dietary supplements	444 (100.0)	219 (49.3)	225 (50.7)	
Age				
18-40	129 (29.1)	71 (55.0)	58 (45.0)	**0.043**
41-60	174 (39.2)	73 (42.0)	101 (58.0)	
> 60	141 (31.8)	75 (53.2)	66 (46.8)	
Gender				
Female	324 (73.0)	160 (49.4)	164 (50.6)	0.968
Male	120 (27.0)	59 (49.2)	61 (50.8)	
Educational status				
Middle school and below	306 (68.9)	137 (44.8)	169 (55.2)	**0.004**
High school and above	138 (31.1)	82 (59.4)	56 (40.6)	
Place of residence				
Urban	340 (76.6%)	181 (53.2)	159 (46.8)	**0.003**
Rural	104 (23.4%)	38 (36.5)	66 (63.5)	
Have a job				
Yes	86 (19.4%)	51 (59.3)	35 (40.7)	**0.039**
No	358 (80.6%)	168 (46.9)	190 (53.1)	
General health status				
Very good/good	155 (34.9)	74 (47.7)	81 (52.3)	0.875
Middle	218 (49.1)	110 (50.5)	108 (49.5)	
Bad/very bad	71 (16.0)	35 (49.3)	36 (50.7)	
BMI				
< 30 kg/m^2	255 (57.4)	124 (48.6)	131 (51.4)	0.733
≥ 30 kg/m^2	189 (42.6)	95 (50.3)	94 (49.7)	

*Column percentage, **Row percentage, BMI: Body mass index

regression analysis regarding the factors affecting the use of herbal products/dietary supplements by the participants are presented in Table 4.

One hundred seventeen (53.4%) of the participants stated the source of information about the products they used as friends/relatives, and 82 (37.4%) of them obtained these products by collecting them from nature. One hundred sixty five (73.3%) of the participants who used herbal products/dietary supplements thought that the products they used were beneficial. One hundred and sixty-one (70.9%) did not inform their doctor about the products they used, and 186 (81.9%) wanted to get information about these products from healthcare professionals. The reasons for the participants' use of herbal products/dietary supplements, the sources of information about these products, the places provided, and the benefits of these products are presented in Table 5.

The opinions of the participants regarding herbal products/dietary supplements are presented in Table 6.

During the study, 459 patients were reached. The collected data were checked by the researchers, and 444 participants without missing data were included in the analyses.

Table 2. Herbal products/dietary supplements used by the participants (n= 219)

	n	%		n	%
Honey	126	57.5	Cinnamon	8	3.6
Linden	74	33.8	Vitamin C	7	3.2
Ginger	60	27.4	Vitamin D	6	2.7
Lemon	53	24.2	Black pepper	6	2.7
Carob	24	10.9	Propolis	6	2.7
Thyme	20	9.1	Vinegar	6	2.7
Peppermint	20	9.1	Bee pollen	5	2.3
Grape/mulberry molasses	20	9.1	Radish	5	2.3
Turmeric	19	8.7	Olive oil	4	1.8
Rosehip	16	7.3	Onion	4	1.8
Pine cone molasses/sirup	15	6.8	Highland tea	4	1.8
Black cumin	12	5.5	Zinc	3	1.4
Garlic	11	5.0	Fennel	3	1.4
Sage	10	4.6	Quince leaf	3	1.4
Green tea	9	4.1	Parlsey	3	1.4
Daisy	8	3.6	Other*	48	21.9

*Cherry stalk, fig leaf, inula molasses, fish oil, hibiscus, rosemary, royal jelly, Korean red ginseng (n= 2), marjoram, alkanet (hava civa in Turkish), eucalyptus, Hindi oil, Reishi mushroom, dried fruit tea, glucosamine, Ag ions, saponins, nutmeg, blueberry, multivitamin, coenzyme Q10, olive leaf, lemon balm, flavonoid-polysaccharide fraction, apricot tea, hazelnut shell, hazelnut leaf, orange peel, clove, kiwi tea, peach tea, sumac tea, black grape seeds, St. John's wort, quail eggs, white and black mulberry, cashew, almond, cress, yarrow (n= 1)

Table 3. Use of herbal products/dietary supplements and characteristics of disease/symptoms and treatment (n= 444)

	Total	User	Non-user	*p* value
	n (%)*	n (%)**	n (%)**	
Disease/symptoms				
Post-COVID syndrome	78 (17.6)	49 (62.8)	29 (37.2)	**0.017**
Respiratory airway and allergic diseases	160 (36.0)	77 (48.1)	83 (51.9)	
Respiratory symptoms	124 (27.9)	62 (50.0)	62 (50.0)	
Other	82 (18.5)	31 (37.8)	51 (62.2)	
Duration of diagnosis/symptoms				
< 3 years	286 (64.4)	144 (50.3)	142 (49.7)	0.788
3-10 year	118 (26.6)	55 (46.6)	63 (53.4)	
> 10 years	40 (9.0)	20 (50.0)	20 (50.0)	
Medicine use status				
Yes	279 (62.8)	143 (51.3)	136 (48.7)	0.290
No	165 (37.2)	76 (46.1)	89 (53.9)	
Regular use of medicines				
Yes, regular	208 (74.6)	100 (48.1)	108 (51.9)	0.056
No, irregular	71 (25.4)	44 (61.1)	28 (38.9)	
Treatment satisfaction				
Very good/good	213 (48.0)	108 (50.7)	105 (49.3)	0.942
Middle	43 (9.7)	23 (53.5)	20 (46.5)	
Bad	23 (5.2)	12 (52.2)	11 (47.8)	
Problems in the treatment				
Yes	39 (14.0)	18 (46.2)	21 (53.8)	0.492
No	240 (86.0)	125 (52.1)	115 (47.9)	
FEV1/FVC ratio* **				
Obstructive disease	51 (60.0)	27 (52.9)	24 (47.1)	1.000
Restrictive disease	34 (40.0)	18 (52.9)	16 (47.1)	
Asthma symptom control level** **				
Well-controlled	15 (15.0)	3 (20.0)	12 (80.0)	**0.034**
Poorly controlled	37 (37.0)	19 (51.4)	18 (48.6)	
Uncontrolled	48 (48.0)	28 (58.3)	20 (41.7)	

*Column percentage, **Row percentage, ***Evaluated in patients with respiratory airway diseases (n= 85), ****Evaluated in asthma patients (n= 100), COVID: Coronavirus disease, FEV1: Forced expiratory volume in 1 second, FVC: Forced vital capacity

Table 4. Logistic regression analysis of the factors affecting participants' uses of herbal products/dietary supplements (n= 444)

	OR (95% CI)	*p* value
Age		
18-40	1	
41-60	0.9 (0.5-1.6)	0.706
› 60	2.0 (1.1-3.8)	**0.042**
Gender		
Female	1	
Male	1.2 (0.7-2.0)	0.525
Educational status		
Middle school and below	1	
High school and above	2.0 (1.1-3.6)	**0.018**
Place of residence		
Rural	1	
Urban	1.8 (1.1-3.0)	**0.018**
Have a job		
Yes	1	
No	1.5 (0.9-2.7)	0.139
General health status		
Very good/good	1	
Middle	1.3 (0.8-2.0)	0.311
Bad/very bad	1.4 (0.7-2.6)	0.293
BMI		
‹ 30 kg/m^2	1	
≥ 30 kg/m^2	1.4 (0.9-2.3)	0.141
Disease/symptoms		
Other diseases	1	
Post-COVID syndrome	2.7 (1.3-5.5)	**0.007**
Respiratory airway and allergic diseases	1.1 (0.6-2.2)	0.684
Respiratory symptoms	1.7 (0.9-3.3)	0.100
Duration of diagnosis/symptoms		
‹ 3 years	1	
3-10 year	1.0 (0.6-1.7)	0.953
› 10 years	1.1 (0.5-2.4)	0.890
Regular use of medicines		
Yes, regular	1	
Non-use medicine	0.7 (0.4-1.1)	0.146
No, irregular	1.6 (0.9-2.9)	0.117

Hosmer-Lemeshow *p*= 0.821, Nagelkerke R^2= 0.12, BMI: Body mass index, OR: Odds ratio, CI: Confidence interval, COVID: Coronavirus disease

Table 5. Characteristics associated with the use of herbal products/dietary supplements by the participants (n= 219)

	n	%
Reasons for participants to use herbal products/ dietary supplements*		
Reducing disease symptoms	127	57.9
Strengthen the immune system	113	51.6
The idea that it is natural and harmless	101	46.1
Support medical treatment	73	33.3
To treat the disease	55	25.1
Relieving medication side effects	5	2.3
Sources of information about the products used*		
Friend/relatives	117	53.4
No information source	70	31.9
Internet and social media	38	17.3
Television, newspaper	19	8.7
Doctor	15	6.8
Other healthcare professionals	4	1.8
Herbalist	2	0.9
Where the used products are supplied*		
From nature	82	37.4
Herbal shop	78	35.6
Market	67	30.6
Friend/relatives	24	10.9
Pharmacy	9	4.1
Internet/television	4	1.8
Other**	4	1.8
Benefit from the products used		
Yes	165	73.3
No	25	11.1
Indecisive	35	15.6

*More than one option is marked, **Firm (n= 3), doctor (n= 1)

Table 6. Opinions of the participants about herbal products/dietary supplements (n= 444)

		Use of herbal products and dietary supplements					
		Yes		No		Total	
		n	%	n	%	n	%
Do you think using herbal products/dietary supplements in addition to modern medicine supports this treatment?	Yes	182	83.1	115	51.1	297	66.9
	No	23	10.5	59	26.2	82	18.5
	Indecisive	14	6.4	51	22.7	65	14.6
Do you think that herbal products/dietary supplements can also cause harm?	Yes	153	69.9	166	73.8	319	71.8
	No	36	16.4	23	10.2	59	13.3
	Indecisive	30	13.7	36	16.0	66	14.9
Do you think herbal products/dietary supplements alone are effective against diseases?	Yes	10	4.6	3	1.3	13	2.9
	No	197	90.0	213	94.7	410	92.3
	Indecisive	12	5.5	9	4.0	21	4.7
Do you think that herbal products/dietary supplements should be approved by the Ministry of Health?	Yes	121	55.3	141	62.7	262	59.0
	No	41	18.7	32	14.2	73	16.4
	Indecisive	57	26.0	52	23.1	109	24.5
Do you think herbal products/dietary supplements are completely ineffective?	Yes	12	5.5	11	4.9	23	5.2
	No	196	89.5	202	89.8	398	89.6
	Indecisive	11	5.0	12	5.3	23	5.2
Do you think that concomitant medication use with herbal products or dietary supplements can cause problems?	Yes	52	23.7	53	23.6	105	23.6
	No	87	39.7	80	35.6	167	37.6
	Indecisive	80	36.5	92	40.9	172	38.7

DISCUSSION

In this study, the use of herbal products/dietary supplements in patients who applied to the Chest Diseases Clinic in a tertiary health institution and the factors affecting their use were evaluated.

The frequency of use of herbal products/dietary supplements for all participants was 49.3%, 62.8% in post-COVID syndrome, 50.0% in patients with subacute/chronic respiratory symptoms, 48.1% in respiratory airway diseases and allergic diseases, and 37.8% in other diseases. In studies conducted in Germany and the United States of America, it was reported that 61.8% and 41.4% of the participants, respectively, used herbal products/dietary supplements for respiratory disorders.[8,17] In studies conducted with participants with respiratory system diseases in Türkiye, the frequency of use was found to be between 64.5% and 90.8%.[13,14] Studies have mostly focused on certain disease groups such as asthma, COPD, allergic diseases, and lung cancer. Studies have shown that the frequency of use of herbal products/dietary supplements varies between 28.8% and 70.1% in COPD patients, 7.8% and 60% in allergic rhinitis patients, and 24.7% and 48.1% in lung cancer patients.[11,12,18-22] There is no study investigating the use of herbal products in patients with post-COVID syndrome. In a study conducted by telephone with COVID-19 patients in a quarantine center in India during the COVID-19 pandemic, it was found that 25.8% of patients applied traditional treatment methods both during and after treatment.[23] In studies conducted in the community during the pandemic period, it has been observed that the frequency of use of herbal products/dietary supplements varies between 18% and 64%.[24,25] According to the data obtained from this study, the frequency of herbal product/dietary supplement use is high and similar to the data in the literature.

When the use of herbal products/dietary supplements was evaluated according to sociodemographic and personal characteristics, a significant relationship was found between age, education level, and place of residence. In studies conducted during the COVID-19 pandemic, it has been shown that the use of these products increases with age.[26,27] The reason for this may be the increase in the incidence of chronic diseases with increasing age. In most of the studies conducted on patients with asthma, allergic rhinitis, lung cancer, and during the COVID period, it was determined that the use of these products increased as the level of education increased.[14,19,22,28,29] The data obtained in our study are compatible with the literature findings. It has been reported that the use of herbal products/dietary supplements is higher among individuals with chronic diseases in Thailand, those living in rural areas, and those living in urban areas among participants with respiratory system diseases in Türkiye.[13,30] In our study, similar results were found in a study conducted in Türkiye.

A significant correlation was found between the use of herbal products/dietary supplements by the participants, the diagnosis, and the level of asthma symptom control (in asthma patients). Previous studies have determined that there is a positive relationship between the use of herbal products and the diagnosis of asthma.[12,20,30] In this study, it was found that the use of herbal products/dietary supplements was higher in asthma patients with inadequately controlled and uncontrolled symptoms than in patients with controlled symptoms. Similar to our findings, a significant relationship was found between the inability to control asthma symptoms and the use of different traditional methods in studies conducted in Canada and England. The use of herbal products was one of the commonly used methods.[31,32] During the COVID-19 pandemic period, the inability to determine the treatment protocol to be applied, especially at the beginning of the pandemic, and the long duration of medicine and vaccine studies have led to an increase in the tendency of society to use these products. In our study, a higher frequency of use was found in patients with post-COVID syndrome compared with the other disease groups. This may be due to the uncertainty caused by the pandemic process and the fact that patients turn to these products to eliminate the long-term effects of COVID-19. In studies conducted during previous pandemics, it has been reported that the tendency to traditional and complementary therapies has increased among people, and the use of herbal products has been preferred primarily.[33]

In this study, the majority of the participants who used herbal products/dietary supplements stated that they found the products beneficial. The findings in the literature support our study, and it has been reported that the perceived effectiveness of these products is high.[12,19,20,30] In a study conducted with patients with respiratory system diseases in Türkiye, it was reported that 87.5% of patients using herbal products stated that they benefited from the products they used, and 90% of them recommended these products to others.[13] In our study, the main reasons for the participants to use these products were to relieve symptoms and strengthen the immune system. In a study conducted with university students in Saudi Arabia, 55.5% of the participants used herbal products to prevent and control respiratory tract infections and strengthen the immune system.[5]

Information on herbal products and dietary supplements can be obtained from many sources. Obtaining information from scientific sources or healthcare professionals is important for public health. As in this study, in previous studies, participants' sources of information about these products were mostly friends and family/relatives.[22,28,34] Television/media/newspaper, internet/social media, and herbalists, although to a lesser extent, doctors, pharmacists, and other health personnel are also expressed as sources of information.[19,20,29] In a study conducted in Germany, individuals who used herbal products in the last 12 months declared the internet 68.2%, pharmacists 54.2%, and family members 45.6% declared the internet as their source of information.[8]

In this study, it was determined that 70.9% of the participants who used herbal products/dietary supplements did not inform their doctor about this issue, and 81.9% wanted to obtain information about these products from healthcare professionals. In the literature, some studies conducted with asthma and COPD patients found that more than half of the individuals did not inform their doctor or other healthcare professionals.[18,20,33,34] In some studies, contrary to these findings, it has been determined that individuals should inform doctors before or while using these products.[28,35] It is important for the progress of treatment and public health that healthcare professionals, especially doctors and pharmacists, question the use of natural products by patients and raise awareness on this issue.

Although the regulation of herbal products/dietary supplements varies according to country or region, these products are available in the market with or without a prescription because of the differences in the legislation of herbal products/dietary supplements in Türkiye. In a study conducted in Thailand, it was determined that patients mostly collect the products they use from nature and also obtain them from herbal shops and pharmacies.[30] In Türkiye, it has been determined that the places of supply for products of natural origin are mostly herbal shops or markets.[36] In this study, similar to the literature, it was determined that the participants collected herbal products/dietary supplements from nature and obtained them from herbal shops and markets. In the Black Sea Region, most of the individuals living in urban areas as well as those living in rural areas have a connection with the village and live in harmony with nature. Therefore, it is expected that these products will mostly be collected from nature.

Due to the increasing demand and use of naturally sourced products, there are also quality, efficacy, and reliability problems related to these products. Herbal products contain a large number and varying amounts of secondary metabolites, which are responsible for their clinical effects and show pharmacological activity. The type and amount of secondary metabolites vary according to the way the plant is collected, harvest time, drying, storage, and processing methods. In addition, it is possible that the desired quality product is not obtained because of adulteration, contamination, wrong plant identification, or labeling with other plants or active substances.[37]

When the attitudes of the participants toward herbal products/dietary supplements were evaluated, it was determined that the majority of them thought that these products supported treatment, similar to the literature.[38] In addition, it can be said that awareness of herb-drug interactions does not need to be at a sufficient level.

This research was conducted during the COVID-19 pandemic. This study investigates the use of herbal products/dietary supplements in individuals with respiratory disease (including asthma, COPD, lung cancer, as well as post-COVID syndrome, interstitial lung diseases, and pulmonary embolism) more comprehensively than studies in the literature, and it is thought to provide important scientific data.

Study limitations

An equal number of patients could not be reached in the groups determined by disease prevalence. Because of the design of the study, the data obtained may not be generalizable to the population.

CONCLUSION

According to our research results, approximately half of the patients with respiratory diseases use herbal products/dietary supplements at a high frequency. The use of these products by patients varies in terms of sociodemographic and disease-related characteristics. The fact that patients with post-COVID syndrome use more herbal products/dietary supplements than other disease groups in this study shows that patients primarily resort to these products in an unknown situation. Considering the information sources and places of supply of the participants about these products, the quality of the products should be increased and they should be controlled by the health authorities to prevent the problems caused by the use of irrational herbal products. It is noteworthy that the majority of patients who use herbal products/dietary supplements do not inform their doctors about this. It is important for healthcare professionals to question the use of herbal products by patients and to provide counseling on this subject to prevent possible adverse effects and herb-drug interactions.

Ethics

Ethics Committee Approval: Ethics committee approval of the study was received from the Karadeniz Technical University Faculty of Medicine, Scientific Research Ethics Committee (date: 24.11.2021, number: 24237859-856, protocol number: 2021/329).

Informed Consent: Participants were informed about the content and purpose of the study, and their consent was obtained.

Authorship Contributions

Concept: T.S., U.Ö., Y.B., Design: T.S., U.Ö., Y.B., Data Collection or Processing: T.S., U.Ö., Y.B., T.Ö., A.K.A, Analysis or Interpretation: T.S., A.K.A., Literature Search: T.S., A.K.A., Writing: T.S., U.Ö., Y.B., T.Ö., G.R., A.K.A.

Conflict of Interest: No conflict of interest was declared by the authors.

Financial Disclosure: The authors declared that this study received no financial support.

REFERENCES

1. Cohen M, Levine SM, Zar HJ. World Lung Day: impact of "the big 5 lung diseases" in the context of COVID-19. Am J Physiol Lung Cell Mol Physiol. 2022;323:338-340.
2. Yong SJ. Long COVID or post-COVID-19 syndrome: putative pathophysiology, risk factors, and treatments. Infect Dis (Lond). 2021;53:737-754.
3. Kerstjens HA, Groen HJ, van Der Bij W. Recent advances: Respiratory medicine. BMJ. 2001;323:1349-1353.
4. Özsürekci C, İleri İ, Çalışkan H, Yildirim F, Candemir B, Çavuşoğlu Ç, Doğrul RT, Göker B. Opinions, acceptance and use about complementary-alternative medicine among elderly individuals and effect of frailty. Ankara Eğt. Arş. Hast. Derg. 2020;53:177-182.
5. Syed W, Samarkandi OA, Sadoun AA, Bashatah AS, Al-Rawi MBA, Alharbi MK. Prevalence, beliefs, and the practice of the use of herbal and dietary supplements among adults in Saudi Arabia: an observational study. Inquiry. 2022;59:469580221102202.
6. Mark JD, Chung Y. Complementary and alternative medicine in pulmonology. Curr Opin Pediatr. 2015;27:334-340.
7. Ogbu CE, Oparanma C, Ogbu SC, Ujah OI, Okoli ML, Kirby RS. Trends in the use of complementary and alternative therapies among US adults with current asthma. Epidemiologia (Basel). 2023;4:94-105.
8. Welz AN, Emberger-Klein A, Menrad K. The importance of herbal medicine use in the German health-care system: prevalence, usage pattern, and influencing factors. BMC Health Serv Res. 2019;19:952.
9. Dişli M, Yeşilada E. Herbal medicinal products in Turkey (standardization, production and adulteration of herbal products in Turkey). J Biotechnol and Strategic Health Res. 2019;3(Suppl):13-21.
10. Abadoglu O, Cakmak E, Kuzucu Demir S. The view of patients with asthma or chronic obstructive pulmonary disease (COPD) on complementary and alternative medicine. Allergol Immunopathol (Madr). 2008;36:21-25.
11. Erbaycu AE, Gülpek M, Tuksavul F, Uslu Ö, Güçlü SZ. Effect of socio-demographic and tumor related factors on use of various herbal and other mixtures in lung cancer (use of complementary treatment in lung cancer). Thorac Res Pract. 2009;11:117-120.
12. Koshak AE. Prevalence of herbal medicines in patients with chronic allergic disorders in Western Saudi Arabia. Saudi Med J. 2009;40:391-396.
13. Erarslan ZB, Ay S, Kültür Ş. A questionnare-based study on medicinal plant use in respiratory diseases. J Fac Pharm Ankara. 2020;44:437-451.
14. Demir M, Kulakaç N. The use of complementary and alternative medicine in the patients who have respiratory disorders in Turkey. J Alt Med Res. 2016;2:117.
15. Sadatsafavi M, McTaggart-Cowan H, Chen W, Mark FitzGerald J. Economic burden of asthma (EBA) study group. Quality of life and asthma symptom control: room for ımprovement in care and measurement. Value Health. 2015;18:1043-1049.
16. Ulubay G, Dilektaşlı AG, Börekçi Ş, Yıldız Ö, Kıyan E, Gemicioğlu B, Saryal S. Turkish thoracic society consensus report: ınterpretation of spirometry. Turk Thorac J. 2019;20:69-89.
17. Rashrash M, Schommer JC, Brown LM. Prevalence and predictors of herbal medicine use among adults in the United States. J Patient Exp. 2017;4:108-113.
18. George J, Ioannides-Demos LL, Santamaria NM, Kong DC, Stewart K. Use of complementary and alternative medicines by patients with chronic obstructive pulmonary disease. Med J Aust. 2004;181:248-251.
19. Molassiotis A, Panteli V, Patiraki E, Ozden G, Platin N, Madsen E, Browall M, Fernandez-Ortega P, Pud D, Margulies A. Complementary and alternative medicine use in lung cancer patients in eight European countries. Complement Ther Clin Pract. 2006;12:34-39.
20. Argüder E, Bavbek S, Sen E, Köse K, Keskin O, Saryal S, Misirligil Z. Is there any difference in the use of complementary and alternative therapies in patients asthma and COPD? A cross-sectional survey. J Asthma. 2009;46:252-258.

21. Şahin ZA, Şahin M. The view of patients with Choronic Obstructive Pulmonary Disease (COPD) on Complementary and Alternative Medicine (CAM) in Eastern Turkey. Afr J Tradit Complement Altern Med. 2013;10:116-121.

22. Bonizzoni G, Caminati M, Ridolo E, Landi M, Ventura MT, Lombardi C, Senna G, Crivellaro M, Gani F. Use of complementary medicine among patients with allergic rhinitis: an Italian nationwide survey. Clin Mol Allergy. 2019;17:2.

23. Charan J, Bhardwaj P, Dutta S, Kaur R, Bist SK, Detha MD, Kanchan T, Yadav D, Mitra P, Sharma P. Use of complementary and alternative medicine (CAM) and home remedies by COVID-19 patients: a telephonic survey. Indian J Clin Biochem. 2021;36:108-111.

24. Kretchy IA, Boadu JA, Kretchy JP, Agyabeng K, Passah AA, Koduah A, Opuni KFM. Utilization of complementary and alternative medicine for the prevention of COVID-19 infection in Ghana: a national cross-sectional online survey. Prev Med Rep. 2021;24:101633.

25. AlNajrany SM, Asiri Y, Sales I, AlRuthia Y. The commonly utilized natural products during the COVID-19 pandemic in Saudi Arabia: a cross-sectional online survey. Int J Environ Res Public Health. 2021;18:4688.

26. AlKharashi NA. The consumption of nutritional supplements and herbal products for the prevention and treatment of COVID-19 infection among the Saudi population in Riyadh. Clin Nutr Open Sci. 2020;39:11-20.

27. Amuzie CI, Kalu KU, Izuka M, Nwamoh UN, Emma-Ukaegbu U, Odini F, Metu K, Ozurumba C, Okedo-Alex IN. Prevalence, pattern and predictors of self-medication for COVID-19 among residents in Umuahia, Abia State, Southeast Nigeria: policy and public health implications. J Pharm Policy Pract. 2022;15:34.

28. Schäfer T. Epidemiology of complementary alternative medicine for asthma and allergy in Europe and Germany. Ann Allergy Asthma Immunol. 2004;93(2Suppl1):5-10.

29. Ahmed I, Hasan M, Akter R, Sarkar BK, Rahman M, Sarker MS, Samad MA. Behavioral preventive measures and the use of medicines and herbal products among the public in response to Covid-19 in Bangladesh: a cross-sectional study. PLoS One. 2020;15:e0243706.

30. Peltzer K, Pengpid S. The use of herbal medicines among chronic disease patients in Thailand: a cross-sectional survey. J Multidiscip Healthc. 2019;12:573-582.

31. Chen W, Fitzgerald JM, Rousseau R, Lynd LD, Tan WC, Sadatsafavi M. Complementary and alternative asthma treatments and their association with asthma control: a population-based study. BMJ Open. 2013;3:e003360.

32. Shaw A, Noble A, Salisbury C, Sharp D, Thompson E, Peters TJ. Predictors of complementary therapy use among asthma patients: results of a primary care survey. Health Soc Care Community. 2008;16:155-164.

33. Hwang JH, Cho HJ, Im HB, Jung YS, Choi SJ, Han D. Complementary and alternative medicine use among outpatients during the 2015 MERS outbreak in South Korea: a cross-sectional study. BMC Complement Med Ther. 2020;20:147.

34. Alshagga MA, Al-Dubai SA, Muhamad Faiq SS, Yusuf AA. Use of complementary and alternative medicine among asthmatic patients in primary care clinics in Malaysia. Ann Thorac Med. 2011;6:115-119.

35. Dehghan M, Ghanbari A, Ghaedi Heidari F, Mangolian Shahrbabaki P, Zakeri MA. Use of complementary and alternative medicine in general population during COVID-19 outbreak: a survey in Iran. J Integr Med. 2022;20:45-51.

36. Kaner G, Karaalp C, Seremet-Kürklü N. Determining the frequency use of herbal products and factors affecting the use herbal products among university students and their families. Turk Hij Den Biyol Derg. 2017;74:37-54.

37. Passalacqua G, Compalati E, Schiappoli M, Senna G. Complementary and alternative medicine for the treatment and diagnosis of asthma and allergic diseases. Monaldi Arch Chest Dis. 2005;63:47-54.

38. El Khoury G, Ramadan W, Zeeni N. Herbal products and dietary supplements: a cross-sectional survey of use, attitudes, and knowledge among the lebanese population. J Community Health. 2016;41:566-573.

Turk J Pharm Sci 2024;21(3):243-251
DOI: 10.4274/tjps.galenos.2023.91126

ORIGINAL ARTICLE

GC-MS Profiling and Pharmacological Potential of *Physconia venusta* (Ach.) Poelt

Ibtissem ZEGHINA[1]*, Ibtissem EL OUAR[1,2], Maya Abir TARTOUGA[1], Mohamed Badreddine MOKHTARI[1], Daniel ELIEH-ALI-KOMI[3,4], Lynda GALI[5], Chawki BENSOUICI[5]

[1]University of Frères Mentouri Constantine, Faculty of Science of Nature and Life, Department of Animal Biology, Laboratory of Immunology and Biological Activities of Natural Substances, Constantine, Algeria
[2]Research Center of Pharmaceutical Sciences, Constantine, Algeria
[3]Charité -Universitätsmedizin Berlin, Institute of Allergology, Corporate Member of Freie Universität Berlin and Humboldt-Universität zu Berlin, Berlin, Germany
[4]Fraunhofer Institute for Translational Medicine and Pharmacology (ITMP), Allergology and Immunology, Berlin, Germany
[5]Research Center of Biotechnology, Constantine, Algeria

ABSTRACT

Objectives: Lichens are complex symbiotic organisms that generate various bioactive compounds with significant therapeutic value. We investigated the chemical composition and bioactivity of the acetone extract of the Algerian lichen *Physconia venusta* (Ach.) poet.

Materials and Methods: Phytochemical screening was performed using gas chromatography-mass spectrometry (GC-MS). The antibacterial activity was assessed against *Escherichia coli, Pseudomonas aeruginosa, Salmonella enteritidis, Salmonella typhi, Staphylococcus aureus, Listeria monocytogenes,* and *Bacillus subtilis* using an agar diffusion test with the determination of the minimal inhibition concentration (MIC), while the antioxidant activity was determined using different chemical methods (DPPH, ABTS, CUPRAC, reducing power, superoxide anion scavenging, β-carotene bleaching, and metal chelate). In addition, cytotoxic activity was tested using *Artemia salina* (Brine shrimp) bioassay.

Results: The studied extract exhibited intense antibacterial activity against *E. coli* and *S. aureus* with inhibition diameters of 28 ± 0.01 and 22 ± 0.01 mm, respectively, with a MIC value of 6.25 mg/mL and a selectivity index of 2.8. The obtained extract showed different antioxidant trends depending on the selected assay. GC-MS analysis revealed many secondary metabolites.

Conclusion: *P. venusta*, a type of lichen, is a potential source of bioactive substances that could be used in pharmaceuticals.

Keywords: *Physconia venusta,* antioxidant, brine shrimp lethality assay, antibacterial, GC-MS, usnic acid

INTRODUCTION

Lichens are symbiotic organisms composed of fungi (mycobiont) and green algae or/and cyanobacteria (photobiont).[1] To treat skin, respiratory, and digestive issues, traditional medicine practices more than 52 lichen species worldwide. More than 1000 compounds with various activities, including anti-inflammatory, anti-proliferative, cytotoxic, and anticancer properties, have been described in previous research.[2] More than 1085 lichen species have been identified in Algeria, 64 of which are indigenous.[3]

Their use as bioindicators of air pollution has received the most scientific attention. However, there have been very few scientific studies on lichen chemistry in this highly diverse country. Antibiotic resistance in bacteria is a major problem affecting public health. It has been increasing for several decades, making it more challenging to treat patients, lengthening the time spent providing care, and increasing infection-related morbidity. Antibiotic resistance has, according to the OMS 2017 report, alarmingly increased on a global scale. The ability to cure widespread infectious diseases is threatened by the emergence and dissemination of new resistance mechanisms.[4] Treatment is becoming more difficult and occasionally impossible for a growing array of infections, including pneumonia, tuberculosis, sepsis, and foodborne

*Correspondence: zeghina.ibtissem@umc.edu.dz, Phone: +213658353559, ORCID-ID: orcid.org/0000-0002-9065-3421
Received: 27.01.2023, Accepted: 26.07.2023

illnesses, because antibiotics lose their potency. The estimate is that by 2050, an effective antibiotic will only be available if new drugs are developed or discovered.[5] Therefore, there is an urgent need for novel antibacterial agents. Researchers from all around the world have recently paid close attention to the quest for novel antibacterial compounds in medicinal plants.[6] Medicinal plants contain a variety of antibacterial molecules like alkaloids, glycosides, terpenoids, saponins, steroids, flavonoids, tannins, quinines, and coumarins.[7] Usnic acid is a di-benzofuran compound known as a secondary lichen metabolite. Numerous studies have documented this substance's biological properties, which include antibacterial, anti-inflammatory, antioxidant, antiviral, and antitumoral effects.[8]

This study aimed to investigate the phytochemical profile of *Physconia venusta* (Ach.) Poelt (Kingdom: *Fungi*, phylum: *Ascomycota*, Class: *Lecanoromycetes*, Order: *Teloschistales,* Family: *Physciaceae*, Genus: *Physconia*), (Catalog #: WIS-L-0136263, Occurrence ID: 773fe232-313e-42b9-a4d6-5689e4a6b748, www.lichenportal.org) by measuring its levels and usnic acid content.

One of the rare lichens with a distribution centered in Italy, Morocco, and Algeria is *P. venusta (Ach.)* Poet, whose phytochemicals have not received much attention.[9]

We investigated the antibacterial activity of the obtained extract against seven bacterial strains known for their resistance to antibiotics and multiple nosocomial and chronic infections. Finally, the antioxidant capacity of the same extract was assessed as persistent bacterial infections often associated with a high production of free radicals in the body.

MATERIALS AND METHODS

Lichen collection

A lichen sample of *Physconia venusta* (Figure 1) was collected from Elmeridje forest-Constantine in northeast Algeria. The specimen was identified by Dr. Philippe Clerc (Conservatory and Botanical Garden of Geneva, Chambésy, Switzerland). The sample was dried at room temperature and then ground to obtain a fine powder, which was stored in the dark until extraction.

Preparation of the acetone extract from P. venusta

Acetone has been effectively used to extract antioxidants, including phenolics, because of its chemical properties, such as the capability of dissolving hydrophilic and lipophilic compounds, giving better yields and supporting the biological activities of phytochemicals, avoiding problems with pectins, and allowing lower temperatures for sample preservation.[10,11] The extraction procedure consists of macerating 20 g of powder in 100 mL of acetone at room temperature for 72 hours. The following filtering, the mixture was concentrated in a rotary evaporator (Buchi 23022A120 Rotavapor Cole-Parmer, USA). The obtained extract was stored at 20 °C.

Chemical characterization

Total phenolic content

The total phenolic content was determined using the Folin-Ciocalteu reagent according to the method described by Müller et al.[12] In brief, 20 µl of the extract was mixed with 100 µl of Folin-Ciocalteu reagent (diluted at 1:10) and 75 µl of sodium carbonate (7.5%). The mixture was then incubated in the dark for 2 hours, and absorbance was measured at 765 nm. A blank was prepared similarly by replacing the extract with the solvent used.

Total flavonoid content

The total flavonoid content was measured according to the method of Topçu et al.[13] with some modifications for a 96-well microplate assay. Briefly, 50 µl of the extract (1 mg/mL) was mixed with 130 µl of methanol, 10 µl potassium acetate (CH_3COOK), and 10 µl aluminum nitrate [Al $(NO_3)_3$, $9H_2O$]. The mixture was incubated at room temperature for 40 minutes, and absorbance was measured at 415 nm.

Gas chromatography-mass spectrometry (GC-MS) analysis

A Perkin Elmer (Clarus SQ 8C GC/spectrometer, Germany) was used to perform quantitative and qualitative analyses of the chemical composition (gas chromatography linked to mass spectrometry). The oven temperature was initially set to 50 °C and held for 5 minutes. A 30 °C/min ramp was applied up to 270 °C, which was held for an additional 5 minutes. MS spectra were acquired in the electron impact ionization mode, ranging from 50 to 600 a.m.u. Various components were identified by different retention times detected by a mass spectrophotometer. The compounds were identified by comparing the data with existing software libraries like WILEY8.LIB, NIST11.lib and PUBCHEM lib.[14]

Quantification of usnic acid by high-performance liquid chromatography (HPLC)

HPLC analysis was performed according to the method described by Cansaran-Duman et al.[15] All used chemicals were HPLC grade from Sigma-Aldrich, Germany. A 1 mg/mL stock solution of usnic acid was prepared in acetone. All the standards were placed in an autosampler and analyzed. Calibration curves of usnic acid were obtained using seven samples of various concentrations using linear regression analysis (Figure 2).

The analysis was performed on an Agilent 1220 infinity LC system equipped with a diode array detector; a reverse phase C18 column was used. Mobile phase A was a mixture of methanol and phosphate buffer pH 7.4 (70:30 *v/v*) with a flow rate of 0.8 mL/min to detect usnic acid at 245 nm by comparing the retention times with pure standard. For sample analysis, 5 mg of the extract was added to 10 mL of acetone at room temperature; and the mixture was filtered using a 0.45 µm filter. 20 µl of the filtered solution was injected into the HPLC system. All experiments were performed in triplicate.

Antimicrobial activity

Microorganisms and media

The Constantine Research Center in Biotechnology-Algeria provided the bacterial strains including four Gram-negative:

Figure 1. Algerian *Physconia venusta* photographed in the Elmeridje forest-Constantine, Algeria

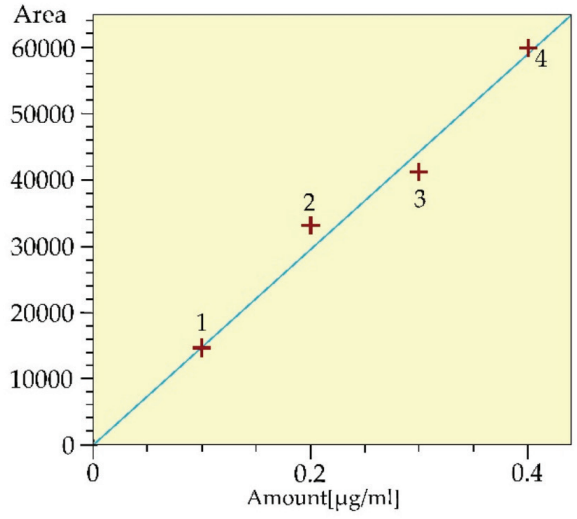

Figure 2. Calibration curve of usnic acid (Sigma); R_2= 0.9896

Escherichia coli (ATCC25922TM), *Pseudomonas aeruginosa* (ATCC27853TM), *Salmonella enteritidis* (ATCC13076TM), *Salmonella typhi* (ATCC14028TM), and four Gram-positive bacteria: *Staphylococcus aureus* (ATCC25923TM), *Listeria monocytogenes* (ATCC 15313TM), *Bacillus* sp. (ATCC16404TM), and *Bacillus subtilis* (ATCC6633TM).

A suspension containing 10^8 colony-forming units (CFU)/mL was prepared from an 18-hour fresh bacterial culture by adjusting the absorbance to 0.1 at 625 nm in physiological water (0, 9%).

Agar disk diffusion

The antimicrobial effect on agar was investigated using the disk diffusion method as previously described.[16] Sterile paper disks of 6-mm size were soaked with acetone extract or usnic acid sigma (15 µl/disk) at two different concentrations (50 mg/mL and 1 mg/mL, respectively) in triplicate and allowed to dry at room temperature under sterile conditions. The plates were then incubated at 37 °C for 24/48 hours. Paper disks loaded with dimethyl sulfoxide (DMSO) were also used as negative controls, whereas gentamicin was used as a positive control. The inhibition zones were reflective of the antimicrobial effectiveness of the extract.

Minimal inhibition concentration (MIC)

MIC was determined by the broth microdilution method using 96-well microtiter plates according to the method described by Londone Bailon et al.[17] For this purpose, a series of dilutions with concentrations ranging from 50 to 0.15 mg/mL and from 1 to 0.0075 mg/mL of the extract and the usnic acid were used in the experiment against every tested strain. 50 µl of a bacterial inoculum (107 CFU/mL) was transferred in each well containing 50 µl of lichen extract or usnic acid solution. After 24 hours of incubation at 37 °C, absorbance was measured at 630 nm, and the MIC was determined. This later corresponded to the lowest concentration, which completely inhibited bacterial growth. A DMSO solution was used as the negative control, and a culture medium with bacteria was used as the positive control. All experiments were performed in duplicate.

Brine shrimp cytotoxicity test

Brine shrimp (*Artemia salina*) eggs (JBL Artemio Mix, Germany) were hatched in seawater (10 g/1L of seawater). The solution was incubated at 28 °C for 48 hours under artificial lighting and aeration provided by an aquarium pump. After incubation, the *nauplii* (larvae) were separated from the remaining eggs and used in the toxicity assay. The effect of the acetone extract on Brine shrimp larvae viability was assessed using the method reported by Sarah et al.[18] Ten larvae of *Artemia* (*nauplii*) were transferred to test tubes containing 100 µL of the extract at different concentrations, where the content was then adjusted to 5 mL by seawater (70%). After 24 hours of incubation, the amount of surviving larvae in each tube was determined. Potassium dichromate was used as the positive control. The percentage of mortality was calculated using the formula below:

$$\%\ death = \frac{(number\ of\ death\ nauplii)}{(total\ number)} \times 100$$

The LC_{50} (lethality of 50% of the larvae) was determined from the regression curve plotted by the mortality rates at different concentrations.

Antimicrobial selectivity index (SI)

The antimicrobial SI is defined as the ratio between the concentrations leading to 50% lysis of cells and the minimum concentration inhibiting bacterial growth (SI = LC_{50}/MIC), which is also indicated as a therapeutic index.[19] SI was calculated using the following equation:

$$SI = LC_{50}\ (mg/mL)/MIC\ (mg/mL)$$

Where LC_{50} refers to the concentration of the sample inducing 50% lethality of *Artemia nauplii* and MIC represents the MIC.

Antioxidant activity

DPPH free radical scavenging assay

The free radical-scavenging activity was determined using the 2,2-diphenyl-1-picrylhydrazyl (DPPH) radical.[20] Briefly, in

a 96-well plate, 160 µL of DPPH (0.1 mM) solution was added to 40 µL of samples at different concentrations (4000, 800, 400, 200, 100, 50, 25, 12.5 µg/mL). The plate was kept in the dark at room temperature for 30 minutes. The absorbance was read at 517 nm. Butylated hydroxytoluene (BHT), butylated hydroxyanisole (BHA), and ascorbic acid were used as standard antioxidants. The scavenging capacity of the DPPH radical was calculated using the following equation:

$$\text{DPPH scavenging effect (\%)} = \left(\frac{Ac\text{-}As}{Ac}\right) \times 100$$

Results were given as IC_{50} value (mg/mL) corresponding to the concentration of the sample inducing a 50% reduction of the initial absorbance of DPPH solution.

ABTS assay

The ABTS scavenging activity was evaluated according to the method described by Londone Bailon et al.[17] The ABTS solution was prepared by mixing 7 mM ABTS with 2.45 mM potassium per sulfate for 16 hours. The $ABTS^{+\bullet}$ solution was then diluted in distilled water to an absorbance of 0.708 ± 0.025 at 734 nm. In a 96-well microplate, 40 µL of the sample at different concentrations was mixed with 160 µL of the $ABTS^{+\bullet}$ solution. After 10 minutes of incubation, absorbance was measured at 734 nm. BHA, BHT, and ascorbic acid were used as antioxidant standards. The inhibition percentage was calculated using the equation represented in the DPPH free radical scavenging assay section.

Superoxide anion scavenging activity

The superoxide radical scavenging ability was assessed by measuring the inhibition of O^{2-} generation using alkaline DMSO, as reported by Mazouz et al.[21] The reaction mixture consisted of 40 µL of acetone extract, 130 µL of alkaline DMSO (20 mg NaOH in 100 mL of DMSO), and 30 µL *nitroblue tetrazolium* test solution (1 mg/mL in DMSO). The mixture was incubated at 25 °C for 5 minutes, and absorbance was measured at 560 nm. Ascorbic acid was used as a positive control. The scavenging activity was determined using the formula represented in the DPPH free radical scavenging assay section.

Reducing power

The reducing power was achieved according to the method reported by Bendjabeur et al.[22] In a 96-well microplate, 10 µl of sample solution at different concentrations was mixed with 40 µl of phosphate buffer (0.2 M, pH 6.6) and 50 µl of potassium ferricyanide (1%). The mixture was incubated at 50 °C for 20 minutes, followed by adding 50 µl of trichloroacetic acid (10%), 40 µl of distilled water, and 10 µl of ferric chloride ($FeCl_3$, 0.1%). The microplate was vigorously shaken, and absorbance was immediately read at 700 nm. BHA, BHT, and ascorbic acid were used as antioxidant standards. The results were reported as absorbances, and the value of $A_{0.5}$ was calculated from the regression curve. $A_{0.5}$ corresponds to the concentration giving an absorbance of 0.5, which was determined from the regression curve.

Cupric reducing antioxidant capacity assay (CUPRAC)

CUPRAC was determined according to the method described by Apak et al.[23] The reaction medium included 40 µl of the sample at different concentrations, 50 mL of $CuCl_2$ (10 mM), 50 mL of neocuproine (7.5 mM in ethanol), and 60 mL of acetate ammonium (CH_3COONH_4, 1 M). After 1 hour of incubation, absorbance was measured at 450 nm. The results were reported as absorbance values and compared with BHA, BHT, and ascorbic acid.

β-carotene bleaching assay

The ability of the *P. venusta* extract to inhibit β-carotene bleaching was investigated according to the method of Ferhat et al.[24] with some modifications for this purpose, β carotene/linoleic emulsion was prepared by dissolving 0.5 g of carotenes in 1 mL of chloroform, 25 mL of linoleic acid, and 200 mg of tween 40. After removing the chloroform under vacuum using a rotary evaporator, the emulsion absorbance was adjusted to 0.8-0.9 at 470 nm by adding hydrogen peroxide. Then, 160 mL of the emulsion was mixed with 40 mL of the extract or standards. Finally, the microplate was incubated for 2 hours at 50 °C, and the absorbance was measured at 470 nm at different reaction times (t= 0 minutes and t=120 minutes). Ethanol was used as a control, and BHA and BHT were used as antioxidant standards. The results were given as IC_{50} using the following equation:

$$\textit{Inhibition (\%)} = \frac{As\ (t=0)\text{-}As\ (t=120)}{Ac\ (t=0)\text{-}Ac\ (t=120)} * 100$$

Where As (t= 0) and As (t= 120) are the absorbances of the sample at 0 and 120 minutes, respectively, Ac (t= 0) and Ac (t= 120) correspond to the absorbances of the control at 0 and 120 minutes.

Ferrous ions' chelating activities

The ferrous chelating activity was measured according to the method described by Decker and Welch.[25] Briefly, in a 96-well microplate, 40 µL of sample solution at different concentrations, 40 µl $FeCl_2$ (0, 2 mM), and 80 µl of ferene solution (0.5 mM) were mixed. After 10 minutes of reaction, the absorbance was measured at 593 nm. The metal chelating activity was calculated using the equation represented in the DPPH free radical scavenging assay section.

Statistical analysis

All measurements were performed in triplicate, and results were presented as means ± standard deviation. Student's t-test was used to determine the statistical significance of antioxidant activity using SPSS software. $p < 0.05$ was considered to be statistically significant.

RESULTS

Total polyphenol content

The results showed that the acetone extract of *P. venusta* contains a high level of total phenolic and flavonoid contents; the values were 123.42 ± 3.75 µg GAE/mg and 60.55 ± 0.81 µg QE/mg extract, respectively (Figure 3).

GC-MS analysis

The extract GC-MS profile revealed the presence of 13 different compounds, which were characterized and identified by comparison of their mass fragmentation patterns with those similar to those in the NIST library database. Among the identified compounds, Eugenol, Benzoic acid, 2, 4-dihydroxy-3, 6-dimethyl-, methyl ester, n-Hexadecanoic acid, 9,12-Octadecadienoic acid (Z, Z)-, Tributyl acetyl citrate, Cyclopenta[a,d]cycloocten-5-one, 1,2,3,3a, 4,5,6,8,9,9a,10,10a-dodecahydro-7- (1-methylethyl)-1,9a-dimethyl-4-methylene, Hexanedioic acid, dioctyl ester, 2-Pentanoic acid, 5- (decahydro-5,5,8a-trimethyl-2-methylene-1-na phthalenyl)- 3-methyl-, [1S-[1α(E),4aβ,8aα]]-,3-Buten-2-one,3-methyl-4- (1,3,3-trimethyl-7-oxabicyclo [4.1.0] heptan-1-yl)-, 9,12-Octadecadienoic acid (Z, Z)-, octyl ester-, 9,10Anthracenedione, 1,8-dihydroxy-3-methoxy- 6-methyl- and Tetracosapentaene,2,6,10,15,19,23 hexamethyl- (Figure 4), (Table 1).

Quantification of usnic acid by HPLC

The content of usnic acid, one of the main compounds specific to lichens, in the extract was determined by HPLC. The results showed that the extract contained 0.0425 mg/mL of usnic acid (Figure 5), (Table 2).

Antibacterial activity

The antimicrobial effect of *P. venusta* acetone extract was assessed using disk diffusion and microdilution. The extract exhibited various antibacterial activities depending on the bacterial strains (Table 3). The largest inhibitory zone was recorded against *S. aureus* with 30 mm ± 0.01, followed by *E. coli* with 28 mm ± 0.01. The extract MIC was determined to be 6.25 mg/mL. However, usnic acid was only active on three bacterial strains, *E. coli, S. aureus,* and *B. subtilis*, at MIC 0.03 mg/mL, 0.03 mg/mL, and 0.015 mg/mL, respectively. However, no effect against *S. typhi* was observed by the lichen extract and usnic acid. By comparing the inhibition zone of usnic acid with that of the extract, it can be inferred that usnic acid is the most active component against both strains, *S. aureus and B. subtilis*. Notably, the extract and usnic acid have a more potent effect than the antibiotic gentamicin.

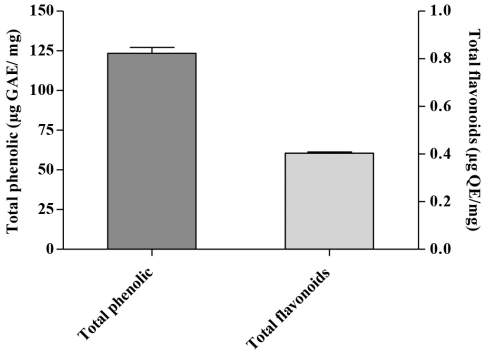

Figure 3. Total phenolic and flavonoids in the acetone extract of the lichen *Physconia venusta*

Antioxidant activity

The antioxidant potential of *P. venusta* extract was evaluated using different methods, and the results are presented in Table 4 as IC_{50} and $A_{0.5}$ values. The acetone extract of *P. venusta* exerted an interesting scavenging activity against the radical ABTS and the anion superoxide (IC_{50} = 20.00 ± 2.28 µg/mL and 24.80 ± 4.43 µg/mL, respectively). In contrast, it exhibited a weak effect against the DPPH radical. The extract also displayed a moderate ability to reduce ferric and cupric ions, incapacity to bleach β-carotene, and an excellent capability to bind ferreous ions (IC_{50} of 26.42 ± 2.98 µg/mL) compared with standard EDTA (IC_{50} = 12.11 ± 0.32 µg/mL).

DISCUSSION

Lichens are promising sources of bioactive molecules of pharmaceutical and nutritional interest. The emergence of antibiotic-resistant bacteria in healthcare is a serious concern. In the current research, the effect of the acetone extract of *P. venusta* on seven bacterial strains known for their resistance to antibiotics; *E. coli, P. aeruginosa, S. enteritidis, S. typhi, S. aureus, L. monocytogenes, and B. subtilis,* was investigated. The effect of the studied extract was compared with that of usnic acid, the essential metabolite found in lichens. The data showed that our extract has an antibacterial effect against the seven (7)

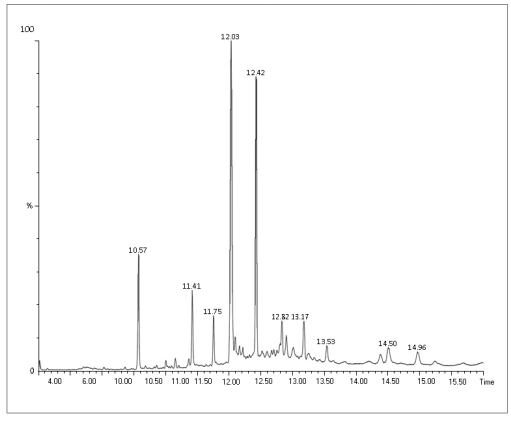

Figure 4. GC-MS chromatogram of *Physconia venusta* acetone extract
GC-MS: Gas chromatography-mass spectrometry

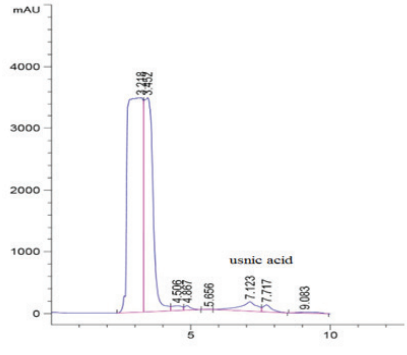

Figure 5. HPLC analysis of usnic acid in *Physconia venusta* acetone extract (retention time: 7,123 minute)
HPLC: High-performance liquid chromatography

strains at MIC 6.25 mg/mL, but the highest growth inhibition was observed against *S. aureus*.

Similarly, usnic acid showed an inhibition diameter close to that exhibited by the extract against the same bacterial strain, *S. aureus*, indicating that it is the principle active compound against this strain. The same observation was registered against *B. subtilis*, proving that usnic acid is the most active compound. Similar results were reported by Gupta et al.[26] with the acetone extract of the lichen *Bulbothrix setschwanensis*, which exhibited an antibacterial effect against *S. aureus* and *E. coli* at MIC 6.25 mg/mL. The study of Kosanić and Ranković[27] demonstrated that the acetone extract from *U. barbata* inhibited *S. aureus* at a MIC of 0.5 mg/mL and the usnic acid MIC was 0.125 mg/mL.[28] It also determined that extracts from the lichen *U. florida* showed an interesting antibacterial effect against methicillin-resistant and methicillin-sensitive strains of *S. aureus* with MICs of 100 and 850 µg/mL, respectively. Moreover, according to Londone Bailon et al.,[17] usnic acid extracted from *U. florida* has shown an antibacterial effect against the same bacteria with MICs of 100 and 750 µg/mL, respectively.

It has been reported that most of the antimicrobial molecules from lichens are polyphenols. Depsides, depsides, dibenzofurans, *etc*., isolated from lichens have also demonstrated significant antimicrobial effects. The suppression of topoisomerase, which is necessary for microbial replication, by polyphenols because of their affinity for binding to a variety of proteins, including enzymes, can also account for their antibacterial activity.[20]

On the other hand, the study of Pompilio et al.[29] showed that usnic acid induces cell wall damage and inhibits bacterial growth through the reduction of protein synthesis, which affects bacterial adhesion during the early stages of biofilm formation. It also reduces the pathogenic potential of *S. aureus* by affecting the expression of relevant virulence factors such as lipase and thermonuclease. The brine shrimp assay was performed to investigate whether the extract exerted more

Table 1. Identification of metabolites in the acetone extract of *Physconia venusta* by GC-MS analysis

	RT (minute)	Area %	Amount %	Compound detected	Molecule formula	Synonym
1	9.02	4.831	5.12	Eugenol	$C_{10}H_{12}O_2$	Eugenic acid
2	10.566	4.831	5.82	Benzoic acid, 2,4-dihydroxy-3,6-dimethyl-, methyl ester	$C_{10}H_{12}O_4$	Atraric acid
3	11.412	3.547	8.44	n-Hexadecanoic acid	$C_{16}H_{32}O_2$	Palmitic acid
4	11.747	1.958	10.18	n-Hexadecanoic acid	$C_{16}H_{32}O_2$	Palmitic acid
5	12.027	19.232	10.50	9,12-Octadecadienoic acid (Z,Z)-	$C_{18}H_{32}O_2$	Alpha-linoleic acid
6	12.417	12.618	6.61	Tributyl acetyl citrate	$C_{20}H_{34}O_8$	Acetyl tributyl citrate
7	12.822	2.211	11.50	Cyclopenta[a,d]cycloocten-5-one,1,2,3,3a, 4,5,6,8,9,9a,10,10a-dodecahydro-7-(1-methylethyl)-1,9a-dimethyl-4-methylene	$C_{20}H_{30}O$	Adipic acid
8	12.892	1.107	5.75	Hexanedioic acid and dioctyl ester	$C_{22}H_{42}O_4$	Copalic acid methyl ester
9	13.172	2.146	11.16	2-Pentanoic acid, 5- (decahydro-5,5,8a-trimethyl- 2-methylene-1-na phthalenyl)-3-methyl-, [1S-[1α(E),4aβ,8aα]]-	$C_{21}H_{34}O_2$	-
10	13.533	1.259	6.55	3-Buten-2-one, 3-methyl-4- (1,3,3-trimethyl-7-oxabicyclo[4.1.0]heptan-1-yl)-	$C_{14}H_{22}O_2$	-
11	14.378	0.885	4.60	9,12-Octadecadienoic acid(Z,Z)-,octyl ester-	$C_{26}H_{48}O_2$	Physcion (parietin)
12	14.498	1.887	9.81	9,10Anthracenedione, 1,8-dihydroxy-3-methoxy-6-methyl-	$C_{16}H_{12}O_5$	-
13	14.958	1.516	7.88	Tetracosapentaene,2,6,10,15,19,23 hexamethyl-	$C_{30}H_{52}$	

GC-MS: Gas chromatography-mass spectrometry, RT: Retention time

Table 2. Usnic acid content and retention time in the *Physconia venusta* acetone extract

	Usnic acid content (mg/mL)	% of usnic acid in dry weight	Retention time (minute)
P. venusta acetone extract	0.0425 ± 0.02	0.85 ± 0.01	7.123 ± 0.01

toxicity than an antibacterial effect; the results showed a SI > 1, indicating the extract's safety on living cells. In addition to their ability to be resistant to antibiotics, the seven selected strains can persist inside the host organism's cells and induce chronic inflammation.[30] This latter is characterized by excessive production of free radicals, leading to an imbalance between oxygen and nitrogen species (reactive oxygen species and reactive nitrogen species).[31] Thus, causing various tissue injuries like protein oxidation, lipid peroxidation, and DNA damage. Therefore, a dual-action antibacterial and antioxidant molecule would be of great therapeutic interest.[32,33]

The antioxidant activity of the extract was evaluated by different assays to consider the diverse mechanisms of action of bioactive compounds. The extract exhibited a potent free radical scavenging effect against ABTS and superoxide anions and an essential capacity for chelating ferrous ions. This ability to sequester transition metals is considered a valuable property of antioxidant compounds, which hinder the generation of free radicals such as OH• *via* the Fenton reaction, in which transition metals such as Fe^{2+} and Cu^{2+} play a significant role as catalysts. The action of antioxidants then form complexes characterized by a low redox potential while preventing them from participating in the reaction.[34]

The antioxidant activity of lichens has been the subject of different studies. Extracts from lichen species; *Cladonia furcata, Hypogymnia physodes, Lasallia pustulata, Parmelia*

Table 3. Antibacterial effects of *Physconia venusta* extract and usnic acid

Bacterial strains	Inhibition zone of the acetone extract (mm)[a]	Inhibition zone of usnic acid (mm)	% inhibition in liquid medium*	MIC of usnic acid (mg/mL)	MIC of the acetone extract (mg/mL)	SI	Gentamicin	Pristinamycin	DMSO
Escherichia coli (ATCC25922TM)	28 ± 0.01	-	50.90	0.03	6.25	2.8	2	15 ± 0.01	-
Pseudomonas aeruginosa (ATCC27853TM)	19 ± 0.01	-	34.54	-	6.25	2.8	1.7	-	-
Salmonella enteritidis (ATCC13076TM)	20 ± 0.02	-	36.36	-	6.25	2.8	-	-	-
Staphylococcus aureus (ATCC25923TM)	30 ± 0.01	27 ± 0.01	60	0.03	6.25	2.8	2.4	37 ± 0.01	-
Bacillus subtilis (ATCC6633TM)	10 ± 0.01	7 ± 0.02	18.18	0.015	6.25	2.8	-	17 ± 0.02	-
Listeria monocytogenes (ATCC 15313TM)	10 ± 0.01	-	18.18	-	6.25	2.8	-	-	-
Salmonella typhi (ATCC14028TM)	-	-	-	0.015	-	-	-	17 ± 0.01	-

Values are represented as mean ± SD of three measurements, a diameter of the disk (6 mm), (-) no inhibition, *values represent the inhibition percentages of *P. venusta* against different bacterial strains at 6.25 mg/mL using the microdilution method, ATCC: American Type Culture Collection, SI: Selectivity index, MIC: Minimum inhibitory concentration, DMSO: Dimethyl sulfoxide, SD: Standard deviation

Table 4. Antioxidant activity of the *Physconia venusta* acetone extract

Bacterial strains	DPPH (IC_{50} µg/mL)	ABTS (IC_{50} µg/mL)	O_2^- scavenging activity (IC_{50} µg/mL)	Reducing power ($A_{0.5}$ µg/mL)	CUPRAC ($A_{0.5}$ µg/mL)	β-carotene bleaching (IC_{50} µg/mL)	Fe^{2+} chelating activity (IC_{50} µg/mL)
P. venusta extract	> 800	20.00 ± 2.28[a]	24.80 ± 4.43[a]	162.67 ± 54.9[c]	164.78 ± 72.27[c]	NA	26.42 ± 2.98[a]
BHA	6.14 ± 0.41[a]	1.29 ± 0.30[a]	NT	9.29 ± 0.22[a]	5.35 ± 0.71[a]	0.91 ± 0.0[a]	NT
BHT	12.99 ± 0.41[b]	1.81 ± 0.10[a]	NT	8.41 ± 1.46[a]	8.97 ± 3.94[a]	1.05 ± 0.0[a]	NT
Ascorbic acid	4.39 ± 0.01[a]	3.04 ± 0.05[a]	7.59 ± 1.16[a]	3.62 ± 0.29[a]	8.31 ± 0.15[a]	NT	NT
EDTA	NT	NT	NT	NT	NT	NT	12.11 ± 0.32[b]

Values are mean ± SD of three measurements (n= 3). *BHA, BHT, ascorbic acid, and EDTA are the standards used. Values with different subscripts (a, b, c) in the same column are significantly different ($p < 0.05$),
DPPH: 2,2 diphenylpicrylhydrazyl, ABTS: 2,2′-azino-bis (3-ethylbenzothiazoline-6-sulfonic acid), BHA: Butylated hydroxyanisole, BHT: Butylated hydroxytoluene, SD: Standard deviation, NT: Not tested, EDTA: Ethylenediaminetetraacetic acid

caperata, Parmelia sulcata, Cetraria islandica, Usnea ghattensis, and *Usnea ghattensis* have shown an intense antioxidant activity.[35] Furthermore, compared with our data, the study of Ranković et al.[36] reported IC_{50} values relatively close to our results (0.78 to 6.25 mg/mL) for *C. furcata, H. physodes,* and *Umbilicaria polyphylla* extracts. However, extracts from *P. glauca* and *P. furfuraceae* lichens have a lower ability to reduce DPPH radicals, with IC_{50} values of 656.98 and 95.33 µg/mL, respectively.

The antioxidant properties of *P. venusta* can be attributed to its phenolic content or other secondary metabolites exclusively found in lichens. The antioxidant effect of polyphenols is broadly reported because of their structure bearing hydroxyl groups, and the number and location of these groups determine their antioxidant properties.[37] In the identical spectra, Fernández-Moriano et al.[44] showed a positive correlation between the antioxidant activity and the phenolic content of 10 *Parmeliaceae* lichen extracts*: Usnea contexta Motyka, Usnea aurantiacoatra, Parmelia omphalodes, Myelochroa irrugans, and Lethariella canariensis. Hypotrachyna cirrhata, F. haysomii, F. euplecta, F. caperata, and B. setschwanensis.*

Moreover, many components isolated from lichens exhibited strong scavenging activity. The antioxidant activity of usnic acid was further assessed *in vivo* and *in vitro*. It was reported to reduce oxidative damage by increasing glutathione peroxidase, constitutive nitric oxide synthase, and superoxide dismutase activities *in vivo*.[38] It is a potent scavenger of peroxyl radicals assessed by ORAC.[38] Other compounds like depsides, artistic acid, 8'-methylmenegazziaic, psoromica, and protocetraric acid also have free radical scavenging activity.[39] Lichens produce many of the fatty acids commonly found in higher plants; the major fatty acid compositions are oleic, linoleic, and palmitic acid.[40] Molina et al. [41] studied the lichen *Physconia distorta* and suggested a close relationship between the synthesis of secondary metabolites and fatty acid metabolism. Mycobiota grown in a glucose-enriched medium favored the production of fatty acids. The antibacterial activity of fatty acids such as linoleic acid, palmitoleic acid, oleic acid, and their esters is well-known against Gram-negative and Gram-positive bacteria. Linoleic acid, in addition to its anticancer properties,[42] has been reported to inhibit the growth of *S. aureus* by increasing its permeability.[43] According to Table 1, we could identify several chemicals, most of which have biofunctions; however, as the main limitation of our study, we did not directly and individually assess their properties. In addition, we recommend using further bacteria to have a more trusted view and insight into the extract and its components on antimicrobial properties.

CONCLUSION

In the current investigation, *P. venusta* extract was shown to possess antibacterial activity against several tested bacterial strains that were resistant to antibiotics and caused nosocomial and chronic illnesses. This study also demonstrated that usnic acid, the most researched lichen component, had potent antibacterial properties against *B. subtilis* and *B. aureus*. The *P. venusta* extract also has an essential ability to scavenge free radicals. Because of its potent properties, *P. venusta* is an excellent natural source for the development and discovery of novel compounds with significant pharmaceutical potential.

Ethics

Ethics Committee Approval: Not required.

Informed Consent: Not required.

Authorship Contributions

Surgical and Medical Practices: I.Z., M.A.T., M.B.M., Concept: I.Z., I.E., C.B., Design: I.Z., I.E., C.B., Data Collection or Processing: I.Z., Analysis or Interpretation: I.Z., M.B.M., D.E-A-K., L.G., Literature Search: I.Z., M.A.T., M.B.M., D.E-A-K., Writing: I.Z., D.E-A-K.

Conflict of Interest: No conflict of interest was declared by the authors.

Financial Disclosure: The authors declared that this study received no financial support.

REFERENCES

1. Selbmann L, Zucconi L, Ruisi S, Grube M, Cardinale M, Onofri S. Culturable bacteria associated with Antarctic lichens: Affiliation and psychrotolerance. Polar Biology. 2009;33:71-83.
2. Shahidi F, Ambigaipalan P. Phenolics and polyphenolics in foods, beverages and spices: Antioxidant activity and health effects-A review. J Funct Foods. 2015;18:820-897.
3. Rafika B, Tarek H. Lichen diversity in the Edough Peninsula. North East of Algeria. 2018.
4. Lomazzi M, Moore M, Johnson A, Balasegaram M, Borisch B. Antimicrobial resistance-moving forward? BMC Public Health. 2019;19:858.
5. Vivas R, Barbosa AAT, Dolabela SS, Jain S. Multidrug-resistant bacteria and alternative methods to control them: an overview. Microb Drug Resist. 2019;25:890-908.
6. Dave P. Evaluation of antioxidant activities by use of various extracts from abutilon pannosum and grewia tenax in the kachchh region. MOJ Food Processing & Technology. 2017:5.
7. Mir H, Elieh Ali Komi D, Pouramir M, Parsian H, Moghadamnia AA, Seyfizadeh N, Lakzaei M. The hepatoprotective effects of *Pyrus biossieriana* buhse leaf extract on tert-butyl hydroperoxide toxicity in HepG2 cell line. BMC Res Notes. 2021;14:298.
8. Shcherbakova A, Strömstedt AA, Göransson U, Gnezdilov O, Turanov A, Boldbaatar D, Kochkin D, Ulrich-Merzenich G, Koptina A. Antimicrobial and antioxidant activity of Evernia prunastri extracts and their isolates. World J Microbiol Biotechnol. 2021;37:129.
9. Valdés B. Results of the fifth "Iter Mediterraneum" in Morocco, 8-27 June, 1992. Bocconea 2013;26:5-12.
10. Garcia Viguera C, Zafrilla P, Tomás-Barberán FA. The use of acetone as an extraction solvent for anthocyanins from strawberry fruit. Phytochemical Analysis. 1998;9:274-277.
11. Garcia Rowe J, Garcia Gimenez MD, Saenz Rodriguez MT. Some lichen products have antimicrobial activity. Z Naturforsch C J Biosci. 1999;54:605-609.

12. Müller L, Gnoyke S, Popken AM, Böhm V. Antioxidant capacity and related parameters of different fruit formulations. LWT-Food Science and Technology. 2010;43:992-999.

13. Topçu G, Ay M, Bilici A, Sarıkürkcü C, Öztürk M, Ulubelen A. A new flavone from antioxidant extracts of *Pistacia terebinthus*. Food Chem. 2007;103:816-822.

14. Kerboua M, Ahmed MA, Samba N, Aitfella-Lahlou R, Silva L, Boyero JF, Raposo C, Lopez Rodilla JM. Phytochemical Investigation of new algerian lichen species: *Physcia mediterranea* nimis. Molecules. 2021;26:1121.

15. Cansaran-Duman D, Aras S, Atakol O. Determination of Usnic acid content in some lichen species found in anatolia. Journal of Applied Biological Sciences 2008;2:41-44.

16. Srivastava P, Upreti DK, Dhole TN, Srivastava AK, Nayak MT. Antimicrobial property of extracts of indian lichen against human pathogenic bacteria. Interdiscip Perspect Infect Dis. 2013;2013:709348.

17. Londone Bailon P, Sanchez Robinet C, Alvarez Guzman G. In vitro antibacterial, antioxidant and cytotoxic activity of methanol-acetone extracts from Antarctic lichens (Usnea antarctica and Usnea aurantiaco-atra). Polar Sci. 2019;22:1004-1077.

18. Sarah QS, Anny F, Misbahuddin M. Brine shrimp lethality assay. Bangladesh J Pharmacol. 2017;12:5.

19. Bézivin C, Tomasi S, Lohézic-Le Dévéhat F, Boustie J. Cytotoxic activity of some lichen extracts on murine and human cancer cell lines. Phytomedicine. 2003;10:499-503.

20. El Aanachi S, Gali L, Neghmouche Nacer S, Bensouici C, Dari K, Aassila H. Phenolic contents and in vitro investigation of the antioxidant, enzyme inhibitory, photoprotective, and antimicrobial effects of the organic extracts of *Pelargonium graveolens* growing in Morocco. Biocatalysis and Agricultural Biotechnology. 2020;29:101819.

21. Mazouz W, El Houda Haouli N, Gali L, Vezza T, Bensouici C, Mebrek S, Hamel T, Galvez J, Djeddi S. Antioxidant, anti-alzheimer, anti-diabetic, and anti-inflammatory activities of the endemic halophyte Limonium spathulatum (Desf.) kuntze on LPS-stimulated RAW264 macrophages. S Afr J Bot. 2020;135:101-108.

22. Bendjabeur S, Benchabane O, Bensouici C, Hazzit M, Baaliouamer A, Bitam A. Antioxidant and anticholinesterase activity of essential oils and ethanol extracts of Thymus algeriensis and *Teucrium polium* from Algeria. J Food Meas Charact. 2018;12:2278-2288.

23. Apak R, Güçlü K, Ozyürek M, Karademir SE. Novel total antioxidant capacity index for dietary polyphenols and vitamins C and E, using their cupric ion reducing capability in the presence of neocuproine: CUPRAC method. J Agric Food Chem. 2004;52:7970-7981.

24. Ferhat M, Erol E, Beladjila KA, Çetintaş Y, Duru ME, Öztürk M, Kabouche A, Kabouche Z. Antioxidant, anticholinesterase and antibacterial activities of *Stachys guyoniana* and *Mentha aquatica*. Pharm Biol. 2017;55:324-329.

25. Decker EA, Welch B. Role of ferritin as lipid oxidation catalyst in muscle food. J Agric Food Chem. 1990;38:674-677.

26. Gupta VK, Verma S, Gupta S, Singh A, Pal A, Srivastava SK, Srivastava PK, Singh SC, Darokar MP. Membrane-damaging potential of natural L-(-)-usnic acid in Staphylococcus aureus. Eur J Clin Microbiol Infect Dis. 2012;31:3375-3383.

27. Kosanić M, Ranković B. Antioxidant and antimicrobial properties of some lichens and their constituents. J Med Food. 2011;14:1624-1630.

28. Shrestha G, St Clair LL, O'Neill KL. The immunostimulating role of lichen polysaccharides: a review. Phytother Res. 2015;29:317-322.

29. Pompilio A, Riviello A, Crocetta V, Di Giuseppe F, Pomponio S, Sulpizio M, Di Ilio C, Angelucci S, Barone L, Di Giulio A, Di Bonaventura G. Evaluation of antibacterial and antibiofilm mechanisms by usnic acid against methicillin-resistant *Staphylococcus aureus*. Future Microbiol. 2016;11.1315-1338.

30. Grant SS, Hung DT. Persistent bacterial infections, antibiotic tolerance, and the oxidative stress response. Virulence. 2013;4:273-283.

31. Butcher LD, den Hartog G, Ernst PB, Crowe SE. Oxidative stress resulting from Helicobacter pylori infection contributes to gastric carcinogenesis. Cell Mol Gastroenterol Hepatol. 2017;3:316-322.

32. Mirabdaly S, Elieh Ali Komi D, Shakiba Y, Moini A, Kiani A. Effects of temozolomide on U87MG glioblastoma cell expression of CXCR4, MMP2, MMP9, VEGF, anti-proliferatory cytotoxic and apoptotic properties. Mol Biol Rep. 2020;47:1187-1197.

33. Pizzino G, Irrera N, Cucinotta M, Pallio G, Mannino F, Arcoraci V, Squadrito F, Altavilla D, Bitto A. Oxidative stress: harms and benefits for human health. Oxid Med Cell Longev. 2017;2017:8416763.

34. Hsu B, Coupar IM, Ng K. Antioxidant activity of hot water extract from the fruit of the Doum palm, Hyphaene thebaica. Food Chemistry. 2005;98.317-328.

35. Kosanić M, Ranković B, Vukojević J. Antioxidant properties of some lichen species. J Food Sci Technol. 2011;48:584-590.

36. Ranković BR, Kosanić MM, Stanojković TP. Antioxidant, antimicrobial and anticancer activity of the lichens Cladonia furcata, Lecanora atra and Lecanora muralis. BMC Complement Altern Med. 2011;11:97.

37. Hamiche S, Bensouici C, Messaoudi A, Gali L, Khelouia L, Rateb ME, Akkal S, Badis A, El Hattab M. Antioxidant and structure-activity relationship of acylphloroglucinol derivatives from the brown alga Zonaria tournefortii. Monatshefte für Chemie-Chemical Monthly. 2021;152:431-440.

38. Cetin Cakmak K, Gülçin İ. Anticholinergic and antioxidant activities of usnic acid-an activity-structure insight. Toxicol Rep. 2019;6:1273-1280.

39. White PA, Oliveira RC, Oliveira AP, Serafini MR, Araújo AA, Gelain DP, Moreira JC, Almeida JR, Quintans JS, Quintans-Junior LJ, Santos MR. Antioxidant activity and mechanisms of action of natural compounds isolated from lichens: a systematic review. Molecules. 2014;19:14496-14527.

40. Kerboua M, Monia AA, Samba N, Silva L, Raposo C, Díez D, Rodilla JM. Phytochemical composition of lichen *Parmotrema hypoleucinum* (J. Steiner) hale from Algeria. Molecules. 2022;27:5229.

41. Molina M, Crespo A, Vicente C, Elix JA. Differences in the composition of phenolics and fatty acids of cultured mycobiont and thallus of Physconia distorta. Plant Physiology and Biochemistry. 2003;41:175-180.

42. Elieh Ali Komi D, Shekari N, Soofian-Kordkandi P, Javadian M, Shanehbandi D, Baradaran B, Kazemi T. Docosahexaenoic acid (DHA) and linoleic acid (LA) modulate the expression of breast cancer involved miRNAs in MDA-MB-231 cell line. Clin Nutr ESPEN. 2021;46:477-483.

43. Greenway DL, Dyke KG. Mechanism of the inhibitory action of linoleic acid on the growth of *Staphylococcus aureus*. J Gen Microbiol. 1979;115:233-245.

44. Fernández-Moriano C, González-Burgos E, Divakar PK, Crespo A, Gómez-Serranillos MP. Evaluation of the antioxidant capacities and cytotoxic effects of ten *Parmeliaceae* lichen species. Evid Based Complement Alternat Med. 2016;2016:3169751.

Turk J Pharm Sci 2024;21(3):252-258
DOI: 10.4274/tjps.galenos.2023.88935

ORIGINAL ARTICLE

Screening of Antimicrobial, Antibiofilm, and Cytotoxic Activities of Some Medicinal Plants from Balıkesir Province, Türkiye: Potential Effects of *Allium paniculatum* Flower

Özlem OYARDI[1]*, Mayram HACIOĞLU[2], Ebru ÖZDEMİR[3], Meryem Şeyda ERBAY[4], Şükran KÜLTÜR[4], Çağla BOZKURT GÜZEL[2]

[1]Gazi University Faculty of Pharmacy, Department of Pharmaceutical Microbiology, Ankara, Türkiye
[2]İstanbul University Faculty of Pharmacy, Department of Pharmaceutical Microbiology, İstanbul, Türkiye
[3]Altınbaş University Faculty of Pharmacy, Department of Pharmaceutical Botany, İstanbul, Türkiye
[4]İstanbul University Faculty of Pharmacy, Department of Pharmaceutical Botany, İstanbul, Türkiye

ABSTRACT

Objectives: Plant extracts are important natural resources that may have antimicrobial and antibiofilm effects against pathogens. This study was conducted to investigate the *in vitro* antimicrobial activities of methanol extracts of some medicinal plants (*Achillea nobilis* subspecies *neilreichii* (A. Kern.) Velen., *Aetheorhiza bulbosa* (L.) Cass, *Allium paniculatum* L, *Asphodelus aestivus* Brot., *Ballota nigra* L., *Cistus laurifolius* L., *Cistus salviifolius* L., *Dioscorea communis* (L.) Caddick and Wilkin, *Galium verum* L., *Hypericum triquetrifolium* Turra, *Paliurus spina-christi* Mill., *Primula vulgaris* Huds. subspecies *rubra* (Sm.) Arcang., *Ranunculus arvensis* L. and *Teucrium polium* L.) from Balıkesir province in Türkiye.
Materials and Methods: Preliminary antimicrobial activity screening was conducted for all extracts. Antibiofilm activity studies were conducted on mature *Candida albicans* biofilms. Moreover, the cytotoxicities of *A. paniculatum* flower extract on A549 and Vero cell lines were determined using a colorimetric tetrazolium-based assay.
Results: *A. paniculatum* flower, *P. vulgaris* root, *C. laurifolius, C. salviifolius,* and *A. nobilis* displayed good activity [minimum inhibitory concentrations (MIC): 9.75, 156, 312, 312 and 312 µg/mL, respectively] against *C. albicans* American Type Culture Collection 10231. Biofilm studies were conducted on these plant extracts. The methanol extract of *A. paniculatum* flower decreased the number of *C. albicans* [colony-forming unit (CFU)/mL] in mature biofilm statistically at 32 x MIC and higher concentrations ($p < 0.01$). *A. paniculatum* flower extract had a cytotoxic effect (killing more than 50% of cells) at high concentrations, and its effect on Vero cells was similar to that on A549 cells.
Conclusion: This study demonstrated the importance of the methanol extract of *A. paniculatum* flower as a natural alternative against *C. albicans* infections, including biofilms.
Keywords: *Allium paniculatum*, antibiofilm activity, antimicrobial activity, cytotoxic activity

INTRODUCTION

Researchers around the world have been exploring the benefits of medicinal herbs for treating various diseases for many years.[1] An important part of these studies is investigating their effects against human pathogens. The effectiveness of antibiotics against pathogens is gradually disappearing, and plants are an important resource for researchers.

The treatment of bacterial and fungal infections has become a significant health concern in recent years because of the rise of multidrug resistance. Apart from the challenge of antibiotic

*Correspondence: ozlemyrd@gmail.com, Phone: +90 312 202 30 10, ORCID-ID: orcid.org/0000-0001-9992-7225
Received: 16.05.2023, Accepted: 26.07.2023

resistance, the formation of biofilm by bacteria and fungi on medical devices inserted into the body, such as urinary catheters, central venous catheters, and contact lenses, further complicates the management of these infections.[2,3] Biofilm is a community of microorganisms that irreversibly bind to a specific surface or living tissue and are embedded in a self-secreted extracellular matrix. Biofilms show more resistance to antibiotics and host defense systems than planktonic cells. Therefore, high doses of antibiotics must be used for treatment, resulting in unwanted side effects.[4,5] Because biofilm formation on catheters and medical devices is a major challenge for treatment, biofilm removal is difficult except for device removal and/or replacement, which is an undesirable or high-risk procedure. Therefore, it is important to investigate natural antimicrobial agents for biofilm treatment.[6,7]

Studies have shown that some plant extracts can inhibit quorum sensing, thus preventing the formation of biofilms and being effective on mature biofilms. Therefore, plant extracts can be an effective source for antibiofilm therapy, because of the active molecules found in their structure.[8]

Balıkesir province in Türkiye is located in western Anatolian, on the border between the Marmara and Aegean regions with a surface area of 14.299 km^2. It is adjacent to Bursa in the northeast, Kütahya and Manisa in the southeast, İzmir in the southwest, the Aegean Sea and Çanakkale in the west. Because of its climatic characteristics, geological structure, and geographic location, the region features diverse flora. For this purpose, in this study, *in vitro* studies were conducted with 14 plants (17 different extracts) belonging to the Balıkesir province. The following plants were used in the study; *Achillea nobilis* L. subspecies *neilreichii* (A. Kern.) Velen., *Aetheorhiza bulbosa* (L.) Cass., *Allium paniculatum* L, *Asphodelus aestivus* Brot., *Ballota nigra* L., *Cistus laurifolius* L., *Cistus salviifolius* L., *Dioscorea communis* (L.) Caddick and Wilkin, *Galium verum* L., *Hypericum triquetrifolium* Turra, *Paliurus spina-christi* Mill., *Primula vulgaris Huds.* subspecies *rubra* (Sm.) Arcang., *Ranunculus arvensis* L. and *Teucrium polium* L. These plants have a very important ethnobotanical value, and their importance for treating different diseases has been recorded in the literature. The selected plants are commonly used for wound healing, diarrhea, urinary tract infections, stomach pain, fungal infections, and cough by local people in Balıkesir.[9-13]

A. paniculatum belongs to the *Amaryllidaceae* family and the genus *Allium* L. The genus *Allium* contains many species that are frequently used as food and natural remedies.[14] The local name of *A. paniculatum* in Balıkesir is "yoğurtçuk". The aerial part is cooked as a meal with eggs and is freshly eaten.[15] In this study, the antimicrobial and antibiofilm properties of medicinal plant extracts from the Balıkesir province were investigated. Further studies were conducted with *A. paniculatum*, which showed promising antibiofilm activity against *Candida* spp. Moreover, the cytotoxic activity of *A. paniculatum* was screened on the A549 and Vero cell lines using the 3-(4,5-dimethylthiazol-2-yl)-2,5-diphenyltetrazolium bromide (MTT) assay.

MATERIALS AND METHODS

Collection and identification of plants

The plant species were collected from Savaştepe and Kepsut (Balıkesir). Studied species, herbarium numbers, and localities are given in Table 1. The plants were identified and the voucher specimens were deposited in the ISTE (Herbarium of the Faculty of Pharmacy of İstanbul University).

Plant extracts

Plant materials were air-dried and extracted by percolation at room temperature with 95% methanol. Then, the obtained

Table 1. Studied species information

Species	Locality	Herbarium number
Achillea nobilis subspecies *neilreichii*	Balıkesir, Kepsut; Kayacıklar village, 440 m.	ISTE 109654
Aetheorhiza bulbosa	Balıkesir, Savaştepe forest, 300 m.	ISTE 109632
Allium paniculatum	Balıkesir, Savaştepe; Karaçam village, 285 m.	ISTE 109758
Asphodelus aestivus	Balıkesir, Kepsut; Örenli village, 550 m.	ISTE 109969
Ballota nigra	Balıkesir, Kepsut; Bükdere village, 630 m.	ISTE 109820
Cistus laurifolius	Balıkesir, Kepsut; Bükdere village, 660 m.	ISTE 109587
Cistus salviifolius	Balıkesir, Kepsut; Serçeören village, 720 m.	ISTE 109591
Dioscorea communis	Balıkesir, Kepsut; Bükdere village, 600 m.	ISTE 109674
Galium verum	Balıkesir, Savaştepe; Soğucak village, 430 m.	ISTE 109947
Hypericum triquetrifolium	Balıkesir, Kepsut; Örenli village, 550 m.	ISTE 109716
Paliurus spina-christi	Balıkesir, Savaştepe; Kocaören village, 522 m.	ISTE 109894
Primula vulgaris subspecies *rubra*	Balıkesir, Kepsut; Örencik village, 730 m.	ISTE 109887
Ranunculus arvensis	Balıkesir, Savaştepe; Madenmezar village, 450 m.	ISTE 109890
Teucrium polium	Balıkesir, Kepsut; Örenharman village, 535 m.	ISTE 109781

methanolic solvents were then concentrated in a rotavapor at a low temperature. The resulting dense extract was dried in a lyophilizer. Dried extracts were stored at -180 ˚C.

Broth microdilution assay

The broth microdilution assay was performed to determine the *in vitro* antimicrobial activities of the plant extracts according to the Clinical and Laboratory Standards Institute guidelines against *Staphylococcus aureus* American Type Culture Collection (ATCC) 6538, *Staphylococcus epidermidis* ATCC 12228, *Enterococcus faecalis* ATCC 29212, *Escherichia coli* ATCC 8739, *Proteus mirabilis* ATCC 43071, *Pseudomonas aeruginosa* ATCC 27853, *Klebsiella pneumoniae* ATCC 4352, and *Candida albicans* ATCC 10231.[16,17] The plant extracts were weighed in the desired amount, and dimethylsulfoxide (DMSO) (Sigma, St. Louis, MO, USA) was used to prepare the concentrations. Two-fold serial dilutions were performed on the extracts, ranging from 1250-0.6 µg/mL, in the microplate and treated with 5 x 10^5 colony-forming unit (CFU)/mL for the bacteria and 0.5 x 10^3 to 2.5 x 10^3 CFU/mL for the yeast final inoculum and incubated at 37 ˚C. The lowest concentration at which no growth was observed the next day was determined as the minimum inhibitory concentration (MIC). In addition, DMSO was tested against the test microorganisms. The studies were repeated at least three times.

Inhibitory effects of plant extracts on C. albicans mature biofilms

Considering the results of the study, *the in vitro* effects of the methanol extracts of *A. paniculatum* flower, *C. laurifolius, C. salviifolius, P. vulgaris* root, and *A. nobilis* on mature *C. albicans* biofilms were investigated because they were determined to have inhibitory effects on *C. albicans* planktonic cells. The overnight culture of *C. albicans* ATCC 10231 was diluted in Brain Heart Infusion Broth at 1 x 10^6 CFU/mL, and the prepared suspensions were transferred to 96-well polystyrene flat bottom microplates and incubated at 37 ˚C for 24 hours. After biofilm formation, the medium was carefully aspirated, and the wells were washed twice using sterile phosphate-buffered saline (PBS). The desired concentrations of plant extracts were added to the appropriate wells and incubated for an additional 24 hours. After incubation, the wells were washed twice with PBS. Finally, PBS was placed in the wells and sonicated for 5 minutes in an ultrasonic cleaner, and the biofilm was disintegrated. Microplates were then vortexed at 900 rpm. This process was repeated twice, and the collected supernatants were diluted and planted onto Tryptic Soy Agar. The CFU values were determined by counting the colonies. The logarithms of the CFU values were implemented in the GraphPad Prism program, and the results were expressed graphically.

Cell culture and effects of A. paniculatum flower extract on cells

The effects of *A. paniculatum* flower`s methanol extract, which was found to be significantly effective on both planktonic and biofilm cells of *C. albicans*, on the human lung cancer cell line (A549, ATCC®-185™) and African green monkey kidney cell line (Vero, ATCC® continuous cell line-81™) were determined. Culture media included Dulbecco's modified Eagle's medium (DMEM; Gibco; USA) supplemented with 10% fetal bovine serum (FBS; Gibco; USA) and 1% Penicillin-Streptomycin (Sigma, USA). 10^4 cells were cultured in wells of the 96-well flat-bottom microplate. Then, they were kept for 24 hours at 37 ˚C in a humidified incubator containing 5% CO_2. After incubation, increasing concentrations of the extract (9.75-1250 µg/mL) were placed into the corresponding wells and incubated for an additional 24 hours. To determine the viability of cells, MTT assay was performed. Following exposure, MTT stock solution (5 mg/mL) was prepared in PBS. After discarding the medium from the wells, 10 µL of MTT solution and 90 µL DMEM without phenol red were added to all wells and kept in the incubator for 3 hours. In addition, positive and negative controls were added, and upon incubation, the supernatants were removed. To dissolve the formazan crystals formed in the wells, 100 µL DMSO was added to the wells, and the plate was left in a shaker for 10 minutes. Optical density$_{570}$ was measured using a microplate reader (EON-BioTek Instruments, Winooski, VT, USA).

Statistical analysis

To evaluate the results statistically, GraphPad Prism 8 was used. Results are represented as mean value ± standard deviation. The data was subjected to One-Way analysis of variance (ANOVA), and subsequently, Tukey's post hoc test was employed. A significance level of $p < 0.05$ was used to determine statistical significance.

RESULTS

Antimicrobial activities of the extracts

The antimicrobial activity results are shown in Table 2. All studied extracts displayed better antimicrobial activity against *C. albicans* than against bacteria. According to the antibacterial activity results, *C. salviifolius* methanol extract showed the highest activity against *S. aureus*. The antimicrobial efficacy of any extract against *E. coli* and *K. pneumoniae*, which are important Gram-negative pathogens, could not be determined. However, significant activities were observed against *C. albicans,* especially for the methanol extract of *A. paniculatum* flower (9.75 µg/mL). Methanol extracts of *P. vulgaris* root, *C. laurifolius*, *C. salviifolius*, and *A. nobilis* subspecies *neilreichii* above ground showed 156, 312, 312 and 312 µg/mL MIC values against *C. albicans*, respectively.

Antibiofilm activity

Because the effects of antimicrobial agents against the biofilms of microorganisms are much lower than planktonic forms, and therefore high doses are needed for treatment, biofilm studies have been conducted with at least four times the MIC values of the extracts. According to the MIC (µg/mL) values of plant extracts; 4 x MIC and 8 x MIC of *C. laurifolius, C. salviifolius,* and *A. nobilis*; 4 x MIC, 8 x MIC and 16 x MIC of *P. vulgaris*; 8 x MIC, 16 x MIC, 32 x MIC, 64 x MIC, and 128 x MIC of *A. paniculatum* were prepared. The inhibitory properties of the studied concentrations on *C. albicans* ATCC 10231 mature biofilms were investigated.

Table 2. Antibacterial and antifungal activities of the plant extracts (µg/mL)

	Microorganisms							
Plant extracts	***S. aureus* ATCC 29213**	***S. epidermidis* ATCC 12228**	***E. faecalis* ATCC 29212**	***E. coli* ATCC 25922**	***K. pneumoniae* ATCC 4352**	***P. aeruginosa* ATCC 27853**	***P. mirabilis* ATCC 14153**	***C. albicans* ATCC 10231**
A. bulbosa tuber	1250	› 1250	625	› 1250	›1250	› 1250	› 1250	› 1250
A. paniculatum bulbous	› 1250	› 1250	› 1250	› 1250	› 1250	› 1250	› 1250	› 1250
A. paniculatum flower	› 1250	› 1250	› 1250	› 1250	› 1250	› 1250	› 1250	9.75
A. aestivus root	› 1250	› 1250	› 1250	› 1250	› 1250	› 1250	› 1250	› 1250
B. nigra leaf	› 1250	› 1250	› 1250	› 1250	› 1250	› 1250	› 1250	› 1250
C. laurifolius leaf	625	› 1250	› 1250	› 1250	› 1250	625	› 1250	312
C. salviifolius leaf	312	› 1250	1250	› 1250	› 1250	625	625	312
D. communis root	1250	› 1250	› 1250	› 1250	› 1250	› 1250	› 1250	› 1250
D. communis leaf	› 1250	› 1250	› 1250	› 1250	› 1250	› 1250	› 1250	› 1250
G. verum aerial part	› 1250	› 1250	› 1250	› 1250	› 1250	› 1250	› 1250	› 1250
H. triquetrifolium aerial part	› 1250	› 1250	› 1250	› 1250	› 1250	› 1250	› 1250	› 1250
P. spina-christi root	625	› 1250	› 1250	› 1250	› 1250	625	625	› 1250
P. vulgaris subspecies *rubra* root	› 1250	› 1250	1250	› 1250	› 1250	› 1250	› 1250	156
P. vulgaris subspecies *rubra* leaf	› 1250	› 1250	› 1250	› 1250	› 1250	› 1250	› 1250	› 1250
R. arvensis aerial part	› 1250	› 1250	› 1250	› 1250	› 1250	› 1250	› 1250	› 1250
T. polium aerial part	› 1250	› 1250	› 1250	› 1250	› 1250	› 1250	› 1250	› 1250
A. nobilis subspecies *neilreichii* aerial part	› 1250	› 1250	› 1250	› 1250	› 1250	› 1250	› 1250	312

According to the results, 32 x MIC, 64 x MIC, and 128 x MIC concentrations of *A. paniculatum* flower methanol extract significantly inhibited *C. albicans* biofilm, whereas no effect was detected in other extracts (Figure 1).

Cytotoxicity

After determining the significant effects of the methanol extract of *A. paniculatum* flower on *C. albicans*, its cytotoxicity to A549 and Vero cell lines was also determined. When the results were analyzed statistically, it was revealed that all studied concentrations caused a statistically significant reduction ($p < 0.05$) in the percentage of viable cells (Figure 2). Based on these findings, 312.5 µg/mL and higher concentrations of the extract inhibited cell viability by more than 50% in both cell lines. Cytotoxicity was higher in Vero cells when lower concentrations were compared.

DISCUSSION

Because of the increasing antibiotic resistance to pathogens, the search for new antimicrobial agents is a high priority. There is a growing trend toward natural products as an alternative drug source, and the antimicrobial properties of plants are being widely studied as a solution against multidrug-resistant pathogens.[18] This study was undertaken to understand the *in vitro* properties of 17 plant extracts belonging to the Balıkesir province of Türkiye. In addition to investigating the antimicrobial activities of the herbal extracts used in our study, the possible

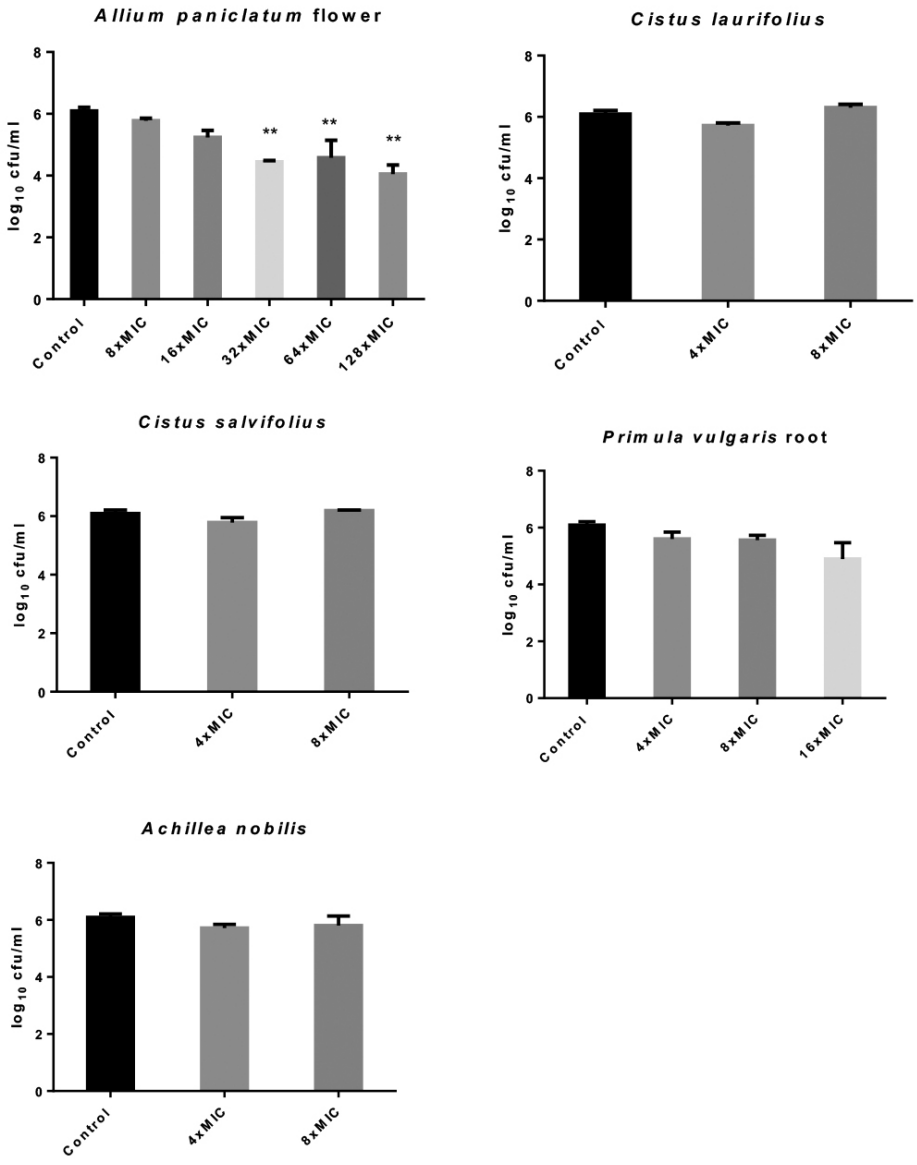

Figure 1. Antibiofilm activities of extracts against *Candida albicans*, $^{**}p < 0.01$

cytotoxicities of the extracts, which had promising antimicrobial effects, were also investigated.

The traditional uses of medicinal plants provide an idea for activity studies. In this study, traditionally utilized plants for their beneficial effects on wound healing in the Balıkesir province of Türkiye were selected for the activity studies. Wound infection is widely prevalent and is a significant clinical obstacle to wound healing. Consequently, exploring the potential antimicrobial properties of plants traditionally employed in wound healing practices is promising. The tuber part of *A. bulbosa* was taken with water for hemorrhoids, intestine problems, constipation, heel cracked, and allergy. The roots of *A. aestivus* are grated and cooked with tarhana (Turkish soup mixture) and applied to the skin for abscesses. The infusion of *B. nigra* leaves is used for colds and stomachaches. The roots of *D. communis*

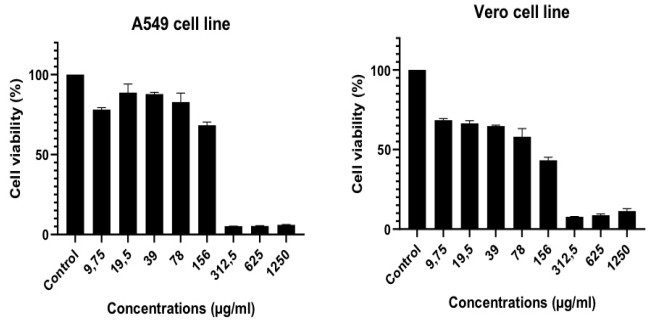

Figure 2. Effects of *Allium paniculatum* flower extract on A549 and Vero cell viability (%)

are used as a decoction for hemorrhoids. The aerial part of *G. verum* is crushed and applied to the skin for wound healing. The infusion prepared from the aerial part of *H. triquetrifolium* is used externally for wound treatment. The roots of *P. spina-christi* are used for allergy and itching. The aerial part of *R. arvensis* is applied on the skin for eczema, abscess, joint pain, and allergy. The aerial part of *A. nobilis* subspecies *neilreichii* is used to treat acne, wound healing, abdominal pain, cough, pain relief, and gynecological diseases. The aerial part of *A. paniculatum* is eaten for health.[11-13,19]

In the Balıkesir region, the roots of *P. vulgaris* are collected and sold by the local people for rheumatism treatment. According to Kahraman et al.,[20] the butanol fraction of *P. vulgaris* roots exhibited the strongest wound-healing efficacy. Primulasaponin I (1) and primulasaponin I methylester (2) were identified as the main active molecules using activity-guided fractionation and isolation procedures.[20] In our study, although the methanol extract derived from *P. vulgaris* root demonstrated efficacy against *C. albicans* (MIC: 156 µg/mL), it did not exhibit noteworthy activity against other tested bacteria.

Ethnomedicinal applications of *Cistus* species are prevalent. The aerial part of *C. laurifolius* is used for diarrhea, urinary tract infections, stomach pain, fungal infection between the fingers, cough, and kidney stones. The aerial part of *C. salviifolius* is used for snake bites, burns, wound healing, diarrhea, urinary tract infections, and prostate.[11-13] Based on the findings of this study, *C. salviifolius* methanol extract showed the highest antibacterial activity (MIC: 312 µg/mL) against *S. aureus* compared with all other extracts. The efficacy of *C. salviifolius* against *S. aureus* has also been confirmed by a previous study conducted by Álvarez-Martínez et al.[21] tested *C. salviifolius* extracts against 100 *S. aureus* clinical isolates and MIC_{50} values were found as 50-80 µg/mL. In addition, it was shown that higher antibacterial activity against methicillin-resistant *S. aureus* isolates than sensitive ones was observed because it contains hydrolyzable tannins and flavonoids such as myricetin and quercetin derivatives.[21] High-performance liquid chromatography revealed the presence of (+)-catechin, (-)-epigallocatechingallate, quercetin-3-O-rutinoside, quercetin-3-O-glucoside, kaempferol-3-O-glucoside, and luteolin in hydroethanolic extracts of five *Cistus* species, including *C. laurifolius* and *C. salviifolius*.[22] Three flavonoids were identified as the primary active components from the *C. laurifolius* ethanol extract: 3,7-O-dimethylquercetin, 3,7-O-methylkaempferol, and 3-O-methylquercetin, which are responsible for strong antinociceptive and anti-inflammatory activities.[23] Therefore, further studies should be conducted to understand its antimicrobial activity better. However, because the highest antimicrobial activity was determined against *C. albicans* in our study, biofilm studies were continued with *C. albicans*.

Although *C. albicans* is a harmless commensal fungus found in the oral cavity or gastrointestinal tract, it is also an opportunistic pathogen that can cause infections. Antimicrobial resistance threatens the treatment of *C. albicans*. In this study, the efficacy of some plant extracts against *C. albicans* was promising. *A. paniculatum* flower extract showed the highest activity (MIC: 9.75 µg/mL), followed by *P. vulgaris* root extract (MIC: 156 µg/mL), *C. laurifolius* (MIC: 312 µg/mL), *C. salviifolius* (MIC: 312 µg/mL), and *A. nobilis* extracts (MIC: 312 µg/mL). According to the MIC results, the methanol extract of the bulb of *A. paniculatum* was found to be ineffective against all microorganisms, including *C. albicans*, whereas the methanol extract of the flower displayed high activity against *C. albicans*. Different parts of *A. paniculatum* have different total flavonoid and phenolic contents; therefore, their antioxidant and enzyme inhibitory properties may vary.[14] The reason for the different antimicrobial activities may be the different contents of the extracts.

Antimicrobials may be up to 1000 times less effective on biofilms than planktonic cells; therefore, biofilms are challenging to eradicate.[24] In this study, it was shown that at least 32 times the MIC value (312 µg/mL) of the methanol extract of *A. paniculatum* flower significantly inhibited *C. albicans* biofilms. The leaves and bulbs of *Allium* plants are known for their antimicrobial properties because of their high thiosulfinate content, especially allicin, polyphenols, and flavonoids. In a recent study, Barbu et al.[25] investigated the antimicrobial activity of hydroalcoholic extracts of six *Allium* species, including *Allium sativum* L. and *Allium ursinum* L. According to their results, both extracts have shown antimicrobial activity against *Candida* species and *S. aureus*. Different studies on the *Allium* genus but different species have also determined the efficacy against *Candida* and *Candida* biofilms.[26,27] However, to date, there have been very few studies on *A. paniculatum* in the literature, but no data showing anti-*Candida* activity.

Organosulfur compounds (such as allicin, ajoenes, dialkenyl and dialkyl sulfides) and saponins found in the structure of *Allium* species have antimicrobial and cytotoxic properties.[28] Although these studies are generally carried out with the bulbs of *Allium* species, it has been shown that the methanol extract obtained from the flowers also contains saponins.[29] Mskhiladze et al.[29] demonstrated that the methanolic extract of *A. leucanthum* flowers inhibited the growth of A549 cells (IC_{50} of 15 ± 3 µg/mL). In our study, the methanol extract of *A. paniculatum* flowers, another *Allium* species, at concentrations of 9.75 µg/mL and higher, statistically inhibited the growth of A549 cells, but more than 50% inhibition occurred after 312.5 µg/mL. Furthermore, it was determined that the cytotoxic effect on cancer cells was similar to that on normal, non-cancerous Vero cells.

CONCLUSIONS

Consequently, the incidence, diagnosis, and clinical severity of *Candida* infections have dramatically increased in recent years. According to our results, *A. paniculatum* was found to be effective on both planktonic and biofilm cells of *C. albicans*, making this plant extract a potent source of antifungal drugs or adjuvant treatment for *Candida* infections. Nevertheless, further analysis studies should be conducted to determine which active compound of *A. paniculatum* has antimicrobial and cytotoxic effects to understand its anticandidal activity better. To determine the suitability of these plant extracts for clinical use, further in-depth investigations are needed.

Ethics

Ethics Committee Approval: There is no requirement for ethical approval.

Informed Consent: Not required.

Authorship Contributions

Concept: Ö.O., M.H., E.Ö., Ş.K., Ç.B.G., Design: Ö.O., M.H., M.Ş.E., Data Collection or Processing: Ö.O., M.H., E.Ö., Ş.K., Ç.B.G., Analysis or Interpretation: Ö.O., E.Ö., M.Ş.E., Ş.K., Ç.B.G., Literature Search: Ö.O., M.H., M.Ş.E., Writing: Ö.O., M.H.

Conflict of Interest: No conflict of interest was declared by the authors.

Financial Disclosure: This work was supported by a grant from the Research Fund of the University of İstanbul (İstanbul, Türkiye), project number: TSA-2019-31201.

REFERENCES

1. Dev S. Impact of natural products in modern drug development. Indian J Exp Biol. 2010;48:191-198.
2. El-Tarabily KA, El-Saadony MT, Alagawany M, Arif M, Batiha GE, Khafaga AF, Elwan HAM, Elnesr SS, E Abd El-Hack M. Using essential oils to overcome bacterial biofilm formation and their antimicrobial resistance. Saudi J Biol Sci. 2021;28:5145-5156.
3. Nett J, Andes D. Candida albicans biofilm development, modeling a host-pathogen interaction. Curr Opin Microbiol. 2006;9:340-345.
4. Kou J, Xin TY, McCarron P, Gupta G, Dureja H, Satija S, Mehta M, Bakshi HA, Tambuwala MM, Collet T, Dua K, Chellappan DK. Going beyond antibiotics: natural plant extracts as an emergent strategy to combat biofilm-associated infections. J Environ Pathol Toxicol Oncol. 2020;39:125-136.
5. Wu H, Moser C, Wang HZ, Høiby N, Song ZJ. Strategies for combating bacterial biofilm infections. Int J Oral Sci. 2015;7:1-7.
6. Cavalheiro M, Teixeira MC. *Candida* Biofilms: Threats, challenges, and promising strategies. Front Med (Lausanne). 2018;5:28.
7. Di Domenico EG, Oliva A, Guembe M. The current knowledge on the pathogenesis of tissue and medical device-related biofilm infections. Microorganisms. 2022;10:1259.
8. Taraszkiewicz A, Fila G, Grinholc M, Nakonieczna J. Innovative strategies to overcome biofilm resistance. Biomed Res Int. 2013;2013:150653.
9. Gürdal B, Kültür S. An ethnobotanical study of medicinal plants in Marmaris (Muğla, Turkey). J Ethnopharmacol. 2013;146:113-126.
10. Kültür S. Medicinal plants used in Kirklareli Province (Turkey). J Ethnopharmacol. 2007;111:341-364.
11. Nath EO. An ethnobotanical study in Savaştepe and Kepsut region (Balıkesir). PhD thesis. Istanbul University, Institute of Health Science, 2016.
12. Polat R, Satıl F. An ethnobotanical survey of medicinal plants in Edremit Gulf (Balıkesir-Turkey). J Ethnopharmacol. 2012;139:626-641.
13. Tuzlaci E, Aymaz PE. Turkish folk medicinal plants, Part IV: Gönen (Balikesir). Fitoterapia. 2001;72:323-343.
14. Emir A, Emir C, Yıldırım H. Chemical and biological comparison of different parts of two *Allium species: Allium paniculatum* L. subsp. villosulum (Hal.) Stearn and *Allium paniculatum* L. subsp. paniculatum L. Chem Pap. 2021;75:411-419.
15. Özdemir Nath E, Kültür Ş. Wild edible plants of Savaştepe district (Balıkesir, Turkey). Marmara Pharm J. 2017;21:578-589.
16. Clinical and laboratory standards institute. Methods for dilution antimicrobial susceptibility tests for bacteria that grow aerobically (7th ed). Approved standard M7-A7. Wayne, PA, USA; 2006.
17. Clinical and laboratory standards institute. Performance standards for antimicrobial susceptibility testing; (2nd) informational supplement. M100-S21. Wayne, PA, USA; 2011.
18. Abreu AC, McBain AJ, Simões M. Plants as sources of new antimicrobials and resistance-modifying agents. Nat Prod Rep. 2012;29:1007-1021.
19. Özdemir Nath E, Kültür Ş. An ethnobotanical study of medicinal plants in Savaştepe (Balıkesir-Turkey). Clin Exp Health Sci. 2022;12:954-980.
20. Kahraman C, Sari S, Küpeli Akkol E, Tatli Cankaya I. Bioactive saponins of primula vulgaris huds. promote wound healing through inhibition of collagenase and elastase enzymes: *in vivo, in vitro* and in silico evaluations. Chem Biodivers. 2022;19:e202200582.
21. Álvarez-Martínez FJ, Rodríguez JC, Borrás-Rocher F, Barrajón-Catalán E, Micol V. The antimicrobial capacity of *Cistus salviifolius* and Punica granatum plant extracts against clinical pathogens is related to their polyphenolic composition. Sci Rep. 2021;11:588.
22. Nur Onal F, Ozturk I, Aydin Kose F, Der G, Kilinc E, Baykan S. Comparative Evaluation of Polyphenol Contents and Biological Activities of Five Cistus L. Species Native to Turkey. Chem Biodivers. 2023;20:e202200915.
23. Küpeli E, Yesilada E. Flavonoids with anti-inflammatory and antinociceptive activity from Cistus laurifolius L. leaves through bioassay-guided procedures. J Ethnopharmacol. 2007;112:524-530.
24. Olsen I. Biofilm-specific antibiotic tolerance and resistance. Eur J Clin Microbiol Infect Dis. 2015;34:877-886.
25. Barbu IA, Ciorîță A, Carpa R, Moț AC, Butiuc-Keul A, Pârvu M. Phytochemical characterization and antimicrobial activity of several *Allium* extracts. Molecules. 2023;28: 3980.
26. Galdiero E, Di Onofrio V, Maione A, Gambino E, Gesuele R, Menale B, Ciaravolo M, Carraturo F, Guida M. *Allium ursinum* and *Allium oschaninii* against *Klebsiella pneumoniae* and *Candida albicans* Mono- and Polymicrobic Biofilms in *in vitro* static and dynamic models. Microorganisms. 2020;8:336.
27. Ng TS, Looi LJ, Ong BS, Chong PP. Antifungal and anti-biofilm effects of shallot (*Allium ascalonicum*) aqueous extract on Candida albicans. J Herbmed Pharmacol. 2018;7:236-242.
28. Lanzotti V, Scala F, Bonanomi G. Compounds from *Allium species* with cytotoxic and antimicrobial activity. Phytochem Rev. 2014;13:769-791.
29. Mskhiladze L, Legault J, Lavoie S, Mshvildadze V, Kuchukhidze J, Elias R, Pichette A. Cytotoxic steroidal saponins from the flowers of *Allium leucanthum*. Molecules. 2008;13:2925-2934.